Characterization of Carbon Dioxide Sequestrating bacterium for Production of Biomaterials

Thesis submitted to

Jawaharlal Nehru University

in partial fulfillment of the requirements

for the award of the degree of

DOCTOR OF PHILOSOPHY

Submitted By:

MANISH KUMAR

SCHOOL OF ENVIRONMENTAL SCIENCES

JAWAHARLAL NEHRU UNIVERSITY

NEW DELHI-110067

2018

जवाहरलाल नेहरू विश्वविधालय
Jawaharlal Nehru University
SCHOOL OF ENVIRONMENTAL SCIENCES
New Delhi - 110067, INDIA

July, 2018

CERTIFICATE

This is to certify that the thesis entitled "**Characterization of Carbon Dioxide Sequestrating bacterium for Production of Biomaterials**" comprises the work done at Environmental Microbiology and Biotechnology Lab, School of Environmental Sciences, Jawaharlal Nehru University, New Delhi, for the partial fulfillment of the degree of Doctor of Philosophy. This work done is original and has not submitted in part or full for any degree or diploma in any other University/institute.

Manish Kumar
MANISH KUMAR
(Candidate)

Thakur
PROF. I.S.THAKUR
(Supervisor)

AL Ram 7/7/18
PROF. AL.RAMANATHAN
(Dean)

प्रो. एल. रामानाथन/Prof. AL. Ramanathan
डीन / Dean
पर्यावरण विज्ञान संस्थान
School of Environmental Sciences
जवाहरलाल नेहरू विश्वविद्यालय, नई दिल्ली-६७
Jawaharlal Nehru University, New Delhi-67

DEDICATED TO MY

BE-LOVING FAMILY

ACKNOWLEDGEMENT

It is a matter of great pride and privilege to have worked at the prestigious Jawaharlal Nehru University for my Ph.D. entitled ***"Characterization of Carbon Dioxide Sequestrating bacterium for Production of Biomaterials"****, under the supervision and guidance of Prof. I.S.Thakur.*

I express my sincere gratitude to ***Prof. I.S. Thakur****, who provided me an opportunity to work in Lab 201, School of Environmental Sciences, JNU and pursue my research interests throughout the duration of my Ph.D. His valuable inputs and ideas kept me on my toes and motivated me to always aim higher and do better than before. Working under his mentorship, has enriched my knowledge base and expanded my life skills, which I am sure will hold me in good stead through my life. I would also like to acknowledge our Hon'rable Dean Prof. AL. Ramanathan and my Doctoral Research Committee members Prof. P. Raj of School of Environmental Sciences, JNU and Dr. Rajesh Mishra of School of Biotechnology, JNU, for their invaluable support.*

I would also like to thank all my respected teachers of my M.sc and Ph.D who thoroughly encouraged me to believe in my abilities. Special thanks to Prof. S.Bhatacharya, Prof. A. K. Atri, Prof. S. Mukhrjee, Prof N. J. Raju, Dr. Meenakshi Dua, Prof. D. Mohan, Prof. S.C. Garkoti, Dr. Ilora Ghosh, Dr. Kashturi Mukopadhay, Dr. N. Siva Sir my B.TECH faculties Dr. Sudipto Bhatacharya, Dr. Sharad Pandey, Dr. Shashi and one of my favourite school teacher Mandal Sir for their sensible suggestion which motivates me toward the research.

The journey of my Ph.D. would not have been the same had I not have the support of my lab mates, who have been a part of my journey at different periods of time. I take this opportunity to acknowledge them, starting from my respected seniors Dr. Shaili Srivastava, Dr. Anjali Singhal, Dr. Moonmoon Hiloidhari, Dr. Umesh Chandra Naik , Dr. Mihir Tanay Das, Dr.Smita Sunduram, Dr. Randhir Bharti, Dr. Jyoti Singh, Dr. Manoj Singh, Dr. Ritu Tripathi, Dr. Pooja Ghosh, Dr. Arti Mishra, Dr. Asmita Gupta, Dr. Moni Kumari, Dr.Madan Kumar, Dr. Rashmi and Kristiniya; my dear juniors Rashmi (Rathour Saab), Khushboo (KK), Badiwali Neha, Raj (New pahalwan in Lab), Juhi (Vanashthali), Radha (Radhe Radhe), Anupreet (Jashmith), Chhotiwali Neha, Disha, Bhawna (Modi), specially juniors to making lab atmosphere cheerful and enjoyable. I also extend my heartfelt gratitude to all the SES staff member lab assistants Rawat Sir, Mr. Narendra, Ramakant Sir, Ramesh Jee, Hoshiyar Sir for their cooperation and support. I would like to thank the generous support

and information shared by Dr. Randhir Kumar Bharti, related to my research topic from very beginning, Dr. Madan Kumar for his guidance in experimental planning, discussion and valuable inputs, Dr. Pooja Ghosh, Dr. Asmita Gupta and KK for writing manuscript and my thesis without which it would be really difficult to submit my work on time.

Although, each and every individual I interacted with during the four years of making this work possible, my special thanks goes to all those without who's' support this work would not have been possible. The whole genome analysis was done in collaboration with Dr. Praveen Verma at National Institute of Plant Genome Research. I would like to acknowledge him and all his lab members for their kind and generous support, especially Dr. Sandhya verma, Rajesh Gazara for the bioinformatics analysis.

The successful completion of this work was possible because of the kind and invaluable technical support that I received from the skilled and well trained staff of advanced instrumental research facilities (AIRF), JNU. I would therefore like to thank to all the staff members of AIRF including Dr. Ajay for GC-MS and NMR analyses, Dr. Ruchita Pal for timely conducting all SEM analyses, Dr. Gajendra Saini and Sharma Sir for TEM analysis, Dr. Manoj Pratap Singh for FT-IR analysis, and Mr. Plabon Borah for LC-MS analysis.
I would also like to thank the Department of science and technology (DST), New Delhi, Government of India, for providing research grants. I express my gratitude to the financial, administrative, hostel, sanitary and health care support lent by Jawaharlal Nehru University.

How can I forget my M.sc and Ph.D classmates, seniors and juniors of SES, hostel-mates, my B.TECH friends, and my schoolmate, how has contributed directly or indirectly in my research work as well as my life specially, Arohi, Anshu, Baba, Anita, Praveen, Amrit, Priyeshu, Manav, Dolley, Kittu, Kamal, Mukesh, shillu, Jyoti, Kopal, Anju, Ravi sir, somya ma'am, meena sir, chinu sir, swati ma'am, Arif sir, Madhav sir, Chandu sir, Anurag sir (my senior come junior), Mr. Tsrering, Captain, Shailesh sir, Mr. Mandal, Prachi ma'am, prince sir, Devendar ma'am, Harpreet ma'am, Madhvi ma'am, Sumo, Rangaswami, Manish (Paanda), Dipawali, Nashim jee, Sarvagaya, Nancy, Sunayna, Akhansh, Shudhanshu, Tarun jee, Khakhi jee, Shushant, Pratima, Horrila, Prakhar, Parul, Laakhe, Meena, Ankit, Deepak, Naarad, Sunny, Manu, Mantri, Chandu, Chandu (my body), Dinkar, Tunni, Mukesh, Brajesh, Pramodh, Ashu, Neeraj and many more……

I would also like to thanks Badminton Club, Cricket club members, and sports staff of JNU starting with, Soami sir, Ravinder sir, Jagat sir, Arun sir, Bipul sir, Luv sir, Koyal ma'am, Bhupi jee, Jaahid jee, Prati, Swati, Mirtunjay sir, Krishna jee, Khan saab, Kunal and

specially ADPE of Sports JNU Dr. Vikram sir and Rakesh sir for their valuable support and encouragement, which make me refresh when I get exhausted some time from Lab work.

Finally no word of thanks is enough for pillar of my life, my ***loving and supportive family****, who has always stood by my side in all walks of life. The unconditional love and support of my mother, father, brother, Bhabi, niece, and nephew have been the fuel of my life. I can never thank them enough for all that they have done to make me "Me" and to enable me achieve all that I have so far. As this four year ordeal concludes, another would begin and thus, the journey of life will continue to surprise and enchant with the unknown. Uri Alon rightly said that science demands a leap into the unknown. My sincere efforts to unravel the unknown would continue as I end this journey and embark upon a new one*...!!

Jully 2018 Manish Kumar

Abbreviation

α	Alpha
β	Beta
γ	Gamma
µg	Microgram
µL	Microliter
mM	Micromolar
ANOVA	Analysis of Variance
BSA	Bovine Serum Albumin
CBB	Calvin-Benson-Bassham
RuBisCO	Ribulose-1,5-bisphosphate carboxyl-ase/oxygenase
CA	Carbonic anhydrase
PRK	Phosphoribulokinase
CV	Coefficient of Variance
DMEM	Dulbecco's Modified Eagle's Medium
DMSO	Dimethyl Sulfoxide
DNS	3,5- Dinitrosalicylic acid
EROD	7-ethoxyresorufin-O-deethylase
FTIR	Fourier Transform Infrared Spectroscopy
GC-MS	Gas Chromatography-Mass Spectroscopy
XRD	X-ray diffraction
TEM	Transmission Electron Microscopy
SEM	Scanning Electron Microscopy
ICPMS	Inductively coupled plasma mass spectrometry
LB	Luria Bertani Broth

MM	Mineral Media
LC-MS	Liquid chromatography-mass spectrometry
MSM	Mineral Salt Medium
MTT	(3-(4,5-Dimethylthiazol-2-yl)-2,5-Diphenyltetrazolium Bromide
NCBI	National Centre for Biotechnology Information
RAST	Rapid Annotations using Subsystems technology
KAAS	KEGG Automatic Annotation Server
PCR	Polymerase Chain Reaction
PHA	Polyhydroxyalkanoates
PHV	Polyhydroxy Valerate
RPM	Revolutions Per Minute
RSM	Response Surface Methodology
bp	base pair
DNA	Deoxyribonucleic Acid
EDTA	Ethylene diamine tetra acetate
h	Hour
kb	Kilobase pair
kDa	Kilo dalton
mg	Milligram
min	Minute
s	Second
mL	Milliliter
mM	Millimolar
nm	Nanometer
^{o}C	Degree centigrade
PAGE	Polyacrylamide gel electrophoresis
PBS	Phosphate buffered saline

cdw	Cell dry weight
SDS	Sodium dodecyl sulphate
v/v	volume/volume
w/v	weight/volume

TABLE OF CONTENT

TABLE OF CONTENT.....i-vii

LIST OF FIGURE.....vii-xi

LIST OF TABLES.....xii-xiii

1. INTRODUCTION .....…….1-9

2. REVIEW OF LITERATURE.....10-39

2.1 Overview of emission and sequestration of CO_2.....……..12

2.1.1 Terrestrial CO2 sequestration.....13

2.1.2 Biological CO_2 sequestration.....14

2.1.3 Carbon dioxide sequestrating chemoautotrophic microorganism……..15

2.2 Development of carbon concentrating mechanism……..17

2.2.1 Carboxysomes……...19

2.3 Carbon fixation pathways……20

2.3.1 Calvin cycle or Calvin-Benson-Bassham (CBB) cycle or reductive pentose pathway…….....22

2.3.2 Reductive TCA cycle or reverse citric acid cycle…….23

2.3.3 Reductive acetyl CoA pathway or Wood-Ljungdahl pathway…….24

2.3.4 3-hydroxypropionate cycle……...26

2.4 Genomics investigation of carbon dioxide sequestration……28

2.4 Biorefinery approach of CO_2 sequestration by bacteria for production of biomaterials……...29

2.4.1 Production of biofuels……..30

2.4.2 Production of biopolymers and bioplastic……33

2.4.3 Production of extracellular polymeric substances (EPS)…….34

2.4.4 Production of chemicals……...36

2.4.5 Production of calcium carbonate……..37

2.4.6 Preparation of Bioactive glasses and its cytotoxicological evaluation…….....37

2.4.7 Optimization of process parameters…….38

3. Characterization of chemolithotrophic bacteria for sequestration of carbon dioxide by whole genome sequencing…….40-74

3.1 Introduction…….....40

3.2 Materials and methods…….....42

3.3 Results and Discussion…….44

3.3.1 General Genomic Features of *Serratia* sp. ISTD04…….....44

3.3.2 GO analysis…….....54

3.3.3 CO_2 sequestration and metabolic diversity…….....56

3.3.4 Transcriptional regulators, Membrane transporters and Proteins…….....59

3.3.5 Biosynthesis of fatty acids and Polyhydroxyalkanoate (PHA)…….....71

3.3.5.1 Cluster analysis for important genes responsible for PHA biosynthesis…….....73

3.4 Conclusion……73

4. Utilization of calcium carbonate precipitated by bacteria during carbon dioxide sequestration for preparation of biocomposite material by sol-gel process……75-95

4.1 Introduction……....75

4.2 Materials and methods…….....78

4.2.1 Production of $CaCO_3$ crystal by *Serratia* sp. ISTD04…….78

4.2.2 Synthesis of biocomposite material by sol-gel process……...79

4.2.3 Preparation of biocomposite material sample for its characterization…….....80

4.2.4 Characterization of biocomposite material……..81

4.2.4.1 SEM-EDX analysis of biocomposite material……..81

4.2.4.2 FT-IR analysis…….....81

4.2.4.3 XRD analysis…….....82

4.2.5 Measurement of ionic concentration in the SBF, 1.5SBF, DMEM and change in pH of the medium……...82

4.2.6 Cytotoxicity test……..82

4.2.6.1. Cell culture……..83

4.2.6.2 Preparation of the extracts……83

4.2.6.3 MTT assay……....83

4.3 Results and Discussion……...84

4.3.1 SEM analysis of biocomposite material……..……84

4.3.1.1 EDX analysis of biocomposite material……...86

4.3.2 FT-IR analysis…….....87

3.3 XRD analysis…….89

4.3.4 Measurement of pH and ions released in the medium……....91

4.3.5 Cytotoxicity test by MTT- assay…….....92

4.4 Conclusions……94

5. Production, characterization and optimization of process parameter for polyhydroxyalkanoate by carbon dioxide sequestering chemolithotrophic oleaginous bacteria……96-123

5.1 Introduction…….....96

5.2 Materials and methods…….....98

5.2.1 Microorganism and culture condition……98

5.2.2 Screening of strain for PHA production…….....99

5.2.2.1 Microscopic visualization…….....99

5.2.2.2 Fluorometric visualization…….....99

5.2.2.3 Spectrofluorometric analysis of PHA accumulation…….....99

5.2.3 Confirmatory analysis of PHA production…….....100

5.2.3.1 FTIR analysis…….....100

5.2.3.2 GC-MS analysis…….....100

5.2.3.3 Transmission electron microscopy…….....101

5.2.4 Optimization of PHA production…….....101

5.2.4.1 Culture conditions for Optimization Experiments…….....101

5.2.4.2 Determination of Biomass, isolation and determination of PHA

weight in cells……...101

5.2.4.3 Box–Behnken Design and Statistical Analysis…….....102

5.3 Results and discussion…….....104

5.3.1 Strain selection for PHA production…….....104

5.3.2 Crystal violet staining…….....104

5.3.3 Fluorescence Microscopic visualization of PHA production…….....105

5.3.4. Spectrofluorometric analysis of PHA accumulation…….....106

5.3.5. GC-MS analysis of PHA and lipids…….....107

5.3.6 Analysis of PHA by FT-IR……..….....110

5.3.7 TEM viewing of PHA granules within the cells…….....111

5.3.8 Process optimization by RSM…….....112

5.3.8.1 Statistical analysis…….....114

5.3.8.2 Interactive effects of factors on weight of PHA and biomass…….....117

5.3.8.3 Validation Results…….....120

5.4 Conclusion…….....123

6. Production, characterization and application of extracellular polymeric substance produced by carbon dioxide sequestering chemolithotrophic bacteria……124-168

6.1 Introduction……124

6.2 Materials and methods…….....126

6.2.1 Chemicals and reagents…….…...126

6.2.2 Microorganism and culture condition…….....126

6.2.3 Isolation and purification of EPS…….....127

6.2.4 Morphological observation of *Serratia* sp. ISTD04 by scanning electron microscopy (SEM)…….....127

6.2.5 Chemical characterization of EPS…….....128

6.2.5.1 Estimation of total carbohydrate content of EPS……128

6.2.5.2 Estimation of reducing sugar of EPS…….....……...128

6.2.5.3 Estimation of protein content of EPS…….....128

6.2.5.4 Estimation of fatty acid content of EPS…….....128

6.2.6 Structural composition analysis of EPS…….....129

6.2.6.1 SEM-EDX analysis of EPS…….....129

6.2.6.2 FT-IR analysis…….....129

6.2.6.3 GC-MS analysis…….....….....130

6.2.6.4 NMR analysis…….....131

6.2.7 Optimization of EPS production and scale up……..……131

6.2.7.1 Culture conditions for optimization of EPS production by

Serratia sp. ISTD04……..……131

6.2.7.2 Scale-up the production of EPS…….....131

2.8 Determination of flocculating activity…….....132

6.2.9 Application of EPS in dyes decolorization…….....132

6.2.10 Proteomics and genomics study of chemolithotrophic bacterium

Serratia sp. ISTD04 for production of EPS…….....133

6.3 Results and discussion……..133

6.3.1 Production of EPS by *Serratia* sp. ISTD04…….....133

6.3.2 Morphological observation of *Serratia* sp. ISTD04 grown in MM- media…….....134

6.3.3 Chemical characterization of EPS…….....135

6.3.3.1 Estimation of total carbohydrate content of EPS…….....….....135

6.3.3.2 Estimation of reducing sugar content of EPS…….....136

6.3.3.3 Estimation of protein concentration of EPS…….....…….....137

6.3.3.4 Estimation of fatty acid content in EPS…….....…….....138

6.3.4 Structural compositional analysis of EPS…….....….....139

6.3.4.1 SEM-EDX analysis of EPS……...……139

6.3.4.2 Functional group analysis by FT-IR…….....…….....142

6.3.4.3 Monosaccharide composition and Linkage analysis by GC-MS…….....….....143

6.3.4.4 Structural configuration analysis of EPS by ^{13}C and ^{1}H NMR…….....….....146

6.3.5 Optimization of production of EPS by *Serratia* sp. ISTD04……..147

6.3.6 Scale-up the production of EPS at fermentor level…….....151

6.3.7 Application of EPS produced by *Serratia* sp. ISTD04…….....….....154

6.3.7.1 Determination of flocculating activity of EPS…….....154

6.3.7.2 Determination of dyes decolorization efficiency of EPS…….....155

6.3.8 Proteomics and genomic analysis of chemolithtrophic bacteria

Serratia sp. ISTD04 for production of EPS…… ……157

6.3.8.1 Proteomics analysis by Nano LC-MS/MS…….….....157

6.3.8.2 Genomic analysis of *Serratia* sp. ISTD04 for production of EPS.....161

6.4 Conclusion……..…….....169

7. SUMMARY AND CONCLUSION.....170-172

8. REFERENCES…….....173-207

LIST OF FIGURE

Fig. No.		Page No.
1.1	Suggested bacterial CaCO3 precipitation mechanism under high-pH and high-Ca2+ extracellular conditions. (Adapted from Hammes and Verstraete, 2002).	6
2.1	Different Routes of carbon capture and sequestration (Adapted from Nanda et al., 2016).	13
2.2	Schematic representation of physiological features of CO2 concentrating bacteria.	16
2.3	Schematic representation CCM and microbial precipitation of calcite (Adapted from Riding, 2006).	18
2.4	Carbon concentration and the carboxysome (Adapted from Yeates et al., 2008).	20
2.5	Representation of Calvin cycle or Calvin-Benson-Bassham (CBB) cycle or Reductive pentose pathway.	23
2.7	Representation of Reductive acetyl CoA pathway or Wood–Ljungdahl pathway.	25
2.8	Representation of Dicarboxylate/4-hydroxybutyrate cycle.	26
2.9	Representation of 3-Hydroxypropionate pathway/malyl-CoA pathway (3HP).	27
2.10	Representation of 3-Hydroxypropionate/4-hydroxybutyrate cycle.	27
2.11	Carbon sequestering mechanisms, overall carbon dioxide fixation pathways and mode of carbon utilization in diverse autotrophic organisms, for production of biomaterials.	30
3.1	Schematic representation of NGS sequencing and analysis pipeline followed in case of *Serratia* sp. ISTD04	43
3.2	Circos Plot of genes compared with the genome for *Serratia* sp. ISTD04. Circles from outside to inside represent; (A) scaffold arrangement (B) gene position on the scaffolds (C) genes in selected pathways (D) GC skew and (E) GC content.	46

3.3	**Classification of proteins in subsystem features using RAST analysis and annotation server and their abundance in different functional groups shown in *Serratia* sp. ISTD04.**	**54**
3.4	**Pictorial representation of GO analysis of *Serratia* sp. ISTD04 genome and proteins involve in (a) biological processes, (b) cellular components and (c) molecular functions.**	**55**
3.5	**Representation of transcriptional regulators identified by Nr-blast in the genome of *Serratia* sp. ISTD04.**	**70**
3.6	**Protein identified by Nr- blast in the genome of *Serratia* sp. ISTD04.**	**71**
3.7	**Gene clusters identified in *Serratia* genome responsible for PHA production. The contignumber and size of DNA fragment selected for cluster analysis has been represented.**	**73**
4.1	**Schematic representation of steps involved in preparation of biocomposite material by sol-gel process (modified from Chen et al., 2010 and Hench et al., 1971).**	**80**
4.2	**(SEM analysis of biocomposite material, all the images at same magnification (a) without immersion (b) Bioactivity in SBF (c) Bioactivity in 1.5 SBF (d) Bioactivity in DMEM.**	**84-85**
4.3	**Elemental composition analysis of Sintered biocomposite material (a) before immersion (b) in SBF (c) in 1.5SBF (d) in DMEM for 25 days by EDX.**	**86**
4.4	**FT-IR spectra of sintered biocomposite material and immersed material in SBF, 1.5SBF and DMEM.**	**88**
4.5	**(a) XRD pattern of un-sintered (600°C) and sintered (1200°C) biocomposite material.** **(b) XRD of sol-gel derived biocomposite material immersed in DMEM, SBF and 1.5SBF for 25 days.**	**89-90**
4.6	**(a) MTT assay of the effect of the biocomposite material (MG-63) in direct contact with cells after 24 h, 3 and 6 days of culture. Vertical lines represent ±SD.** **(b) MTT assay performed with the biocomposite material extracts and osteoblastic cells after 24 h and 3 days of culture. Vertical lines represent ±SD.**	**92-93**

5.1	**Staining of *Serratia* sp. ISTD04 with crystal violet showing violet cell clumps.**	**105**
5.2	**Staining of *Serratia* sp. ISTD04 with Nile red showing fluorescence.**	**106**
5.3	**Nile red fluorescence at 575 nm and 590 nm emission wavelengths along with growth at 595 nm of *Serratia* sp. ISTD04 measured every 24 h for 8 days.**	**107**
5.4	**GC-MS chromatogram of PHA produced by *Serratia* sp. ISTD04 showing the peak of 3- Hydroxyvalerate.**	**109**
5.5	**FT-IR spectra of PHA synthesized by *Serratia* sp. ISTD04.**	**110**
5.6	**Transmission electron micrograph (X 15000 magnification) of *Serratia* sp. ISTD04 in (a) control and (b) 72 h cultures showing PHA granules marked by black arrow.**	**112**
5.7	**Actual response values obtained from the experiments were compared with the response predicted by BBD model for (a) PHA production and (b) Biomass production.**	**114**
5.8	**3-D surface plot showing the interaction of A= Glucose concentration (%), B = pH and C = Bicarbonate concentration (mM) on weight of (i) PHA (a,b,c) and (ii) biomass (d,e,f) both measured in g per 100 mL culture by *Serratia* sp. ISTD04.**	**119-120**
5.9	**Ramps indicate the optimized conditions of factors (glucose concentration%, pH, bicarbonate (mM)) for production of PHA and biomass by *Serratia* sp. ISTD04, predicted by model.**	**121**
6.1	**(a) EPS precipitated by ice cold isopropanol (b) EPS purified by isopropanol, acetone and oven dried.**	**134**
6.2	**SEM images of *Serratia* sp. ISTD04 during EPS production at different time intervals; (a) 0h, (b) 48 h, and (c) 72h in media supplemented with 50 mM NaHCO3 and glucose (0.5%).**	**135**
6.3	**Standard curve of Glucose for phenol- sulfuric acid assay.**	**136**
6.4	**Standard curve of Glucose for 3,5- dinitrosalicyclic acid assay.**	**137**
6.5	**Standard curve of BSA for Bradford assay.**	**138**
6.6	**SEM viewing of purified EPS extracted from *Serratia* sp. ISTD04 at various magnifications (a-d).**	**139-140**
6.7	**Elemental composition of EPS in terms of abundance, as detected by**	**141**

	EDX spectrometer (a) peaks of the elements detected (b) relative Atomic wt. percent of the abundant elements.	
6.8	**FT-IR spectra of EPS produced by *Serratia* sp. ISTD04.**	**142**
6.9	**(a) GC-MS analysis of monomers composition of EPS produced by Serratia sp. ISTD04 (b) Linkage analysis of EPS.**	**144-145**
6.10	**(a) ^{13}C and (b) ^{1}H NMR analysis of EPS extracted from *Serratia* sp. ISTD04.**	**146-147**
6.11	**Representation of optimization parameters for production of EPS (a) Glucose % (w/v) (b) NaHCO3 Conc (mM) (c) pH.**	**149**
6.12	**Bacterial growth in 20 L fermentor and subsequent production of EPS at various time intervals.**	**152**
6.13	**Production and precipitation steps of EPS produced by *Serratia* sp. ISTD04 in 20 L fermentor.**	**153**
6.14	**Determination of bioflocculating activity of bacterial culture broth EPS, culture supernatant EPS by Kaoline test (Jar test) using distilled water as blank.**	**154**
6.15	**Representation of dyes decolorization efficiency of EPS produced by *Serratia* sp. ISTD04 (1) Trypan blue (2) Acridine orange (3) Methyl orange (4) Bromothymol blue (5) Aniline blue (6) Crystal violet.**	**156**
6.16	**Whole cell proteins (triplicate) separated by SDS-PAGE gel from *Serrati*a sp. ISTD04.**	**158**
6.17	**Representation of 96 proteins identified by LC-MS/MS in *Serratia* sp. ISTD04 and its functional classification.**	**161**
6.18	**Represention of putative gene clusters with contig number, position and size identified in *Serratia* sp. ISTD04 genome responsible for polysaccharide biosynthesis.**	**168**

LIST OF TABLE

Table No.	Table	Page No.
2.1	Comparative table of microorganism for production of biomaterials with advantage and disadvantage.	11-12
2.2	CO_2 fixation pathways and theirs key enzymes in various organisms	21
2.3	Production of biofuels and bio-based materials by CO2 concentrating chemoautotrophic microorganisms.	34-35
3.1	General genome features of *Serratia* sp. ISTD04.	44-45
3.2	Important genes involve in various pathways represented on Circos plot.)	47-50
3.3	Representation of proteins involve in various pathways, analyzed by KEGG-KAAS pathway analysis.	51-52
3.4	Representation of Proteins identified against the Nr- blast search.	61-69
4.1	Elemental composition analysis (qualitatively) of Sintered and immersed biocomposite material in SBF, 1,5SBF and DMEM by EDX.	87
4.2	Representation of peaks and their corresponding annotation of biocomposite material.	88
4.3	ICP-MS analysis of ions present in the medium before and after immersion in SBF, 1.5SBF and DMEM.	92
5.1	Box –Behnken design of independent variables for process parameters optimization.	103
5.2	GC-MS data table for PHA and FAMEs produced by *Serratia* sp. ISTD04.	109
5.3	Peaks observed in FT-IR spectrum of PHA synthesized by *Serratia* sp. ISTD04 and their corresponding annotations.	111
5.4	Behnken design for actual and predicted response of PHA yield and Biomass.	113

5.5	**ANOVA Results for Response Surface Quadratic model of PHA yield.**	**115**
5.6	**ANOVA Results for Response Surface Quadratic model of Biomass.**	**116**
5.7	**Weight of PHA and Biomass obtained from *Serratia* sp. ISDT04 culture (g per 100 mL culture) before and after optimization.**	**122**
6.1	**Peaks observed in FTIR spectrum of EPS produced by *Serratia* sp. ISTD04.**	**143**
6.2	**Optimization of process parameters for production of EPS by *Serratia* sp. ISTD04**	**148**
6.3	**Production of EPS by pure culture of bacteria using different carbon sources.**	**151**
6.4	**Identification and functional classification of proteins involve in different major pathway of *Serratia* sp. ISTD04 grown in MSM containing $NaHCO_3$ as sole carbon source.**	**158-160**
6.5	**Genes and protein identified in the clusters analysis of *Serratia* sp. ISTD04 for biosynthesis of EPS.**	**163-167**

Chapter 1:

INTRODUCTION

1. INTRODUCTION

Emission of Global Warming Gases (GWGs) is the mainly responsible causes, which trigger the global warming and subsequently climate shift. Carbon dioxide (CO_2), being the most rampant of GWGs, concentration has increases by somehow 32% since the Industrial Revolution, from approximately 280 part per million (ppm) to 400 ppm until now (**De Silva et al., 2015; Cheah et al., 2016**). The power sector is the foremost CO_2 emitter requires strict CO2 management technology and thus various strategies have been made so far to move forward to achieve "low carbon society" (**Cheah et al., 2015; Li et al., 2015**). In current years, endeavours have been made to extend technologies and processes for CO_2 capture, storage and utilization (CCU), which includes liquids, solids, membranes as adsorbents and biological methods (**Choi and Drese, 2009; Rahaman et al., 2011; Olson et al., 2012**). However, CO_2 is incredibly striking as reaction media in biphasic catalysis as it is copious, harmless, non-flammable easily available and renewable carbon source for production of value added products such as fuels and chemicals (**Peters et al., 2011**). Therefore, catalytic mechanism and reaction media are developed based on economic feasibility and activation of CO2 for uses it as eco-friendly carbon source. Considerable development is made so far in catalytic utilization of CO_2, as a substitute of reaction medium, reactant, reagent and promoter due to its exclusive physical properties (**Cokoja et al., 2011; Trusler, 2017**). Several chemical processes, photochemical, electrochemical, biochemical and microwave-assisted conversion of CO_2 are reported since last five decades (**Choi and Drese, 2009; Leung et al., 2014**). To understand the molecular mechanism adopted by biological system for utilization of CO2 and developing the advance technology, it is important to know the basic chemistry of CO2. Although CO2 is a nonpolar molecule, but it contains two polar C=O bonds and exhibits two varying reaction sites, such as electrophilic carbon atom and nucleophilic oxygen atoms. The chemical bonding of a third atom of oxygen and some other atom with carbon atom is exergonic reaction and as a result CO_2 can be transformed into carboxylates, lactones, carbamates, urea, isocyanates and carbonates (**Choi and Drese, 2009**). Apart from oxidised form of CO_2 its reduced form such as formates, oxalates, formaldehyde, carbon monoxide, methanol and methane are produced by endergonic reaction mechanism (**Jessop, 2006**). Therefore, major challenge for scientific and technological community is to utilize CO_2 as a C-1 building block. CO_2 is a copious and reusable C1 carbon

source and through the catalytic conversion it can be used as an eco-friendly and inexpensive source of carbon. CO_2 thoroughly form a C–O (carbon– oxygen), C–N (carbon–nitrogen), C–C (carbon–carbon), and C–H (carbon-hydrogen) bond by chemical reaction and it can be converted into valuable chemicals and fuels such as carbonates, dialkyl carbonates, and polycarbonates (C–O bond); oxazolidinones, quinazolines, urea derivatives, carbamates, isocyanates, and polyurethanes (C–N bond); carboxylic acids and its derivatives (C–C bond); and formic acid derivatives and methanol (C–H bond). There are more possibilities of these compounds to synthesize in biological system due to presence of their inherent biocatalyst and genes (**Sakakura et al., 2007**). Although synthetic conversion of CO2 possible through chemical reactions despite that, biological systems are more prominent in utilization of CO2 (**Bharti et al., 2014a; Kumar et al., 2017c**). Scientific investigation has been started to introduce biotechnology and synthetic biology approach in biological CO_2 capture and utilization (CCU), can be an alternative to enhance the utilization of CO_2 by prokaryotic microbes at industrial level (**Hicks et al., 2017**). A phylogenetically assorted assemblage of prokaryotes fixes CO2 into organic carbon. Till date, six metabolic routs for CO_2 fixation in prokaryotic organisms have been reported as represented in **Table 1** (**Jajesniak et al., 2014; Kumar et al., 2017c**). Based on the presence of diverse enzymatic machinery and their extent of oxygen sensitivity, generally the pathways can be classified into two groups such as aerobic and anaerobic. Diverse groups of microorganisms able to assimilate CO_2 through the Calvin-Benson-Bassham (CBB) cycle, transforming the inorganic carbon into complex organic compounds (**Bar-Even et al., 2010**). In the terrestrial setting such as surface soil, sediments, the oxygentolerant reductive pentose phosphate pathway, CBB pathway, the hydroxypropionate bicycle, and the 3-hydroxypropionate-4-hydroxybutyrate cycle are significant. The key enzyme of CBB cycle is ribulose-1,5-bisphosphate carboxylase (RuBisCO), which can fixes the CO_2 into inorganic carbon and it present in eukaryotes such as plants and algae as well as prokaryotic chemolithoautotrophic bacteria (**Bharti et al., 2014c; Kumar et al., 2017b**). The oxygen-sensitive CO_2 fixation pathways, reductive tricarboxylic acid (rTCA) cycle, reductive acetyl-CoA pathway or Wood–Ljungdahl pathway and the dicarboxylate-4-hydroxybutyrate cycle are of meticulous interest in anaerobic marine sedimentary layer overlying prospect of CO_2 capture and storage (CCS) sites (**Cotton et al., 2018; Huber et al., 2008; Bar-Even et al., 2010; Ye et al., 2016**). These

mechanisms are merely present in prokaryotes and explicit microorganisms. Microorganisms exhibiting these mechanisms have been recommended as contender species for CCS monitoring.

Table.1.1 CO_2 sequestration pathways in different microorganisms and their important carboxylating enzymes.

Name of the carbon dioxide fixing pathway	CO_2 fixing enzyme	Organisms	Carbon/Energy source	References
Calvin cycle	RuBisCO (EC: 2.1.1.127)	Plants *Scenedesmus* sp. *Leptolyngbya* sp. Bacteria	Light/CO_2	Bar-Even et al., 2010; Tripathi et al 2015; Singh and Thakur 2015 Bharti et al. 2014
3-hydroxy Propionate cycle	Acetyl-CoA carboxylase(EC: 6.4.1.2) Propionyl-CoA carboxylase(EC: 6.4.1.3)	*Chloroflexus aurantiacus*	Light	Bar-Even et al., 2010; Herter et al., 2001
Wood-Ljungdahl pathway	Formate dehydrogenase (EC: 1.2.1.2) CO dehydro genate/ Acetyl-CoA synthase (EC:2.3.1.169)	*Clostridium ljungdahlii*	Hydrogen	Ragsdale, 1997
Reductive TCA cycle	2-Oxoglutarate synthase (EC: 1.2.7.3) Isocitrate dehydrogenase (EC:1.1.1.87)	*Chlorobium thiosulfatophilum*	Light Sulfur	(Bar-Even et al., 2010; Kim et al., 1992)
Dicarboxylate/4-hydroxybutyratecycle	Pyruvate synthase (EC: 1.2.7.1)	*Ignicoccus hospitalis*	Hydrogen	(Bar-Even et al., 2010; Huber et al.,

	Phosphoenol pyruvatecarboxylase (EC:4.1.1.31)		Sulfur	2008)
3-hydroxypropionate /4-hydroxybutyrate cycle	Acetyl-CoA carboxylase(EC: 6.4.1.2) Propionyl-CoA carboxylase(EC: 6.4.1.3)	*Metallosphaera sedula*	Hydrogen Sulfur	(Bar-Even et al., 2010; Berg et al., 2007)

In CBB cycle, the carboxylation reaction of ribulose 1,5-bisphosphate to give two molecules of 3-phosphoglycerate (3PG) is catalysed by RuBisCO. Out of these two molecules of 3PG, one molecule is goes to central metabolic pathways, whereas the other is employ to carry forward the cycle. However, particularly RuBisCO is inefficient carboxylase, along with its attraction toward CO_2, it also binds O_2 (oxygenase activity) leading to photorespiration and unnecessary metabolites formation (**Schwander et al., 2016**). This inadequacy of RuBisCO is challenging due to the low CO_2 and high O2 concentrations of these gases in atmosphere. To balance the unevenness between the high requirement of inorganic carbon and low ambient CO_2 concentration, biological organisms come together with chemoautotrophs, which are evolved with CO_2 concentrating mechanisms (CCMs). The major components of CCM include active bicarbonate (HCO_3^-) uptake transporters, a suit for restrict carbonic anhydrases (CAs) strategically inside the cells and for RuBisCO a subcellular micro-compartment in which most RuBisCO is located which is called as carboxysome. Inorganic carbon entered via either CO_2 diffusion through the cellular membranes or the active transportation of HCO_3^- by using membrane pumps. The fastest enzyme CA acting on $HCO3^-$ and quickly convert it into CO_2 for successive utilization by RuBisCO (**Bose and Satyanarayana, 2017**). Inorganic carbon fixation prospective is endorsed to their large allocation especially in moist conditions, ability to produces more biomass, rapid uptake of CO_2 and its fixation in biomass and finally its conversion into high commercial value metabolites. In term of technology level, β-proteobacteria, clostridia and archaea could sooner or later surpass the photosynthetic microbes. It is imperative to extend biotechnological approach viz. robust strain selection (biomass, growth pattern, rate of CO_2 fixation, diversity of product and quantity), cheaper growth inducer in media along with CO_2, physiological parameters (gas concentration), bioprocess technique (batch

mode, continuous mode) and design of bioreactor (continuous stirred tank reactor, fixed bed reactor, membrane reactor) for CCU and biomaterials production (**Jajesniak et al., 2014**).

Recent progress and advancement in the field of molecular analysis technologies like proteomics, genomics and transcriptomics, increase the understanding about complex microbial system. For bacteria, next generation sequencing (NGS) has become a popular and promising technique. The easily accessible construction tools for preparation of genomic library, fast and better quality sequencing and entrenched data analysis pipelines for genome re-sequencing and assembly, signify its cost effectiveness and better reliability of results (**Vuyisich et al., 2014)**. The more and more accessible genomic, metabolomics and proteomic data related to phototrophic and chemotrophic microbes, push the researcher to think about the potential application of microbes for utilization of CO_2 along with production of value added biomaterials and important biological enzymes (**Bharti et al., 2014b; Badger et al., 2006**).

Most of the bacterial species are capable to precipitate carbonates in an alkaline environment rich in Ca^{2+} ions. Carbonate precipitation is associated with metabolic pathways like photosynthesis, nitrogen and sulfur cycles, and ion exchange (Ca^{2+}/H^{+}). The calcium carbonate precipitation by the bacteria has been described that involvement of stoichiometric interactions between positively charged Ca^{2+} ions and the negatively charged bacterial cell wall (**Hammes and Verstraete., 2002**). These Ca^{2+} ion-cell wall interactions produce changes in the overall charge of the cell wall. This process allowing interaction between differently charged bacteria. Due to changes in the overall ionic charge, bacteria aggregate to increase the size of the biomineral, and in turn, bacteria become the nucleus of the biomineral (**Ferrer et al., 1988; Rivadeneyra et al., 1998**).

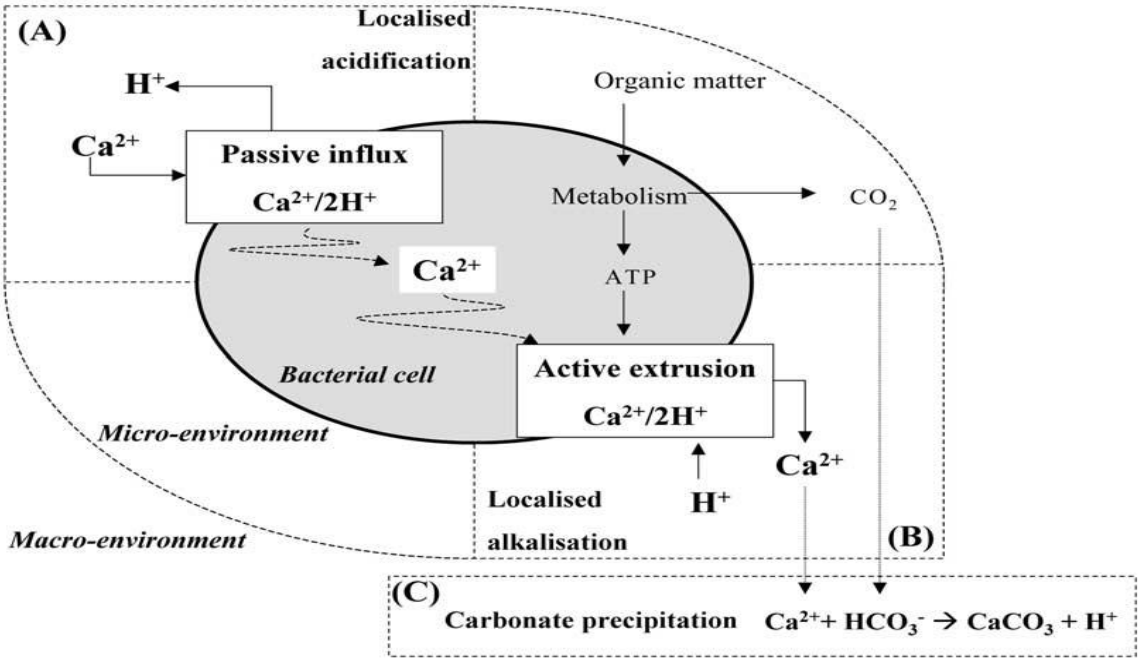

Fig.1.1 Suggested bacterial $CaCO_3$ precipitation mechanism under high-pH and high-Ca^{2+} extracellular conditions. (Adapted from **Hammes and Verstraete, 2002**).

Larry Hench from university of Florida was the first who invented bioactive glass in 1969. He decided to prepare a biodegradable glass. The molar composition of bioactive glass 46.1 mol. % SiO_2, 24.4 mol. % Na_2O, 26.9 mol. % CaO and 2.6 mol. % P_2O_5, later termed 45S5 **(Hench et al. 1971**). The name ‘‘Bioglass’’ was trademarked by the University of Florida as a name for the original 45S5 composition. It should therefore only be used in reference to the 45S5. The mechanism for bone bonding is attributed to a hydroxycarbonate apatite (HCA) layer on the surface of the glass, following initial glass dissolution (**Hench et al., 1971**). HCA is similar to bone mineral and is thought to interact with collagen fibrils to integrate (bond) with the host bone. The osteogenic properties of the glass are thought to be due to the dissolution products of the glass, i.e. soluble silica and calcium ions that stimulate osteogenic cells to produce bone matrix (**Hench et al. 2006**). Glass can be made using two processing methods, the traditional melt-quenching route and the sol–gel route. The sol–gel process has great versatility by which bioactive glasses can be made as nanoporous powders or monoliths or as nanoparticles simply by changing the pH of the process (**Brinker et al. 1990**).There are now several types of bioactive

glass like the conventional silicates, such as Bioglass 45S5, phosphate-based glasses and borate-based glasses. Surprisingly, after 40 years of research on bioactive glasses by numerous research groups, no other bioactive glass composition has been found to have better biological properties than the original Bioglass 45S5 composition.

Rising level of greenhouse gases (GHGs) such as CO_2, methane nitrous oxide (N_2O, chloroflorocarbons (CFCs) leading to climate shift. Simultaneously accumulation of non-degradables substances such as plastics, pesticides triggers environmental degradation. The production of petroleum-derived plastics has been increasing globally 299 million tons in 2013, which was 3.9% higher than 2012s (**Yan et al., 2006; Kumar et al., 2016d**). Polyhydroxyalkanotes (PHAs) is biological polymers having characteristics such as, biodegradable, biocompatible and thermostable. It is stored as intracellular reserve materials in diverse group of organism, preferably when carbon source is excess and nutrient condition is limiting in media (**Gupta et al., 2017; Kumar et al., 2018**). Accumulation of PHA in microbes is one of the endurance tactics to avoid pressure exerted by environment on the microbes inhabiting in various ecological niches, such as marine sediments, microbial mats, rhizosphere, marbles mine and in the artificial ecosystems (**Kumar et al., 2017c**). *R. eutropha* store PHAs within its cytoplasm as source of carbon commonly known as bioplastics (**Yu, 2014**). PHA granules usually consist of short chains of poly 3-hydroxybutyrate (PHB) and poly 3-hydroxybutyrate-co-3-hydroxyvalerate (PHBV) (**Kumar et al., 2016e**). With the help of genetic engineering technology considerable research has been carried out to produce PHA copolymers that reveal improved mechanical strength than PHB using wide varieties of carbon sources such as, glucose, fructose, plant oils and sodium bicarbonate (**Kumar et al., 2017c**). *Ideonella* sp. is reported to store PHA intracellular from captured inorganic carbon, similarly Serratia sp. ISTD04 use sodium bicarbonate as carbon source and produced polyhydroxyvalerate (PHV) 48% of it dry biomass (**Yu, 2014; Kumar et al., 2016c**). A few products that can be derived from PHB, though chemical and enzymatic methods such as, (R)-3-hydroxybutyric acid (3HB), methyl ester of 3HB, crotonic acid, acetoacetic acid and 1,3- butanediol (**Yu, 2014; Tanaka et al., 2011**). A number of haloarchaeal genera have been able to produced PHA such as, *Haloarcula*, *Haloferax*, *Halobiforma* and *Haloquadratum*, (**Yu, 2014**). Purified PHA extracted from biological origins having properties similar to petroleum derived plastics polyproplylene

like its biocompatibility, biodegradability and thermal stability, make this polymers as a commercially interested products.

Biomineralization of CO_2 by precipitating calcium carbonate, performed by microorganisms have been advance and successful tactic of point source CCS (**Bose and Satyanarayana, 2017**). Extracellular polymeric substance (EPS) is excretory materials of organisms secreted into their own environment (**Subramanian et al., 2010; Kumar et al., 2017c**). The microbial EPS is mainly made up of carbohydrates and non-carbohydrates components that are secreted by microbes, during cell lysis or non-availability of carbon source in the surrounding environment (**More et al., 2014**). To identify the pathways of EPS production in microorganism, proteomics, genomics and metabolomics are the emerging and imperative approach, which quite helpful in finding the mechanism of its production (**Singh et al., 2014; Kumar et al., 2017b**). EPS can be produced by diverse groups of organism, which includes archaea, bacteria and eukaryotes and its physical, chemical, biological and rheological attributes change according to nutrient load, carbon source, temperature, pH and nature of microorganisms (**Shen et al., 2013; Gupta and Thakur, 2016**). EPS production is widely distributed in most of the Gram-negative bacteria such as *Rhizobium* sp., *Agrobacterium* sp., *Azoarcus* sp. *Zoogloea* sp., *Azotobacter vinelandii*, *Haemophilus* sp., *Xanthomonas campestris*, *Pseudomonas* sp. (**Gupta and Thakur, 2016**). Bacterial species such as *Leuconostoc mesenteroides*, *Lactobacillus* sp., *Streptococus bovis*, they belongs to Gram-positive bacteria have been also reported for production of EPS (**Jiang, 2011**). Attributable to its unique properties like its functionality, biocompatibility and biodegradability, this novel biological materials have potential application in many fields such as bioflocculant, cementing materials, fabrics, detergents, recovery of microbial oil, pharmaceutical, food additives, metals removal, dyes removal and waste water treatment (**Gupta and Thakur, 2016**). EPS assist the microorganism to conquer the environmental limits such as metal toxicity, limiting nutrient circumstance, food accessibility, energy scarceness, it act as protecting barrier for the microorganism surviving in unfavorable environmental conditions (**Kumar et al., 2017b**).

Increasing concentration of CO_2 may propel the researcher to thing about advance microbial technology to sequester the CO_2 using biotechnological approach and simultaneously

production of valuable biomaterials. Based upon these facts and knowledge, the current research objectives are:

1. **Characterization of chemolithotrophic bacteria for sequestration of carbon dioxide by whole genome sequencing.**
2. **Utilization of calcium carbonate precipitated by bacteria during carbon dioxide sequestration for preparation of biocomposite material by sol-gel process.**
3. **Production, characterization and optimization of process parameter for polyhydroxyalkanoate by carbon dioxide sequestering chemolithotrophic oleaginous bacteria.**
4. **Production, characterization and application of extracellular polymeric substance produced by carbon dioxide sequestering chemolithotrophic bacteria.**

Chapter 2:

REVIEW OF LITERATURE

2. REVIEW OF LITERATURE

The increase in concentration of carbon dioxide (CO_2) by anthropogenic activities such as change in land use pattern, deforestation, industrialization, transportation and modern life style leads to global climate shift, which is one of the critical environmental challenges that the world is facing today. The atmospheric concentration of CO_2 is presently 408 ppm (**CO_2 earth, 2017**). As one of the potent Global Warming Gas (GWG), CO_2 has increased by approximately 43% since industrial revolution and is expected to further increase to 60% in 2100 if the current trend continues (**Kumar et al., 2016d**). Mitigation strategy of CO_2 can be attained mainly by three possible ways: primarily by improving energy efficiency of existing engine technology and proper fossil fuel utilization, secondly by CO_2 sequestration and the lastly by facilitating the uses of unconventional fuels such as biohydrocarbon, biodiesel, etc. (**Bharti et al., 2014a**). Storage and utilization of captured CO_2 by autotrophic biota and some microorganism such as algae, cyanobacteria, chemoautotrophic and chemolithoautotrophic bacteria having CO2 fixing mechanism supported by key enzyme like Ribulose- 1,5-bisphosphate carboxylase/oxygenase (RuBisCO) and facilitated by enzyme like carbonic anhydrase (CA) is one of the mitigation options (**Bharti et al., 2014b**). Bacteria possess significant advantages over photosynthetic organism e.g. higher plants and microalgae, which have been the main focus of attention, for production of environmental friendly fuel oil as well as biomaterials. Fatty acids, alcohols and alkanes are fundamental organic components for production of biofuel. Bacteria are capable of synthesizing intracellular as well as extracellular fatty acid (**Bharti et al., 2014a**). Intracellular fatty acid is used by bacteria as precursor molecules for biosynthesis of their own cell envelopes (**Moazami et al., 2011**). Bacteria synthesize fatty acids similar to plants, using acetyl-CoA with ATP as the source of energy and NADPH as the source of reducing equivalents (**Bharti et al., 2014b**). Hydrocarbons such as alkanes and alkenes are produced directly from fatty acid metabolites by decarboxylation of fatty aldehydes (**Schirmer et al., 2010**). Microorganisms obtain their food and energy via assorted adaptation in environment for survival. Accumulation of polyhydoxyalkanoate (PHA) is survival strategy adopted by microorganisms against the stress responses exerted by environment (**Kumar et al., 2016d**). Among prokaryotes, biosynthesis of PHA is well known in Gram positive and Gram negative bacteria (**Belova et al., 1997**). Unlikely, more than 80 diverse types of PHA have been reported in bacteria (**Lee, 1996**). Various PHA

biosynthesis pathways have been design by the nature in microorganisms based on their living habitats survival pattern and energy requirements. Extracellular polymeric substances (EPS) are high molecular weight substances usually called as exopolysaccharides. EPS is a secretary product of microorganism into the surrounding medium (**Gupta and Thakur, 2016**). The main components of these polymers are monosaccharide and some non carbohydrates such as protein, nucleic acids, lipids, phosphate, acetate and succinate (**More et al., 2014**). Microbial EPS plays a considerable role in dealing with microbes and their environments and stress; habitually serving as a source of energy in nutrient limiting conditions and as a protective barrier during adverse environmental conditions (**Kumar et al., 2017b**).

Table.2.1 Comparative table of microorganism for production of biomaterials with advantage and disadvantage.

Microorganisms	Advantage	Disadvantage
Cyanobacteria	1. Grow easily with moderate nutritional requirements. 2. Cultivation is simple and inexpensive. 3. Higher rate of photosynthetic and growth as compared to algae and higher plants. 4. Contain considerable amount of lipids. 5. Wide range of fuels potentially obtained from cyanobacterial biomass (H_2, ethanol, diesel, methane). 6. Easily Genetically modified.	1. Optimum Temperature, pH, intensity of light affect productivity. 2. Required proper C:N ratio for their growth. 3. Agitation required for their growth increase the operational cost.
Algae	1. Widely distributed 2. Easy cultivation 3. Fast growth. 4. Higher cell density. 5. Fast CO_2 utilization. 6. High fatty acid content. 7. Production of value added byproducts such as proteins, fertilizers. 8. Easily Genetically modified.	1. Light requirement (*e.g.*, intensity, wavelength). 2. Water requirement. 3. More phosphorous required as fertilizer. 4. Fuels derived from algae having imbalance saturated and unsaturated fatty FAMEs composition, lead to low fuel properties.
Bacteria	1. Aerobic microorganisms and easier cultivation 2. Diverse carbon sources and carbon utilization pathways. 3. Natural ability to store lipids and PHA as reserve food material. 4. Balance fuel properties composition.	1. Fermentation process is still under development. 2. Higher chances of contamination.

	3. Easily Genetically modified.	
Archaea	1. CH_4 produced by methanogens. 2. Ability to accumulate PHA in some archaeal species. 3. Admirable sources of thermostable enzymes (*e.g*., carbonic anhydrases).	1. Fermentation process is still under development. 2. Difficult to maintained growth conditions. 3. Genetic modification is difficult.

2.1 Overview of emission and sequestration of CO_2

Based on the information available by **Millennium Development Goals indicators (2014)**, approximate contribution of anthropogenic emission of CO_2 by various countries is as follows- European Union (~4000 t), United Kingdom (~571 t), Canada (450 t), United States of America (5826 t), Japan (1095 t), Australia (330 t). Sequestration of CO_2 is also known as "Carbon capture". It is a technique for the longterm storage of CO_2 or their related form to either mitigate or adjourn global warming and circumvent dangerous climate shift. It has been provided as a way to slow down accumulation of GWGs in atmospheric and marine ecosystems, which is released by natural and anthropogenic activities. Although technologies have been developed for utilizing CO_2 as a chemical feedstock, but still at an industrial level CO_2 utilization is limited. Very few industries can utilize CO_2 for production of different chemicals such as urea (~70 Mt CO_2/year), inorganic carbonates and pigments (~30 Mt CO_2/year), methanol (~6 Mt CO_2/year), salicylic acid (~20 kt CO_2/year) and propylene carbonate (a few kt CO_2/year) (**Jajesniak et al., 2014**). On the contrary, photosynthetic organisms fix around 100 Gt of carbon into biomass annually (**Field et al., 1998**).

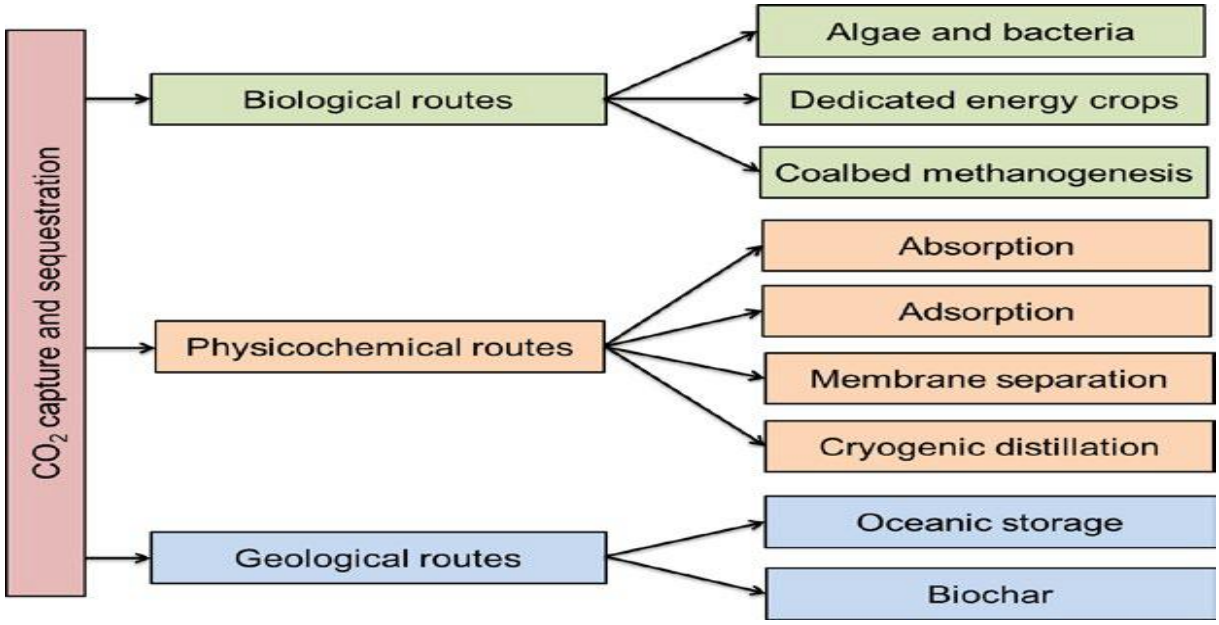

Figure.2.1 Different Routes of carbon capture and sequestration (Adapted from Nanda et al., 2016).

2.1.1 Terrestrial CO2 sequestration

Carbon (C) is an indispensable element for sustaining life on the planet. Naturally it can be found in organic and inorganic forms with a very small rate of exchange between these two forms (**Schnitzer, 1991**). At around 18% (about 50% on a dry basis), the concentration of C in living matter is almost 100 times greater than the average concentration of C in the earth (0.19%). Thus, for sustainability of life on the planet, recycling of C is must. Photoautotroph use light energy of the sun and convert atmospheric CO_2 to organic matter by photosynthesis. This C is returned back to the atmosphere from fixed organic matter as CO_2 by respiration, combustion, and decay (**Shively et al., 2001**). Thus it is a continuous process through which atmospheric CO_2 is utilized naturally through photosynthesis and stored as organic matter in biomass and soils. For thousands of years, this cycle remained in balance, and the CO_2 concentration in the atmosphere remained fairly constant. However, in the last 100 years or so, fossil fuel burning, deforestation, changes is land use pattern, and other factors have disturbed this natural balance, consequentially increasing atmospheric CO_2 concentration (**Sheikh et al., 2014**). There is global concern that rising levels of GWGs in the atmosphere, predominantly CO_2, are contributor in

global climate shift. Atmospheric CO_2 concentration has increased significantly from preindustrial levels of 280 ppm to 384 ppm and recently 408 ppm (**CO2 earth, 2017**).

2.1.2 Biological CO_2 sequestration

Biological sequestration or biosequestration is the process of capturing and storage of the atmospheric greenhouse gases such as CO_2 by biological processes. This process may be enhanced by increasing photosynthesis through practices like reforestation, preventing deforestation and genetic modification. Some other methods include, enhanced soil carbon trapping in agriculture fields or by the use of microorganisms, which can utilize CO2 emitted from natural as well as anthropogenic activities (**Fowles, 2007; Elbakidze and McCarl, 2007**). Biological based CO_2 trapping methods are another prospective way for improvement in CO2 capture technology that includes algae, bacteria, cyanobacteria and archaea. The concept of these systems is based on the natural tendency of living organisms to react with atmospheric CO_2. The important enzymes involved in the process such as RuBisCO, phosphoribulokinase (PRK), CA which help and facilitate the sequestration of CO_2 by organism (**Figueroa et al., 2008; Bharti et al., 2014b**). Inorganic compounds are utilized by the chemolithoautotrophic bacteria as electron donors for energy requirement and growth. They are categorized into two major groups based on their electron donors: Obligate lithotrophs, which includes hydrogen, sulphide, sulphur, metal, ammonia, nitrite oxidizing bacteria and facultative lithotrophic bacteria such as CO-oxidizer (**Saini et al., 2011**). Soil microorganisms chemolithoautotrophically sequester the CO_2 and play significant role in removal of GWGsby Calvin-Benson-Bassham (CBB) cycle which helps in reducing global warming and subsequent climate change (**Videmšek et al., 2009**). However, some chemolithotrophic bacteria such as Epsilonproteo bacteria have been accounted to follow the reductive tricarboxylic acid pathway for fixation and assimilation of CO_2 (**Campbell et al., 2006**). The key enzyme involved in the CBB cycle is RuBisCO. CA is reported as facilitator of CO_2 towards active sites of RuBisCO (**Bharti et al., 2014b**). Both enzymes are important for CO_2 sequestration. CA performs the catalysis of hydration reaction of CO_2 is present in most living organisms including autotrophs and heterotrophs (**Smith and Ferry, 2000**). Other supportive enzymes involved in CO_2 sequestration pathway are PRK, phosphoenolpyruvate carboxylase, phosphoenolpyruvate carboxykinase, phosphoenolpyruvate carboxy-transfer

enzyme, pyruvate carboxylase, malic enzyme and isocitrate dehydrogenase (**Zhang et al., 2011; Bharti et al., 2014b**).

2.1.3 Carbon dioxide sequestrating chemoautotrophic microorganism

Living organisms able to assimilate CO_2 are not only restricted to photosynthetic organisms viz. plants, algae, cyanobacteria but there are many CO_2-assimilating bacteria and archaea, such as green nonsulfur bacteria, deinococci, methanococcus, thermococcus (**Matter et al., 2016; Kumar et al., 2017b**). Many of the known prokaryotic chemolithotrophic microbes use the inorganic carbon as a source of energy in absence of light by fixing inorganic carbon for their growth and survival. Fixation of inorganic carbon by chemolithotrophes has been an important phenomena performed by microbes under extreme environmental conditions such as hydrothermal vents, chemocline of anoxic marine basins and sediments (**Noble et al., 2012; Kumar et al., 2017b**). It is believed that chemoautotrophy carbon fixation in costal marine sediments is reasonably minor process due to the relatively lower microbial biomass yield and favourable condition for chemical oxidation reactions. Besides that, true chemoautotrophs have to vie with mixotrophs and heterotrophs, which are proficient to oxidize reduced sulphur compounds, significantly available in active coastal marine sediments accumulating huge amounts of organic substances (**Noble et al., 2012**). However, current research recommends that up to 0.29 Pg C y−1 could be potentially fixed by chemoautotrophic microorganisms in near shore and shelf sediments globally compared to 0.92 Pg C y−1 of total mineralized carbon, signifying a major role of chemolithotrophic microbes to run the sediment carbon cycle (**Hillebrand et al., 2016**). A recent report predicted, a group of unculture Gammaproteobacteria play vital role in reoxidation phenomenon that takes place in costal marine sediments (**Moreira and Pires, 2016**). Research effort on chemoautotrophic bacteria has been started to gaining attention, which could be further potentially transferred to industrial-level bioprocesses, due to small generation time (doubling time) and easy to handle. Chemoautotrophic microbial communities from diverse ecological niches are concurrent to sediment type or geographic region, mainly reliant upon site-specific geochemical and physical conditions (**Bharti et al., 2014b; Srivastava et al., 2015a**). Natural assemblages of chemoautotrophic bacterial communities react to increasing CO_2 levels by modified their community structure, changes in their functional ranges, and shifted biomass measurements. Aerobic prokaryotes require an input

of energy and reducing equivalents for assimilation of CO_2 into organic carbon whereas anaerobic prokaryotes often use low-potential sources as reducing equivalents (**Hicks et al., 2017**). The application of microbial technologies at industrial scale, still it is a challenging approach for production of desired materials, due to its inherent characteristics such as, growth pattern, types of metabolites produce, thermal-stability and tolerance to inhibitors. The application of genetic engineering and enabling technology make it possible to apply microbes as a promising candidate for production of chemicals and biomaterials at industrial level. Chemoautotrophic microorganism, capable to assimilates CO_2 are found in a wide range of ecological niches, ranging from environments with low, moderate to environments with extreme conditions (**Bose and Satyanarayana, 2017; Kumar et al., 2017b**).

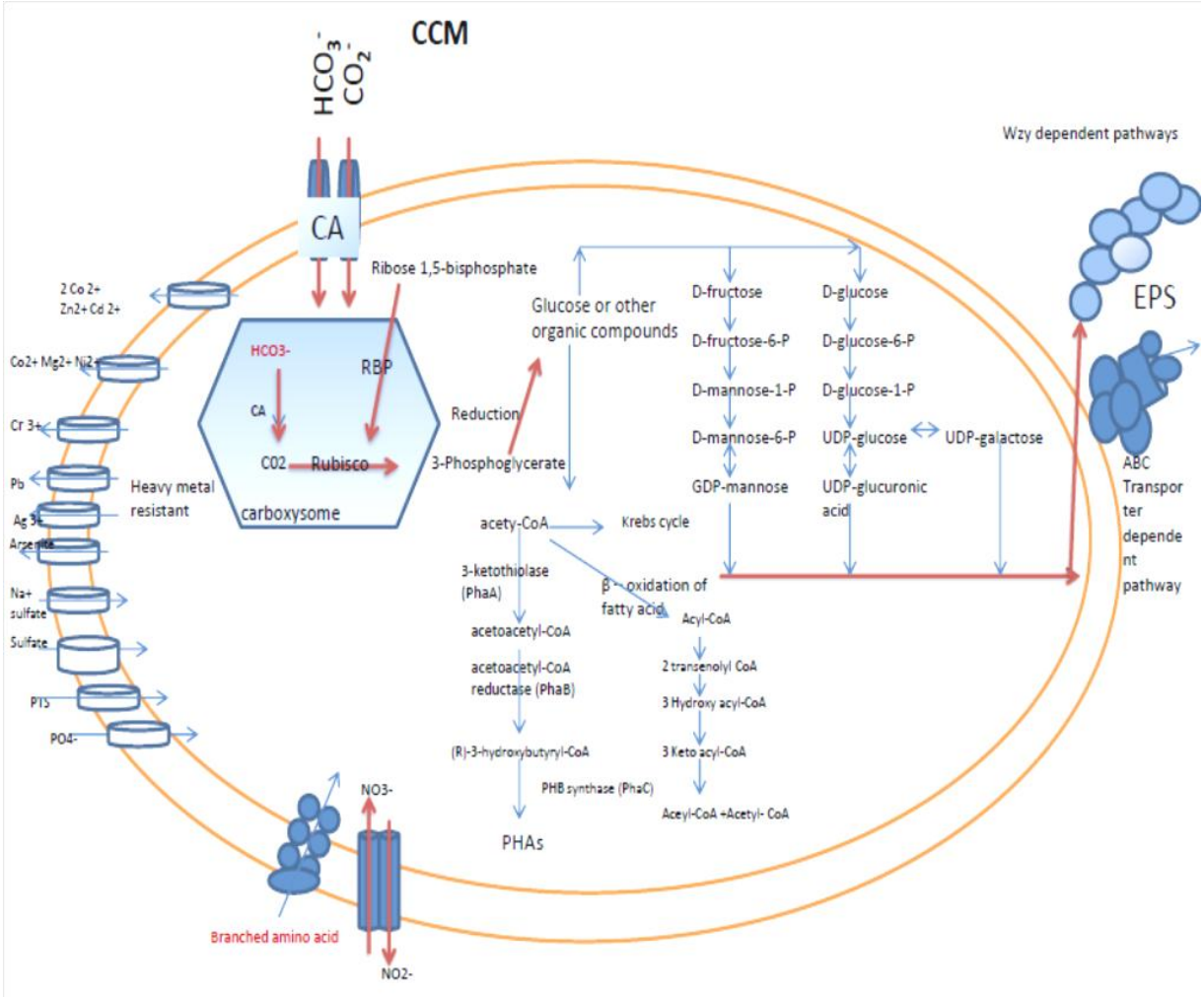

Fig. 2.2 Schematic representation of physiological features of CO_2 concentrating bacteria.

2.2 Development of carbon concentrating mechanism

2.7 billion years back, cyanobacteria was the only oxygenic photosynthetic microorganism existing on the earth (**Buick, 1992**). During that time the gaseous composition was changing in the environment where CO_2 has turned down and O_2 ascended. This phenomenon has forced evolutionary pressure on existing cyanobacteria to evolve tactics for efficiently utilizing inorganic C for photosynthesis. In environmental response to this they have acquired an effective photosynthetic CO_2 concentrating mechanism (CCM) for convalescing the carboxylation reaction by their comparatively bungling RuBisCO (**Badger and Price, 1992**). This CCM is possibly the most effective mechanism present in CO_2 fixing organisms, which can concentrate CO_2 up to 1000-times in the region of the active site of RuBisCO (**Sawaya et al., 2006**). According to **Karlsson et al. (1998)**, when green alga, *Chlamydomonas* reinhardtii, and several other green algae and CO2 fixing microbes were exposed to lower Ci (inorganic carbon) levels (in solutions equilibrated with ambient air containing 0.035% CO_2, for instance), a Ci-concentrating mechanism is encouraged to actively supply CO_2 to RuBisCO. Thus, CCM is a multi-module CO_2 concentrating machinery of cyanobacteria and many other chemoautotrophic bacteria that recompenses for low levels of accessible Ci and deprived CO_2 fixation kinetics (**Kerfeld et al., 2010**). The essential module of the CCM is the carboxysome, a bacterial micro component (BMC) that co-requisite RuBisCO and CA (**Yeates et al., 2008**). Bacteria that contain carboxysomes are generally found in environments with CO2 concentrations lower than the Michaelis constant (K_M) for CO_2 of RuBisCO. To fulfill their desire of C, microbes rely on CCM that gathers within the cytosolic pool of Ci, essentially in the form of bicarbonate, at many times the extracellular concentration (**Kim et al., 2012**). However, RuBisCO is unable to utilize bicarbonate but it rather utilizes CO_2. It is scientifically proven that co-sequestration of bicarbonate with the help CA, rapidly converts cytosolic bicarbonate to CO_2 within the carboxysome. This efficiently increases the confined steady state CO_2 levels well above the KM of RuBisCO and allows the enzyme to perform their function at a fully saturated state (**Cannon et al., 2010**). The enzyme CA, which is involved in the catalysis of both the dehydration of bicarbonate to CO_2 and its hydration to bicarbonate play an important role in CCM (**Cannon et al., 2010**). The conversion of accumulated cytosolic pool of bicarbonate into CO2 within the carboxysome has been performed by CA (**Bharti et al., 2014b**). Probably the protein shell

imposed a diffusive restriction to the efflux of generated CO2 from the carboxysome resulting in the localized increment of CO_2 around the active site of RuBisCO within the carboxysome (**Sawaya et al., 2006**). Number of active CO_2 and bicarbonate transporters plays an important role in accumulation of bicarbonate in the cytosol and this bicarbonate acts as a substrate for the carboxysome (**Badger and Price, 2003**).

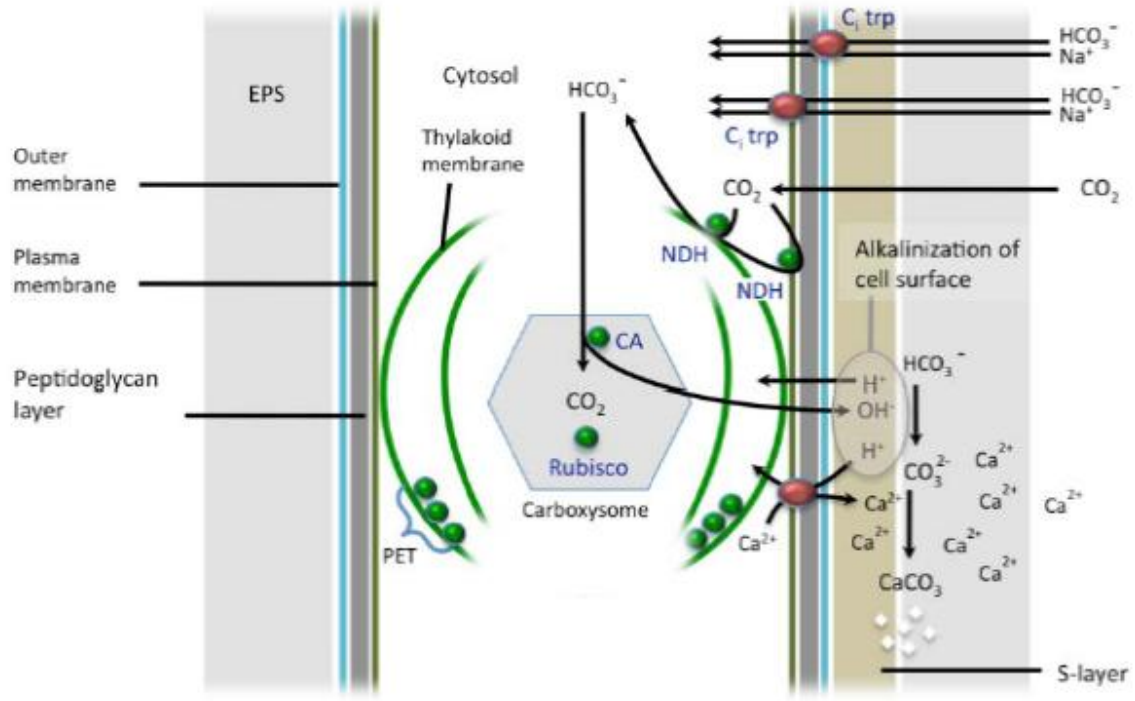

Figure.2.3 Schematic representation CCM and microbial precipitation of calcite (Adapted from Riding, 2006).

The role of EPS is very imperative in microbial precipitation of carbonate through diverse mechanisms (**Arp et al., 1999; Défarge, 2011; Trichet and Défarge, 1995**). For example, anionic component of the EPS can attract cationic metals ions such as Ca^{2+} and Mg^{2+} and as result trigger the carbonate formation. In contrast, by strongly bounded divalent cations the EPS can hamper carbonate formations. Also, carbonate precipitation if favored by EPS by creating heterogeneous microenvironment that supports metabolic growth of different microbial community by serving as carbon and energy supply for heterotrophic microbes (**Dupraz et al.,**

2004). The mineralogy of precipitated calcite crystals is highly influenced by characteristics of the EPS (**Kawaguchi and Decho, 2002**).

2.2.1 Carboxysomes

The earliest BMC (bacterial microcompartment) to be revealed was the carboxysome (**Shively et al., 1973**). Carboxysome is tightly packed molecular layer having hexameric units with diminutive pores size, which allow only smaller metabolites to passes through it such as bicarbonate, 3PGA, and 5RuBP (**Tsai et al., 2007**). It present in all cyanobacterial and several non-photosynthetic autotrophic bacterial species. Carboxysomes were first visualized by electron microscopy in 1961 as polyhedral structures intracellular in cyanobacteria and subsequently identified in chemoautotrophic bacteria (**Yeates et al., 2008**). Depending on species type and growth condition, approximately 5–20 of these icosahedral structures mainly present in individual microbes, measure 100 to 200 nm in diameter and visible per individual cell by transmission electron microscopy (**Cannon et al., 2010**). These organelles contain most of the cell's RuBisCO, which is the key enzyme, involve in CO_2-fixation process by CBB-cycle; hence the name called carboxysome (**Cannon et al., 2010**). The carboxysome is a bacterial organelle that encapsulates the enzymes to increase the CO_2 fixation efficiency (**Bharti et al., 2014b**). The outer layer of the carboxysome is evocative of a viral capsid and composed of many copies of very few small proteins. **Tsai et al., (2007**) described the structure of the carboxysomal outer shell protein CsoS1A from the chemoautotrophic bacterium Halothiobacillus neapolitanus. The CsoS1A protein forms hexameric units that packed tightly to form a molecular layer, perforated by narrow pores. Genome sequences of several cyanobacteria and chemoautotrophs became accessible during the pastdecade, the subsistence of two types of carboxysomes, differentiated on the basis of their protein composition, became manifested (**Badger and Price, 1992**). The α-type carboxysome is present in all chemoautotrophs. Cyanobacteria that having RuBisCO form IA, such as *Prochlorococcus* sp. and marine species of *Synechococcus* sp. Cyanobacteria that contain form IB RuBisCO, illustrated by well known species having β-carboxysomes such as *Synechocystis* PCC6803 and *Synechococcus* PCC7002 and PCC7942 (**Badger and price, 2003**). According to current scrutiny, bicarbonate enters the carboxysome and gets converted into CO2 by enzymatic activity of CA (**Cannon et al., 2010**). After that, RuBisCO catalyzes the generation reaction 3-phosphoglyceric acid (3PGA) with utilizing CO_2 and ribulose bisphosphate

(RuBP) as substrate inside the carboxysome. No other Calvin cycle enzymes are known to be encapsulated inside the carboxysome, so 3PGA is assumed to leave the carboxysome (**Tsai et al., 2007**).

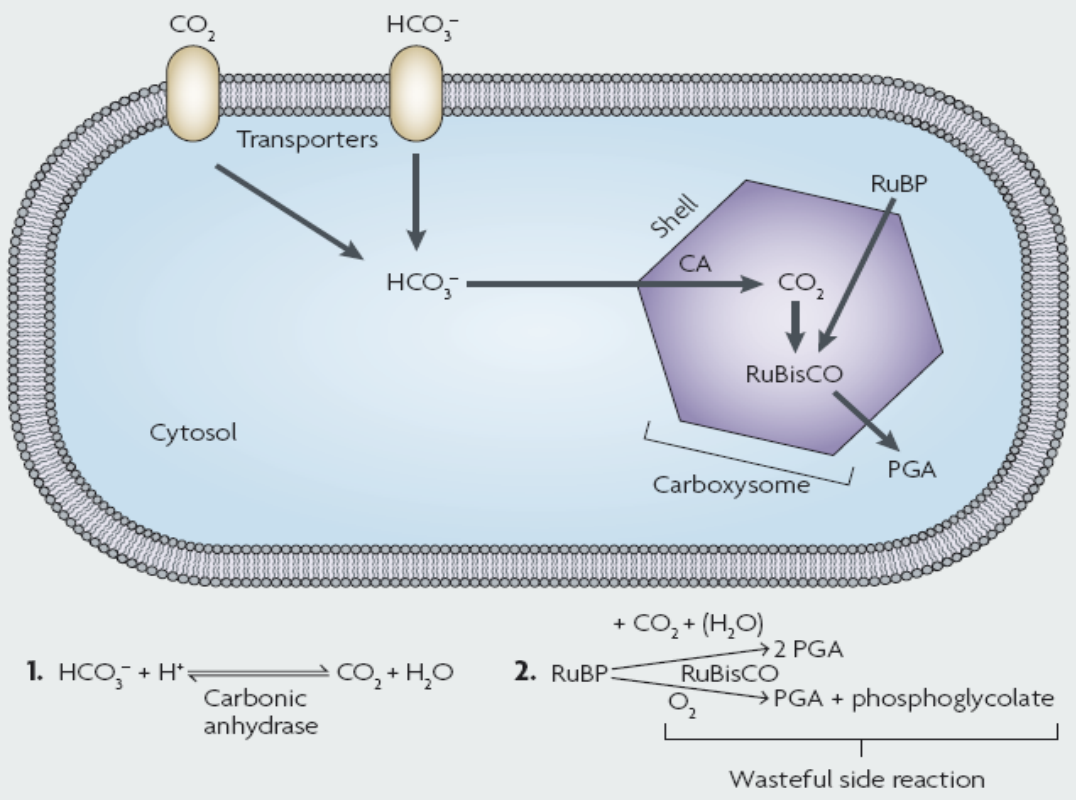

Fig.2.4 Carbon concentration and the carboxysome (Adapted fromYeates et al., 2008).

2.3 Carbon fixation pathways

Carbon fixation is the conversion of CO_2 to organic compounds by living organisms. Organisms which can utilize and fix carbon are called autotrophs. It is well documented that autotrophic organisms obtain C from CO_2. CO_2 assimilating microorganisms are ubiquitous in nature, widespread and belong to both archaeal and bacterial domains (**Wood, 1991; Saini et al., 2011**). Within archeal domain, they belong to phyla Euryarchaeota and Crenarchaeota. While among bacterial domain, they belong to the phyla Aquificae, Actinobacteria, Chloroflexi (green nonsulfur bacteria), Proteobacteria, Chlorobi, Firmicutes and Thermodesulfobacteria. Four pathways are well known by which autotrophic organisms fix CO_2 (**Thauer, 2007**).

Table.2.2 CO2 fixation pathways and theirs key enzymes in various organisms.

Carbon Fixation Pathways	**Alternate name**	**Organisms**	**Key enzymes**
1. Calvin-Benson-Bassham cycle (CCB)	Reductive pentose phosphate cycle	Plants, algae, cyanobacteria, proteobacteria mycobacteria	RuBisCO
2. Reductive tricarbocylic acid cycle (rTCA)	Reductive citric acid cycle/Reverse Krebs cycle/Arnon-Buchanon cycle	Proteobacteria, green sulfur bacteria, aquaficae bacteria	PEP carboxylase 2-Oxogluteratesynthase Isocitrate Dehydrogenase Pyruvate synthase
3. Wood-Ljungdahl pathway (W-L)	Reductive acetyl-CoA pathway	Euryarchaeota, proteobacteria, plantomycetes, spirochaetes	Formate dehydrogenase Carbon monoxide dehydrogenase(CODH) Formylmethanofuran Dehydrogenase(FMFD)
4. 3-Hydroxypropionate 4-hydroxybutyrate cycle (3HP-4HB)		Aerobic crenarcheota	Acetyl-CoA/Propionyl-CoA carboxylase
(A) Dicarboxylate 4-hydroxybutyrate cycle (DC-4HB)		Anaerobic crenarcheota	Pyruvate synthase PEP carboxylase
(B) 3-Hydroxypropionate bi-cycle (3-HP)	Fuchs-Holo cycle	Green non-sulfur bacteria	Acetyl-CoA carboxylase Propionyl-CoA carboxylase

2.3.1 Calvin cycle or Calvin-Benson-Bassham (CBB) cycle or reductive pentose pathway

The first autotrophic CO_2 fixation pathway was elucidated by Calvin about 50 years back in photoautotrophic organisms. Besides the photosynthetic eukaryotic organisms, numerous prokaryotic microorganisms have also been known to perform Calvin cycle for CO_2 fixation (**Saini et al., 2011**), and many more have been shown to at least harbor RuBisCO (**Bharti et al., 2014b**). It seems that the Calvin cycle is operated by purple nonsulfur bacteria (*Rhodobacter, Rhodospirillum, Rhodopseudomonas*) (**Paoli and Tabita, 1998**), and purple sulfur bacteria (*Chromatium*), cyanobacteria (*Synechococcus*, *Anacystis*, *Anabaena*) (Berberoglu et al., 2008), along with hydrogen bacteria (*Ralstonia, Hydrogenovibrio*) (**Hügler et al., 2003**) and other chemoautotrophs like *Thiobacillus* (**Atomi, 2002**). The Calvin cycle requires 13 enzymatic reactions (**Kumar et al., 2016a; Saini et al., 2011**). Among all the RuBisCO-mediated reactions, the one which can fix CO_2, require one molecule of RuBP, CO_2, and H_2O which gets converted into two molecules of 3-phosphoglycerate (3- PGA). The role of the other 12 reactions is to regenerate RuBP (**Berg, 2011**). Overall, after 3 molecules of CO_2 are fixed to 3 molecules of RuBP, 6 molecules of 3-PGA are formed. Out of six 3-PGA, five are used to regenerate 3 molecules of RuBP. The remaining single molecule of 3- PGA is further used in the biosynthesis of cellular material. Three enzymes can be considered unique to the Calvin cycle (**Saini et al., 2011; Berg, 2011**) which includes RuBisCO, PRK, and sedoheptulose bisphosphatase (SBPase). The activities of the other enzymes are shared with the gluconeogenesis pathway and the pentose phosphate cycle (**Atomi, 2002**).

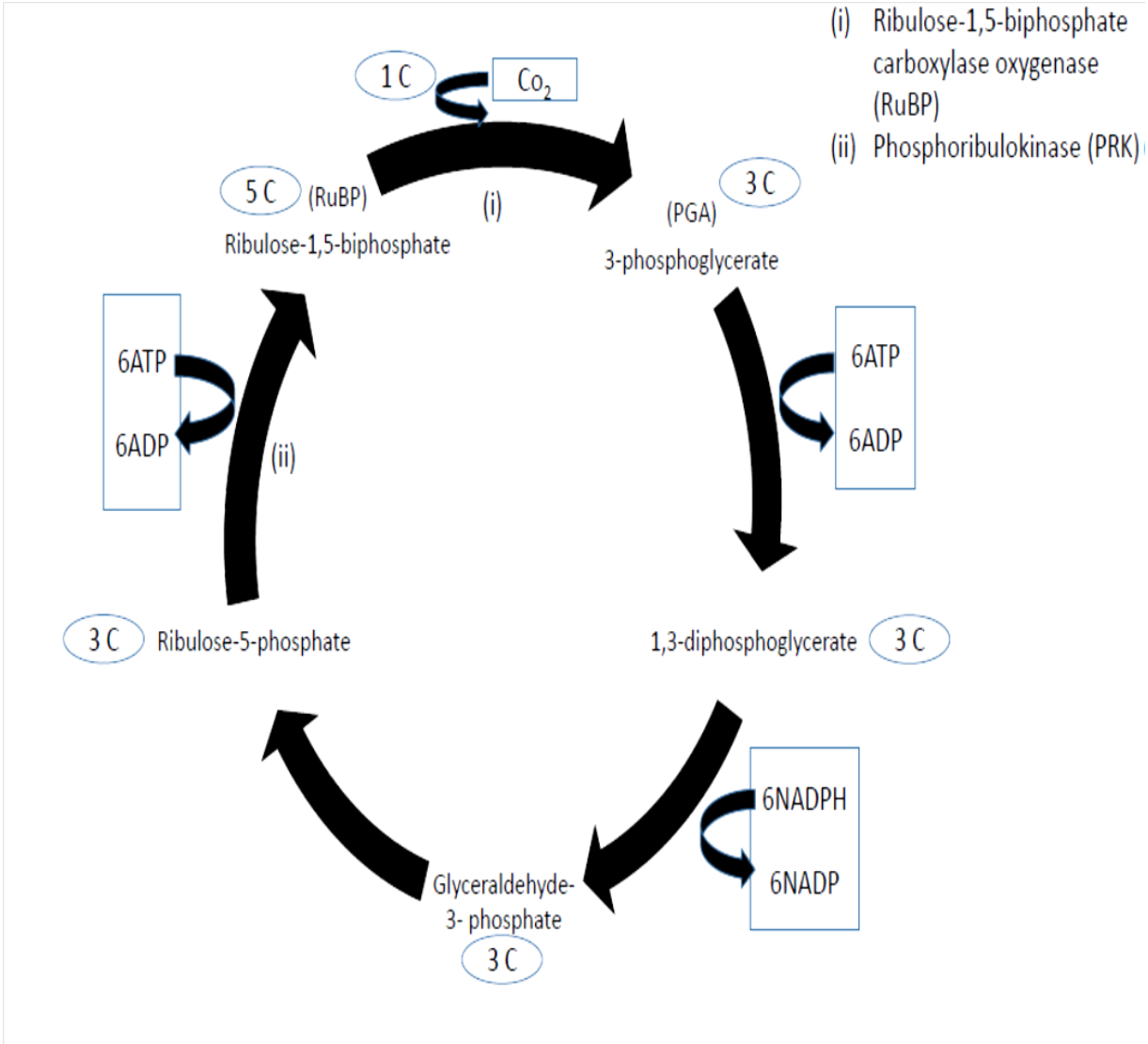

Fig.2.5 Representation of Calvin cycle or Calvin-Benson-Bassham (CBB) cycle or Reductive pentose pathway.

2.3.2 Reductive TCA cycle or reverse citric acid cycle

In 1966, a new autotrophic pathway i.e. Reductive TCA cycle was reported in green sulfur bacterium Chlorobium thiosulfatophilum (**Buchanan and Arnon, 1990**). As the name indicates, it is reverse of citric acid cycle and operates in reductive direction of TCA cycle. It is a cyclic pathway which can operates in bacterial and archaeal domains. Microorganisms present in extreme environments, such as high temperature, anaerobic conditions, acidic conditions, such as Crenarchaeota- *Thermoproteus* neutrophilus (**Schafer et al., 1986**) and *Pyrobaculum* islandicum

(**Hu and Holden, 2006**), *Hydrogenobacter* thermophilus (Shiba et al., 1985), Hydrogenobacter hydrogenophilus (**Hügler et al., 2007**), Thermocrinis rubber (**Hügler et al., 2007**) usually acquire different CO_2 fixation mechanisms. Reductive TCA pathway initiates with cleavage of citrate to acetyl-CoA and oxaloacetate by the action of enzyme ATP-citrate lyase (ACL), which is the key enzyme of this pathway. This pathway is one of the alternative pathway of Calvin cycle. Along with this pathway at present there are two more pathways, such as the reductive acetyl coenzyme A (CoA) pathway, and the 3- hydroxypropionate cycle (**Hugler, et al., 2005**).

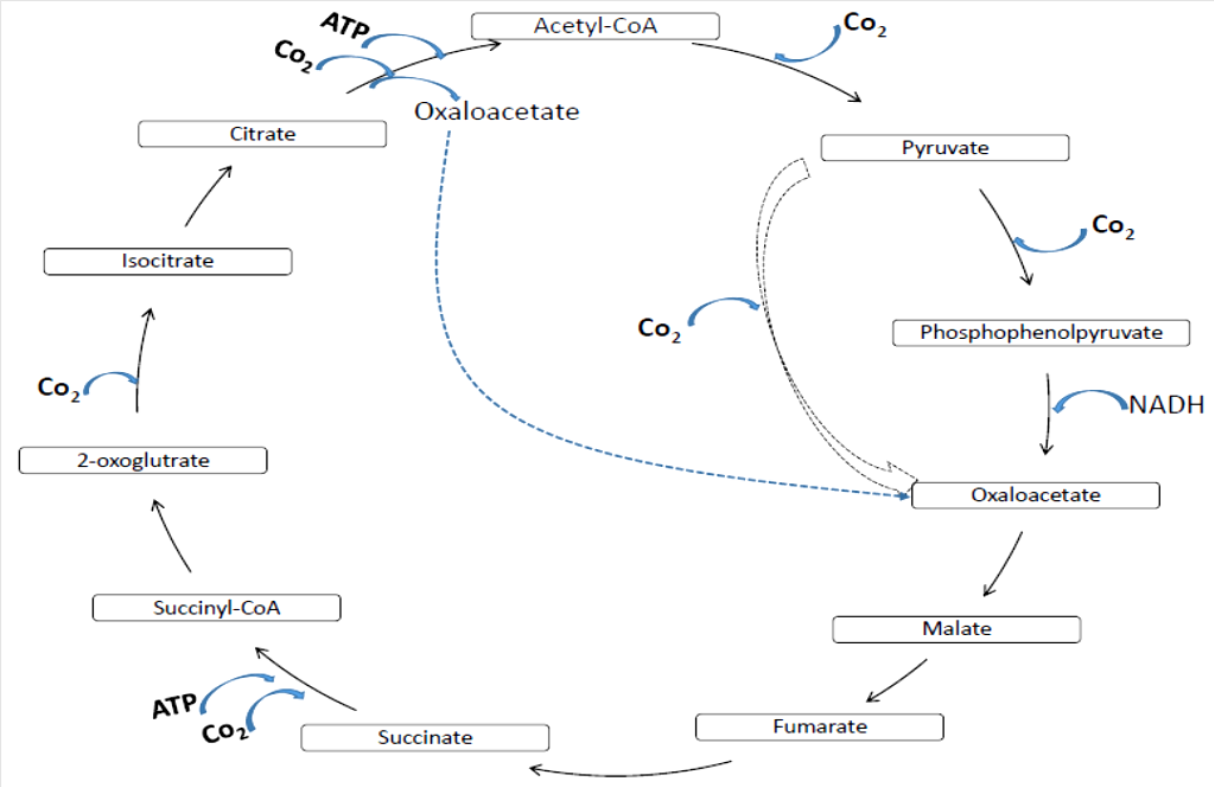

Fig.2.6 Representation of Reductive TCA cycle or reverse citric acid cycle.

2.3.3 Reductive acetyl CoA pathway or Wood-Ljungdahl pathway

Reductive acetyl CoA pathway is the third pathway for CO_2 fixation operates in many microbes. Using this pathway autotrophic acetogens and methanogens synthesize acetic acid and methane from CO_2 (**Ragsdale and Wood, 1985**). This cycle operates in strict anaerobic organisms which include some Proteobacteria, Planctomycetes, Spirochaetes and Euryarchaeota. The pure culture of *Clostridium* thermoaceticum was used as a representative organism to

explicate the mechanism of this pathway. Unlike other CO_2 fixing pathway, it does not rivet regeneration of the primary CO_2 acceptor (**Hu et al., 1982**). This pathway enables certain organisms to use hydrogen as a donor of electron and CO2 as an acceptor of electron as well as a building block for biosynthesis of cellular materials (**Berg et al., 2010**). It is initiated with the simultaneous oxidation-reduction of two molecules of CO_2. They enter the pathway through two unusual paths which were called as Western and Eastern branches of the pathway. The exact role of carbon monoxide dehydrogenase (CODH) in the reductive acetyl-CoA pathway was reported in 1985. CODH plays four crucial roles in the pathway such as oxidation of CO to CO_2, reduction of CO_2 to CO, formation of C-1 intermediate from CO and finally the synthesis of acetyl- CoA through condensing C-1 intermediate with methyl and CoA group (**Ragsdale and Wood, 1985**). The Eastern branch also called as methyl branch, reduces CO_2 to the methyl group of an acetate molecule. During reduction to methyl group CO_2 goes through many steps and each step involves the contribution of various enzymes and cofactors.

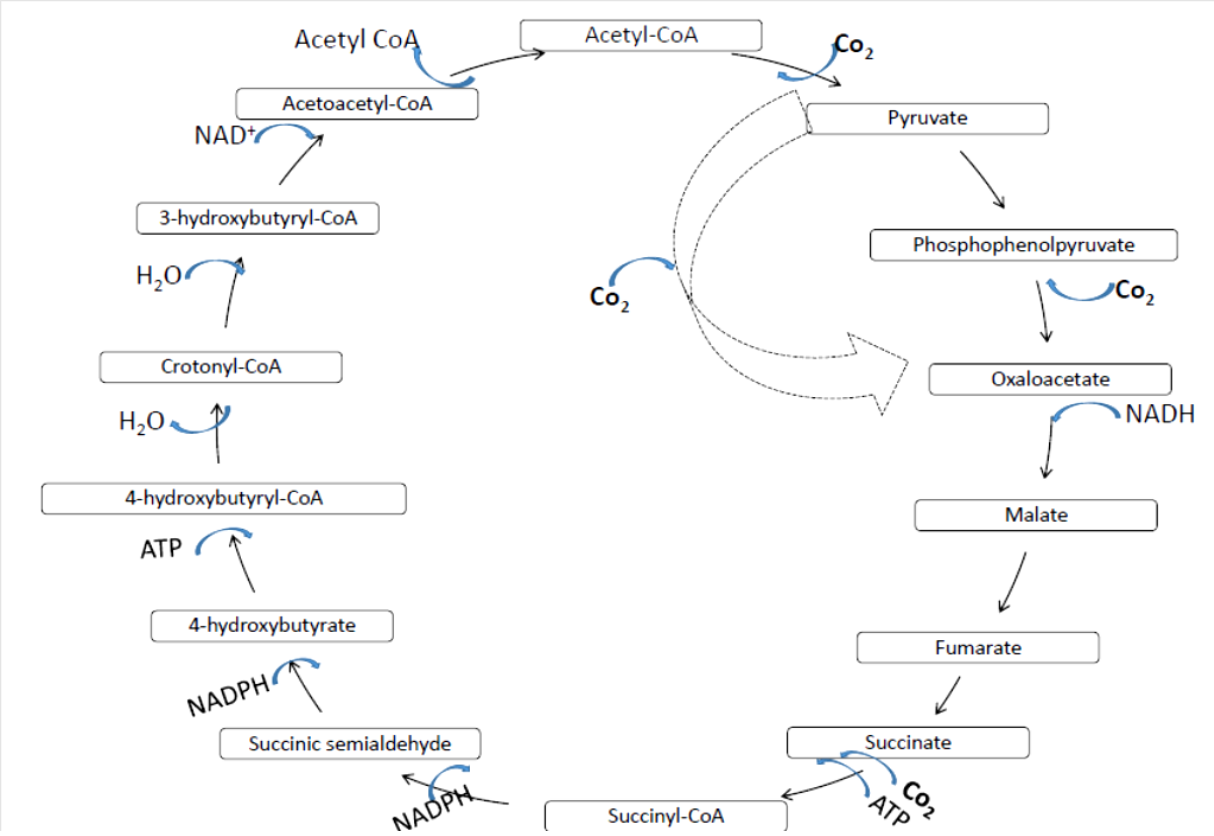

Fig.2.7 Representation of Reductive acetyl CoA pathway or Wood–Ljungdahl pathway**.**

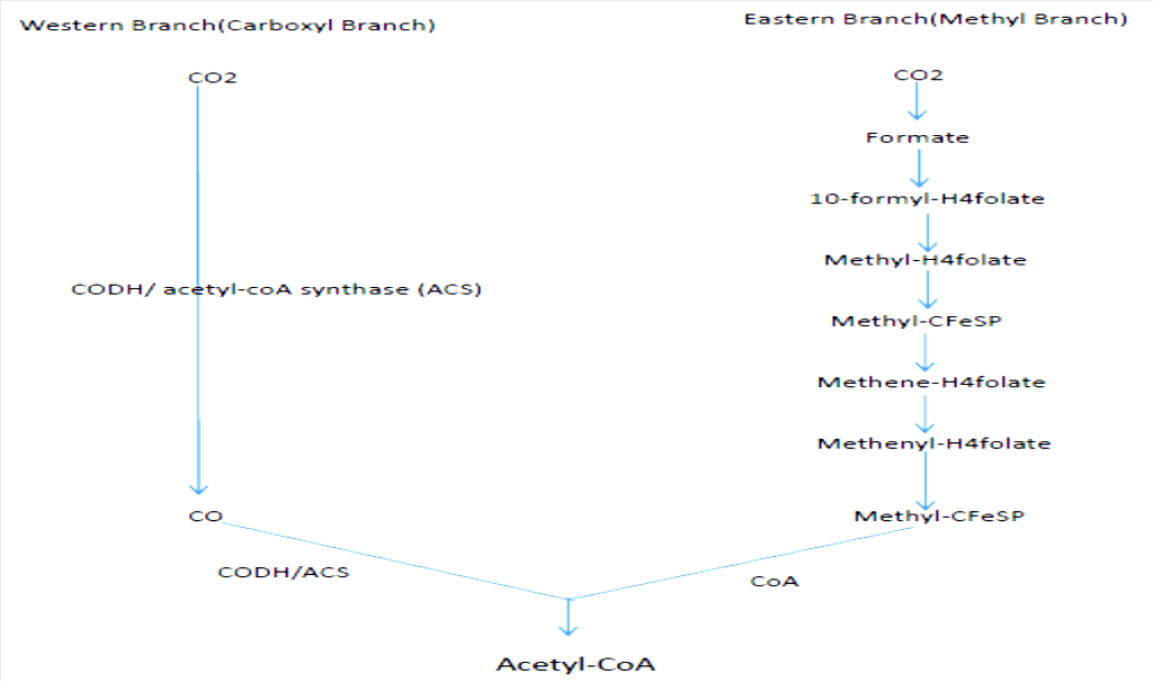

Fig.2.8 Representation of Dicarboxylate/4-hydroxybutyrate cycle.

2.3.4 3-hydroxypropionate cycle

The 3-hydroxypropionate bicycle is found in some green non-sulphur bacteria of the family Chloroflexaceae. This pathway has not been known to take place elsewhere, which makes this pathway a remarkable invention. The conversion of acetyl-CoA along with two bicarbonates to succinyl-CoA utilizes the same intermediates as in the hydroxypropionate– hydroxybutyrate cycle, but most of the enzymes are completely different. Furthermore, cleavage of malyl-CoA, regenerate acetyl-CoA and glyoxylate; this regenerated glyoxylate requires second cycle for its assimilation and therefore termed as bicycle (**Berg et al., 2010**). In the initial part, CO_2 fixation leads to the formation of glyoxylate and acetyl-CoA and the later on of this pathway involves the assimilation of glyoxylate, with propionyl-CoA, to ultimately form a dicarboxylic CoA ester, which is further cleaved to generate pyruvate and acetyl-CoA (**Hügler et al., 2003**). The acetyl-CoA formed in the later stage consents to stopping of the cycle with combining with initial part of the cycle, while the produced pyruvate acts as a precursor molecules for all subsequent metabolic reaction (**Tabita, 2009**).

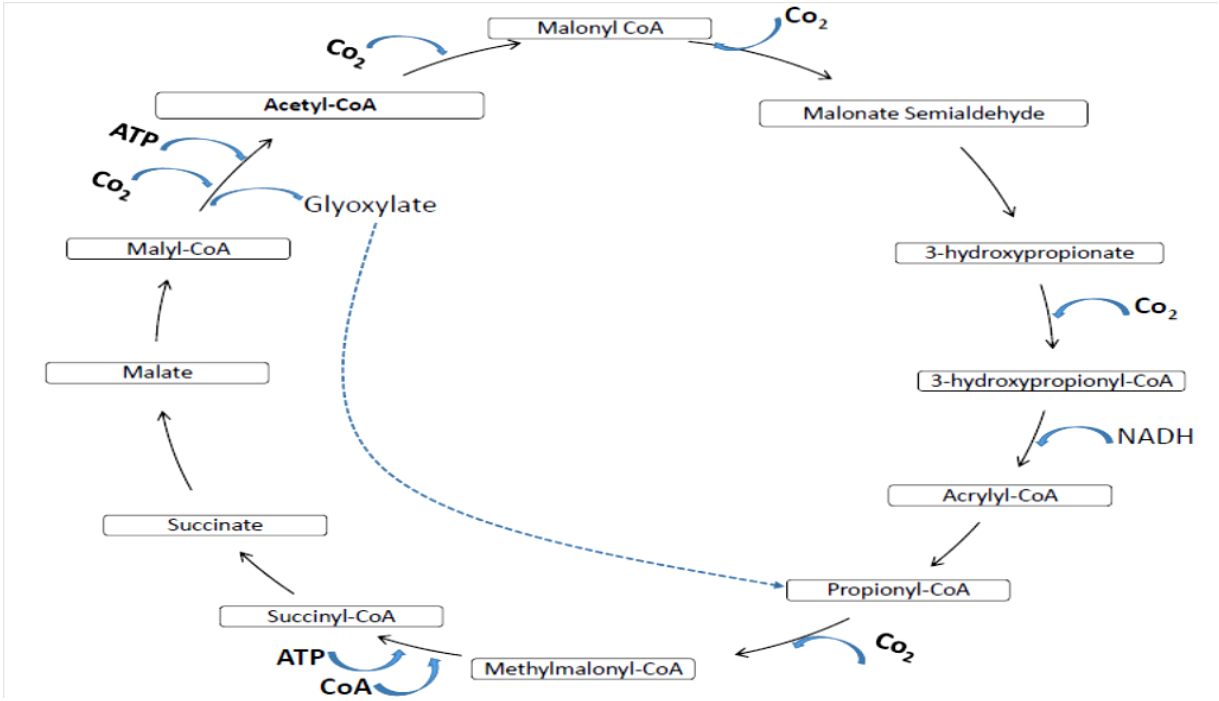

Fig.2.9 Representation of 3-Hydroxypropionate pathway/malyl-CoA pathway (3HP)**.**

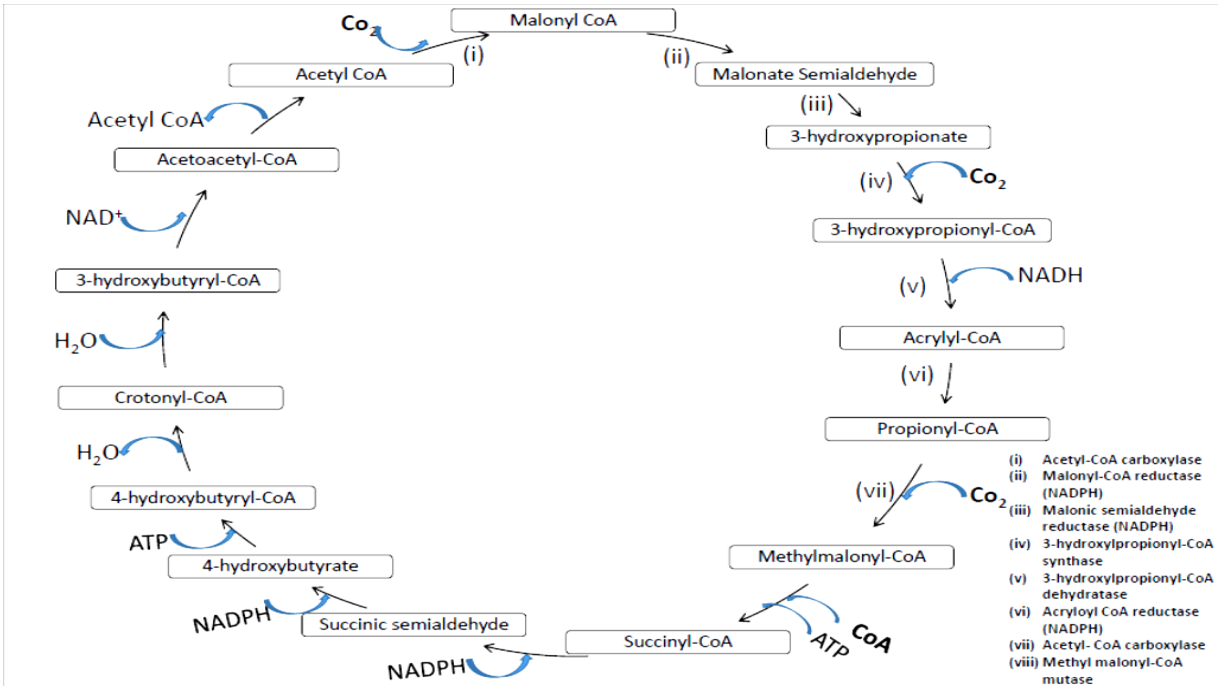

Fig.2.10 Representation of 3-Hydroxypropionate/4-hydroxybutyrate cycle.

2.4 Genomics investigation of carbon dioxide sequestration

Introduction of advance and sophisticated molecular techniques such as genomics, transcriptomics and proteomics and progresses made in instrumental advancement, open the platform to understand more about the complex microbial system. For bacteria, next generation sequencing (NGS) has become a popular practice. The accessibility of kits for construction of genomic library, quick and high quality sequencing, and well established data interpretation pipelines for genome re-sequencing and assembly, significantly make it a cost effective approach as well as better reliability of these generated results (**Vuyisich et al., 2014)**. The commercialization and utility of bacterial genome sequencing has led to further complex applications in the field of clinical and agricultural , outburst discovery and monitoring, human health sector, biocatalysis (**Vuyisich et al., 2014)**, environmental remediation **(Dunbar et al., 2012**). The progressively more accessible genomic, metabolomics and proteomic information about the phototrophic and chemotrophic microbes, open the scope of potential application of microbial community for sequestration of CO_2 along with production of value added biological materials and important enzymes (**Bharti et al., 2014b; Badger et al., 2006**). Rigorous investigation has been performed on genomic and proteomic analysis of CO2 sequestering microbes, which includes bacterial and archeal domains such as *Rhodospirillum rubrum* (**Harpel et al., 2002**), *Rhodobacter capsulatus* (**Horken and Tabita, 1999**) *Rhodobacter sphaeroides* (**Wang et al., 1993**), *Ralstonia eutropha* (*Alcaligenes eutrophus*) (**Hansen et al., 1999**), *Hydrogenovibrio* marinus (**Hayashi et al., 1999**), *Thiobacillus denitrificans* (**Hernandez et al., 1996**), *Anacystis* nidulans (**Bainbridge et al., 1998**), *Synechococcus* sp. *PCC6301* (**Newman and Gutteridge, 1994**), *Azospirillum thiophilum* (**Orlova1, et al., 2016),** *Pseudonocardia dioxanivorans CB1190* (**Grostern1 and Alvarez-Cohen1, 2013) *Cupriavidus* metallidurans Strain CH34** (**Janssen et al., 2010**), autotrophic *Acetogens* (**Shin et al., 2016**), *Thermococcus* kodakaraensis *KODI, Methanococcus* j*annaschii, Archaeoglobus fulgidus* (**Atomi, 2002)** and many more whose genome sequences have been published.

2.4 Biorefinery approach of CO_2 sequestration by bacteria for production of biomaterials

The promising bio-based cost-cutting measure is an emerging sector with notable future potential and provides many business prospects (**Luoma et al., 2011**); in this context it comprises the concept of biorefinery (**Clark et al., 2006**). There are many applied descriptions for biorefinery, but in common terms, utilization of renewable raw materials (biomass) for production of energy and broad range of daily use commodities in an cost effective and sustainable manner (**Li et al., 2010; Aresta et al., 2013; Gnansounou and Pandey, 2017**). The extensive use of fossil fuels such as oil, coal, and natural gas by modern society raises a question- how we can manage the natural resources and achieve the goal of sustainable development (**Venkata Mohan et al., 2016**). The biorefineries concurrently produce biofuels as well as biomaterials along with minimizing the environmental damage by utilizing the waste (**Venkata Mohan et al., 2014; Abraham et al., 2015**). Hydrocarbons and triacylglycerol are the major metabolic products of CO_2 sequestration in bacteria along with production of EPS, PHA and $CaCO_3$ (**Kumar et al., 2017b**). Bacteria synthesize fatty acids similar to plants, using acetyl-CoA with ATP as the source of energy and NADPH as the source of reducing equivalents. (**Schirmer et al., 2010**). It occurs in three step process, firstly fatty acid elongase elongates hexadecanoic acid to an even carbon number fatty acid, after that fatty acid reductase catalyzes and reduces the fatty acid to aldehydes and finally decarboxylation of the aldehyde is catalyzed by aldehyde decarboxylates to yield alkanes (**Messner and Sleytr, 1992**). It has been reported that odd carbon number alkanes are found in larger proportion as compared to even carbon number alkane in higher plants while they contain even carbon fatty acid as the major fatty acid components. In contrast, in some bacteria, equal proportion of even and odd carbon number alkanes has been reported, where even carbon fatty acids were predominant inside the bacteria (**Schirmer et al., 2010**). As the decarboxylation pathway does not passably explain this mechanism, we are forced to think about the occurrence of another alkane biosynthesis pathway in the bacteria (**Wang and Lu, 2013**).

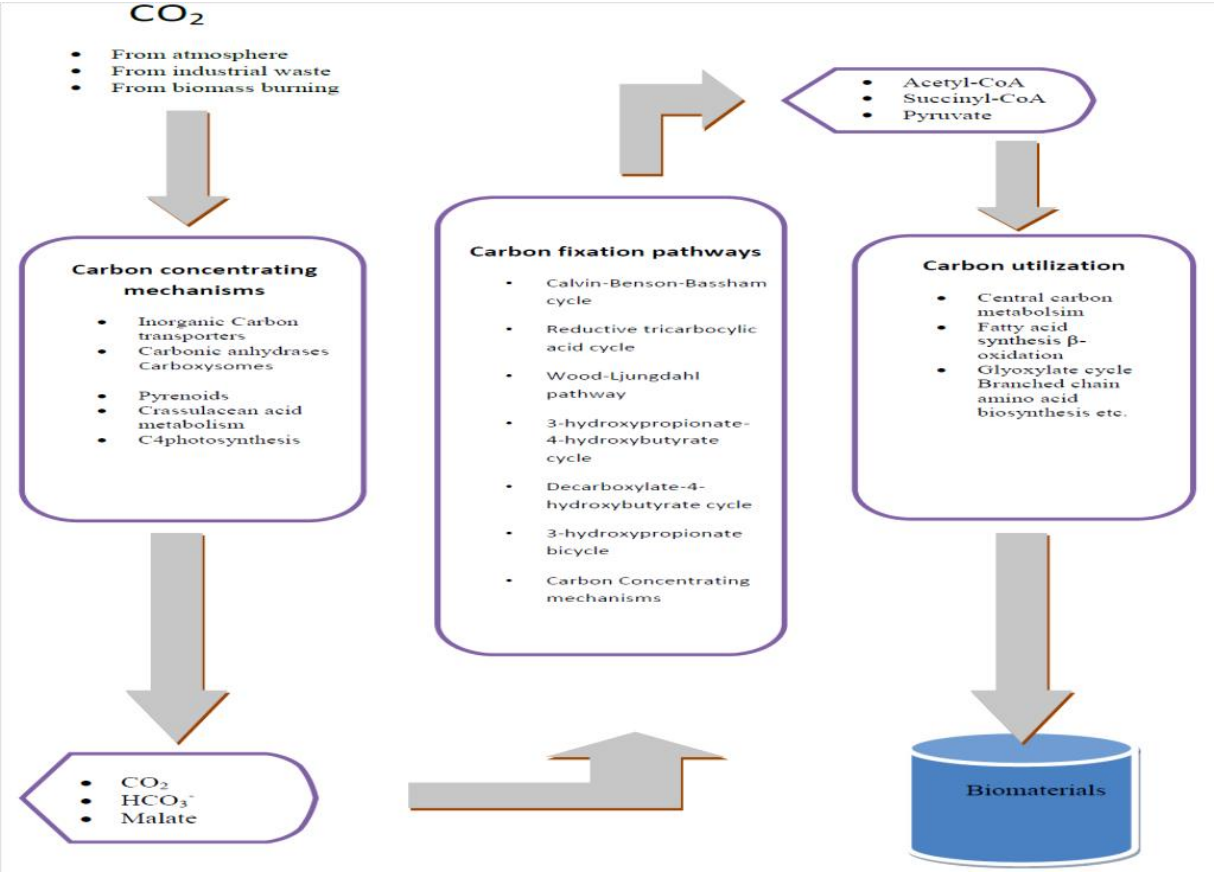

Fig.2.11 Carbon sequestering mechanisms, overall carbon dioxide fixation pathways and mode of carbon utilization in diverse autotrophic organisms, for production of biomaterials.

2.4.1 Production of biofuels

To reduced emission of greenhouse gases, biofuel with carbon capture and storage (BECCS) technology is an upcoming greenhouse gas mitigation strategy which produces negative CO_2 emissions. Typically the name biofuel itself represent the liquid fuels, such as ethanol and biodiesel that are used as substitute of fuels like petroleum, diesel and jet fuel (**Singh and Thakur, 2015; Tripathi et al., 2015**). Biofuels also comprise solid and gaseous fuels like wood pellets and biogas or syngas respectively. Production methodology of biofuel includes chemical, biochemical and thermochemical conversion practices. Chemolithotrophic bacteria can accumulate up to 2–60% of lipids of dry bacterial biomass and it is the major biomolecules of cell biomass. Fatty acids and triglyceride are the main component of microbial oils and lipids, which can further transesterified into alcoholic esters that's why this process is centre of

attention (**Bharti et al., 2014a**). It is manifested that extracting the lipid from chemoautotrophic bacteria is a challenging job because of it is high energy-intensive, lower biomass yield and the cost involve in scale up the production processes. The improvement in chemical and physical technology for the extraction and purification of the lipids from dry bacterial biomass is providing a cost effective alternatives for production of biofuel from chemoautotrophic bacteria. The fundamental chemistry involve in biodiesel production is quite simple and generally occurs via transestrification of triglyceride (lipid) with a mono-alcohol such as, ethanol or methanol in the presence of acid or base as catalyst (**Kumar et al., 2017a; Madhavan et al., 2017**). The most general method practice in production of biodiesel is alkali catalyzed transestrification; as a result, the converted product is fatty acid methyl esters (FAMEs) and glycerol. When the raw materials (oils) contains large amount of free fatty acids (FFAs), uses of acid catalysts are the preferable option, in which FFAs are simultaneously esterified and transesterified into FAMEs (**Kumar et al., 2016c**). Sulphuric acid, hydrochloric acid, boron trifluoride, phosphoric acid and sulfonic acids were the first used as homogenous catalyst for transesterification of lipids (**Ma and Hannab, 1999**). In recent times, heterogeneous catalysts are becoming more striking option, due to their good adsorbability, easy to handle, regenerability, minimal operational cost and its ample use in a continuous reactor. So far, heterogeneous solid catalysts including zeolites, silica molecular sieves doped with metals, such as aluminium, titanium, sulphated zirconia, tungstated zircon, sulfonated tin oxide, Amberlyst-15,75 and Nafion NR50 have been used (**Madhuvilakku and Shakkthivel, 2013**). Use of intracellular as well as extracellular lipase as a biological catalyst is again one of the alternative of enzymatic diesel production, in both the cases (intra as well as extracellular lipase) biological catalyst were immobilized on solid support such as biochar or activated charcoal (**Khosla et al., 2017; Singh et al., 2015**). These techniques are highly proficient as compared to use of free enzymes, because its reduced the steps involve in downstream processes and recycling operations (**Khosla et al., 2017**). Very few information available principally, which can relate the production of lipids from chemolithotrophic bacteria (**Kumar et al., 2017c**). CO_2 concentrating chemolithotrophic Serratia sp. ISTD04, produced 466 mg extracellular lipids/L of bacterial culture filtrate and 64.7% intracellular lipids of dry bacterial biomass (**Bharti et al., 2014a,b**)**.** For production of good quality biodiesel, the constituent of fatty acid plays an imperative role. Higher content of saturated fatty acid in biodiesel than unsaturated fatty acid is problematic during winter season, due to jamming of fuel

injector pipeline but simultaneously, it offers elevated oxidation reliability and improved energy efficiency of the fuel (**Knothe, 2008; Kumar et al., 2016c**). For production of fatty acid-derived biofuel R. eutropha has been engineered as model organism, provided CO2 and H2 as the only carbon source and electron donor, respectively in chemolithotrophic growth media (**Müller et al., 2013**). In has been reported that, in genetically modified R. eutropha, electrochemically generated formate from CO_2, used as carbon source produce isobutanol and 3-methyl-1-butanol which can further use as biofuel (**Li et al., 2012**). For production of useful metabolites such as, ethanol, acetate, acetone, lactate, butanol, 2,3-butanediol, valeroate, caproate, carpylate *Clostridium* sp. follow different rout and utilize various carbon sources such as, simple and complex carbohydrates, CO_2/H_2 and CO. (**Tracy et al., 2012; Sillers et al., 2008; Yu et al., 2012**). Archaea reside in extreme environment, such as high temperature (thermophiles and hyperthermophiles) or low temperature (psychrophiles), acidic condition (acidophiles), saline environment (halophiles) and anaerobic condition (methanogens). Methanogenes, which can use CO_2 or CO and $HCOO^-$ as carbon source and H_2 as energy source for production of methane, such as *hydrogenotrophic* methanogens, *Methanothermobacter* thermautotrophicus, *Methanothermobacter* marburgensis, *Methanobrevibacter* aboriphilus, *Methanocaldococcus* jannaschii, *Methanosarcina* barkeri (**Hu et al., 1982; Henstra et al., 2007**)**.** These assemblages of microbes provide an opportunity for production of non-conventional energy along with source of robust thermostable enzymes which can be further significantly use in industrial CO_2 capture, such as CA (**Bose and Satyanarayana, 2017**). The discovery of novel archaeal isolates and the advancement in genetic engineering tools, archaea would undoubtedly unparallel producer of wide range of products in gas fermentation processes. Production of bioalcohols have principally reported in *Rhodobacter* and *Synechococcus* by utilizing CO_2 as carbon source (**Connor and Atsumi, 2010; Hanai et al., 2007**). In recent year, production of isopropanol is achievable biologically which can be used as moderately substitute of gasoline, also propylene is dehydrated product of Isopropanol, which can be further used in preparation of polypropylene, which is called as plastics (**Hanai et al., 2007**). In current years with the help of microbial technology, advanced generation biofuels, such as isobutanol and n-butanol are able to produced (**Kolodziej and Scheib, 2014**). Further isobutanol is readily transformed through well-known processes to wide range of hydrocarbons such as, isobutylene and paraxylene.

2.4.2 Production of biopolymers and bioplastic

Rising level of greenhouse gases (GHGs) such as CO_2, methane nitrous oxide (N_2O, chloroflorocarbons (CFCs) leading to climate shift. Simultaneously accumulation of non-degradables substances such as plastics, pesticides triggers environmental degradation. The production of petroleum-derived plastics has been increasing globally 299 million tons in 2013, which was 3.9% higher than 2012 (**Yan et al., 2006; Kumar et al., 2016d**). Polyhydroxyalkanotes (PHAs) is biological polymers having characteristics such as, biodegradable, biocompatible and thermostable. It is stored as intracellular reserve materials in diverse group of organism, preferably when carbon source is excess and nutrient condition is limiting in media (**Gupta et al., 2017; Kumar et al., 2018**). Accumulation of PHA in microbes is one of the endurance tactics to avoid pressure exerted by environment on the microbes inhabiting in various ecological niches, such as marine sediments, microbial mats, rhizosphere, marbles mine and in the artificial ecosystems (**Kumar et al., 2017c**). R. eutropha store PHAs within its cytoplasm as source of carbon commonly known as bio-plastics (**Yu, 2014**). PHA granules usually consist of short chains of poly 3-hydroxybutyrate (PHB) and poly 3-hydroxybutyrate-co-3-hydroxyvalerate (PHBV) (**Kumar et al., 2016e**). With the help of genetic engineering technology considerable research has been carried out to produce PHA copolymers that reveal improved mechanical strength than PHB using wide varieties of carbon sources such as, glucose, fructose, plant oils and sodium bicarbonate (**Kumar et al., 2017c**). *Ideonella* sp. is reported to store PHA intracellular from captured inorganic carbon, similarly *Serratia* sp. ISTD04 use sodium bicarbonate as carbon source and produced polyhydroxyvalerate (PHV) 48% of it dry biomass (**Yu, 2014; Kumar et al., 2016d**). A few products that can be derived from PHB, though chemical and enzymatic methods such as, (R)-3-hydroxybutyric acid (3HB), methyl ester of 3HB, crotonic acid, acetoacetic acid and 1,3- butanediol (**Yu, 2014; Tanaka et al., 2011**). A number of haloarchaeal genera have been able to produced PHA such as, Haloarcula, Haloferax, Halobiforma and Haloquadratum, (**Yu, 2014**). Purified PHA extracted from biological origins having properties similar to petroleum derived plastics polyproplylene like its biocompatibility, biodegradability and thermal stability, make this polymers as a commercially interested products.

2.4.3 Production of extracellular polymeric substances (EPS)

Bacteria participate in biomineralization of CO_2 by precipitating calcium carbonate, offer novel and self-sustaining strategies for point source carbon capture and sequestration. EPS is secretary product of microorganism secreted into the surrounding medium. The matrix of EPS mainly composed of different biochemicals such as carbohydrate and non-carbohydrate components that are secreted by microbes, during cell lysis or availability of carbon source in the medium (**More et al., 2014**). EPS can be produced by wide groups of organism like, archaea, bacteria and eukaryotes and its physiochemical and rheological characteristics change according to nutrient condition, temperature, pH of the media and type of microbes (**Shen et al., 2013; Gupta and Thakur, 2016**). Production of EPS is a very common feature of most of the Gramnegative bacteria such as *Rhizobium* sp. *Agrobacterium* sp., *Azoarcus* sp. *Zoogloea* sp., *Azotobacter* vinelandii, *Haemophilus* sp., *Xanthomonas* campestris, *Pseudomonas* sp. (**Gupta and Thakur, 2016**). Gram-positive bacteria have been investigated for production of EPS, such as *Leuconostoc* mesenteroides, *Lactobacillus* sp., *Streptococus* bovis (**Jiang, 2011**). Due to their uniqueness such its functionality, biocompatibility and biodegradability, these novel biomaterials have prospective relevance in many fields for illustration as cementing materials, fabrics, detergents, recovery of microbial oil, pharmaceutical, food additives, removal of metal in mining and treatment of waste (**Gupta and Thakur, 2016**). Microbial EPS participate and help the microorganism to overcome the environmental constraint such as limiting nutrient condition, elemental toxicity, food availability, energy scarcity which, act as shield for the microorganism surviving in adverse environment (**Kumar et al., 2017b**).

Table.2.3 Production of biofuels and bio-based materials by CO2 concentrating chemoautotrophic microorganisms.

Name of Products	Name of biomaterials	Organisms	References
Biofuel	Biodiesel	*Serratia* sp. ISTD04	Bharti et al., 2014a
	Biodiesel	*Ralstonia eutropha*	Bi et al., 2013
	Bioethanol	*Ralstonia eutropha* H16	Li et al., 2012
	Isobutanol and 3-methyl-1-butanol	*Ralstonia eutropha* H16	Li et al., 2012
	1-butanol	*Clostridium*	Yu et al 2012

	1-propanol,	*tyrobutyricum*	
	1-butanol, isobutanol, 2-methyl-1-butanol, and 3-methyl-1-butanol	*Clostridium acetobutylicum*	Sillers et al., 2008
	Biogas	*Methanothermobacter* sp.	Rittmann et al., 2015
	Bioelectrochemical	*Clostridium ljungdahlii, Methanosarcina barkeri*	ElMekawy et al., 2016
	Electromicrobial	*Ralstonia eutropha* H16	Li et al., 2012
Bioplastic	Polyhydroxybutarate	*Ralstonia eutropha*	Muller et al., 2013
	Polyhydroxyvalerate	*Serratia* sp. ISTD04	Kumar et al., 2016d
	Polyhydroxybutarate	Ideonella sp.	Tanaka et al., 2011
	Polyhydroxybutarate	*Haloarchaeal*	Yu et al., 2014
	Polyhydroxyalkanoates	*Serratia* sp. ISTVKR1	Gupta et al., 2017
Biosurfactants	Biosurfactants	*Bacillus* sp. strain ISTS2	Sundaram and Thakur, 2015
		Bacillus sp. SS105	Maheshwari et al., 2017
Bioflocculant	Exopolysaccharides	*Serratia* sp. ISTD04	Kumar et al. 2017b
	Exopolysaccharides	*Bacillus* sp. ISTVK1	Gupta and Thakur, 2016
Biochemicals	Methyl ketone	*Ralstonia eutropha*	Li et al., 2012
	succinyl-CoA, acetyl-CoA	Autotrophic archaea	Budde et al., 2011
	(R)-3-hydroxybutyric acid (3HB), methyl ester of 3HB, crotonic acid, acetoacetic acid and 1,3-butanediol	*Ralstonia eutropha* and anaerobic archae	Yu, 2014
Biocomposite materials	Calcite, aragonite and vaterite	*Serratia* sp. ISTD04	Srivastava et al., 2015a,b

2.4.4 Production of chemicals

With the advancement in the field of genetic engineering and protein engineering, biomaterials production from CO_2 sequestration by microbes has been comes out in the form of various products like acetone, isoprene, isobutyraldehyde, malic acid, salicylic acid etc. (**Lee et al., 2012**). 2.5-times increase in isoprene production is observed in cyanobacterium of *Synechocystis* genus, due to Heterologous genomic integration of the mevalonic acid pathway genes from *Enterococcus faecalis* and *Streptococcus pneumoniae* in *Synechocystis* genus, which previously expressing heterologous isoprene synthase (**Lindberg et al., 2010**). R eutropha also known as *Cupriavidus* necator is a Gram-negative, soil bacterium. It can be grown autotrophically, heterotrophically and mixotrophically, depending on the types of source of carbon in media. R. eutropha uses H_2 as sole energy source for fixation of CO_2 via the CBB cycle in the deficiency of organic substrates. In autotrophic CO_2 fixation CA has immense significance for enhancing the fixation besides that RuBisCO (**Brigham et al., 2010**). The occurrence of four CA genes in R. eutropha which are capable to capture CO_2 and employ it to produce valuable chemicals was evaluated after analysis of H16 genome sequence. Ferulic acid, the precursor biomolecule to vanillin biotransformation and 2-methylcitric acid are the other valuable materials that can be produced in considerable amount from genetically modified R. eutropha (**Brigham et al., 2012; Bi et al., 2013**). Although the important development in the numeral of impending biochemical produced by R. eutropha, majorly of the discussed methods use organic compounds as a carbon source instead of CO2 (**Fukui et al., 2002**) Using inorganic carbon $HCO3^-$ members of autotrophic archaea, like *Metallosphaera*, *Sulfolobus*, *Archaeoglobus*, and *Cenarchaeum* species, utilize CO2 via the 3-hydroxypropionate-4-hydroxybutyrate (3HP-4HB) cycle, to produce a succinyl-CoA, which is ultimately formed two molecules of acetyl-CoA via 4-HB cycle (**Budde et al., 2011; Huber et al., 2008**). Five genes, which are responsible for CO_2 fixation in archea Metallosphaera sedula was hetrologously expressed in hyperthermophilic archea *Pyrococcus furiosus* as a result, effectively integration of CO_2 into 3HP a key building block chemical (**Keller et al., 2013**).

2.4.5 Production of calcium carbonate

$CaCO_3$ is a vital mineral and ever-present in nature. Calcite, aragonite and vaterite are non-hydrated polymorphs of crystalline $CaCO_3$.Thermodynamically, most stable, metastable and unstable polyform of $CaCO_3$ includes calcite, aragonite and vaterite respectively (**Li et al., 2010**). Carbon capture and storage (CCS) is one of the mitigation strategies to reduce the emission of CO_2 from anthropogenic activities and enhances the energy saving technology to mitigate the climate change (**Sheikh et al., 2014**). Biomineralization of CO_2 by $CaCO_3$ precipitation is a fundamental component of global carbon cycle and takes place in marine, freshwater and terrestrial ecosystems. A number of microbial strains, which are able to calcify and precipitate calcite have been wildly distributed in the nature, such as several cyanobacteria, eukaryotic microalgae, *Bacillus* sp., *Serratia* sp. (**Barabesi et al., 2007; Bharti et al., 2014b**), *Pseudomonas* sp., *Vibrio* sp. and sulphate reducing bacteria but still its physiological function is mysterious (**Ercole et al., 2007**). Since calcium is a key secondary cellular messenger helping in signalling, it is vital that the cells manage the influx and outflux of calcium. Calcification may be the regulatory response of microbes. Bacterial cell wall (S-layer) acts as nucleation site for formation of $CaCO_3$, and was first reported in 1953 in *Spirillum* sp. After that S-layer was subsequently found in several other species of bacteria and archaea (**Messner and Sleytr, 1992**). In Bacillaceae, S-layers may perhaps delineate the periplasmic space and as a result, either delay or control the secretion of exoenzymes.

2.4.6 Preparation of Bioactive glasses and its cytotoxicological evaluation

Bone transplantation is often required to replace injured tissue due to any strain, ailment or osteoogenic disorder. By using the different medical practices, such as autografts, allografts or xenografts most of the bone related problems are resolve. Although these grafting techniques are very popular and give satisfactory results under certain conditions, still they have several limitations such as, accessibility of the material, availability of the donor, surgical problems along with highly prone to inducing contagious diseases amongst others **(Navarroa et al., 2004)**. Attributable to the several limitations of the biogenic grafts, the newly developed synthetic materials and their successfully application in bone grafting provide us an alternative to replace existing grafting technology. Such synthetic alternatives should be artificially prepared to

stimulate bone regeneration and provide support to the newly regenerated tissue. Overall two well known procedures have been applied in tissue engineering: the foremost consists in the expansion of 3-D scaffolds; to trigger the oozing of extra-cellular matrix and enhance the formation of tissue in vitro, seeding of cells are performed in vitro before the implantation. The second strategy is performed in vivo, to develop the perforated interconnected materials according to the competence of host osseous cells which leads to bone regeneration. In this contest, a number of materials, which include polymers and ceramics, have been projected for the improvement of these scaffolds (**Lawrencin et al., 1996; Hutmacher, 2000; Temenoff and Mikos, 2000; Dean-Mo, 1997**). Preparation of biological glasses based it chemical composition such as, calcium sodium silicate, calcium phosphate, calcium silicon phosphate should be an appealing option due to its biodegradability and biocompatibility for the embellishment of tissue engineering materials **(Navarro et al., 2004)**. Mammalian cell line based in-vitro assays (**Navarro et al., 2004**) have been employed for assessing the toxicity of biocomposite material. The use of cell lines for evaluation of cytotoxicity of the material, not only depicts the cellular response of the cell against the material, but also it precisely reduces the time, cost and resources required for experimentation. Cell line based assays will also help to understand the possible mechanism of action and biomarker can be identified when exposed to synthetic material.

2.4.7 Optimization of process parameters

For improving the performance of a system, a process, or a product in order to obtain the maximum benefit from it, determination of the optimum conditions is important. Traditional approach of optimizing one-variableat- a-time (OVAT) for a multivariable system is not only time and labor intensive but often results in missing out the interactive effects between the components (**Bandaru et al., 2006**). Response surface methodology (RSM) is a suitable multivariate statistical technique which not only assists in understanding the interactions of different variables and predicts maximized response, but also is rapid and economical with fewer experiments and minimal resource utilization (**Ghosh et al.,2014**) . Amongst the various RSM designs available, Box–Behnken design (BBD) has been found to be more efficient than the central composite and full factorial designs (**Ferreira et al., 2007**) and has been effectively applied for the optimization of various processes such as dye decolorization, degradation,

biosorption, enzyme, drug, PHA and biodiesel production (**Kumar et al., 2016c; Ghosh et al.,2014**).

Chapter 3:

Characterization of chemolithotrophic bacteria for sequestration of carbon dioxide by whole genome sequencing

3. Characterization of chemolithotrophic bacteria for sequestration of carbon dioxide by whole genome sequencing.

3.1 Introduction

Serratia belongs to genus of Gram-negative, rod-shaped, facultative anaerobic bacteria of the family Enterobacteriaceae. These microorganisms are ubiquitous in nature shows diverse range of habitats, which includes water, soil, plant rhizospher, diminutive mammals and humans (**Li et al., 2015**). Escherichia and Salmonella are also belongs to Enterobacteriaceae family, compare to these microbes there are comparatively very few genome sequence information have been documented. Literature survey shows that, only 17-genomic sequence analysis report of *Serratia* have been deposited to national center for biotechnological information (NCBI) (ftp://ftp.ncbi.nlm.nih.gov/genomes/Bacteria/): S. *marcescens* WW4 screened from paper machine (**Chung et at., 2013**), pathogenic S. *marcescens* Db11 isolated from drosophila, S. *marcescens* FGI 94 shows the association with leaf-cutter ant fungus garden (**Aylward et al., 2013**), S. *proteamaculans* 568 produces chitinase, which is revealed by genomic analysis (**Purushotham et al., 2012**), S. *liquefaciens* ATCC27592 and S. *fonticola* RB-25 screened and isolated from a landfill site (**Ee et al., 2014**), S. *plymuthica* strains AS13 associated with plant (**Neupane et al., 2012**), plant-growth-promoting (PGPR) activities performing strains such as, AS12, AS9, S13 and 4Rx13 and coexisting strain *Serratia symbiotica* Cinara cedri uid82363 shows the association with *B. aphidicola* in aphid (**Muller et al., 2013**). Apart from their opportunistic pathogenic behavior the genus *Serratia* is somewhat illustriously known for production of biomaterials such as, pigments like prodigiosin and pyrimine (**Li et al., 2015**), biosurfactants (**Matsuyama et al., 1986**), fatty acid (**Bharti et al., 2014a; Kumar et al., 2017b**), essences (alkyl-methoxypyrazines) (**Gallois and Grimont, 1985**), important enzymes (**Purushotham et al., 2012; Joshi et al., 1989**), polyhydroxyalkanotes (PHAs) (**Kumar et al., 2016d**).

Atmospheric carbon dioxide (CO_2) is foremost green house gas (GHG) present on the planet earth. Presence of low concentration of CO_2 in the atmosphere affects the substrate (CO_2) utilization efficiency of photosynthetic carbon assimilation by plants and microorganisms, such

as phototrophs and chemotrophes (**Price et al. 1998**). Autotrophic organisms can synthesize all forms of cellular materials exclusively from inorganic carbon. This phenomenon makes autotrophic organisms as essential driving force to run the global carbon cycle. In the global carbon cycle, heterotrophic organisms utilizes the organic carbon to build the cellular materials and again this organic carbon is converted in to inorganic carbon by oxidation and return back in the form of inorganic carbon, these processes makes global carbon cycle completed. To maintain the overall redox balance of the planet earth, continuation of CO_2 and O_2 concentration is the essential parameters in the atmosphere, which is regulated by the autotrophic and heterotrophic activities of the organisms (**Thakur et al., 2018; Kumar et al., 2017c**).

A number of microorganisms are adept to grow in lower concentration of CO_2 by making use of CO_2-concentrating mechanism (CCM). Many microorganisms such as, Cyanobacteria and chemolithototrophic bacteria has been develops CCM to maintain the inorganic carbon concentration in their cytoplasm higher than the surrounding (outside) inorganic carbon concentration. The site of CCM is carboxysomes, which is polyhedral proteinous micro-compartment (**Yeates et al. 2008; Price et al. 1998**). The micro-compartment of carboxysomes are mainly composed with CO_2-fixing enzyme, such as Ribulose- 1,5-bisphosphate carboxylase/oxygenase (RuBisCO) and carbonic anhydrase (CA). The CO_2 fixation potency of the RuBisCO is improved by co-localization of a specified CA that helps in catalyzing the dehydration reaction of the cytoplasmic bicarbonate and provides CO_2 as substrate at which the RuBisCO start acting (**Yeates et al. 2008; Murray et al. 2003**).

Considering all these facts *Serratia* sp. ISTD04 was isolated from marble mining rocks of the palaeoproterozoic metasediments of the Aravali Supergroup, Rajasthan, India, by enrichment in minimal salt media with $NaHCO_3$ as sole carbon source. In this study bacterium was characterized for chemolithotrophic fixation of carbon dioxide by whole genome sequence analysis using NGS platform. The bioinformatics studies were carried out to recognize the genesand pathways involve in sequestration of carbon dioxide along with production of biomaterials such as, fatty acid, PHA and EPS.

3.2 Materials and methods

Whole-genome shotgun sequencing of *Serratia* sp. strain ISTD04 was performed on the Illumina Miseq platform and resulted in 2,073,386 paired-end reads of 151-bp length. After filtering the raw reads using NGS tool kit (v2.3.1), high-quality 1,485,793 paired-end reads were obtained. The genome assembly was performed using Velvet (v1.2.10) (**Zerbino and Birney, 2008**), SOAPdenovo (**Xie et al., 2014**), and gsassembler using a k-mer value of 79 for primary assembly. SSPACE (**Boetzer et al., 2011**) was used to perform scaffolding of the primary assembled contigs that generated 120 scaffolds, with an N50 scaffold size of 1,03,262 bp. The maximum scaffold length was 3,28,633 bp and minimum scaffold length was 210 bp. The NCBI prokaryotic genome annotation pipeline (PGAP) was used for the identification of candidate gene models. Furthermore, Pfam (**Finn et al., 2014**) annotation was carried out to assign functional domains to the predicted gene models. The pathways and the genes involved were predicted with the help of the KEGG Automatic Annotation Server (KAAS) (**Moriya et al., 2007**). An assessment of genes of *Serratia* sp. strain ISTD04 with respect to its genome was carried out with the help of clicO FS (Circular Layout Interactive Converter Free Services). The genomic annotation and study of *Serratia* sp. ISTD04 genome was also executed by Rapid Annotations using Subsystems technology (RAST).

Gene Ontology (GO) search was carried out and the genes identified in genome have been categorized mainly into three functional domains such as, biological processes, cellular component and molecular functions with the help of Blast2GO (**Conesa et al., 2005**). To spot out the prospective contribution of the genes of *Serratia* sp. ISTD04 in biological pathways, genes were mapped to locate canonical pathways in Kyoto Encyclopedia of Genes and Genomes (KEGG) datasets. The outcome of KEGG analysis comprises KEGG Orthology (KO) assignments, their subsequent Enzyme commission (EC) numbers and genes involve in metabolic mechanisms with the help of KAAS (http://www.genome.jp/kaas-bin/kaas main) (**Moriya et al., 2007**). A total of 4,833 genes for *Serratia* sp. ISTD04 were used as input to KEGG-KAAS and genes engaged in various pathways were additionally categorized into 22 different functional pathways (**Kumar et al., 2016a**). The inclusive pipeline of whole genome sequencing and its analysis has been depicted in **Fig.3.1**

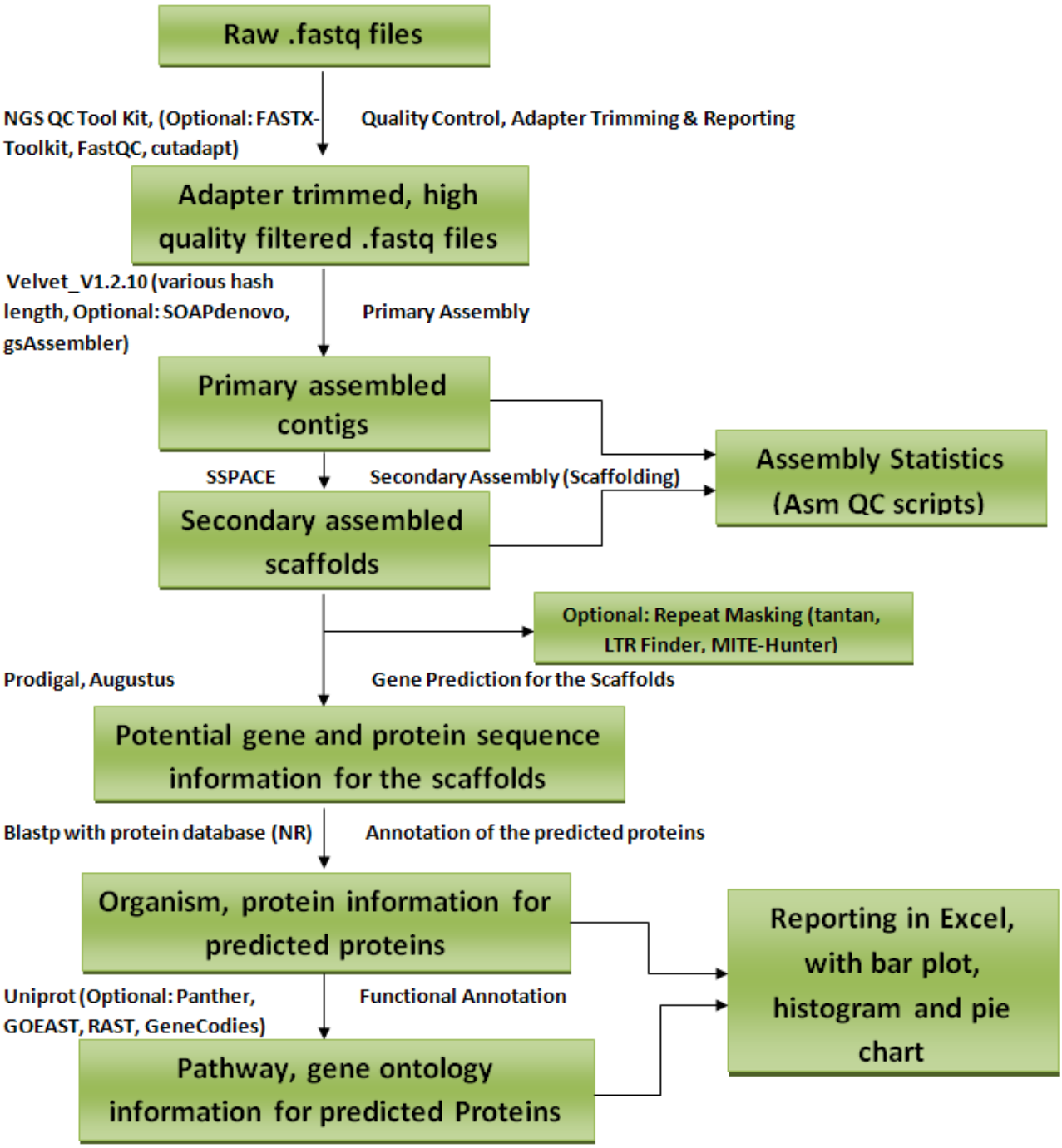

Fig. 3.1 Schematic representation of NGS sequencing and analysis pipeline followed in case of *Serratia* sp. ISTD04.

3.3 Results and Discussion

3.3.1 General Genomic Features of *Serratia* sp. ISTD04

The total genome size of *Serratia* sp. ISTD04 is 5.07 Mb and coverage of 81X was achieved. This whole-genome shotgun project has been deposited at DDBJ/ENA/GenBank under the accession number MBDW00000000.1. The size of genome of this genus deposited to NCBI is in the range of 4.8-6.3 Mb. The genome features for *Serratia* sp. ISTD04 have been depicted in **Table.3.1**. A Circular plot of genes presents a space efficient and clear cut illustration of inter-genic relatedness. Circos Plot showing arrangement of genes and on the genome of *Serratia* sp. ISTD04 is depicted in **Fig.3.2**. **Table.3.2** represent the important genes involve in various pathways such as Carbon dioxide sequestration**,** Fatty acid metabolism and PHA production, Carbohydrate metabolism and EPS production, Nitrogen assimilation and Degradation.

The G+C content in the genome of this strain is 59.98 % and a total of 4,563 protein coding genes were predicted by Prokaryotic Genome Annotation Pipeline (PGAP). The bacterium contained 75 tRNAs, 8 rRNAs (5S rRNAs, 4 16S rRNAs, and 2 of 23S rRNAs) and 12 noncoding RNAs (ncRNAs). In addition, 88 pseudo genes were predicted, among which were 6 frame-shifted pseudogenes. Using PGAP, 3,765 (82.51%) of the total predicted genes were annotated. In addition to that, Pfam annotation was assigned to 4,234 genes (92.78%) and 1,498 genes (32.82%) were predicted by the KAAS tool to be involved in various pathways (**Kumar et al., 2016a**). There were 561 hypothetical proteins were also predicted in the genome of *Serratia* sp. ISTD04 using Nr blast.

Table.3.1 General genome features of *Serratia* sp. ISTD04.

Total bases (genome)	5,069,140 bp
Total no. of scaffolds	120
Average scaffold size	42,242.833 bp
Scaffold N50	103,262 bp
Maximum scaffold size	328,633 bp
Minimum scaffold size	210 bp
G+C content	59.98%

Coverage percentage	81
Total bases (genes)	4,487,315 bp
Average Gene Length	928.474 bp
Gene N50	1,139 bp
Maximum Gene Length	10,016 bp
Minimum Gene Length	72 bp
Total No. of genes	4,833
Protein coding genes	4,563
Nr annotated genes	4,374
Pfam annotated gene	4,234
Hypothetical proteins	561
tRNAs	75
rRNAs	8
NcRNAs	12
Pseudogenes	88

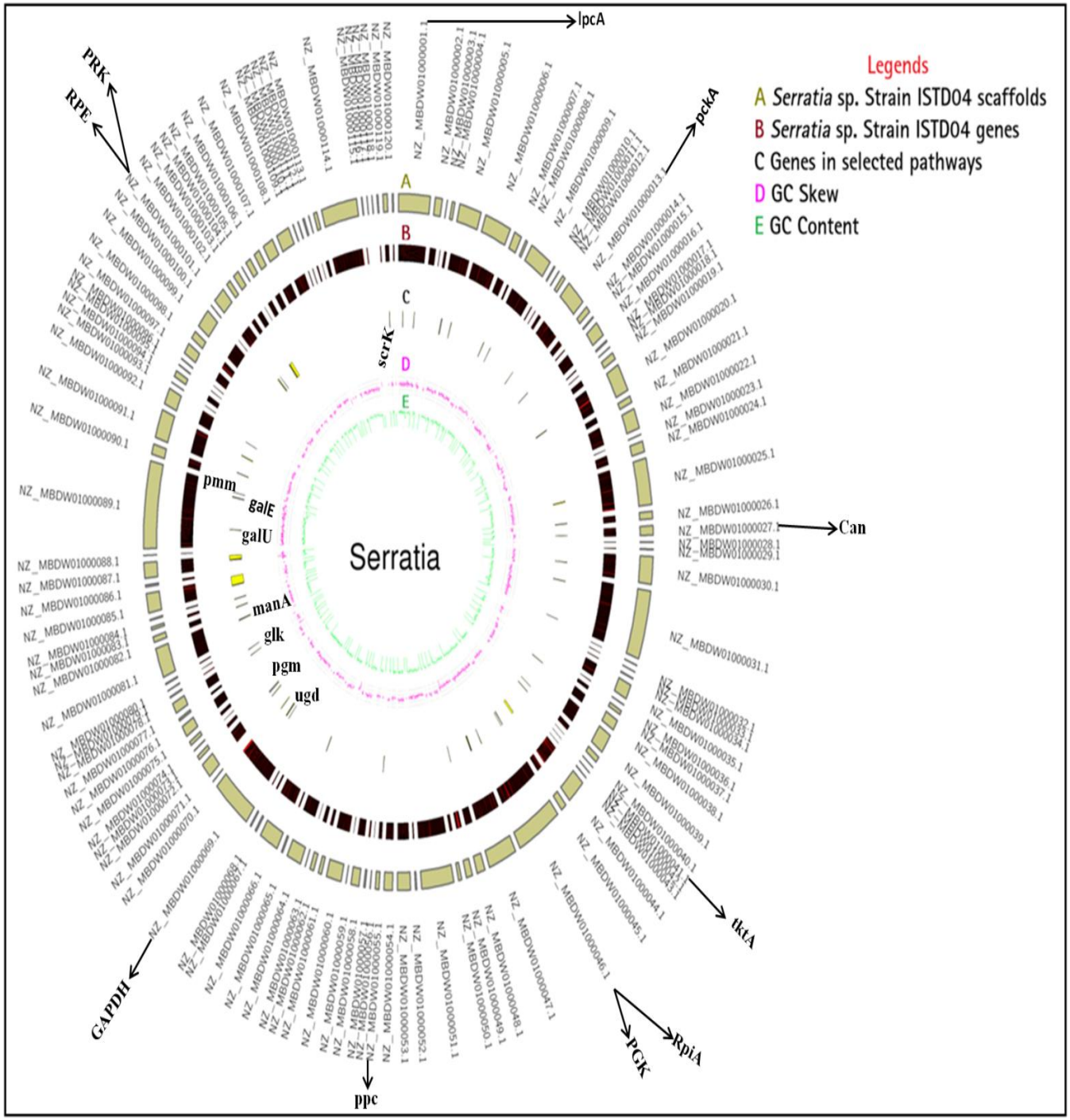

Fig.3.2 Circos Plot of genes compared with the genome for *Serratia* sp. ISTD04. Circles from outside to inside represent; (a) scaffold arrangement (b) gene position on the scaffolds (c) genes in selected pathways (d) GC skew and (e) GC content.

Table.3. 2 Important genes involve in various pathways represented on Circos plot.

Carbon dioxide sequestration pathway					
***Serratia* sp. ISTD04**	**Name of Enzyme**	**Start**	**End**	**Stand**	**Reference sequence**
NZ_MBDW01000101.1	Phosphoribulokinase (PRK)	39694	40563	-	RS21380
NZ_MBDW01000027.1	Carbonic anhydrase (can)	23602	24258	+	RS06440
NZ_MBDW01000046.1	Phosphoglycerate kinase (PGK)	15179	16342	+	RS09745
NZ_MBDW01000069.1	Glyceraldehyde 3-phosphate dehydrogenase (GAPDH)	84456	85451	-	RS15220
NZ_MBDW01000005.1	Triosephosphate isomerase (TPI)	23641	24408	+	RS01160
NZ_MBDW01000046.1	Fructose-bisphosphate aldolase, class II (FBA)	16459	17538	+	RS09750
NZ_MBDW01000082.1	Fructose-bisphosphate aldolase, class I (fbaB)	6003	7052	-	RS17235
NZ_MBDW01000047.1	Fructose-1,6-bisphosphatase I (FBP)	38661	39665	-	RS10880
NZ_MBDW01000005.1	Fructose-1,6-bisphosphatase II (glpX)	18250	19260	+	RS01130
NZ_MBDW01000041.1	Transketolase (tktA, tktB)	10	696	+	RS09165
NZ_MBDW01000001.1	D-sedoheptulose 7-phosphate isomerase (lpcA)	122540	123121	-	RS00600
NZ_MBDW01000101.1	Ribulose-phosphate 3-	15631	16308	+	RS21270

	epimerase (RPE)				
NZ_MBDW01000046.1	Ribose 5-phosphate isomerase A (rpiA)	27544	28200	+	RS09805
NZ_MBDW01000064.1	Malate dehydrogenase NADP+	58544	60823	-	RS14240
NZ_MBDW01000047.1	Malate dehydrogenase (mdh)	43398	44336	+	RS10905
NZ_MBDW01000055.1	Phosphoenolpyruvate carboxylase (ppc)	17173	18991	+	RS13175
NZ_MBDW01000013.1	Phosphoenolpyruvate carboxykinase (ATP) (pckA)	13332	14951	-	RS03190
Fatty acid metabolism and PHA biosynthesis pathway					
NZ_MBDW01000026.1	Pyruvate water dikinase (ppsA)	9718	12096	+	RS06255
NZ_MBDW01000083.1	Fumarate hydratase, class I (fumA, fumB)	6284	7930	-	RS17330
NZ_MBDW01000081.1	Fumarate hydratase, class II (fumC)	70762	72159	+	RS16995
NZ_MBDW01000071.1	Succinate dehydrogenase / fumarate reductase (sdhA,frdA)	35940	37706	+	RS15905
NZ_MBDW01000071.1	Succinyl-CoA synthetase alpha subunit (sucD)	44090	44962	+	RS15930
NZ_MBDW01000071.1	Succinyl-CoA synthetase beta subunit (sucC)	42924	44090	+	RS15925
NZ_MBDW01000038.1	Acetyl-CoA C-	14880	16064	-	RS08595

	acetyltransferase (atoB)				
NZ_MBDW01000009.1	Isocitrate dehydrogenase (IDH1, IDH2)	30228	31481	-	RS02625
NZ_MBDW01000069.1	Aconitate hydratase (acnA)	163283	165955	+	RS15605
NZ_MBDW01000046.1	Acetyl-CoA carboxylase carboxyl transferase (accA)	207558	208517	+	RS10595
NZ_MBDW01000030.1	Methylenetetrahydrofolate dehydrogenase (NADP) (fold)	59425	60291	+	RS06820
NZ_MBDW01000031.1	Phosphate acetyltransferase (pta)	36482	38641	-	RS07200
NZ_MBDW01000031.1	Acetate kinase (ackA)	258090	258980	+	RS07205
NZ_MBDW01000015.1	Acetyl-CoA synthetase (acs)	1	1485	+	RS03710
NZ_MBDW01000087.1	Acyl carrier protein (acpP)	34236	34472	-	RS17880
NZ_MBDW01000087.1	Acyl-carrier-protein S-malonyltransferase (fabD)	35373	36302	+	RS17890
NZ_MBDW01000087.1	3-oxoacyl-[acyl-carrier-protein] synthase III (fabH)	36321	37274	-	RS17895
NZ_MBDW01000040.1	3-oxoacyl-[acyl-carrier-protein] synthase I] (fabB)	10451	11671	-	RS09110
NZ_MBDW01000087.1	3-oxoacyl-[acyl-carrier-protein] synthase II (fabF)	32912	34153	-	RS17875
NZ_MBDW01000044.1	3-oxoacyl-[acyl-carrier protein] reductase (fabG)	78612	79361	-	RS09500
NZ_MBDW01000089.1	3-hydroxyacyl-[acyl-carrier protein] dehydratase (fabA)	94540	95058	+	RS18505

NZ_MBDW01000008.1	Trans-2-enoyl-CoA reductase (NAD+) (fabV)	6658	7857	+	RS02425
NZ_MBDW01000020.1	Long-chain acyl-CoA synthetase (fadD)	36370	37908	+	RS04395
NZ_MBDW01000077.1	Acetyl-CoA acyltransferase (fadA, fadI)	38084	39386	+	RS16620
NZ_MBDW01000048.1	3-hydroxyacyl-CoA dehydrogenase (fadB)	40082	41008	-	RS11400
NZ_MBDW01000069.1	Acetaldehyde dehydrogenase / alcohol dehydrogenase (adhE)	108698	111370	-	RS15350
Carbohydrate metabolism and EPS biosynthesis pathway					
NZ_MBDW01000077.1	Glucokinase (glk)	1446	2408	+	RS16415
NZ_MBDW01000071.1	Phosphoglucomutase (pgm)	11657	13300	+	RS15785
NZ_MBDW01000089.1	UTP--glucose-1-phosphate uridylyltransferase (galU, galF)	306139	307032	-	RS19360
NZ_MBDW01000089.1	UDP-glucose 4-epimerase (gale)	276794	277807	-	RS19280
NZ_MBDW01000069.1	UDPglucose 6-dehydrogenase (ugd)	104331	105674	+	RS15330
NZ_MBDW01000001.1	Fructokinase (scrK)	33986	34900	-	RS00160
NZ_MBDW01000081.1	Mannose-6-phosphate isomerase (manA)	68546	69724	-	RS16985
NZ_MBDW01000089.1	Phosphomannomutase (manB)	277998	279371	-	RS19285
NZ_MBDW01000089.1	Mannose-1-phosphate guanylyltransferase (manC)	279386	280810	-	RS19290

4,833 protein coding genes of *Serratia* sp. ISTD04 were used as input for KEGG-KAAS pathway analysis out of these, 2,326 genes were mainly categorized in to four processes such as, Metabolism, Cellular processes, Genetic information processing, Environmental information processing, further these genes were segregated in to 22 various functional pathway. The functional genes annotated by KEGG-KAAS pathway analysis mainly involve in carbohydrate metabolism, energy metabolism, amino acid metabolism, metabolism of cofactors and vitamins, membrane transport etc. The detail classification of KEGG pathway proteins are depicted in **Table.3.3**.

Table 3.3 Representation of proteins involve in various pathways, analyzed by KEGG-KAAS pathway analysis.

Pathway	**No of Proteins**
Metabolism	
Overview	228
Carbohydrate metabolism	271
Energy metabolism	139
Lipid metabolism	75
Nucleotide metabolism	108
Amino acid metabolism	250
Metabolism of other amino acids	76
Glycan biosynthesis and metabolism	50
Metabolism of cofactors and vitamins	183
Metabolism of terpenoids and polyketides	28

Pathway	No of Proteins
Biosynthesis of other secondary metabolites	34
Xenobiotics biodegradation and metabolism	43
Genetic Information Processing	
Transcription	4
Translation	86
Folding, sorting and degradation	52
Replication and repair	54
Environmental Information Processing	
Membrane transport	279
Signal transduction	139
Cellular Processes	
Transport and catabolism	11
Cell growth and death	18
Cellular community - prokaryotes	144
Cell motility	54

By using RAST annotation and analysis server 4689 coding genes were functionally annotated. Out of these, 58 % of coding genes have been further classified into 26 subsystems features. The distribution of functional proteins involve in various functional activities out of total classified proteins in subsystem has been shown in **Fig.3.3**. The subsystem features count illustrate overwhelming presence of proteins related to general process like, carbohydrate, amino acids and derivatives, cell wall components, prosthetics, cofactors and lipid metabolism. After

normal cellular processes the subsystem feature count is dominated by membrane transport, regulation and cell signaling, respiration and stress response. The sequestration of CO_2 by chemolithotrophic bacteria by CBB pathway is tightly regulated process, particularly RuBisCO is insufficient carboxylase, due to its appeal toward CO2, it also combines to O_2 (oxygenase activity) resulted photorespiration and redundant metabolites production (**Schwander et al., 2016**). This process hampered the activity of RuBisCO due to availability of higher concentration of O_2 in the environment than CO_2. To make this process effective, chemolithotrophes developed the CCM, which takes place in micro-compartment called carboxysome. Inorganic carbon (CO_2, HCO_3^-) entered via either CO_2 diffusion through the cellular membranes or the active transportation of HCO_3^- by using membrane pumps. The action of CA quickly converts HCO_3^- in to CO_2, which is subsequently utilized by RuBisCO (**Bose and Satyanarayana, 2017**). The dominance of these features such as membrane transporters, regulation and cell signaling, respiration and stress response along with existing cellular process and their complementary support indicate the ability of *Serratia* sp. ISTD04 to survive in the presence of HCO_3^- and utilize it, as source of CO_2 (**Bharti et al., 2014b**). The depiction of lipid, fatty acids isoprenoid, membrane transporters and carbohydrate metabolic genes in such a large number support the biomaterials such as fatty acids, PHA and EPS production ability of *Serratia* sp. ISTD04 (**Kumar et al., 2017b**).

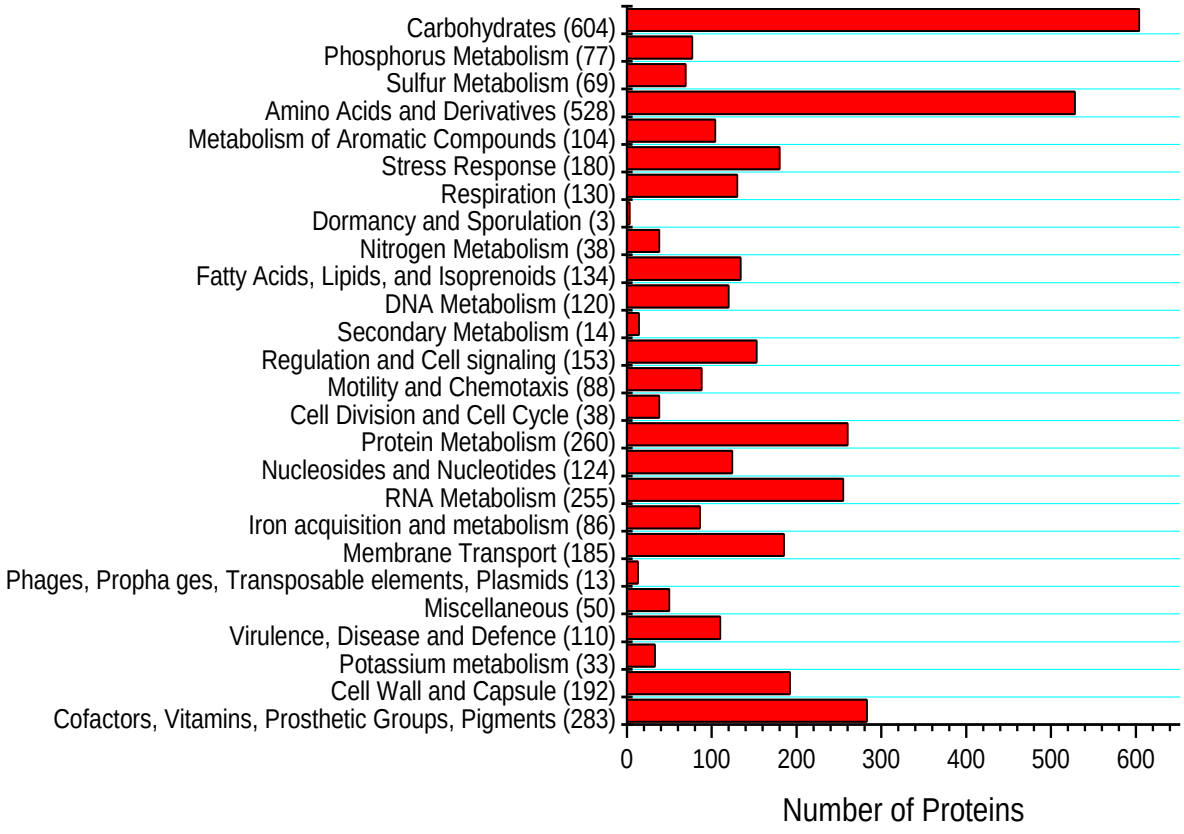

Fig.3.3 Classification of proteins in subsystem features using RAST analysis and annotation server and their abundance in different functional groups shown in *Serratia* sp. ISTD04.

3.3.2 GO analysis

Gene Ontology (GO) study was applied to do the functional characterization of the genome. This analysis revealed the functional contribution of genes and its involvement in metabolic processes, cellular functions and molecular components of the genome of *Serratia* sp. ISTD04 as shown in **Fig.3.4.** The analysis revealed that, the metabolic and cellular process was the overriding process of the genome in the biological processes. The studies of cellular components signify the contribution of membrane and membrane associated proteins. GO molecular functions analysis showed the major contribution of proteins into three imperative functions i.e. binding activity, transportation activity and catalytic activity.

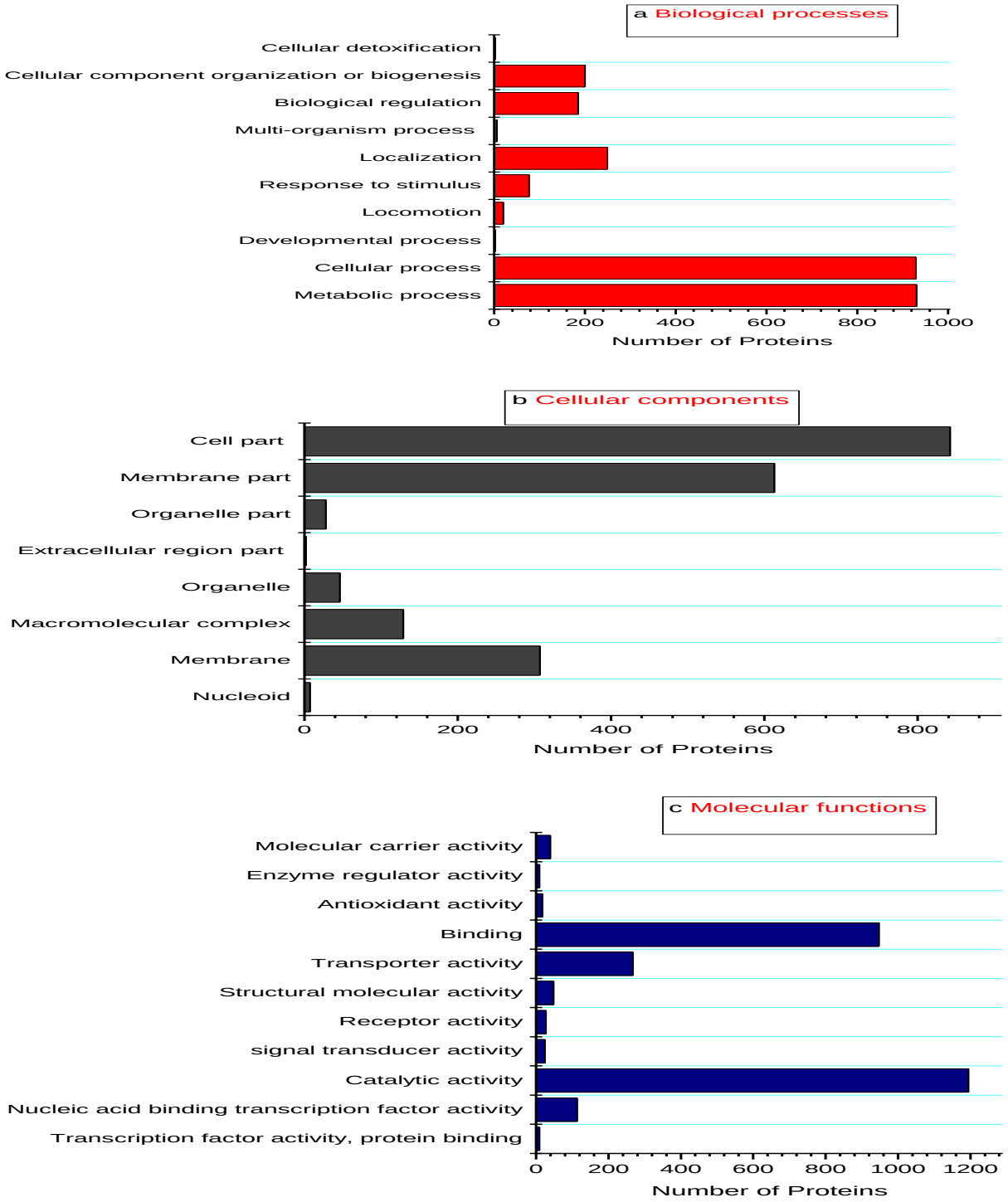

Fig.3.4 Pictorial representation of GO analysis of *Serratia* sp. ISTD04 genome and proteins involve in (a) biological processes, (b) cellular components and (c) molecular functions.

Presence of carbonate dehydrates or CA and its transporters specify their role in transportation of HCO_3^- across the membrane and subsequent its utilization in the form of CO_2. Representation of carboxylase, decarboxylase, isomerase, kinase, aldolase, phosphatase and epimerase in good fraction shows their involvement in sequestration of CO_2. The GO investigation particularly biological process and molecular functions certainly provided the information related to *Serratia* sp. ISTD04 and its enzymatic machinery, which can utilize CO_2 as well as organic compounds (autotrophic and heterotrophic) as carbon source for production of biological materials.

3.3.3 CO_2 sequestration and metabolic diversity

Genomic investigation of *Serratia* sp. ISTD04, authenticate it diversified metabolic mechanism. Along with CO_2 it can utilized various other carbon source. Since this strain was isolated from marble mining rocks of the palaeoproterozoic metasediments, CO_2 sequestration is of specific interest along with production of biological products. Chemoautotrophic bacteria are categorized majorly into two groups: obligate chemoautotrophes and facultative chemoautotrophs. Obligatory chemoautotrophic bacteria are completely dependent on CO2 as sole carbon source, while facultative chemoautotrophs utilize CO_2 via the Calvin cycle along with, it can also utilize diverse range of organic substance as carbon substrate. As compare to others, obligate chemoautotrophs, they are very much specific in their function and its metabolic activities for utilization of dearth of reduced substances are optimized (**Beudeker et al., 1982; Kuenen and Bos, 1989**). Facultative chemoautotrophic bacteria exhibit diverse metabolic activities, which makes them an contender species for utilization of various groups of compounds. In disparity with obligatory autotrophs, facultative autotrophic bacteria exhibit inducible metabolic mechanisms for utilization of wide range of substrates. A distinctive attributes of these microbe is the capability to grow mixotrophically, i.e. simultaneous utilization of substrates facilitating autotrophic and heterotrophic mode of growth (**Shively et al., 1998**). This strain can metabolize monosaccharide (galactose, mannose, fructose), disaccharides (sucrose) polysaccharides (starch) and many organic compounds such as, glucuronate, ascorbate, aldarate, amino sugar, nucleotide sugar, propionate and butanoate. The pathways analysis of this strain revealed that, it may also utilize C5-branched dibasic acid and other glyoxylate,

dicarboxylate and pyruvate as carbon source. KEGG pathway study of carbohydrate metabolism shows that this strain is able to utilize soft carbon source like glucose for his growth and energy requirement. Genomic investigation of *Serratia* sp. ISTD04 clearly depicted that this strain follow CBB cycle for sequester of CO_2 (**Kumar et al., 2016a)**.

Fixation of CO_2 by CBB cycle required 13 catalytic reactions (**Saini et al., 2011**). The principle enzyme involve is CO_2 sequestration via CBB cycle is RuBisCO, which produce two molecules of 3-phosphoglycerate from ribulose-1,5- bisphosphate (RuBP) by carboxylating activity. The rest of the enzymes of the CBB cycle are facilitating regeneration of RuBP. The glycolytic enzymes such as, phosphoglycerate kinase, glyceraldehyde-3-phosphate dehydrogenase, and triosephosphate isomerase, utilizes two molecules of ATP and two of NADH to transform two molecules of 3-phosphoglycerate to glyceraldehyde-3-phosphate and dihydroxyacetone phosphate. After that series of rearrangement reactions takes place to generate ribulose-5-phosphate. Based on the enzymatic participation, such as aldolase, phosphatase and transketolase (APT), the rearrangement mechanisms are categorized into two akin metabolic units. Conversion of glyceraldehyde-3-phosphate and dihydroxyacetonephosphate into xylulose-5-phosphate and erythrose-4-phosphate is performed by the first APT unit; further second APT unit transformed dihydroxyacetonephosphate into xylulose-5-phosphate, ribulose-5-phosphate and erythrose-4-phosphate (**Shively et al., 1998)**. Sedoheptulose bi-phosphate (SBP) is dephosphorylated by the action of sedoheptulose bisphosphatase (SBPase), which have unique activity in comparison to gluconeogenic fructose bisphosphatase (FBPase) in the CBB cycle. In overall rearrangement reaction, pentose phosphate pathways principally provide possible rout. In these circumstances, the second APT unit constituents (aldolase and phosphatase) are traded by transaldolase. The major difference occur using phosphatase in the aldolase/SBPase variant in this process; turn second APT unit irreversible, whereas transaldolase variant make this process reversible. The autotrophic microbial community discover till date make use of the aldolase/SBPase variant of the CBB cycle. Xylulose-5-phosphate and ribose-5-phosphate generated during sequential reactions of the two APT units are further transformed into ribulose-5-phosphate with the help of catalytic reaction of pentose phosphate epimerase and pentose phosphate isomerase, respectively. Finally, the regeneration of RuBP from ribulose-5-phosphate by phosphorylation is performed by another inimitable CBB cycle enzyme, PRK using 1 ATP

molecule. The final outcome of the CBB cycle is 3 molecules of CO_2 generate 1 molecule of triosephosphate by utilizing 9 molecules of ATP and 6 molecules of NADH.

Genomic analysis (PGAP, KEGG pathway analysis) of *Serratia* sp. ISTD04 shows that all the important genes and proteins of CBB pathway are present in this strain **Table.3.2,** but RuBisCO is missing in the sequence (**Kumar et al., 2016a**)**.** Although proteomic analysis of this strain was performed by **Bharti et al (2014b)** and **Kumar et al (2017b)**, reported the presence of both subunits (large and small) of RuBisCO. The second most important enzyme of the CBB cycle, PRK, which is not much acknowledged. PRK protein are octameric in structure with subunit size in the range of 32–36 kDa obtained from *R. eutropha* and the photosynthetic bacteria, *R. acidophila* and Rb. sphaeroides (**Gibson and Tabita, 1987; Rippel and Bowien, 1984; Siebert and Bowien, 1984; Tabita, 1980**). In bacteria PRK activity is strongly controlled by metabolites concentration inside the bacterial cell, with few exceptions like PRK activity of *T.* neapolitanus is controlled by NADH and adenosine monophosphate (AMP) (**MacElroy et al., 1972**). Phosphoenolpyruvate (PEP) and AMP are general inhibitors of PRK (**Shively et al., 1998**). The control of PRK action by NADH and AMP can be explain, as cellular response of the enzyme, which depends on the energy statues of the cell and its redox potential. Genetic and biochemical investigation recognized some of the isoenzyme, which has great impact in CBB cycle along with RuBisCO and PRK. In these categories, first enzyme was FBPase, revealed by **Johnson and MacElroy, 1973.** It is important that, as compare to gluconeogenic enzyme of heterotrophes, the FBPase of autotrophic bacteria *T. neapolitanus* was not activated by acetyl co-A action but mainly repressed by PEP concentration. Later on finding of different FBPase activities in microorganism such as, *T. versutus, N. opaca*, and *X. flavus*, which follow heterotrophic as well as autotrophic growth, the catalytic activities were controlled by two distinct proteins (**Amachi and Bowien, 1979; Meijer et al., 1990; van den Bergh et al., 1995; Wood et al., 1977**). Two distinct and mechanically different types of aldolases have been found in Prokaryotes, Archaea and Eukaryotes. During catalysis reaction of the reactant and the ε-amino group of a lysine residue Class I aldolase catalyzed the formation of Schiff base, while class II aldolase run the catalytic cycle taking bivalent cation as electrophile (**March and Lebherz, 1992**). During heterotrophic growth of *X. flavu*s, activity of aldolase was free from the Fe^{2+} concentration, but in autotrophic growth condition Fe^{2+} increases the aldolase activity 14-

fold (**van den Bergh et al., 1996**). The presence of both the aldolases in *Serratia* sp. ISTD04 confirmed that this strain can perform both autotrophic as well as heterotrophic mode of growth, depends on availability of diverse groups of substrate. Due to, limitation of genomic investigation the specific role of isoenzymes in the metabolic activities have not been evaluated (**Shively et al., 1998)**. It might be possible that these isoenzymes are simply facilitating the CBB cycle enzymatic activities, which is crucial to perform autotrophic growth in presence of CO_2 and increase the rate of CO_2 fixation.

3.3.4 Transcriptional regulators, Membrane transporters and Proteins

Transcription regulators help in regulating the various cellular and metabolic processes by controlling (up regulation or down regulation) the transcription mechanism in the influence of substrates or environmental stimulus. The various transcription regulators (251) was identified by Nr-blast analysis of the genome of *Serratia* sp. ISTD04. Transcriptional regulators recognized with majority belong to HTH-type transcription regulator along with LysR family, GntR family, glycosyl trasferase family transcriptional regulators **Fig.3.5**. The LysR-type transcriptional regulator (LTTR) is diverse group of proteins family, which includes the important protein for CO_2 sequestration like CbbR protein. CbbR protein regulates the CO_2 fixation (*cbb*) operons genes expression, which are important enzymes of the CBB pathway. CbbR-dependent genes regulation takes place in diverse groups of organisms, such as nonsulfur bacteria and sulfur purple bacteria, marine and freshwater chemoautotrophes, cyanobacteria, methylotrophic bacteria, several species of hydrogen- utilizing bacteria, and wide varieties of *Pseudomonas*, *Mycobacterium*, and *Clostridium* species (**Terazono et al., 2001; Wei et al., 2004; Toyoda et al., 2005; Romagnoli and Tabita, 2006; Lee et al., 2009; Esparza et al., 2010; Wang et al., 2011**). In addition to that, CbbR protein also responsible for regulation of carbon fixing gene expression in the chloroplasts of eukaryotes, like red algae (**Minoda et al., 2010**). The transcription regulators like HTH-type transcription regulator and CysB- like protein transcription regulator help in regulation and expression of CO_2 fixing proteins (**Dangel and Tabita, 2015**). Nr-blast search also identified the carboxylase and decarboxylase proteins in genome of *Serratia* sp. ISTD04, which are responsible for fixation of CO_2 in chemolithotrophic bacteria (**Bharti et al., 2014a; Kumar et al., 2017b**) are represented in **Table.3.4, Fig.3.6**.

GntR family proteins are comes under helix-turn-helix domain of bacterial transcriptional regulators, which are broadly distributed in bacteria family and its numbers are numerously variable among bacterial family as reported by **Hoskisson and Rigali (2009)**. GntR family member proteins have been established to participate in regulation of diverse imperative biological processes, which includes primary metabolism, motility, development, production of antibiotic and resistance as well as degradation of aromatic compounds. More recently, involvement of GntR proteins family in formation of biofilm have been also established in *E.* coli, *Enterococcus* faecalis and *Listeria* monocytogenes (**Zhang et al., 2008; Ballering et al., 2009; Wassinger et al., 2013**) and the production of EPS in *Streptomyces* sp. (**Bai et al., 2013**), however regulation of their targeted genes and its mechanisms are remains mysterious. The role of glycosyl transferase family transcriptional regulators and ABC transporter in production of EPS from bacterial strains are well reported previously (**Hidalgo-Cantabrana et al., 2014**). Apart from transcriptional regulators, Nr-blast search of proteins of *Serratia* sp. ISTD04 also identified the potential candidate proteins responsible for EPS biosynthesis such as, UDP-glucose 6-dehydrogenase, phosphoglucomutase, Galactose-1-phosphate uridylyltransferase, UDP-galactose-4-epimerase, Mannose-6-phosphate isomerase, phosphomannomutase, glucans biosynthesis glucosyltransferase H, polysaccharide biosynthesis protein, capsular polysaccharide translocation, glycogen/starch/alpha-glucan phosphorylases family protein (**Ates, 2015; Hidalgo-Cantabrana et al., 2014; Brandt et al., 2016; Kornmann et al., 2003; Pühler et al., 2008)** and many more represented in **Table 3.4**.

Table.3.4 Representation of Proteins identified against the Nr- blast search.

serratia_Id (query) locus tag	**NR_Db_Id (Subject)**	**Description**	**% Identity**	**Alignment length**	**E-value**	**Query cover**
		CO2 Sequestering Enzymes				
BBC05_16825	CDS56108.1	phosphoribulokinase [Serratia symbiotica]	95.156	289	0	100
BBC05_06250	ERK11276.1	Phosphoglycerate kinase [Serratia fonticola AU-AP2C]	98.191	387	0	100
BBC05_13225	KXJ03736.1	glyceraldehyde-3-phosphate dehydrogenase [Serratia marcescens]	97.321	336	0	100
BBC05_19345	ANM79803.1	triose-phosphate isomerase [Serratia marcescens]	99.216	255	0	100
BBC05_13025	SAY44498.1	Fructose-bisphosphate aldolase class 1 [Serratia marcescens]	99.427	349	0	100
BBC05_06255	EFE96163.1	fructose-bisphosphate aldolase, class II [Serratia odorifera DSM 4582]	96.936	359	0	100
BBC05_04065	SAY44197.1	Transketolase [Serratia marcescens]	97.527	283	0	100
BBC05_06310	KXJ00812.1	ribose-phosphate isomerase A[Serratia marcescens]	99.541	218	1.4E-154	100
BBC05_10725	ANM78414.1	ribose -phosphate isomerase B [Serratia marcescens]	97.744	133	1.24E-88	88
BBC05_16715	ANM76785.1	ribulose-phosphate 3-epimerase	99.111	225	6.77E-	100

		[Serratia marcescens]			162	
BBC05_12275	AFV36793.1	carbonic anhydrase [Serratia sp. ISTD04]	99.462	186	4.7E-132	100
BBC05_02415	AGE19010.1	Citrate lyase [Serratia marcescens CUY86136.1]	100	501	0	100
BBC05_07410	CUW02506.1	Malate dehydrogenase [Serratia]	97.756	312	0	100
BBC05_15225	CDS57382.1	NAD-linked malate dehydrogenase [Serratia symbiotica]	93.961	563	0	99
BBC05_10660	KGY55980.1	malic enzyme [Serratia marcescens]	99.868	759	0	100
BBC05_13120	CUW24027.1	Fumarate hydratase class I [Serratia]	96.533	548	0	100
BBC05_12785	SAY43017.1	Fumarate hydratase class II [Serratia marcescens]	99.57	465	0	100
BBC05_05665	CDG15027.1	fumarate reductase [Serratia marcescens]	99.585	241	0	99
BBC05_05670	ANM78186.1	fumarate reductase subunit C family protein [Serratia marcescens]	99.225	129	1.59E-85	99
BBC05_11935	CDS57215.1	succinyl-CoA synthetase alpha chain [Serratia symbiotica]	97.931	290	0	100
BBC05_11930	CRH37540.1	Succinyl-CoA ligase [ADP-forming] subunit beta [Pantoea ananatis]	93.814	388	0	100
BBC05_20805	SAY42786.1	Isocitrate dehydrogenase [NADP] [Serratia marcescens]	99.754	406	0	97

BBC05_11610	SAY43401.1	Aconitate hydratase [Serratia marcescens]	98.876	890	0	100
BBC05_15845	CVF96668.1	Pyruvate synthase [Serratia marcescens]	99.065	1177	0	100
BBC05_03135	ANM80828.1	phosphoenolpyruvate synthase regulatory protein [Serratia marcescens]	98.901	273	0	100
BBC05_03140	ANM76094.1	phosphoenolpyruvate synthase [Serratia marcescens]	99.116	792	0	100
BBC05_01275	SAY45571.1	Phosphoenolpyruvate carboxylase [Serratia marcescens]	99.67	606	0	100
BBC05_21020	SAY42737.1	Bicarbonate transporter BicA [Serratia marcescens]	99.214	509	0	100
		EPS biosynthesis Enzymes				
BBC05_01700	SAY44294.1	Glucokinase [Serratia marcescens]	96.562	320	0	100
BBC05_11790	ETX39330.1	phosphoglucomutase [Serratia marcescens BIDMC 44]	99.817	547	0	100
BBC05_09340	SAY42029.1	Galactose-1-phosphate uridylyltransferase [Serratia marcescens]	96.286	350	0	100
BBC05_15065	KGY57505.1	UDP-galactose-4-epimerase [Serratia marcescens]	94.955	337	0	100
BBC05_11335	SAY43506.1	UDP-glucose 6-dehydrogenase [Serratia marcescens]	97.763	447	0	100
BBC05_00160	SAY41676.1	Fructokinase [Serratia marcescens]	96.382	304	0	100

BBC05_12775	SAY43015.1	Mannose-6-phosphate isomerase [Serratia marcescens]	98.724	392	0	100
BBC05_15070	KGY57506.1	phosphomannomutase [Serratia marcescens]	96.484	455	0	99
BBC05_12775	SAY43015.1	Mannose-6-phosphate isomerase [Serratia marcescens]	98.724	392	0	100
BBC05_19510	AAL78078.1	glucosyl-transferase [Yersinia enterocolitica]	99.611	257	0	100
BBC05_13845	SAY42616.1	Glucans biosynthesis glucosyltransferase H [Serratia marcescens]	99.531	852	0	100
BBC05_19485	KGY51962.1	glycosyl transferase family 9 [Serratia marcescens]	98.333	360	0	100
BBC05_19765	AGQ31694.1	glycosyl transferase [Serratia liquefaciens ATCC 27592]	77.419	279	3.54E-160	93
BBC05_19775	AHY07915.1	polysaccharide biosynthesis protein [Serratia plymuthica]	86.713	429	0	100
BBC05_19785	EZQ64369.1	capsular polysaccharide translocation[Serratia marcescens BIDMC 81]	100	369	0	98
BBC05_23440	ERH70632.1	PTS sugar transporter subunit IIA [Serratia marcescens EGD-HP20]	100	148	3.61E-104	100
BBC05_04915	KKO56354.1	sugar (and other) transporter family protein [Serratia ureilytica]	99.778	450	0	100
BBC05_06740	CUW23703.1	PTS system mannose-specific EIIAB component [Serratia]	86.111	144	8.36E-81	100

BBC05_07750	ANM80863.1	glycosyl hydrolase 20, domain 2 family protein [Serratia marcescens]	96.981	795	0	99
BBC05_01605	ANM80482.1	glycogen/starch/alpha-glucan phosphorylases family protein [Serratia marcescens]	99.376	801	0	100
BBC05_11660	CDG12485.1	sugar ABC transporter, permease protein [Serratia marcescens subsp. marcescens Db11]	99.153	354	0	100
BBC05_12130	SAY42246.1	Biofilm dispersion protein BdlA [Serratia marcescens]	98.848	434	0	100
BBC05_13845	SAY42616.1	Glucans biosynthesis glucosyltransferase H [Serratia marcescens]	99.531	852	0	100
BBC05_13850	ETX49065.1	glucans biosynthesis protein G [Serratia marcescens BIDMC 50]	99.8	500	0	100
BBC05_13855	KXJ03647.1	glucans biosynthesis protein [Serratia marcescens]	98.138	376	0	100
BBC05_15035	AID71053.1	glycosyltransferase, family 2 protein [Aeromonas hydrophila]	37.916	931	0	99
BBC05_15050	AID71050.1	glycosyltransferase [Aeromonas hydrophila]	53.203	359	3.74E-127	99
BBC05_15060	ANF30168.1	dTDP-4-dehydrorhamnose 3,5-epimerase [Hafnia alvei]	74.576	177	2.95E-100	100
BBC05_15075	KGY57507.1	mannose-1-phosphate guanyltransferase [Serratia marcescens]	95.992	474	0	100

BBC05_15135	CUW09536.1	Glycosyl transferases group 1 [Serratia]	52.895	380	1.65E-134	99
BBC05_15145	CUW09503.1	UTP--glucose-1-phosphate uridylyltransferase [Serratia]	90.236	297	0	100
BBC05_15150	AIA49534.1	UTP-glucose-1-phosphate uridylyltransferase [Serratia sp. FS14]	93.96	298	0	100
BBC05_15890	SAY43619.1	PTS system mannose-specific EIIAB component [Serratia marcescens]	98.746	319	0	100
BBC05_15895	AHM74410.1	PTS system mannose-specific EIIC component [Yersinia enterocolitica LC20]	92.105	266	2.53E-156	100
BBC05_15900	BAO34308.1	mannose-specific enzyme IID component of PTS [Serratia marcescens SM39]	100	280	0	100
BBC05_16160	AGO55685.1	glycosyl transferase family 2 [Serratia plymuthica 4Rx13]	83.333	300	0	100
BBC05_16170	AHY07910.1	carbohydrate-binding protein CenC [Serratia plymuthica]	73.844	627	0	100
BBC05_16330	KXJ03416.1	diguanylate cyclase [Serratia marcescens]	92.5	400	0	100
BBC05_19035	AHM73177.1	D-galactose/ D-glucose-binding protein [Yersinia enterocolitica LC20]	93.939	330	0	100
BBC05_06060	SAY44415.1	GDP-mannose pyrophosphatase NudK [Serratia marcescens]	98.421	190	3.35E-137	99

		PHA and fatty acid Biosynthesis Enzymes				
BBC05_01905	SAY44255.1	3-ketoacyl-CoA thiolase [Serratia marcescens]	99.078	434	0	100
BBC05_05470	KGY44449.1	3-hydroxybutyryl-CoA dehydrogenase [Serratia marcescens]	96.091	307	0	100
BBC05_20605	OBY35437.1	trans-2-enoyl-CoA reductase [Providencia rettgeri]	94.737	399	0	100
BBC05_05475	SAY46280.1	Acetyl-CoA acetyltransferase [Serratia marcescens]	97.97	394	0	100
BBC05_07910	AHY05249.1	3-ketoacyl-CoA thiolase [Serratia plymuthica]	95.866	387	0	100
BBC05_20425	AHY08755.1	transporter [Serratia plymuthica]	91.509	318	0	100
BBC05_22110	SAY43217.1	Long-chain-fatty-acid--CoA ligase [Serratia marcescens]	98.242	512	0	100
BBC05_23720	SAY45245.1	Lipid A biosynthesis lauroyl acyltransferase [Serratia marcescens]	98.039	306	0	100
BBC05_07075	ABV42875.1	beta-hydroxyacyl-(acyl-carrier-protein)dehydratase [Serratia proteamaculans 568]	97.576	165	4.87E-116	100
BBC05_11020	ERK10714.1	Lipid A biosynthesis 2-(lauroyl)-lipid IVA acyltransferase [Serratia fonticola AU-AP2C]	93.168	322	0	100
BBC05_13675	CDS58128.1	3-oxoacyl-(acyl-carrier-protein)	93.033	244	5.59E-	100

		reductase [Serratia symbiotica]			162	
BBC05_13670	ERH71201.1	acyl carrier protein [Serratia marcescens EGD-HP20]	100	78	3.76E-46	100
BBC05_13680	KXJ03618.1	malonyl CoA-ACP transacylase [Serratia marcescens]	99.029	309	0	100
BBC05_13685	SAY42651.1	3-oxoacyl-[acyl-carrier-protein] synthase 3 [Serratia marcescens]	98.423	317	0	100
BBC05_14070	AIM21329.1	3-hydroxybutyryl-CoA dehydrogenase [Serratia sp. SCBI]	99.389	491	0	100
BBC05_14075	SAY42575.1	3-oxoadipyl-CoA/3-oxo-5,6-dehydrosuberyl-CoA thiolase [Serratia marcescens]	94.293	403	0	100
BBC05_14290	CFQ45316.1	3-hydroxydecanoyl-ACP dehydratase [Yersinia similis CNB00920]	95.93	172	4.05E-118	100
BBC05_14300	SAY42529.1	3-oxoacyl-[acyl-carrier-protein] synthase 2 [Serratia marcescens]	96.471	425	0	100
BBC05_14585	SAY42471.1	Lipid A export ATP-binding/permease protein MsbA [Serratia marcescens]	97.582	579	0	100
BBC05_16100	ANM76772.1	fatty acid desaturase family protein [Serratia marcescens]	97.784	361	0	100
BBC05_16110	ANM76128.1	fatty acid hydroxylase superfamily protein [Serratia marcescens]	97.613	377	0	100
BBC05_16275	SAY44964.1	Rhamnolipids biosynthesis 3-oxoacyl-[acyl-carrier-protein]	97.348	264	0	100

		reductase [Serratia marcescens]				
BBC05_18290	SAY41407.1	Long-chain-fatty-acid--CoA ligase FadD15 [Serratia marcescens]	95.847	602	0	100
BBC05_19150	AJR01628.1	Putative acetyltransferase [Enterobacteriaceae bacterium bta3-1]	76.536	179	2.13E-92	98
BBC05_06040	EZQ60168.1	fatty acid oxidation complex subunit alpha [Serratia marcescens BIDMC 81]	99.307	721	0	100
BBC05_23675	CDS56366.1	acetyl CoA carboxylase, BCCP subunit [Serratia symbiotica]	88.387	155	5.52E-92	100
BBC05_23680	AHM71842.1	Acetyl-CoA carboxylase subunit A [Yersinia enterocolitica LC20]	96.882	449	0	100
BBC05_03970	AAM85170.1	acetyl CoA carboxylase, carboxytransferase component, beta subunit [Yersinia pestis KIM10+]	91.419	303	0	99
BBC05_07100	KXJ02543.1	acetyl-CoA carboxylase subunit alpha [Serratia marcescens]	99.687	319	0	100

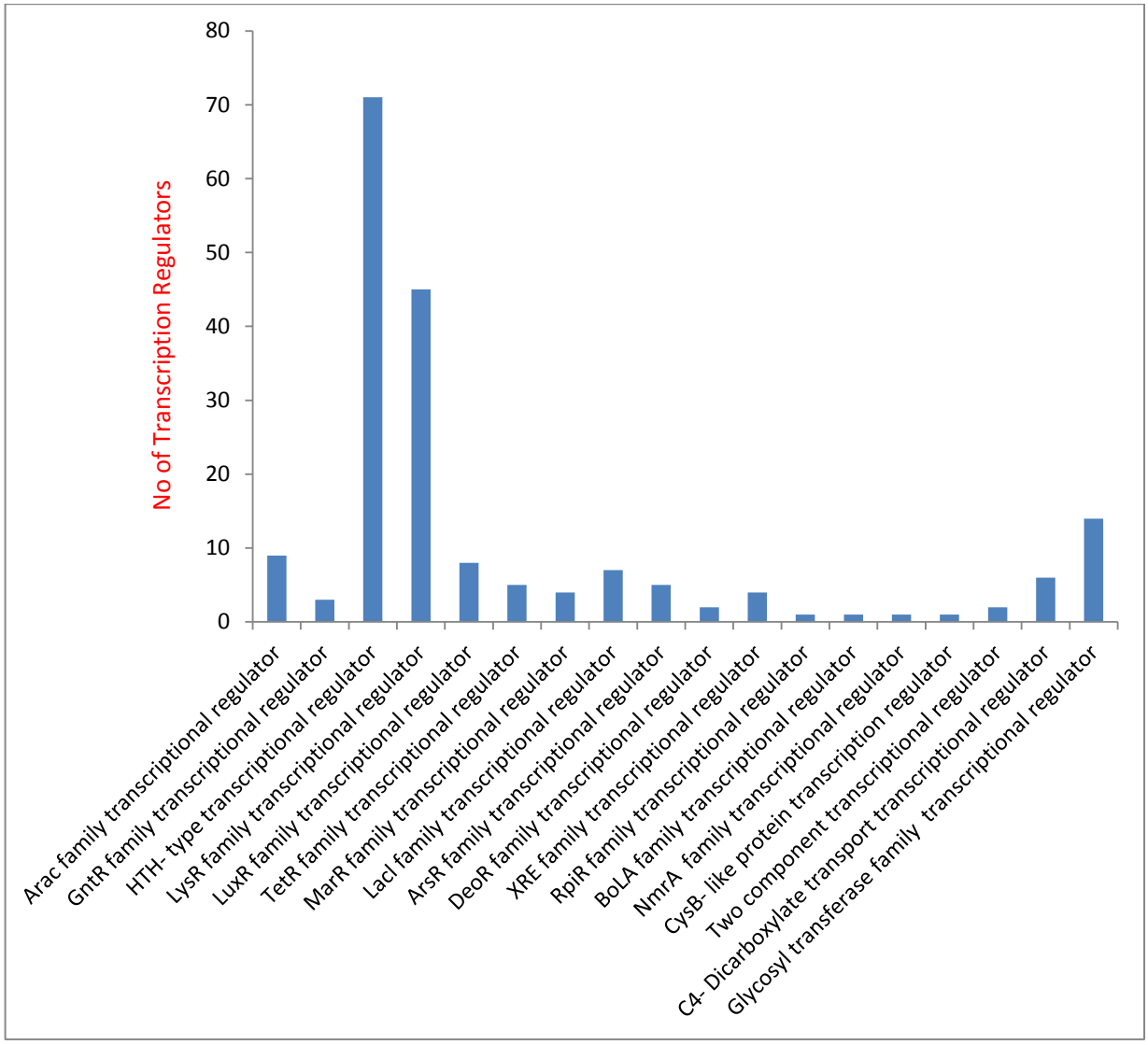

Fig.3.5 Representation of transcriptional regulators identified by Nr-blast in the genome of *Serratia* sp. ISTD04.

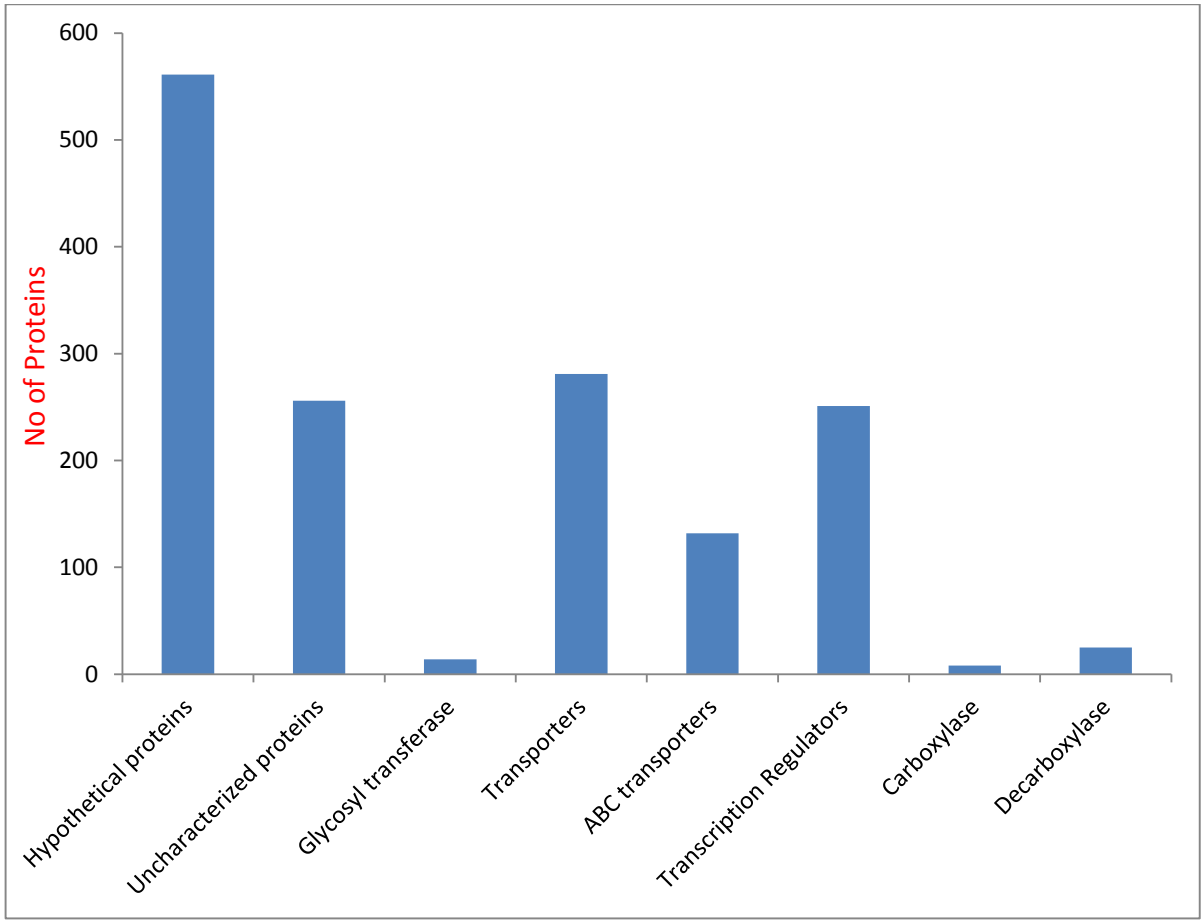

Fig.3.6 Protein identified by Nr- blast in the genome of *Serratia* sp. ISTD04.

3.3.5 Biosynthesis of fatty acids and Polyhydroxyalkanoate (PHA)

Serratia sp. ISTD04 is extensively studied previously for extraction of fatty acid as raw materials for production of biodiesel (**Bharti et al., 2014a, 2014c; Kumar et al., 2017a, 2017b**). PHA is intracellular reserve materials of the microorganism, plays a key role in survival of microbes during long term stress condition. PHA acts as carbon and energy assets of the microorganism, when environmental condition becomes adverse (**Tan et al., 2014**). In bacteria PHA biosynthesis routs are interlinked with the central metabolic pathways, such as glycolysis, Krebs cycle, *β*-oxidation of fatty acid, *de novo* fatty acids biosynthesis, catabolism of amino acid, CBB cycle, and serine pathway (**Khanna and Srivastava, 2005; Madison and Huisman, 1999; Rothermich et al., 2000; Peplinski et al., 2010; Shimizu et al., 2013).** Production and

characterization of polyhydroxyvalerate (co-polymer of polyhydroxybutrate) from *Serratia* sp. ISTD04 have been described comprehensively in chapter five. Synthesis of PHA and its accumulation in bacteria is tightly regulated and control by the expression genes, which are responsible for its synthesis. PHA produced by this strain is polyhydroxyvalerate, which is five carbons PHA. Synthesis of PHA start with the action of β-ketothiolase, which mediate the condensation reaction of two monomeric unit of acetyl-CoA or one monomeric unit of acetyl-propionyl-CoA followed by the formation of activated hydroxyacyl-CoA by the action of acetoacetyl-CoA reductase. Finally PHA synthase (PHA polymerase) action transformed the activated hydroxyacyl-CoA into polyoxoester by releasing CoA (**Rehm, 2010; Możejko-Ciesielska and Kiewisz, 2016**). Synthesis of medium chain length PHA was perform by enzymes enoyl CoA hydratase and hydroxyacyl ACP-CoA transacylase by diverting the metabolic intermediates of fatty acid metabolism, such as enoyl-CoA and hydroxyacyl carrier proteins (**Rehm, 2010; Możejko-Ciesielska and Kiewisz, 2016**). Although extensive research work has been performed and published by the various researchers on the PHA formation mechanism in bacteria, but still we have very less information related to exact catalytic mechanism of the enzymes and its function as well as genomic analysis of PHA producing bacteria (**Schubert et al., 1988**). Three important enzymes are responsible for biosynthesis of PHA in the microorganism, such as β–ketothiolase, acetoacetyl-CoA reductase and PHA synthase. In comparison to former two enzymes, we have very limited information about the PHA synthase, which is the key enzyme of PHA biosynthesis pathways. Under define growth condition; PHA synthase is linked with phospholipids and present on the surface of the PHA granules in *Bacillus megaterium, R. rubrum* (**Merrick and Doudoroff, 1960**), and Zoogloea ramigera **(Fukui et al., 1976; Tomita et al., 1983**) and its help in increase the chain length of PHA polymers or simply polymerization of the PHA . **Griebel and Merrick (1971)** investigated a protein called A-I, in *B. megaterium,* which intervenes between the monomer and the growing chain of the polymer and it perform functions like an acyl carrier protein. Genomic investigation of *Serratia* sp. ISTD04 shows, all the enzymes, which are involve in fatty acid and well as PHA biosynthesis pathways **Table.3.2 and 3.4.** Absence of PHA synthase in the sequence of *Serratia* sp. ISTD04 is justified that, either it might be missed during sequencing or polymerization is

performed by acyl carrier protein, which is described by **Griebel and Merrick (1971)** in *B. megaterium*.

3.3.5.1 Cluster analysis for important genes responsible for PHA biosynthesis

Here we have described the genes, which are responsible for PHA accumulation and the arrangement of genes on the cluster responsible for PHA synthesis in the genome of *Serratia* sp. ISTD04 by antiSMASH ver. 4.1.0 and Rapid Annotations using Subsystems technology (RAST) is shown in **Fig. 3.7**. The cluster analysis predicted the presence of important genes responsible for PHA production, such as β-ketothiolase, acetyl transferase with some precursors proteins like, 3-hydroxybutryl-CoA dehydrogenase, enoyl-CoA hydratase. This cluster is also dominated by transporters and stress tolerant proteins.

MBDW01000089.1 (52414 – 62693) 10.2 KB

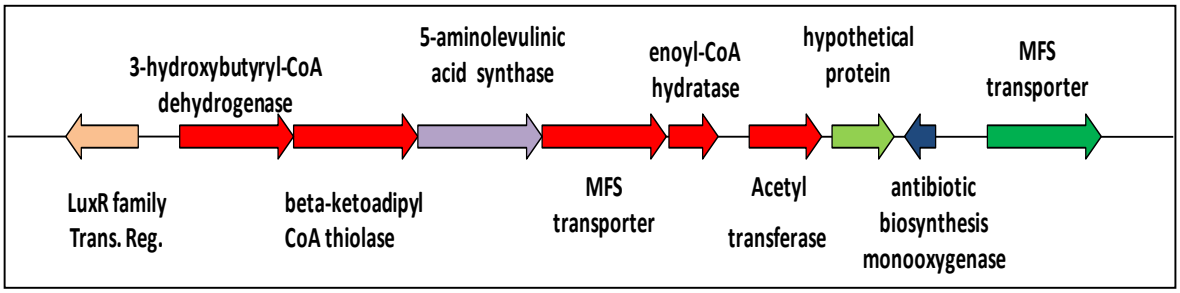

Fig.3.7 Gene clusters identified in *Serratia* genome responsible for PHA production. The contig number and size of DNA fragment selected for cluster analysis has been represented.

3.4 Conclusion

Serratia sp. ISTD04 is a novel organism which performs chemolithoautotrophic carbon dioxide assimilation. Genome analysis of *Serratia* sp. ISTD04 revealed the presence of PRK and other CBB pathway genes. However, the RuBisCo gene could not be identified in the genome assembly. The carbonic anhydrase, an important facilitator enzyme, is also present in the genome. Anaplerotic CO_2 assimilating enzymes *viz*. phosphoenolpyruvate (PEP) carboxylase, malic enzymes, and PEP carboxykinase, are present in the genomic analysis. Transcriptional regulator, such as LTTR, HTH type and CysB- like protein transcription regulator related to CO_2

fixation are also identified in the genome. EPS biosynthesis ability of this strain is also investigated at genomic level, presence of various EPS synthesis enzymes such as UDP-glucose 6-dehydrogenase, phosphoglucomutase, Galactose-1-phosphate uridylyltransferase, UDP-galactose-4-epimerase, Mannose-6-phosphate isomerase, phosphomannomutase, glucans biosynthesis glucosyltransferase H, polysaccharide biosynthesis protein, capsular polysaccharide translocation, glycogen/starch/alpha-glucan phosphorylases family protein and many more in the genome, confirm this strain as an potential candidate for EPS production. Enzymes for fatty acid metabolism such as acetyl-CoA carboxlases, malonyl Co-ACP transacylase, 3-ketoacyl ACP-synthase, and 3-ketoacyl ACP-reductase are present. Enzymes involved in PHA synthesis like β-ketoacyl-CoA thiolase and acetoacetyl-CoA dehydrogenase were also identified in the genome sequence. Therefore, this strain can be applied to simultaneous sequestration of CO_2 and production of value-added biomaterials.

Chapter 4: Utilization of calcium carbonate precipitated by bacteria during carbon dioxide sequestration for preparation of biocomposite material by sol-gel process

4. Utilization of calcium carbonate precipitated by bacteria during carbon dioxide sequestration for preparation of biocomposite material by sol-gel process.

4.1 Introduction

The CO_2, one of the most potent green house gas (GHG), its concentrations (270 ppm) was stable before the industrial revolution, now its increased to 400 ppm. It has been expected that by the middle of current century CO_2 concentrations should be reach up to 600 ppm, and by the end it is probably 700 ppm. Rising CO_2 concentration may induces the autotrophic CO2 fixing organisms to fix the CO_2 different mechanism like CO_2 concentrating mechanisms (CCMs), with the help of carboxylating enzymes such as ribulose 1, 5-bisphosphate carboxylase/oxygenase (RuBisCO) and carbonic anhydrase (CA) (**Kaplan and Reinhold, 1999**). There are penalty of methods available to reduce the atmospheric CO_2 concentration. Fixation of CO_2 by physicochemical methods resulted formation of carbonate mineral and its precipitation in the form of calcite, magnesite and dolomite. CO_2 was naturally fixed by the action of biological organisms (plants and microbes). CO_2 and its dissolved inorganic form (HCO_3^-) are indispensable constituents which are available to microorganisms (**Srivastava et al., 2015a**). To reduces or mitigate the rising level of CO_2, biological method of CO_2 sequestration is the most effective method since some chemolithotrophic microbes are able to fix atmospheric CO_2 and immobilize in the form of useful minerals like calcite, vaterite and aragonite.

The biological precipitation of carbonates minerals has been previously reported. Various groups of bacteria can precipitate carbonates such as *Bacillus cereus*, *Pseudomonas aeruginosa* (**De Muynck *et al.* 2010**), *Bacillus pasteurii* (**Kroll, 1990**), *Pseudomonas putida* (**De Muynck et al., 2008**), *Myxococcus xanthus* (**Rodriguez-Navarro et al., 2003**), *Pseudomonas fluorescens*, *Bacillus subtilis* (**Zamarreno et al., 2009**), and *Serratia* sp.ISTD04 (**Srivastava et al., 2015a,b**). Mostly, the bacterial species can precipitate carbonate minerals in different environmental condition (growth condition) such as salinity, alkalinity, duration and growth media composition

(**Knorre and Krumbein, 2000; Rivadeneyra et al., 2004**). These microbial precipitated carbonate minerals may be used as raw material for synthesis of bioactive glasses.

Bioactive glasses belong to a group of biological active materials have been extensively used in the medical fields such as dentistry and orthopedics. After its discovery these materials customized the functions and capabilities of bioenert material to bioactive material by stimulating a strong positive response in human body in which they are implanted (**Abbasi et al., 2015; Stoor et al 1998)**. A synthetic material can be called as bioactive material if they are able to produce biological response and induce formation of strong chemical bond between implanted material and a soft or hard body tissue (**Hench et al., 1971**). Fixed elemental proportions of the calcium and phosphorous in silicate-based glasses, similar to human bone can induced the formation of strong chemical bond between glasses and body tissue without interrupting fibrous layer of the body tissue (**Hench, 2006**). It has been observed that the glasses containing more than 60% SiO_2 composition, the bond formation among body tissue and glasses will hamper (**Li et al., 1991**). In contrast, it is probable that the activities of bioactive materials will increase with increasing the concentration of CaO in the material, due to dissolution of the calcium ion may induced the formation of the chemical bond (**Laudisio and Branda, 2001**). It has been reported that, in-vivo implantation of these materials has no side effect such as inflammation, toxicity and anti immune response (**Greenspan et al., 1994**). The bonding mechanism of these glasses includes formation of a hydroxyapatite (HAp) layer with the bone when these materials are implanted in the body. The similar types of formation of HAp layer was also observed on the glass surface when these glasses are soaked in to simulated body fluid (SBF) having ion concentrations equivalent to the human blood plasma (**Siriphannon et al., 2002**). Hench from the University of Florida first time synthesized the bioactive glass in 1969 (**Hench et al., 1971)**. At that time, the existing implant materials like metals and polymers was synthesized to be bioinert encountered certain problem; after implantation in the body they start fibrous encapsulation, more willingly than forming a strong bond with the implanted tissues. Hench started his work to solve the existing problem by designing a material that could strongly bond to the bone and cop-up with the complex environment of the human body. He tried to prepare a biodegradable glass having chemical composition Na_2O-CaO-SiO_2-P_2O_5 and higher calcium

composition (**Hench et al., 1971)**. He synthesized such glass having the chemical composition of 46.1 mol. % SiO_2, 24.4 mol. % Na_2O, 26.9 mol. % CaO and 2.6 mol. % P_2O_5 and latterly termed as 45S5 and Bioglass®. This synthesized bioglass strongly bond to the human bone until-unless it could not be detached without breaking the bone. In reality, this bioglass bonds with human bone quickly and encourage new bone formation away from the place where this material implanted. The bond forming mechanism of this material started with formation of HAp layer on the material, following initial glass dissolution (**Hench et al., 1971)**. The discovery of bioglass synthesis by the Hench introduced a new field of bioactive ceramics preparation, lead to synthesis of various new types of materials which includes synthetic hydroxyapatite and several calcium phosphates composed materials (**LeGeros, 2002**).

Commercially production of bioactive glasses has been made popular by existing conventional glass synthesis methods such as melting and quenching. In the interim, various research afford has been made to synthesize the bioactive glasses by adopting the sol–gel process (**Jones et al., 2009**), due to its awful versatility with certain advantages as compare to melting and quenching processes. By adopting the sol–gel process, diverse groups of ceramic or bioactive materials can be synthesized such as very tinny spherical powders, thin film coatings, ceramic fibers, micro-perforated inorganic membranes, monolithic ceramics and glasses and highly perforated aerogelic materials (**Hench, 1997**). Despite its several advantages, this method has not much applied in preparation of bio-glasses or glass ceramics containing Na_2O (**Chen et al., 2010**). All the sol–gel synthesized bioactive glasses series from 49–86S, contain SiO_2, CaO and P_2O_5, but they do not contain Na_2O (**Ramila et al., 2002; Hench, 1997**]. Due to high hydrolytic activity of sodium alkoxide in water, this is the major technical challenge of addition of Na_2O in a sol–gel bioactive glass preparation (**Ramila et al., 2002)**. To overcome this technical problem, many researcher has been used MgO in the sol–gel derived synthesis of bioactive glasses and produced SiO_2–CaO–P_2O_5–MgO glasses (**Balamurugan et al., 2007**). Still, there are some good explanations to use Na_2O in the preparation of bioceramic materials; it provides mechanical strength to the materials without losing its biodegradability. First of all, Na_2O has been used to reduce the melting point of SiO_2-based glasses in the glass industry, while other constituents like CaO and MgO are supplemented to provide stability to the glasses,

otherwise it would be becomes water soluble. Second advantage of using Na_2O is related to crystallization treatment of bioceramics to improve the mechanical strength of the materials. Because mechanically amorphous bioactive materials are easily breakable, to obtained good mechanical properties, the foams of bioactive glass must be sintered at higher temperature for formation crystalline structure (**Chen et al., 2006**). The crystalline structure of bioactive glasses without Na_2O is not bioactive (bioenert) (**Bao et al., 2008**); it means that using Na_2O increase the mechanical strength but simultaneously decreases material degradability. On the contrary, sintered 45S5 Bioglass® having both good mechanical strength as well as adequate biodegradability, might be due to the formation of $Na_2Ca_2Si_3O_9$ crystalline phase (**Chen et al., 2006**). With the above discussion the present objective of this study; utilization of $CaCO_3$ precipitated by *Serratia* sp. ISTD04 for synthesis of bioactive glass by sol-gel process and subsequently evaluation of cytotoxicity of this material on osteosrcoma cell line.

4.2 Materials and methods

All the chemicals and reagents used in the present study were of analytical grade procured from Sigma-Aldrich (St. Louis, MO, USA), Merck (Darmstadt, Germany) or HiMedia unless stated otherwise.

4.2.1 Production of CaCO3 crystal by *Serratia* sp. ISTD04

Previously reported CO_2 sequestering and CaCO3 precipitating *Serratia* sp. ISTD04 was selected for production of $CaCO_3$ as optimized methodology described by **Srivastava et al (2015).** In brief Bacteria were grown aerobically in 200 mL MSM containing 25 mM $CaCl_2$, pH 8, temperature 30 °C and kept in CO_2 incubator shaker (Sanyo, Japan) equipped with an infrared sensor to maintained the 5 % CO_2 concentration for 25 days. After 25 days the precipitated crystals were collected on Whatman No. 1 filter paper (90 mm in diameter, pore size 1.2 μm) by filtration, rinsed with sterile distilled water, and air-dried at 37 °C for 48 h. This collected $CaCO_3$ crystal was further used to synthesize the biocomposite material.

4.2.2 Synthesis of biocomposite material by sol-gel process

The preparation steps of biocomposite material are described in **Fig.4.1**.with slight modification in synthesis process developed by **Chen et al (2010)** and **Hench et al (1971)**. In brief, taken 0.2053 g Si powder, 0.192 g $NaNO_3$, 0.6 g $CaCO_3$ (precipitated by *Serratia* sp. ISTD04) to maintain the molar ratio of SiO_2, Na_2O and CaO respectively similar to crystalline phase $Na_2Ca_2Si_3O_9$. To attain a transparent solution the molar ratio between acidified deionized water (0.25M HNO_3) and the above mention precursor chemicals was kept at 10. Each precursor chemical was supplemented reasonably with slow rate into acidified solution at ambient temperature. Each chemical was added sequence wise in to the solution when the previous added chemical in the solution was mixed completely after that stirred the solution for at least 1 h to complete the mixing process. The prepared gel was dried up at 60 and 200 ℃ for 72 and 40 h, respectively, then aged it at 600 ℃ for 5 h and finally sintering was performed at 1200 ℃ for 2 h. The main objective of sintering the aged gel to obtained Na2O and CaO from the thermal decomposition of sodium nitrate ($NaNO_3$) and calcium carbonate ($CaCO_3$) respectively. The thermal decomposition of $NaNO_3$ and $CaCO_3$ occurs at about 680℃ and 850 ℃, respectively (**Hoshino et al., 1981; Rodriguez-Navarro et al., 2009**), and it has been reported, that the temperature at which 45S5 Bioglass® get fully crystallized is 600 ℃ (**Clupper and Hench, 2003**). Hence, crystallization takes place in the glasses during the thermal decomposition of $NaNO_3$ and $CaCO_3$. To ensure the complete thermal decomposition, crystallization and achieve both satisfactory mechanical properties and biodegradability of the material, the sintering of the material was performed at 1200 ℃ for 2 h (**Chen et al., 2006; Choudhary et al., 2015**).

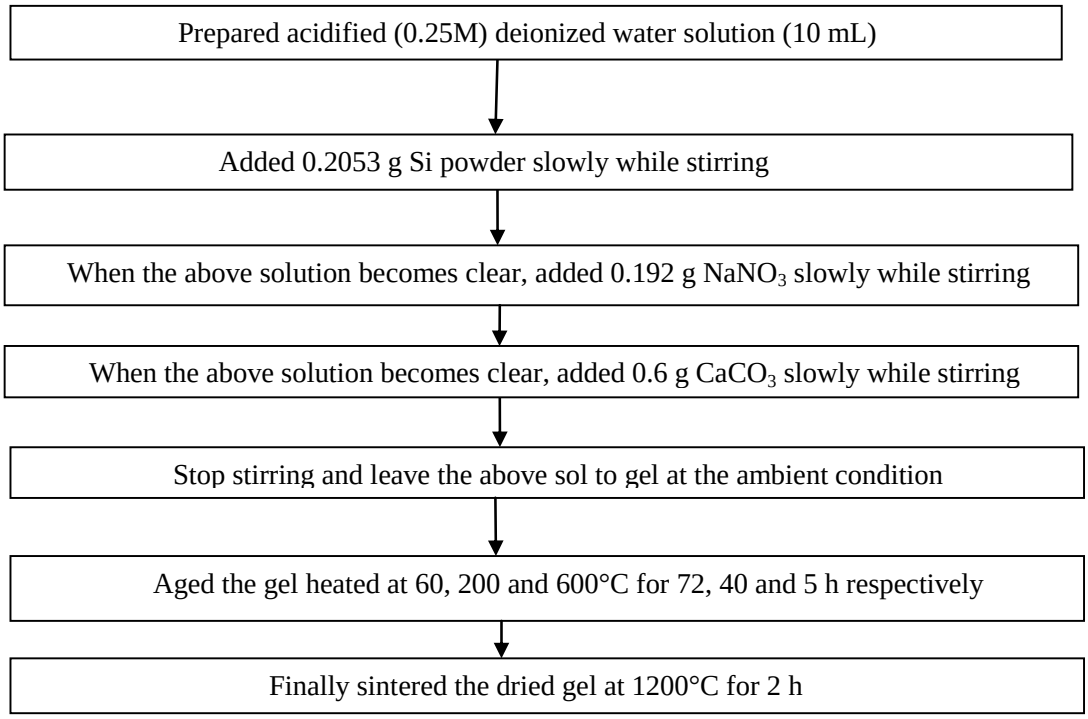

Fig.4.1 Schematic representation of steps involved in preparation of biocomposite material by sol-gel process (modified from **Chen et al., 2010** and **Hench et al., 1971)**.

4.2.3 Preparation of biocomposite material sample for its characterization

The prepared material was grounded in to powdered form by using mortar-pestle and incubated in to Simulated body fluid (SBF), 1.5 SBF and Dulbecco's modified Eagle's medium (DMEM) for 25 days. SBF is a solution with ion compositions similar to human blood, but without any proteins, hormones, glucose, or vitamins (**Plewinski et al., 2013**). 1.5 SBF contains ions concentration 1.5 times more than SBF and help in rapid formation of HAp (**Tanahashi et al., 1994**). The SBF and 1.5 SBF solution was prepared as per methodology describe by Kokubo and Tanahashi (**Kokubo and Takadama, 2006; Tanahashi et al., 1994**). 0.5 g powder of synthesized biomaterial was immersed in to SBF (50 mL, pH 7.4) and 1.5 SBF (50 mL, pH 7.4) for 25 days at 37 °C after that centrifuge the mixture at 8000 rpm for 10 min remove the supernatant and kept it for further analysis and the pallet was washed with distilled water dry it at 105 °C and again grounded in to powder form by using mortar-pestle for further characterization. Similarly the grounded 0.5 g powder was also immersed in DMEM (50 Ml, pH 7.4) with 10%

heat-inactivated fetal bovine serum, 0.1% penicillin/streptomycin and placed at 37 °C with 5% CO_2 (**Chen et al., 2010)** for 25 days and prepared the sample by the above described process for its further characterization.

4.2.4 Characterization of biocomposite material

Morphology, morphological changes, elemental composition, bond angles, bonding patterns, mineralogy of the biocomposite material was analysed by Scanning electron microscopy (SEM), Energy Dispersive X-ray (EDX) spectroscopy, Fourier Transform Infrared Spectroscopy (FT-IR), X-ray diffraction (XRD), Inductively coupled plasma mass spectrometry (ICP-MS).

4.2.4.1 SEM-EDX analysis of biocomposite material

SEM analysis was performed for viewing morphology and morphological changes takes place in biocomposite material after immersion in SBF, 1.5 SBF and DMEM. The dried powder of prepared material was mounted on aluminum stubs and sample was coated with 90 Å thick gold-palladium coating in polaron Sc 7640 sputter coater (Carl Zeis, Germany) for 30 min. Coated samples were viewed at 20 KV with scanning electron microscopy (Leo Electron Microscopy Ltd., Cambridge) at various magnification.

Energy Dispersive X-ray (EDX) spectroscopy of dried material was performed for elemental analysis of qualitative analysis of the elemental composition of material. The dried powder was mounted on aluminium stubs and the analysis was performed at 20 kV on Dx4 Prime EDX spectrometer (Bruker, Germany) equipped with X-flash detector.

4.2.4.2 FT-IR analysis

Functional groups analysis of biocomposite material was performed by Fourier Transform Infrared spectroscopy (FT-IR). For FT-IR analysis, dried material powder was properly mixed with potassium bromide (KBr) with the help of motor-pester and compressed to prepare a salt disc of about 3 mm diameter. IR spectroscopy of the disc was recorded Varian 7000 FTIR spectrometer (Perkin-Elmer Inc., Wellesley, MA, USA) at room temperature, in the frequency range of 400 to 4000 cm^{-1}, for 64 scans per sample at a resolution of 4 cm^{-1}.

4.2.4.3 XRD analysis

The dried powder form of prepared material was analyzed by X-ray diffraction pattern for its mineralogical study. For diffraction analysis, X-pertsystem; PANalytical equipped with 'X' pert Pro software having Cu, (K-α) radiations (40 kV, 25 mA). The data was collected over 1 h = 5-80º with step size or offset was 0.001 and counting time 10 s per step. Diffractogram was taken for each sample that gave a specific Pick list in diffractogram. 'X' pert high score software was used for analysis of diffractogram which suggested the presence of minerals in the samples. The analysis of bioactive material by X-ray diffraction method was performed to define its crystal structure (**Chen et al., 2010**).

4.2.5 Measurement of ionic concentration in the SBF, 1.5SBF, DMEM and change in pH of the medium

Measurement of ionic concentration of calcium (Ca), sodium (Na) and phosphorous (P) was performed using Agilent's 7900 inductively Coupled Plasma Mass Spectrometry (ICP-MS) equipped with Ultra High Matrix introduction (UHMI) technology. The 0.5 g sample was immersed in 50 mL of above mention medium and after 25 days supernatant was used to analyze the ions concentration in the medium. Simultaneously the pH of the medium was also measured by using portable pH meter.

4.2.6 Cytotoxicity test

3-(4,5-dimethylthiazol-2-yl)-2,5-diphenyltetrazolium bromide (MTT) assay was used as an overall indicator of cytotoxicity. This method is based on the ability of living cells to reduce dissolved MTT (yellow) into insoluble formazan (blue) in the presence of mitochondrial succinate dehydrogenase (**Mosmann 1983**). In the present study the prepared biocomposite material was tested using two different methods, as described by **Navarro et al (2004)** with slight modification, one involving direct exposure of biomaterial with cultured MG-63 osteosarcoma cell and another wherein the cells were exposed to the extract of the biomaterial.

4.2.6.1. Cell culture

MG-63 osteosarcoma cell line, isolated from a human osteogenic osteosarcoma, were cultured in Dulbecco's Modified Eagle's Medium (DMEM) supplemented with 10% foetal bovine serum, 1% antibiotic antimycotic solution and were maintained at 37 °C in 5 % CO_2 humidified incubator. Fresh culture media was reinstated, replacing the yellow turned culture media every two days. Further, the cells' monolayers rinsed with phosphate buffered saline (PBS) and detached by flushing and incubating them with Trysin-EDTA (0.25%) (5 min at 37 °C) were used for making sub-cultures. Reculturing of the detached cells was done following the two conditions for the cytotoxicity test.

4.2.6.2 Preparation of the extracts

Extracts for indirect test were obtained from the biocomposite material under sterilized conditions. The autoclaved biocomposite material were immersed in complete culture medium (1:50 g/mL ratio) in Falcon tubes and incubated at 37 °C, with occasional stirring. The crude fluid was obtained after 24 h, 3, 6, 12 and 25 days of incubation, the fluid was inoculated in the cell cultures for toxicity analysis.

4.2.6.3 MTT assay

For direct evaluation of cytotoxicity, in a 24 well plate, cells were cultured along with the sterilized biomaterial (10 mg) at a concentration of $7x10^4$ cells/well with 50 µL of DMEM per well. After 30 min of incubation, 500 µL of the culture medium were added to each well. Here, the polysterene standard culture microplate without the biocomposite material was used as negative control. For indirect effect evaluation, in wells seeded with the same concentration of cells as above, the medium was changed for the undiluted extracts (500 µL /well) after confluency. Here also, the supplemented DMEM was used as negative control. In both cases, direct and indirect methods, 50 mM BaP was used as the positive control.

Cytotoxicity was assessed using MTT assay according to **Mosmann (1983)**. In order to measure the cell viability, 1 mL of MTT solution (10% in culture medium) was added after 24 h,

3 and 6 days, to each well for the direct contact method, while MTT solution (1 mL) was added after 24 h and 3 days of culture in the case of indirect method. This was followed by the incubation of cells in dark at room temperature for 3 h and then absorbance measurement at 570 nm using an microplate reader (Biorad, USA). The results were expressed as the averaged absorbance levels of triplicates. The statistical significance ($P < 0.05$) of the differences in the absorbance values was determined using Tukey multiple comparison test.

4.3 Results and Discussion

4.3.1 SEM analysis of biocomposite material

Surface morphology of sintered biocomposite material, before and their bioactivity was observed after immersion in SBF, 1.5 SBF and DMEM for 25 days **Fig.4.1.a,b,c,d**. The surface characteristics such as surface porosity and morphology of the implants help in regulation of cell proliferation, cell attachment and protein adsorption (**Paital and Dahotre, 2009**).

a b

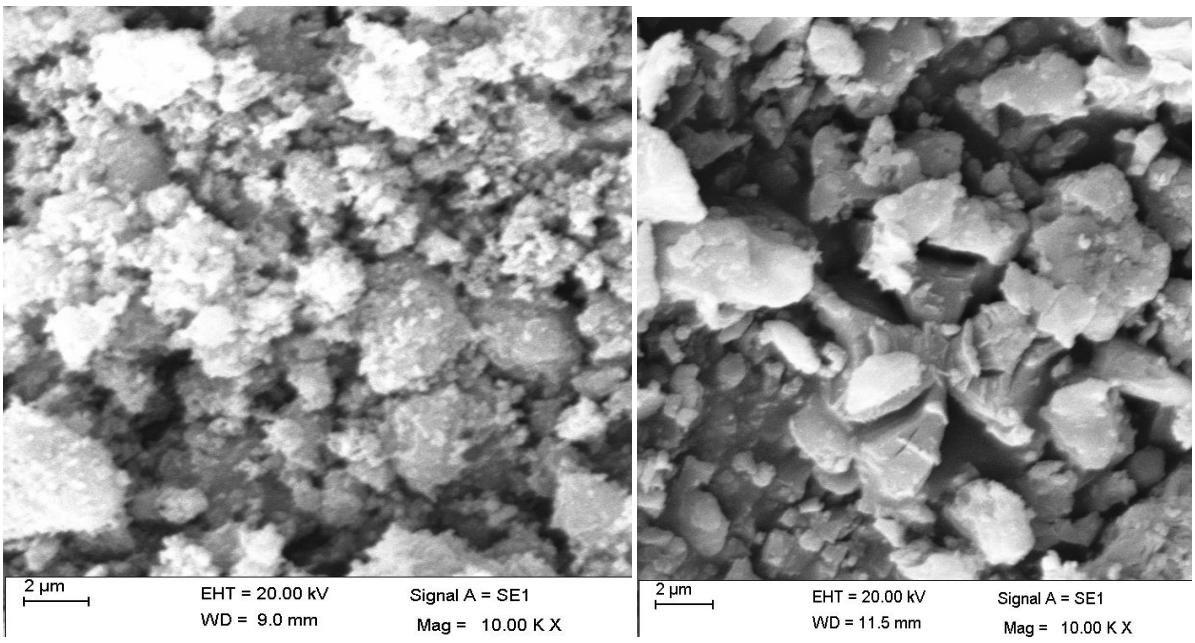

c d

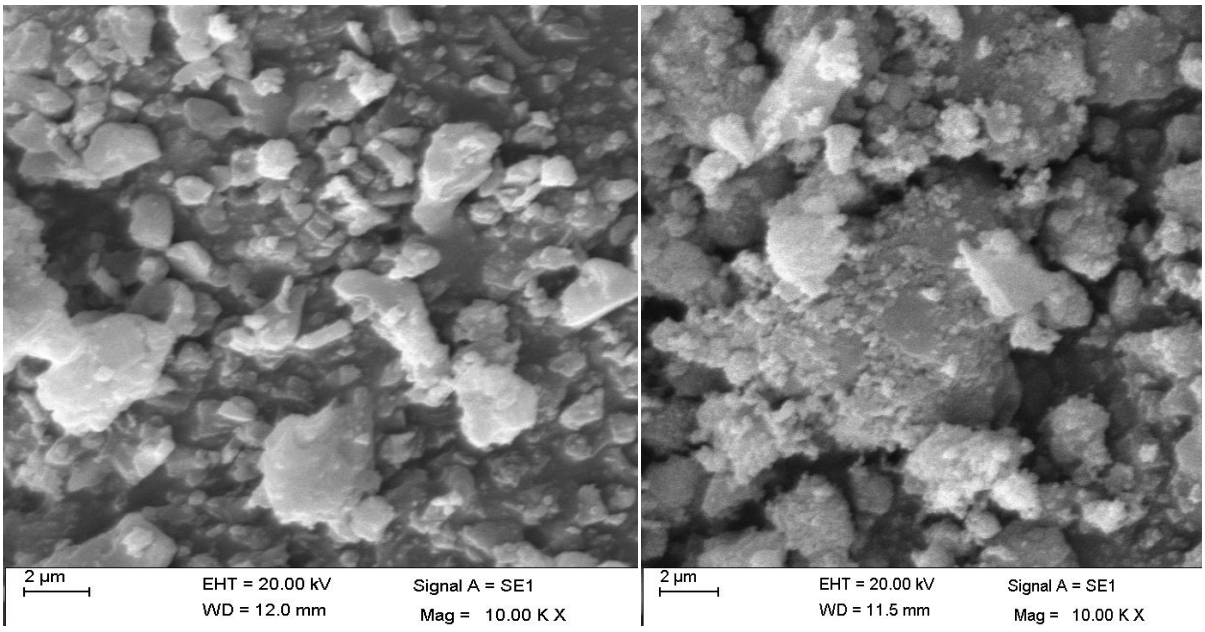

Fig.4.2 SEM analysis of biocomposite material, all the images at same magnification (a) without immersion (b) Bioactivity in SBF (c) Bioactivity in 1.5 SBF (d) Bioactivity in DMEM.

SEM image (**Fig4.2 a**) of sintered biocomposite material powder before immersing in SBF solution and DMEM shows porous surface and agglomerated morphology. Porous property of this sintered material might be due to release of gases during its formation at higher temperature. Porous material facilitates the ion exchange between the ceramics and SBF, accelerates the dissolution reaction and simultaneously apatite formation, it has been documented previously. Porous and agglomerated structure of the material also increases the Interaction between the implanted material and the surrounding tissues (**Saiz et al., 2002; Montenero et al., 2000; Lakshmi et al., 2013**). **Fig.4.2.b,c,d** depicts SEM image of biocomposite material powder after immersion in SBF, 1.5SBF and DMEM for 25 days. It reveals that the biomaterial showing more bioactivity due to deposition of smaller particle like appearance throughout the surface. Appearance of minute constituent cluster reveals the formation of hydroxyapatite. These

morphological changes in the biocomposite material confirm that this material is able to increase the efficiency of biomineralization of hydroxyapatite on the surface of implanted material.

4.3.1.1 EDX analysis of biocomposite material

Elemental composition of sintered biocomposite material as well as immersed material in SBF, 1.5 SBF and DMEM was analyzed by EDX **Table.4.1, Fig.4.2**.

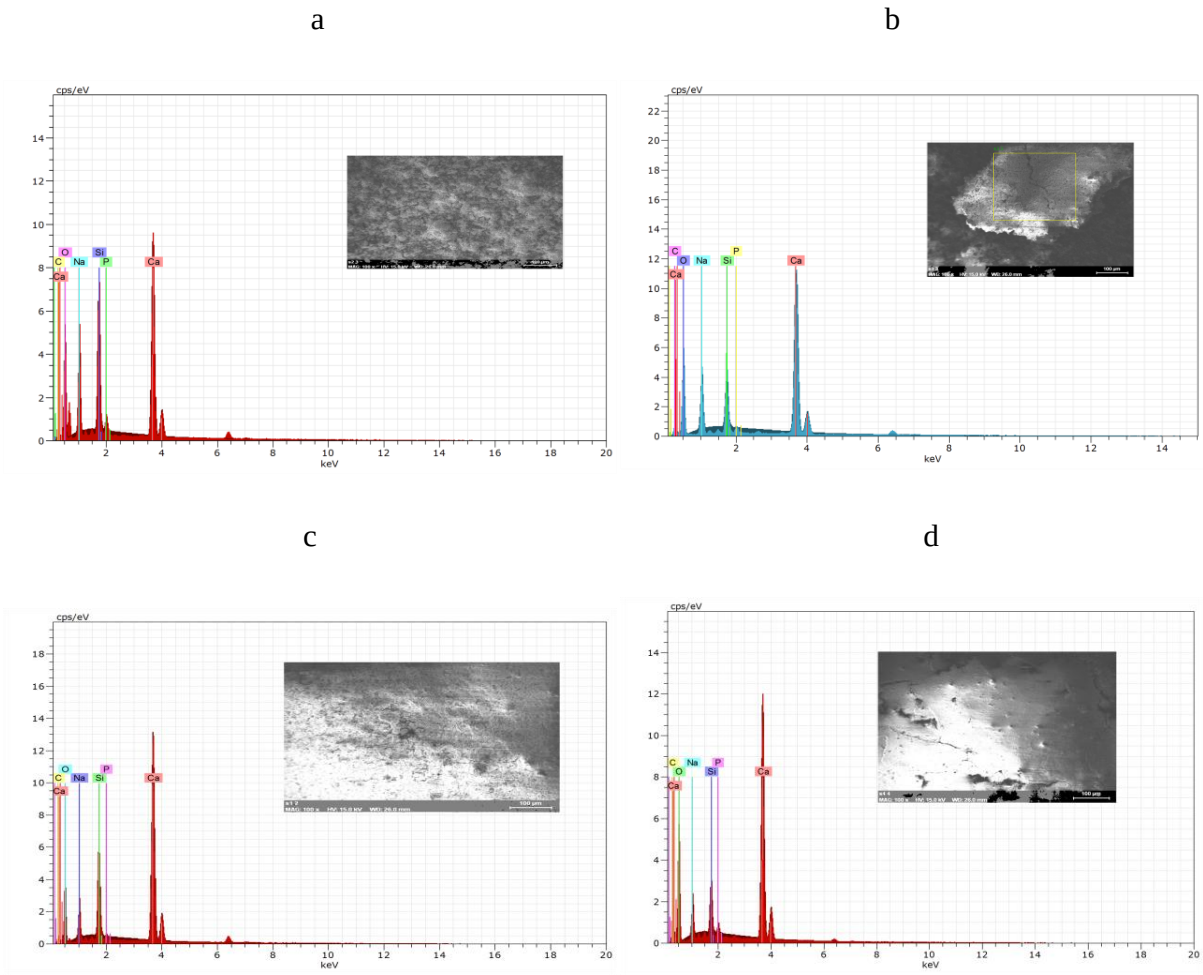

Fig.4.3 Elemental composition analysis of Sintered biocomposite material (a) before immersion (b) in SBF (c) in 1.5SBF (d) in DMEM for 25 days by EDX.

Table.4.1 Elemental composition analysis (qualitatively) of Sintered and immersed biocomposite material in SBF, 1,5SBF and DMEM by EDX.

Sample	At. wt% of Ca	At. wt% of Si	At. wt% of Na	At. wt% of P	At. wt% of C	At. wt% of O
Sintered	15.51	7.15	8.21	0.03	4.41	64.78
SBF	13.45	2.86	5.84	0.41	3.80	73.51
1.5SBF	22.29	6.39	4.44	0.52	1.92	64.44
DMEM	17.43	2.40	3.06	0.38	7.20	69.53

Observation of bicomposite material by SEM analysis revealed morphological changes takes place in biocomposite material after immersion in SBF, 1.5SBF and DMEM for 25 days. However, this kind of morphological changes cannot convincingly identify the chemical composition of mineral precipitates, so the elemental analysis of the sample required. EDX analysis **Table.4.1 Fig.4.3 (a,b,c,d)** revealed that in the sintered sample almost negligible contribution of phosphorous (P) as compare to overall elemental At. wt% of material, but after immersion in SBF, 1.5SBF and DMEM the P At. wt% increased. The increase in P At. wt% in the material could be due to replacement of $SiO4^{2-}$ by $PO4^{3-}$ or $HPO4^{2-}$ may lead to formation of HAp ($(Ca)_5(PO4)_3OH$).

4.3.2 FT-IR analysis

FT-IR analysis of sintered and immersed biocomposite material in SBF, 1.5SBF and DMEM was performed to investigate the functional group present in sample **Table 4.2 Fig.4.4**.

Table.4.2 Representation of peaks and their corresponding annotation of biocomposite material.

Peak(cm^{-1})	**Bonds and Corresponding annotation**
414.69	O-Ca-O bending
640.36 and 682.79	O-Si-O bonding
935.47 and 974.04	Si-O stretching modes
1024.19	Symmetrical stretching vibration of Si-O-Si
1400.31	Distorted carbonate group
1637.56	Bending vibration of H_2O
3439.07	Moisture absorption band (OH)

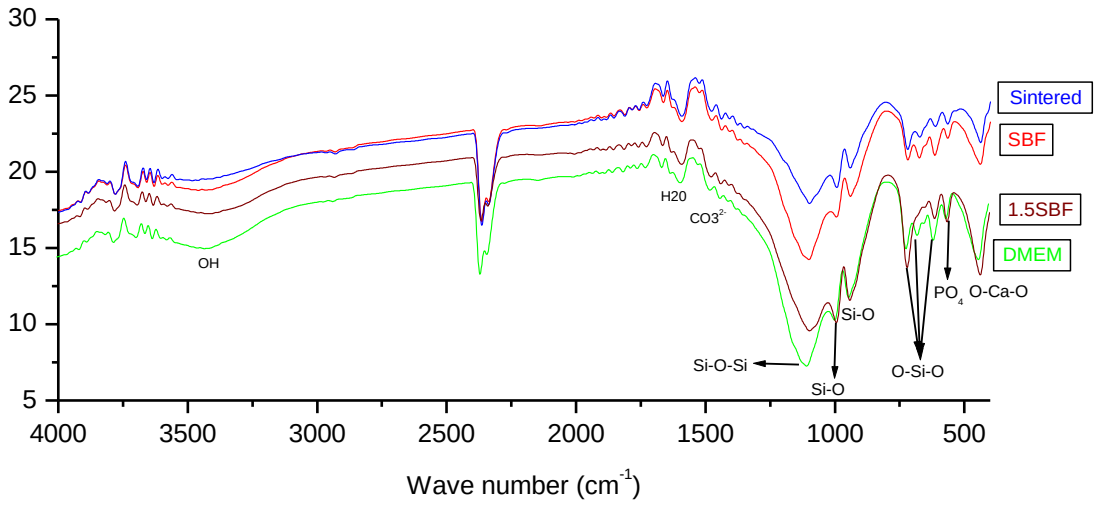

Fig.4.4 FT-IR spectra of sintered biocomposite material and immersed material in SBF, 1.5SBF and DMEM.

Peak obtained at 414.69 represent O-Ca-O bending mode. The O-Si-O peaks were observed at 640.36 and 682.79 $cm^{-1.}$ Peaks at 935.47 and 974.04 cm^{-1} designated to the Si-O stretching modes. Symmetric stretching at 1024.19 cm^{-1} was assigned to Si-O-Si vibration and asymmetric stretching at 1400.31 cm^{-1} is due to the dissolution of CO_2 in silicate bio-ceramics and results in the formation of distorted carbonate group (**Choudhary et al., 2015**). Bending vibration of H_2O was observed at 1637.56 cm^{-1} and broad moisture absorption band was observed at 3439.07 cm^{-1} (**Engin et al., 2006; Choudhary et al., 2015**). Peak of Na_2O bonding was not identified by the FT-IR analysis due to the highly volatile nature of $NaNO_3$ at higher temperature and its dissociated constituent Na_2O (**Chen et al., 2010**).

4.3.3 XRD analysis

Fig.4.5 (a) shows the XRD spectra of the un-sintered (600°C) and sintered biocomposite material. The crystalline phase $Na_2Ca_2Si_3O_9$ was identified in the sintered powders. Before the sintering of the material, the major peaks are identified as calcite ($CaCO_3$) and cristobalite (SiO_2) and XRD pattern shows that the un-sintered material is in amorphous form. After sintering at 1200°C for 2 h the crystallization and transformation of material take place and the major peak identified in the material was wollastonite ($CaSiO_3$).

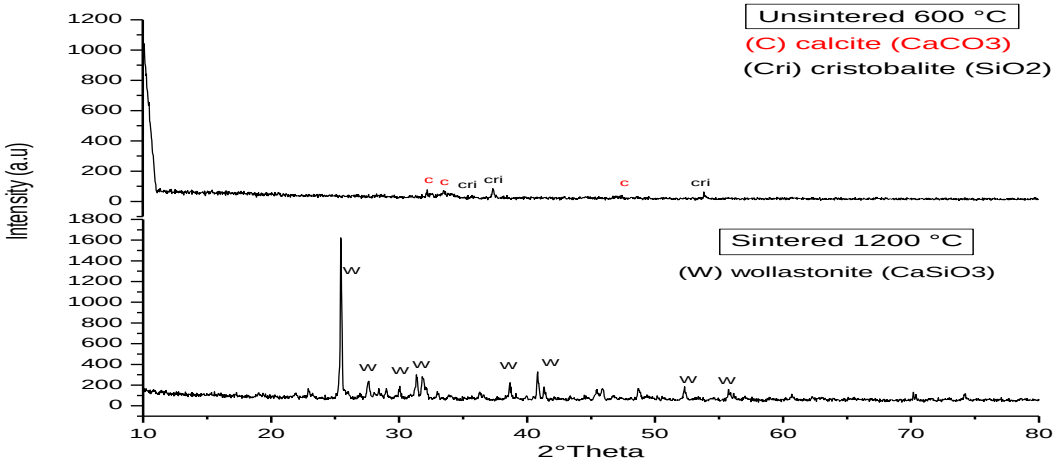

Fig.4.5 (a) XRD pattern of un-sintered (600°C) and sintered (1200°C) biocomposite material.

Silicate based bioactive glasses shows good bioactivity due to presence of silica rich layer on the glass surface, which facilitates the bond formation between bioactive glass and the bone mineral. When bioactive materials are immersed to aqueous phase environment, such as SBF and DMEM to examine its in-vitro and in-vivo bioactivity respectively, both chemical and structural transformation takes place on the surface of materials with respects to time. During dissolution of the material in aqueous environment, cations from material surface exchanged with H^+ ions available in the media, leads to increase in OH^- concentration in the media later on these OH^- ions reacts with silica present in the biocomposite material. As a result of this hydrolysis reaction, breaking of Si-O-Si bonds takes place, leads to formation of new bond silanol (Si-OH) and subsequently increase in the pH of the aqueous medium (**Choudhary et al., 2015)**. The newly formed silanol group act as nucleation site for formation of HAp on the interface of osteogenic tissue and implanted bioactive glass due to utilization of calcium and phosphate ions present in the medium by silanol group. The nature of the materials, circulation of the medium and incubation time is the crucial factors to determine the bioactivity of these bioceramics and glasses (**Liu et al., 2004; Kokubo, 1998; Tavangarian and Emadi, 2011**).

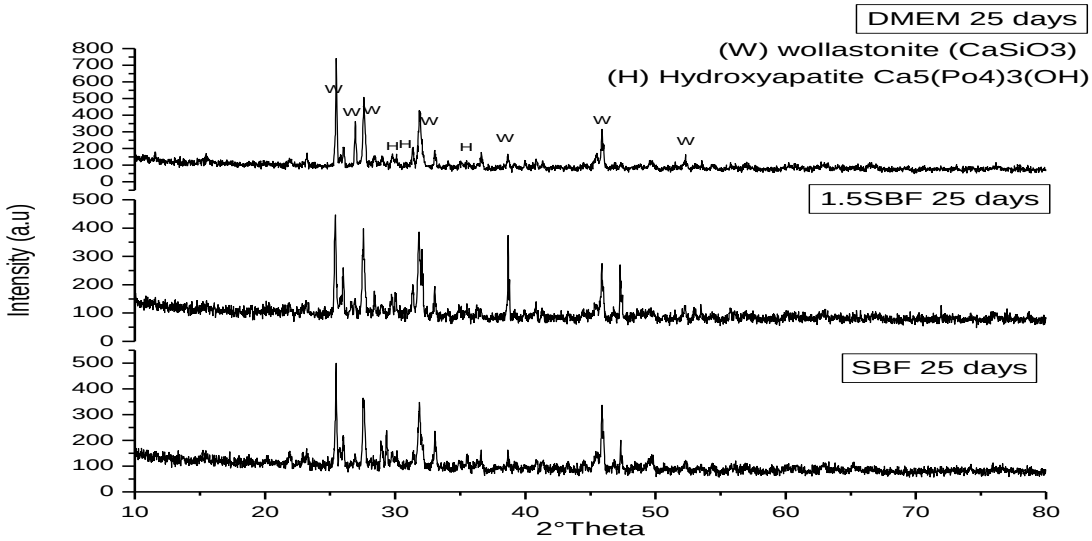

Fig.4.5 (b) XRD of sol-gel derived biocomposite material immersed in DMEM, SBF and 1.5SBF for 25 days.

The XRD analysis of present sol-gel derived biocomposite material **Fig.4.5 (b)** possess the important features similar to melt-derived Na_2O-containg glass ceramics like formation of crystalline phase $Na_2Ca_2Si_3O_9$ after sintering, presence of wollastonite ($CaSiO_3$) forms in the crystallized biocomposite material and remained in the material when incubated in SBF, 1.5SBF and DMEM along with formation of HAp. The formation of HAp in the material signifies that this biocomposite material can have both good bone bonding ability as well as degradability. It has when previously reported that amorphous HAp and associated amorphous calcium phosphates have been shown these type of characteristics (**Hench, 1998**).

4.3.4 Measurement of pH and ions released in the medium

Initially (before immersion) the pH of the medium was 7.4, after incubation for 25 days the pH of the medium are increased to 7.8 (SBF), 7.9 (1.5SBF) and 7.8 (DMEM) **Table.4.3**. The increase in pH of the medium is better explained by the release of Na^+ ions in the medium from the material (**Chen et al., 2010**). As compared to previous report **(Peitl et al., 2001; Clupper et al., 2002; Saravanapavan and Hench, 2003; Chen et al., 2008; Saravanapavan et al., 2003**) the increment of pH of the medium is slow might be due to non-replacement of media though out the immersion, released ion in the medium would slow down further release of ions from the materials into solution (**Chen et al., 2010**). Exchange of ions from the material after immersion in solution was analyzed by ICP-MS **Table.4.3**. ICP-MS analysis revealed that the ion exchange between the crystalline phase biocomposite material and its solution in which this material immersed for 25 days leads to change in the crystalline morphological structure of the biocomposite which is also analyzed by SEM analysis.

Table 4.3 ICP-MS analysis of ions present in the medium before and after immersion in SBF, 1.5SBF and DMEM.

Sample	**SBF**	**1.5SBF**	**DMEM**
Before immersion Ca Conc (ppb) ± RSD	98215± 9.76	141378± 8.13	71326± 7.45
After immersion Ca Conc (ppb) ± RSD	97952± 5.21	128734± 5.21	69831± 4.32
Before immersion Na Conc (ppb) ± RSD	3152198± 12.31	4689581± 11.22	3395821± 5.67
After immersion Na Conc (ppb) ± RSD	3213216± 6.17	4713496± 5.62	3412746± 8.91
Before immersion P Conc (ppb) ± RDS	30472± 3.10	44121± 4.72	27582± 6.72
After immersion P Conc (ppb) ± RSD	29192± 6.47	42191± 10.24	26219± 4.33
Before Immersion pH	7.4	7.4	7.4
After immersion pH	7.8	7.9	7.8

In the present study Na^+ have been exchanged with Ca^{2+} which is confirmed by increase in concentration of Na^+ in the solution and decrease in Ca^{2+} concentration in solution also decreases in P concentration in the solution revealed that might be exchange of PO_4^- takes place with SiO_4^{2-} of the biocomposite although analysis of SiO_4^{2-} was not performed by the ICP-MS. This type of analysis was also reported by the various researchers and the present report is good agreement with previous report (**Chen et al., 2010; Chen et al., 2007**).

4.3.5 Cytotoxicity test by MTT- assay

The results of the MTT assay for effect of direct and indirect contact of the biocomposite material with the osteosacrcoma cells revealed a non-cytotoxic effect as depicted by **Fig.5.6a** and **Fig.5.6b** respectively. The cytotoxicity in all the samples was less than that of BaP (50 mM).

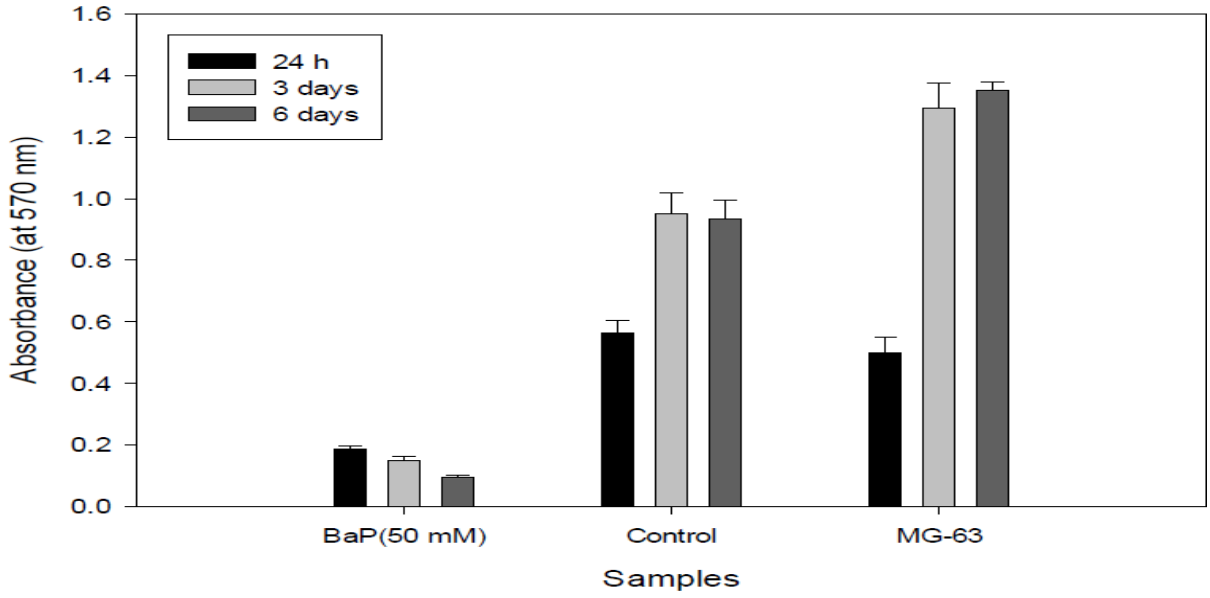

Fig.5.6a MTT assay of the effect of the biocomposite material (MG-63) in direct contact with cells after 24 h, 3 and 6 days of culture. Vertical lines represent ±SD.

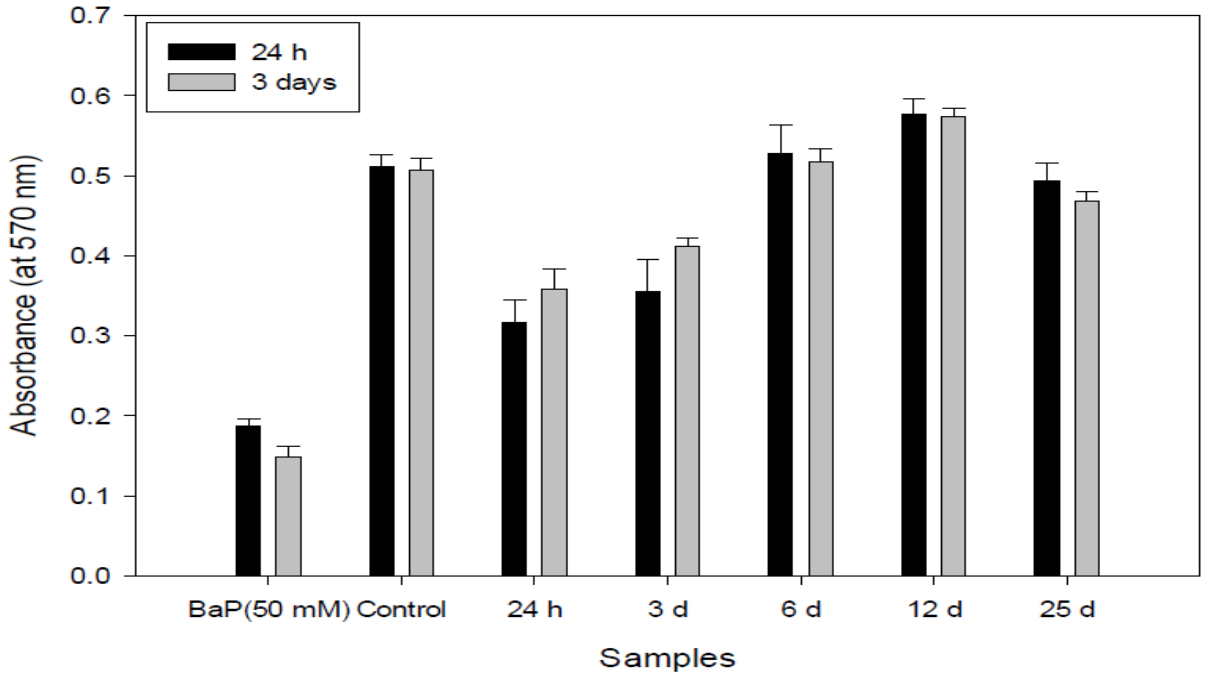

Fig.5.6b MTT assay performed with the biocomposite material extracts and osteoblastic cells after 24 h and 3 days of culture. Vertical lines represent ±SD.

The result of MTT-assay obtained for the direct contact, increase in absorbance **Fig.5.6a** confirmed that increase in the cell viability with time and cell number for both control and treated material, particularly after 3rd days of cell culture. It was observed that in 24 h of cell culture there were not much significant differences occurs between the control (polysterene culture plate with DMEM) and the synthesized biocomposite material, but after 3 and 6 days of culture, the significant increment in absorbance values was observed as compare to control. With increasing cell culture time the direct contact experiment results suggesting that, the viability of cells increased significantly from 3 to 6 days, which confirmed the non-toxic behavior of biocomposite material, also this material enhanced the growth and proliferation of the cells (**Navarro et al., 2004**).

In the other experiment where different time interval construct supernatant was used to grow the cells **Fig.5.6b**, not significant differences in cell viability were observed after 24 h of cell culture between the various construct supernatant and the control sample. In contrast, after 3 days of cell culture, increments in cells viability was observed for the construct supernatant obtained after longer soaking durations. In fact, the major cell viability differences visualized between the construct supernatant obtained after soaked in DMEM for 6 and 12 days and those obtained after soaked in 12 and 25 days were statistically significant ($P < 0.05$). Decrease in cells growth of 25 days sample as compare to control and 12 days sample probably due to increase in ions concentration in the medium. Although this range of ions concentration did not affect the growth of cells so some other study required, like effect of various ions concentration on the cellular growth as well as duration in which the cells are in contact with ions.

4.4 Conclusions

Utilization of $CaCO_3$ precipitated by CO_2 sequestering *Serratia* sp. ISTD04 for the synthesis of biocomposite material powder using the sol-gel technique under ambient environmental condition has been performed successfully. The sol–gel derived and sintered biocomposite material having the essential features of Na_2O-containing bioactive materials, mainly the formation of crystalline phase $Na_2Ca_2Si_3O_9$ during sintering and formation of amorphous hydroxyl apatites without losing its crystallinity when it get immersed in SBF,

1.5SBF and DMEM for 25 days, this study revealed this material have good mechanical properties as well as biodegradability. ICP-MS study of immersed material revealed that exchange of ions takes place between the material and aqueous environment, which favour the formation of hydroxyl apatites. MTT-assay confirmed that this material and their supernatant did not have any cellular cytotoxicity.

Chapter 5: Production, characterization and optimization of process parameter for polyhydroxyalkanoate by carbon dioxide sequestering chemolithotrophic oleaginous bacteria

5. Production, characterization and optimization of process parameter for polyhydroxyalkanoate by carbon dioxide sequestering chemolithotrophic oleaginous bacteria.

5.1 Introduction

The world today is facing twin crises of rising carbon dioxide (CO_2) emission leading to climate change as well as environmental deterioration by accumulation of non-biodegradable compounds such as plastics. On one hand, the concentration of CO_2, the primary green house gas, has increased approximately 43 % since industrial revolution and is projected to increase by 60 % in 2100 if the current trend continues. Such an unabated accumulation of CO_2 in the atmosphere will put our planet at the greatest risk of irreversible changes. CO_2 capture and storage by autotrophic biota and some chemoautotrophic and chemolithoautotrophic bacteria possessing CO_2 fixing enzymes like Ribulose-1,5-bisphosphate carboxyl- ase/oxygenase (RuBisCO), is one of the mitigation options (**Bharti et al., 2014a**).

On the other hand, global plastic production, mostly derived from fossil fuels, has been continuously rising with almost 299 million tons of plastics produced in 2013 which was 3.9 % higher than 2012's output and is projected to further increase at a moderate rate in the coming years (**Kumar et al., 2016e**). Easy synthesis, availability and low cost are the major drivers of the growing plastic industry. However, insufficient recovery, recycling and waste degradation time of 100 to 1000 years is leading to an annual accumulation in millions of tons, of this man made material, mostly at landfills and in oceans. Some bacteria have the capability to naturally accumulate, within their cells, such biopolymers that exhibit similar physical and mechanical properties to oil-based plastics. Therefore, one of the most cost effective and sustainable methods to alleviate this dual challenge of high CO_2 and plastic accumulation is through culturing of such microorganism that are capable of fixing atmospheric CO_2 along with production of easily degradable biopolymers.

Polyhydroxyalkanoates (PHAs) are biodegradable, biocompatible and thermostable biopolymers that are synthesized by several bacteria as intracellular materials for the storage of

carbon/energy usually in the presence of high carbon concentration and growth limiting nutrient environments (**Kumar et al., 2017b**). Structurally, PHAs are polyesters, which contain (*R*)-hydroxyacyl monomeric units. The side chain *R* group of each monomer unit is commonly a saturated alkyl group but may occur in other forms like unsaturated, branched or substituted (**Lu et al., 2009**). Depending on the bacterial strain employed and the growth substrates supplied, PHA can be synthesized as homopolymers or copolymers or even their mixture. On the basis of total number of carbon atoms present in each monomeric unit, PHA may be a short-chain length PHA (scl-PHA) with 3 to 5 carbon atoms, medium-chain length PHA (mcl-PHA) having 6 to 14 carbon atoms, long-chain length PHA (lcl-PHA) containing 15 or more carbon atoms or copolymer of scl-mcl PHA copolymer consisting of monomeric subunits with 4 to12 carbons (**Khanna and Srivastava, 2005**).

Among the nearly 150 different PHA monomers identified till date, Poly (3-hydroxybutyrate) (PHB), poly-β- hydroxyvalerate (PHV) are the most studied and best-characterized form of scl-PHA Other forms, commonly synthesized by microbes are mcl-PHA like poly (3- hydroxyhexanoate) (PHH), poly (3-hydro-xyoctanoate) (PHO) (**Chaitanya et al., 2014**) and copolymers like Poly (3-hydroxybutyrate-*co*-3-hydroxyvalerate) (PHBV) and poly(3-hydroxybutyrate-*co*-3-hydroxyhexanoate) (PHBHHx) (**Noda et al., 2005**). Both Gram positive and Gram negative bacteria have been known to produce PHA and the synthesis may follow different pathways such as an enoyl-CoA hydratase, Methyl malonyl-CoA pathway for PHBV synthesis from sugars represented by *Ralstonia eutropha,* from fatty acids or carbohydrates as represented by the Pseudomonads. *Alcaligens latus, Azotobactor vinilandii, Serratia* sp, *Bacillus* sp. are some other commercially important strains for PHA production (**Thakur et al., 2018**).

An increasing global PHA market has been attracting companies such as Metabolix (U.S.), Meredian Inc. (U.S.), Ecomann (China), Biocycle (Brazil), Biomer (Germany), and Bio-on (Italy) to invest in increasing PHA production capacities. The global bioplastics production capacity was estimated at 1.7 million tonnes in 2014, with a 2 % contribution of PHA. The global bioplastics market is projected to reach 5.8 billion US dollars in 2021 (**Kumar et al., 2016d**). However, the main stumbling block to the growing PHA market is its high cost of production.

Hence, there is a need to search low cost sustainable alternatives along with optimization of process parameters for higher production of these biopolymers. Lately, researchers in this field are focussing more on screening low cost sustainable alternatives along with optimization of process parameters for maximizing production efficiency of these biopolymers (**Zhu et al, 2010; Hong et al., 2009**). One of the statistical techniques' for optimization is Response surface methodology (RSM). Previous studies have reported the use of RSM for increased production of PHAs by different bacterial strains such as *Bacillus coagulans, Rhodobacter sphaeroides* and *R. eutropha (***Kim, 2000*;* Hoseinabadi et al, 2015**). The objectives of this study were to screen a previously described carbon concentrating oleaginous bacterial strain *Serratia* sp. ISTD04 for production of PHA using bicarbonate and glucose as carbon sources, characterization of the PHA, and optimization of the process parameters for enhanced PHA and biomass generation using Response Surface Methodology (RSM).

5.2 Materials and methods

All the chemicals and reagents used in the present study were of analytical grade procured from Sigma-Aldrich (St. Louis, MO, USA), Merck (Darmstadt, Germany) or HiMedia unless stated otherwise.

5.2.1 Microorganism and culture condition

A previously reported carbon concentrating bacterial strain *Serratia* sp. ISTD04 (gene bank accession number- JF276275) isolated from marble rocks of the palaeoproterozoic metasediments of the Aravali Supergroup, Rajasthan, was used for the study of PHA production. The bacterial strain was procured from a chemostat culture maintained at 30 °C, 150 rpm and pH 7.6 in Minimal salt medium (MSM) containing (g L^{-1}): $Na_2HPO_4 \cdot 2H_2O$, 7.8; KH_2PO_4, 6.8; $MgSO_4$, 0.2; $NaNO_3$, 0.085; $ZnSO_4.7H_2O$, 0.05; $ZnCl_2$, 0.02; Ca $(NO_3)_2.4H_2O$, 0.05 and 20 mM $NaHCO_3$ as the sole carbon source (**Bharti et al. 2014b**). Pre-LB cultured biomass of the strain was centrifuged (7000 rpm, 10 min) and the cell pellet transferred to mineral medium (MM) (pH 7.6) (**Numata et al., 2013**) containing (g L^{-1}): KH_2PO_4, 1.5; Na_2HPO_4, 6.78; NaCl, 0.5; $NH_4(CH_3COO)_3Fe$, 0.06; 1M $MgSO_4$, 2 mL L^{-1}; 1M $CaCl_2$, 0.1 mL L^{-1}; 1mL L^{-1} trace metal

solution consisting of (g L^{-1}): $ZnSO_4$, 0.1; H_3BO_3, 0.3; $CuSO_4$, 0.006; $NiCl_2.6H_2O$, 0.020; $Na_2MoO_4.2H_2O$, 0.030; $MnCl_2.2H_2O$, 0.25, supplemented with 20 mM $NaHCO_3$ and 1 % Glucose as carbon sources and incubated under aerobic conditions at 30 °C and 150 rpm for several days.

5.2.2 Screening of strain for PHA production

5.2.2.1 Microscopic visualization

Bacterial cells grown in MM and collected after 72 h incubation were taken on a clean glass slide, heat-fixed, stained with crystal violet for 10 sec followed by destaining with running water (10 sec) and then visualized under optical microscope (**Khandpur et al. 2012**).

5.2.2.2 Fluorometric visualization

PHA accumulation was observed fluorometrically with Nile red according to **Berlanga et al (2006)** but with slight modification. Briefly, 1 mL of the bacterial strain cultured in MM with 20 mM $NaHCO_3$ and 1 % Glucose as carbon sources was harvested at 72 h and cell pellet was washed thrice with PBS (Phosphate buffer saline, pH 7.4), fixed in Ethanol: Acetic acid (1:3) for 10 min, again washed with PBS and finally stained with Nile red (10 µg mL^{-1}) for 5 min. Cells were immobilized by mixing with 1 % low melting agarose in 1:1 ratio and mounted on glass slides prior to visualization under the microscope using epifluorescence (Zeiss HBO 100 fluorescence microscope) for the presence of PHA within the cells as indicated by the intensity of Nile-red fluorescence as measured at 560 nm excitation and 590 nm emission wavelengths.

5.2.2.3 Spectrofluorometric analysis of PHA accumulation

Accumulation PHA within the bacterial cells was observed spectrofluorometrically with Nile red following a modification of the procedure described by **Kimura et al (2004)**. Briefly, *Serratia* sp.ISTD04 was cultured in MM with 20 mM $NaHCO_3$ and 1 % Glucose as carbon sources and incubated under aerobic conditions at 30 °C and 150 rpm for 7 days. Fluorescence of bacterial culture was measured after staining with 10 µg mL^{-1}Nile red at 488 nm excitation

wavelength and 575 nm and 590 nm emission wavelengths for short and medium chain length PHA respectively, every 24 h with 0 h taken as control. The intensity of Nile-red orange fluorescence as measured using Shimadzu RF-5301 PC spectrofluorophotometer, indicated the presence of PHA within the cells. The growth of bacterial cells expressed as optical density (O.D.) at 595 nm on Cary 100 BIO UV-Visible Spectrophotometer was also recorded simultaneously.

5.2.3 Confirmatory analysis of PHA production

5.2.3.1 FTIR analysis

Serratia sp. ISTD04 cultured in MM with 20 mM $NaHCO_3$ and 1 % Glucose as carbon sources was harvested after 72 h and the collected cells were washed with MilliQ water and lyophilized. The accumulated PHAs were extracted from the dried cells with chloroform for 72 h at 70 °C, and then precipitated with 10 volumes of hexane, air dried and weighed (**Numata et al., 2013**). Fourier Transform Infrared Spectroscopy (FTIR) was used to record the PHA spectrum of the dried sample using Varian 7000 FTIR spectrometer (Perkin-Elmer Inc., Wellesley, MA, USA) at room temperature (25 °C). A paste of 0.01 g of the dried sample remaining after hexane precipitation was prepared in KBr and the spectrum was read in the range of 400 to 4000 cm^{-1}, applied for 64 scans per sample at 4 cm^{-1} resolution.

5.2.3.2 GC-MS analysis

To study the PHA content of the bacterial strain, the lyophilized and dried cells were processed according to **Numata et al., 2013**. Briefly, the dried cells were subjected to methanolysis in the presence of methanol (1.7 ml), 98% sulfuric acid (0.3 ml), and chloroform (2.0 ml) at 100 °C for 140 min followed by the addition of 1.0 ml of water to the reaction mixture for phase separation. The lower organic layer was used for gas chromatographic mass spectrometry (GC-MS) analysis on Shimadzu GC-MS-QP 2010 Plus equipped with a capillary column Rtx-5MS (dimensions: 0.25-µm film thickness, 0.25 mm ID, 30 m in length). 1 µL of the sample in chloroform was injected into GC-MS injector port and conditions were set with slight modifications: initial temperature 60 °C for 3 min; temperature increased from 60–320 °C at a

rate of 12 °C min^{-1}, hold time: 8min). Data were matched with the GC-MS inbuilt standard mass spectra library of NIST-05 and Wiley-8.

5.2.3.3 Transmission electron microscopy

Bacterial cells from 0 h (control) and 72 h culture in MM were taken and fixed by chilling to 4°C followed by addition of glutaraldehyde (2.5 %). They were then washed with PBS buffer (0.1 M, pH 7.2) and further fixed using 1% aqueous osmium tetraoxide (as secondary fixative) for 2 h at room temperature. Samples were then dehydrated with a graded series of acetone (50, 70, 90 and 100 %) with incubation of 2 h at each concentration, except for the 70 % ethanol, which was performed overnight. Samples were infiltrated with an araldite mixture CY212 (TAAB Laboratories Equipment, Berks, United Kingdom). Ultrathin sections were cut with a glass knife, counterstained with 2 % uranyl acetate and 0.2 % lead acetate and examined in a TEM (2100F, JEOL, Tokyo, Japan) at an acceleration voltage of 120 kV.

5.2.4 Optimization of PHA production

5.2.4.1 Culture conditions for Optimization Experiments

The optimization experiments were performed with *Serratia* sp. ISTD04, pre-cultured in LB and inoculated in 250 mL Erlenmeyer flasks under aerobic conditions, with 100 ml of MM at 30 °C and 150 rpm for 72 h and were supplemented with three different Bicarbonate concentration (20, 50 and 100 mM), % Glucose concentration (0.25. 0.50, 1.00) and pH ranges (4, 7, 10) as per experimental design. Based on the previous studies carried out on the bacterial strain by **Bharti et al (2014a)**, the ranges and levels of the three variables were selected. Both weight of PHA and biomass, were taken as response.

5.2.4.2 Determination of Biomass, isolation and determination of PHA weight in cells

Cell biomass expressed as cell dry weight per 100 ml of culture broth, was determined after centrifugation (8000 rpm, 15 min.), washing (with MilliQ water) and oven drying (60 °C, 24 h) followed by weighing of dry pellets. For PHA isolation, the biomass (lyophilized cells)

was treated with chloroform as mentioned in section 2.3. The hexane precipitated and dried sample were weighed to determine the PHA yield in grams per 100 mL culture.

5.2.4.3 Box–Behnken Design and Statistical Analysis

Optimization of the carbon sources' concentration and pH for maximum PHA and Biomass yield of *Serratia* sp. ISTD04 was done using Box–Behnken design (BBD) of Response surface methodology (RSM) with the help of Design Expert 9.0.6 software (Stat-Ease Inc., Minneapolis, USA). A set of 17 experiments were carried to evaluate the effects of the three variables viz., % Glucose concentration, pH and Bicarbonate concentration in mM, each with three different concentration levels (low (-1), medium (0) and high (+1)) on two responses, weight of PHA and biomass both measured in grams (g) per 100 mL culture. The experimental design matrix derived from the Box–Behnken model with the coded minimum, medium and maximum levels of the three variables and their actual values chosen for 17 different experimental shown in **Table.5.1**.

The BBD model for predicting the optimal conditions can be expressed in the form of a second order polynomial equation as follows:

$$Y = \beta_0 + \sum \beta_i x_i + \sum \beta_{ij} x_i x_j + \sum \beta_{ii} x^2_{ii} + \varepsilon \quad (1)$$

Where, β_0, β_i, β_{ij} are regression coefficients for the intercept, linear and interactions among different factors, respectively; Y is the predicted response; x_i and x_j are independent factors in coded units and ε is the random error term (**Ghosh et al., 2014**). Analysis of Variance (ANOVA) was used to determine the statistical parameters. The coefficient of regression (R^2) was calculated to find out the goodness of fit of the model. Significance of the model terms and equation was evaluated using F -test. Three dimensional response surface plots were obtained to visualize the individual and interactive effects of factors on the two responses. The level of each factor was optimized for maximum response generation by using the numerical optimization desirability function. Experiments were performed (in duplicate) at the predicted conditions and the results were compared with the model's predicted values to confirm the validation of the model.

Table.5.1 Box –Behnken design of independent variables for process parameters optimization.

	Coding			Actual		
Run	A	B	C	A	B	C
1	+1	0	-1	1	7	20
2	0	0	0	0.5	7	50
3	0	0	0	0.5	7	50
4	0	0	0	0.5	7	50
5	-1	0	+1	0.25	7	100
6	+1	-1	0	1	4	50
7	0	+1	-1	0.5	10	20
8	0	-1	-1	0.5	4	20
9	-1	-1	0	0.25	4	50
10	+1	0	+1	1	7	100
11	0	0	0	0.5	7	50
12	+1	+1	0	1	10	50
13	0	+1	+1	0.5	10	100
14	0	-1	+1	0.5	4	100
15	-1	0	-1	0.25	7	20
16	-1	+1	0	0.25	10	50
17	0	0	0	0.5	7	50

A: Glucose conc. (%) B:pH C: Bicarbonate conc. (mM)

5.3 Results and discussion

5.3.1 Strain selection for PHA production

A previously reported carbon concentrating oleaginous bacterial strain *Serratia* sp. ISTD04 (gene bank accession number- JF276275) isolated from marble rocks of the palaeoproterozoic metasediments of the Aravali Supergroup, Rajasthan, was used for the screening and study of PHA production in MM medium (pH 7.6) supplemented with 20 mM $NaHCO_3$ and 1 % Glucose as carbon sources and incubated under aerobic conditions at 30 °C and 150 rpm for several days. The strain has been previously reported to have extracellular lipid production along with possessing a carbon concentrating mechanism (**Bharti et al., 2014c**). The presence of two key enzymes involved in carbon capture viz., carbonic anhydrase and ribulose-1,5-bisphosphate carboxylase/oxygenase (RuBisCO) has been reported in this strain (**Bharti et al., 2014a and 2014b**). It has also been established that the strain has the potential of carbon dioxide (CO2) sequestration and biodiesel production (**Bharti et al., 2014c**).

The biosynthesis of PHA and fatty acids or lipids proceed through a common intermediate that is, (R)-3-hydroxyacyl-CoA, resulting from β-oxidation (Ren et al., 2000). Studies have been conducted on directing the metabolism of microorganisms for the production PHA via fatty acid pathways (**Magdouli et al., 2015**). *Serratia* sp, a gram-negative bacteria in the family Enterobacteriaceae, has commercially been used for the production of various enzymes, biosurfactants, bioplastics, and antioxidants. Lugg et al (2008) showed about 50% of cell dry weight accumulation of PHB in *Serratia* sp. In a recent study using *Serratia* ureilytica, isolated from PHA producing bioreactor was found to produce 51 % of cell dry weight PHBV using volatile fatty acids as substrate (**Reddy and Mohan, 2015**). Hence, based on the above literature, *Serratia* sp. ISTD04, being oleaginous bacterial strain was selected for study of PHA production along with carbon sequestration in the presence of bicarbonate and glucose as carbon sources.

5.3.2 Crystal violet staining

Microscopic visualization of heat fixed *Serratia* sp. ISTD04 cells taken from its culture grown in MM supplemented with 20 mM $NaHCO_3$ and 1 % Glucose and stained with crystal

violet (10 sec) followed by destaining with running water showed dark aggregates of the violet colored cells **Fig.5.1**. Crystal violet stain binds to the lipopolysaccharide molecules that are attached to the "outer membrane" of the Gram negative bacteria thus staining the cells. The results, thus qualitatively confirm the presence of PHA in the bacterial strain (**Ogunjobi et al., 2011**).

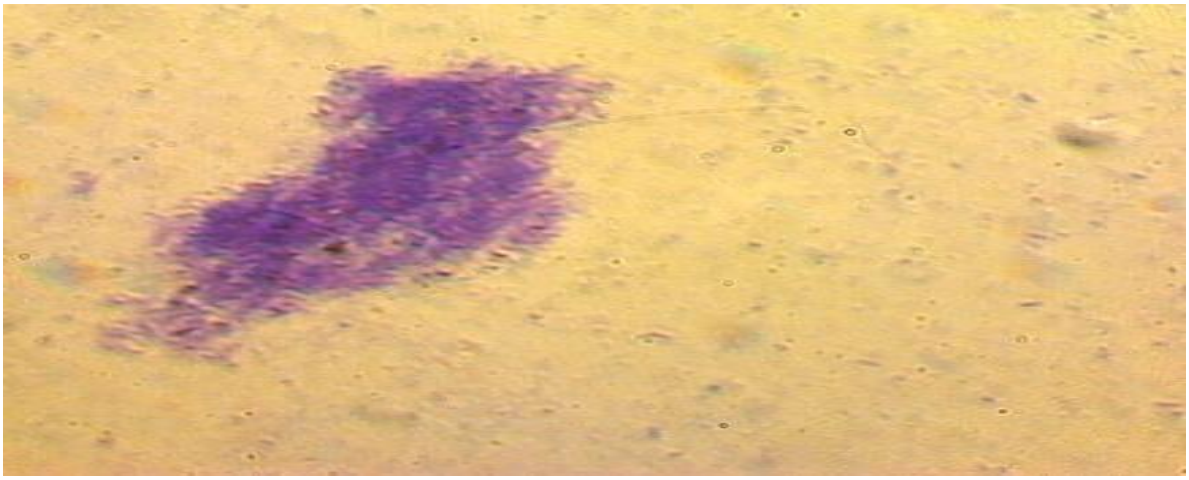

Fig.5.1 Staining of *Serratia* sp. ISTD04 with crystal violet showing violet cell clumps.

5.3.3 Fluorescence Microscopic visualization of PHA production

Serratia sp. ISTD04 was further screened for PHA and lipid accumulation by Nile red fluorescence microscopy at 560 nm and 590 nm excitation and emission wavelengths, respectively. The Nile red stained and LMA fixed bacterial cells were found to show a strong fluorescence after 72 h incubation in MM with 20 mM NaHCO3 and 1 % Glucose as carbon sources **Fig.5.2**. Nile red (9-diethylamino-5H benzo[a] phenoxazine-5-one) is a lipophilic fluorescent dye and is often used to detect the PHA and lipid content of microorganisms such as bacteria and microalgae (**Zuriani et al., 2013; Chen et al., 2011**). Bacteria synthesize and store PHA and lipids as insoluble inclusions within their cells in the presence of abundant carbon sources and under nutrient, particularly nitrogen, limiting conditions. Nile red binds with these lipid and polymer granules within the bacterial cells and gives fluorescence at defined wavelengths. Thus, Nile red fluorescence confirmed the presence of lipidic granules within the bacterial strain.

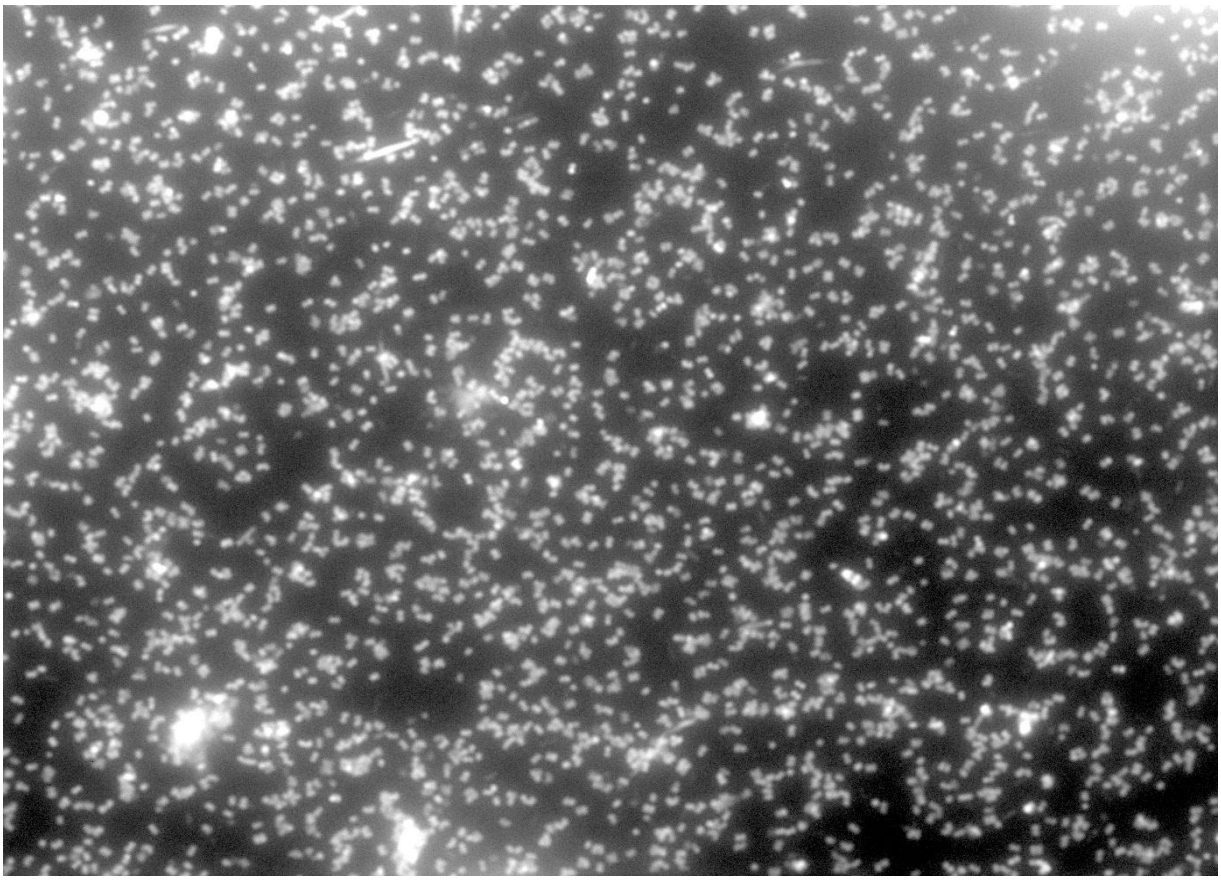

Fig.5.2 Staining of *Serratia* sp. ISTD04 with Nile red showing fluorescence.

5.3.4. Spectrofluorometric analysis of PHA accumulation

Spectrofluorometric monitoring of *Serratia* sp. ISTD04 culture in MM, was done with Nile red dye for PHA and lipid accumulation for 8 days. Simultaneous growth measurement of the bacterial culture was also performed by measuring absorbance at 595 nm using spectrophotometer. **Fig.5.3** shows the fluorescence at 575 nm and 590 nm along with growth curve. Maximum fluorescence was observed at 3th day at 575 nm while bacterial growth attained stationary phase within 1 day. A gradual decline in fluorescence was accompanied by a sharp decline in growth after 3rd day. Lesser fluorescence was observed at 590 nm than at 575 nm on all days. It can be inferred from the results that the strain showed maximum accumulation of PHA and lipids after 72 h. With depletion of carbon sources, there is a rapid fall in bacterial growth in batch cultures. During such starving conditions, PHA serves as a carbon and energy

reserve and is rapidly oxidized to retard the degradation of cellular components, thus increasing strain survivability under adverse conditions (**Chaitanya et al., 2014**). This possibly explains a gradual decline in fluorescence as compared to a sharp dip in bacterial growth after 3rd day of incubation. Nile red is a metachromatic dye and shows orange red fluorescence in hydrophobic environments. The dye is a commonly used vital stain for detection of intracellular lipids and PHA at an excitation wavelength of 488 nm and emission spectra ranging from 570 to 595 nm (**Lee et al., 1998**). The initial gradual detection of fluorescence at the two wavelengths with time may be related to the cellular permeability of the Nile red dye as well as to the size of lipid and polymer granules within the bacterial cells (**Cooksey et al 1987**).

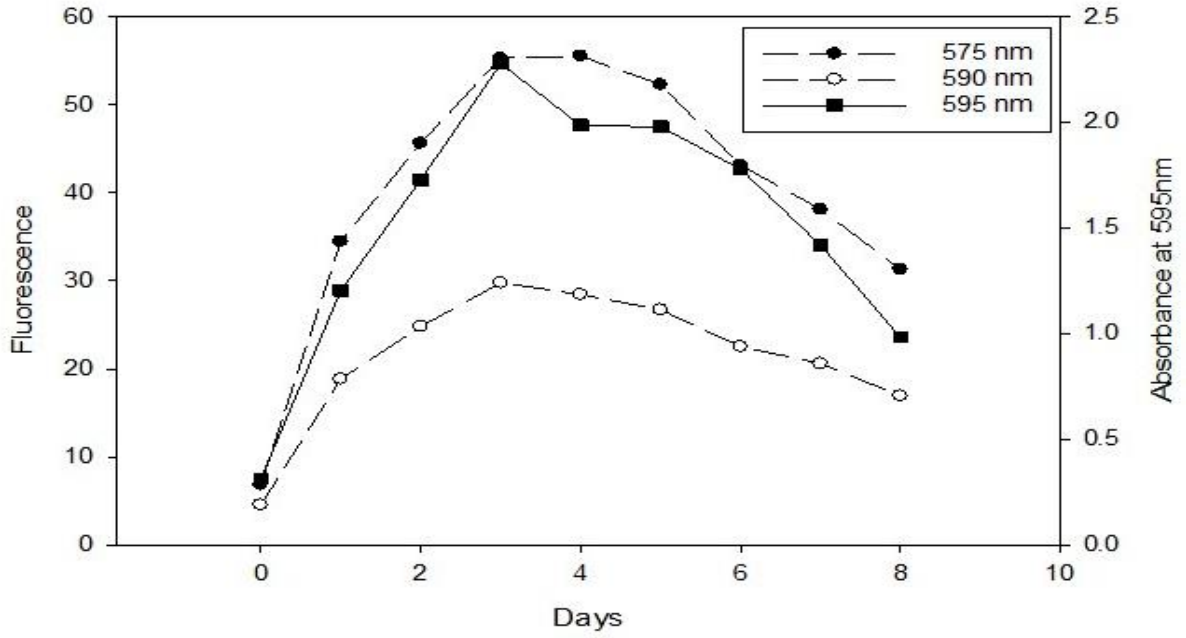

Fig.5.3 Nile red fluorescence at 575 nm and 590 nm emission wavelengths along with growth at 595 nm of *Serratia* sp. ISTD04 measured every 24 h for 8 days.

5.3.5. GC-MS analysis of PHA and lipids

The GC-MS profile of the *in situ* transesterified samples of *Serratia* sp.ISTD04 depict the presence of PHA, 3-hydroxyvalerate (RT 16.35) and Fatty Acid Methyl Esters (FAMES) such as Tetradecanoic acid, 12-methyl-, methyl ester (RT 18.81), Eicosanoic acid, methyl ester

(RT 20.19) and Hexadecanoic acid, 14-methyl-, methyl ester (RT 22.19) within the cells **Fig. 5.4, Table.5.2**. As observed in the result, C_{15}-C_{20} organic compounds are the major constituents of FAMEs, thus establishing the strain to be a potential source of good quality biodiesel as previously reported by **Bharti et al., (2014c).**

The results also confirm that bacterial production of 3-hydroxyvalerate, a monomeric unit of poly (3-hydroxyvalerate) (PHV) which is a non-PHB homopolymer of medium chain length (mcl-PHA). This is the first report of production of homopolymer PHV along with carbon sequestration by bacteria. There have several reports of production of PHB from bacteria. While, 3-hydroxybutanoic acid provides stiffness, 3-hydroxypentanoic acid promotes flexibility to the back bone of the polymer, which is made up of carbon and oxygen atoms. PHV has also been shown to form solution-grown single crystals which have a distinctive crystal and lamellar structure (**Iwata et al., 2001**). *Serratia* sp.ISTD04 has been previously reported to accumulate lipids along with carbon sequestration by **Bharti et al., (2014a)** and a similar profile of production of FAMEs has been reported in MSM media supplemented with 20 mM bicarbonate but without the production of PHV. Therefore, the present study also confirms the role of lipid accumulating, nitrogen deficient MM media in the formation of PHAs by the bacterium.

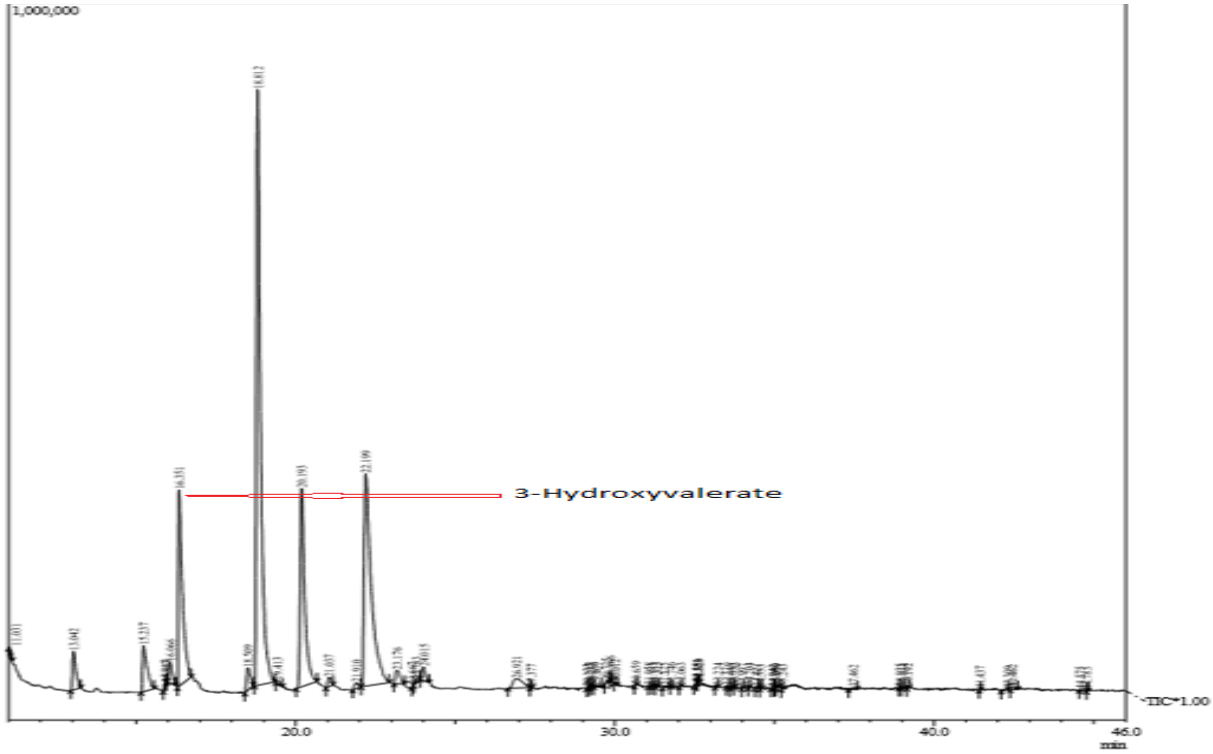

Fig.5.4 GC-MS chromatogram of PHA produced by *Serratia* sp. ISTD04 showing the peak of 3-Hydroxyvalerate.

Table.5.2 GC-MS data table for PHA and FAMEs produced by *Serratia* sp. ISTD04.

Compound name	Formula	R.T. (min.)	% Area
Butanedioic acid, dimethyl ester	$C_6H_{10}O_4$	15.237	3.14
3-hydroxyvalerate	$C_5H_{10}O_3$	16.351	11.90
Tetradecanoic acid, methyl ester	$C_{15}H_{30}O_2$	18.509	1.26
Tetradecanoic acid, 12-methyl-, methyl ester	$C_{16}H_{32}O_2$	18.812	37.58
Eicosanoic acid, methyl ester	$C_{21}H_{42}O_2$	20.193	13.57
Hexadecanoic acid, 14-methyl-, methyl ester	$C_{18}H_{36}O_2$	22.199	23.23
Nonanoic acid, 7-methyl-, methyl ester	$C_{10}H_{20}O_2$	21.037	0.50

5.3.6 Analysis of PHA by FT-IR

Non-destructive attenuated total reflectance FT-IR was carried out of the hexane precipitated PHA sample. The assignment of functional group as shown in **Table.5.3** was done according to previous reports (**Gumel et al. 2012; Mohapatra et al. 2014**). The infrared absorption observed at 3421.71 cm^{-1} was due to the O-H stretching vibration of the hydroxyl group of the polymer chain **Fig.5.5**. Characteristic peaks at 2954.93 $cm^{-1}$and 2924.07 cm^{-1} were respectively assigned to asymmetric methyl group and asymmetric CH_2 of the lateral monomeric chains. The intense peak at 2854.64 cm^{-1} was due to symmetrical methyl group and was possibly a result of the conformational disorder taken place during the crystallization process (**López-Cuellar et al., 2011**). The absorption band observed at 1741.71 cm^{-1} and reported to be a PHA marker band has been assigned to the stretching vibration of carbonyl (C=O) ester bond. The bands observed at 1658.77 and 1469.75 cm^{-1} have been assigned to the stretching vibrations of bacterial intracellular amide (–CO–N–) I and II respectively. Absorption at 1377.17 cm^{-1} and 1259.51 cm^{-1} was assigned to terminal CH_3 groups and asymmetric C–O–C stretching vibration respectively. Several absorption bands observed from 1166.93 cm^{-1} to 619.39 cm^{-1} were assigned to C–O and C–C stretching vibration. Thus, these peaks clearly establish the precipitated material as PHA.

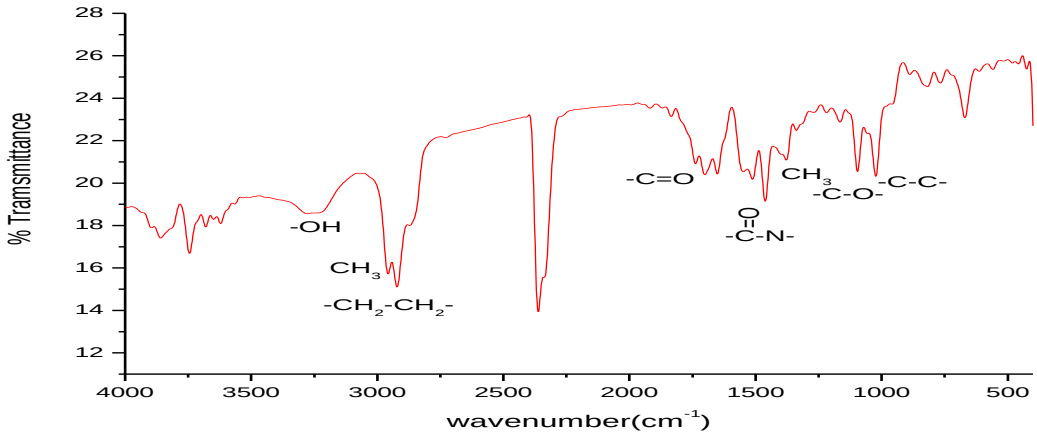

Fig.5.5 FT-IR spectra of PHA synthesized by *Serratia* sp. ISTD04.

Table.5.3 Peaks observed in FT-IR spectrum of PHA synthesized by *Serratia* sp. ISTD04 and their corresponding annotations.

Peak (cm-1)	Bonds and Corresponding annotation
1166.93-619.148	C-O and C-C stretching
1259.51	Asymmetrical –C-O-C stretching vibration
1377.171	Terminal –CH3 group
1659.50 and 1460.39	Bacterial protein and amide II and sp specific
1741.71	PHA marker bond –R-C=O carbonyl ester group
2854.64	Symmetric CH3 group
2924.07	Asymmetrical –CH2 group lateral monomeric chain
2954.93	Asymmetrical –CH3 group
3419.78	-OH- group of polymer chain

5.3.7 TEM viewing of PHA granules within the cells

Transmission electron microscopic studies performed on both controls **Fig.5.6a** and 72 h culture cells **Fig.5.6b** indicated a higher accumulation of PHA granules within the bacterial cells in the 72 h sample. The results further confirm the production of PHA by the strain. Similar images for visualization of PHA granules within the bacterial cells have been shown by **Berlanga et al., (2006)** and **Poblete-Castro et al., (2014)**. There is coating of phospholipids and proteins monolayer over there granules and the associated proteins are involved in the formation of granule and in the synthesis and degradation of PHA (**Pötter and Steinbüchel, 2005**).

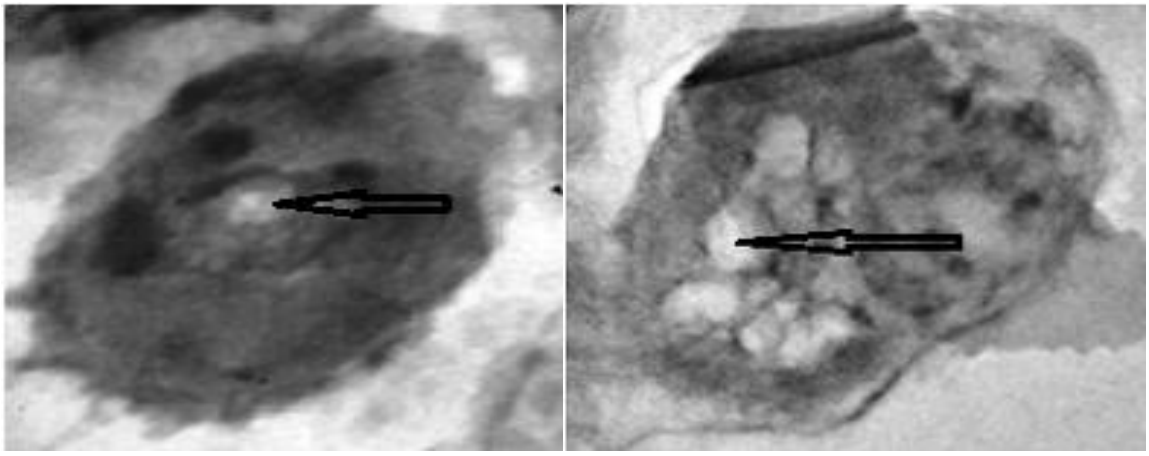

(a) (b)

Fig.5.6 Transmission electron micrograph (X 15000 magnification) of *Serratia* sp. ISTD04 in (a) control and (b) 72 h cultures showing PHA granules marked by black arrow.

5.3.8 Process optimization by RSM

Response surface methodology (RSM) was used for process optimization. Box-Behnken design (BBD), a type of RSM was selected for creating the quadratic response model. Quadratic equations were used to draw the relationship between the three factors (Glucose and bicarbonate concentrations and pH) and two responses (PHA and biomass production). The coefficients of regression equation were calculated and the data was fitted to second-order polynomial equation for weight of PHA and biomass in g per 100 mL culture. The coded equations obtained from Box– Behnken design (BBD) for weight of PHA and biomass by *Serratia* sp. ISTD04 as suggested by software is given below:

PHA(g/100 mL) = +0.079 -7.729E- 003* A +7.146E- 003* B -4.597E- 003* C -2.356E-003* AB +7.371E-003* AC +1.911E-003* BC-0.012* A^2-0.013* B^2-0.014* C^2 (2)

Biomass(g/100mL)= +0.17-0.012* A+0.013* B-4.919E-003* C+1.065E-003* AB +4.008E-003*AC+1.876E-003* BC-5.930E-003* A^2-0.025* B^20.019*C^2 (3)

Where, A = Glucose concentration (%), B = pH and C = Bicarbonate concentration (mM)

Table.5.4. Behnken design for actual and predicted response of PHA yield and Biomass.

	Response1 Weight of PHA(g)		**Response2 Weight of Biomass(g)**	
Run Order	**Actual Value**	**Predicted Value**	**Actual Value**	**Predicted Value**
1	0.042	0.043	0.13	0.14
2	0.082	0.081	0.17	0.18
3	0.081	0.081	0.18	0.18
4	0.081	0.081	0.17	0.18
5	0.050	0.049	0.15	0.15
6	0.041	0.040	0.12	0.11
7	0.066	0.066	0.15	0.15
8	0.054	0.054	0.12	0.13
9	0.054	0.055	0.14	0.14
10	0.048	0.048	0.13	0.13
11	0.080	0.081	0.18	0.18
12	0.049	0.049	0.14	0.14
13	0.055	0.056	0.14	0.14
14	0.036	0.036	0.11	0.11
15	0.073	0.073	0.17	0.17
16	0.072	0.073	0.16	0.17
17	0.082	0.081	0.18	0.18

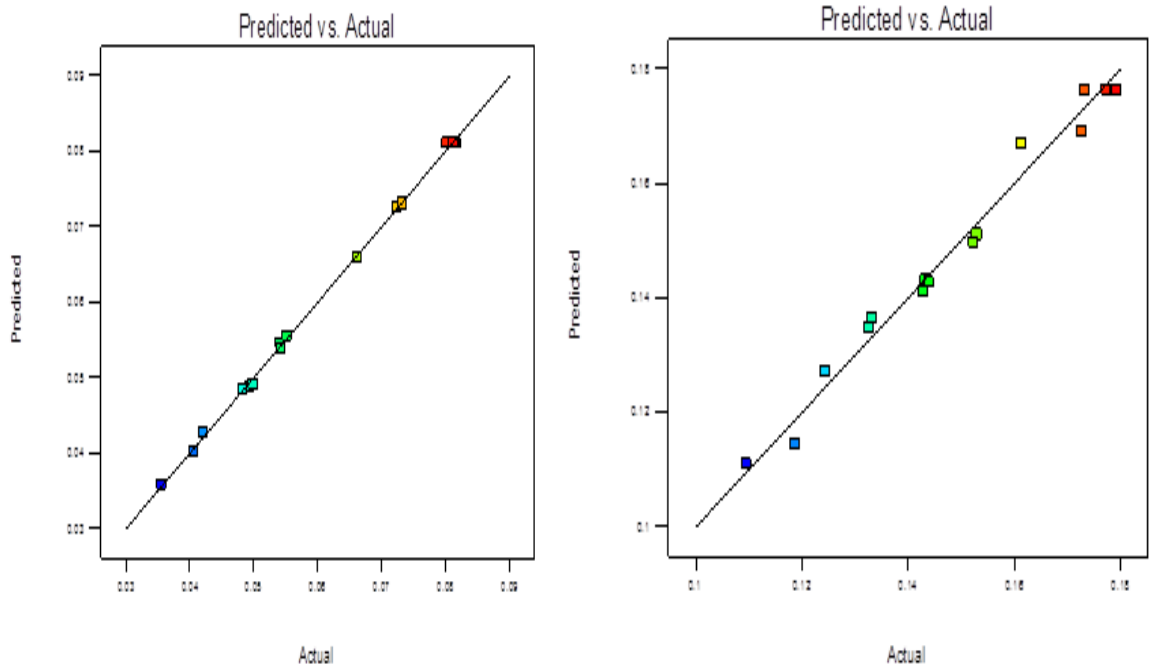

(a) (b)

Fig.5.7 Actual response values obtained from the experiments were compared with the response predicted by BBD model for (a) PHA production and (b) Biomass production.

5.3.8.1 Statistical analysis

The role of individual factors and their double interactions on the response is revealed by comparing the factor coefficients in the coded equations. Positive coefficient values indicate that individual or double interaction factors positively affect the response, whereas the negative coefficient values indicate that the factors decrease the response in the tested range.

The coefficient values in Eqs. (2) and (3) reveal that the weight of PHA and biomass decrease with increase in the two factors glucose and bicarbonate concentration, while increase with increase in pH.

The combined interaction of glucose concentration and pH had a negative effect on weight of PHA but positive effect on the biomass, while of the collective effect of pH and bicarbonate concentration, and glucose concentration and bicarbonate concentration had a positive effect on

both the responses. Analysis of variance (ANOVA) was used to define the adequacy of the model. The results of ANOVA for weight of PHA and biomass are shown in **Table.5.5 and 5.6**.

Table.5.5 ANOVA Results for Response Surface Quadratic model of PHA yield.

Source	**Sum of Squares**	**df**	***Mean Square***	***F Value***	***p-value Prob > F***	
Model	4.278E-003	9	*4.754E-004*	*858.36*	*< 0.0001*	*Significant*
A-Glucose conc.	*4.645E-004*	*1*	*4.645E-004*	*838.72*	*< 0.0001*	
B-pH	*3.761E-004*	*1*	*3.761E-004*	*679.09*	*< 0.0001*	
C-Bicarbonate conc.	*1.608E-004*	*1*	*1.608E-004*	*290.36*	*< 0.0001*	
AB	*2.340E-005*	*1*	*2.340E-005*	*42.26*	*0.0003*	
AC	*2.362E-004*	*1*	*2.362E-004*	*426.43*	*< 0.0001*	
BC	*1.504E-005*	*1*	*1.504E-005*	*27.15*	*0.0012*	
A^2	*4.236E-004*	*1*	*4.236E-004*	*764.84*	*< 0.0001*	
B^2	*7.656E-004*	*1*	*7.656E-004*	*1382.31*	*< 0.0001*	
C^2	*6.938E-004*	*1*	*6.938E-004*	*1252.79*	*< 0.0001*	
Residual	3.877E-006	7	*5.538E-007*			
Lack of Fit	*2.449E-006*	*3*	*8.163E-007*	*2.29*	*0.2206*	*not significant*
Pure Error	*1.428E-006*	*4*	*3.570E-007*			
Cor Total	4.282E-003	16				
R^2	0.99					
R^2_{adj}	0.99					
CV%	1.21					
AP	79.19					

Table.5.6 ANOVA Results for Response Surface Quadratic model of Biomass.

Source	Sum of Squares	df	Mean Square	F Value	p-value Prob > F	
Model	8.014E-003	9	8.904E-004	44.32	< 0.0001	significant
A-Glucose conc.	*1.162E-003*	*1*	*1.162E-003*	*57.84*	*0.0001*	
B-pH	*1.337E-003*	*1*	*1.337E-003*	*66.56*	*< 0.0001*	
C-Bicarbonate conc.	*1.842E-004*	*1*	*1.842E-004*	*9.17*	*0.0192*	
AB	*4.780E-006*	*1*	*4.780E-006*	*0.24*	*0.6406*	
AC	*6.984E-005*	*1*	*6.984E-005*	*3.48*	*0.1045*	
BC	*1.450E-005*	*1*	*1.450E-005*	*0.72*	*0.4237*	
A^2	*1.105E-004*	*1*	*1.105E-004*	*5.50*	*0.0514*	
B^2	*2.610E-003*	*1*	*2.610E-003*	*129.95*	*< 0.0001*	
C^2	*1.276E-003*	*1*	*1.276E-003*	*63.51*	*< 0.0001*	
Residual	1.406E-004	7	2.009E-005			
Lack of Fit	*1.042E-004*	*3*	*3.473E-005*	*3.81*	*0.1143*	*not significant*
Pure Error	*3.642E-005*	*4*	*9.105E-006*			
Cor Total	8.154E-003	16				
R^2	0.98					
R^2_{adj}	0.96					
CV%	2.97					
AP	19.03					

The Model F-value of 858.36 for weight of PHA and 44.32 for biomass by *Serratia* sp. ISTD04 implies that the model is significant. The chance of a larger F-value occurring due to noise is only a 0.01%. The ‘‘Lack of Fit F value’’ of 2.29 and 3.81 for weight of PHA and biomass respectively, implies that that a Lack of fit is not significant relative to the pure error. There is a 22.06 % and 11.43 % chance that ‘‘Lack of Fit F-value’’ this large could occur due to noise for weight of PHA and biomass respectively. The R^2 coefficient provides the proportion of the total variation in the response predicted by the model, certifying a satisfactory adjustment of the quadratic model to the experimental data. A high R^2 value close to 1 is preferable and a reasonable agreement with adjusted R^2 is necessary**.**

"Adeq Precision" (AP) measures the signal to noise ratio. A ratio greater than 4 is desirable. The ratio of 79.19 and 19.033 for weight of PHA and biomass respectively, indicates an adequate signal. This model can be used to navigate the design space as per the model. The coefficient of variance (CV) is the ratio of standard error of estimate to the mean value of the response. It describes the duplicability of the model. A model is normally considered reproducible if its CV % is not greater than 10. As shown in **Table.5.5** and **Table.5.6** the values of CV % are 1.21 and 2.97 for weight of PHA and biomass respectively. Both the values are less than 10, thus confirming the reproducibility of the model.

5.3.8.2 Interactive effects of factors on weight of PHA and biomass

Three-dimensional graphical responses were generated on the basis of the model equations to study the interactive effects of the three factors on the two responses. The response surface plots for weight of PHA and biomass are shown in **Fig.5.8**. These plots depict the relative effects of any two factors while keeping the third factor constant. In case of weight of PHA, efficiency was found to increase up to pH 8 followed by a decline with further increase in pH while it showed increase up to intermediate concentrations of glucose after which there was a decline **Fig.5.8a**. However, for biomass, with more acidic pH, there was a sharp decrease but with increasing concentration of glucose, there was a marginal decline of biomass **Fig.5.8d and c** shows the interactive effects of bicarbonate and glucose concentration on the weight of PHA and suggests that values near to the intermediate points have the most positive effect and there is a jagged dip at higher concentration. According to **Fig.5.8f**, interactive effect of bicarbonate and glucose concentration is not very critical to biomass yield as the curve is relatively flat. Nevertheless, maximum biomass is observed at intermediate bicarbonate concentration while there is a gradual decline in biomass with increasing glucose concentration. The influence of bicarbonate concentration along with pH had similar effect on both the responses. Weight of PHA and biomass showed maximum value at intermediate levels of bicarbonate concentration while a there was a sharp decline above and below pH 8 **Fig.5.8b and c**. Thus, these plots suggest that pH plays a very crucial role in higher response generation followed by bicarbonate concentration while glucose concentration has a moderate effect. Slightly alkaline pH,

intermediate bicarbonate and low glucose concentration have positive effects on both weight of PHA and biomass.

There is a positive effect on both the responses with increase in bicarbonate concentration up to intermediate levels as previously reported by **Bharti et al. (2014a, b)** for biomass generation of this strain. The fact that bicarbonate is more critical to both the responses than glucose (as revealed by the RSM results) as the carbon source is an important finding as it could be beneficial for cost reduction as well as carbon sequestration along with formation of PHA. The high influence of pH on the responses can be explained by the fact that pH and bicarbonate are indirectly correlated that means with increase in bicarbonate concentration in the medium, there is a decrease in pH. This bacterium has a carbon concentrating mechanism and utilizes bicarbonate as a carbon source for growth as previously reported by **Bharti et al., 2014a, b.** As bicarbonate is utilized by the bacterium during growth, the level of bicarbonate in medium falls, and pH increases which is accompanied by an observed increase in PHA production and biomass accumulation up to intermediate levels of bicarbonate and slightly alkaline pH after which both responses begin to decline. The results, thus, confirm the carbon concentrating potential along with PHA production by *Serratia* sp. ISTD04.

PHA

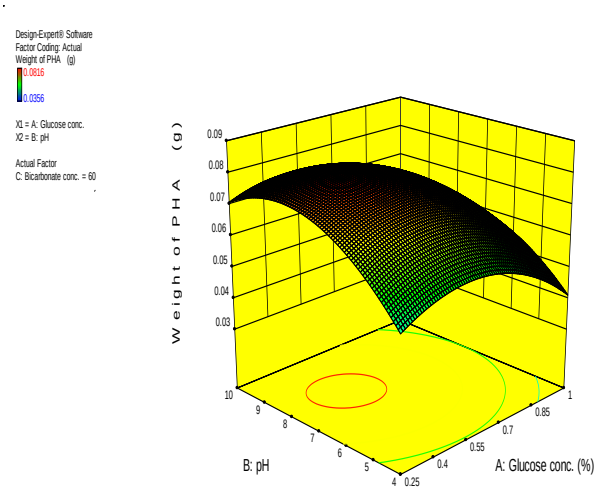

(a)

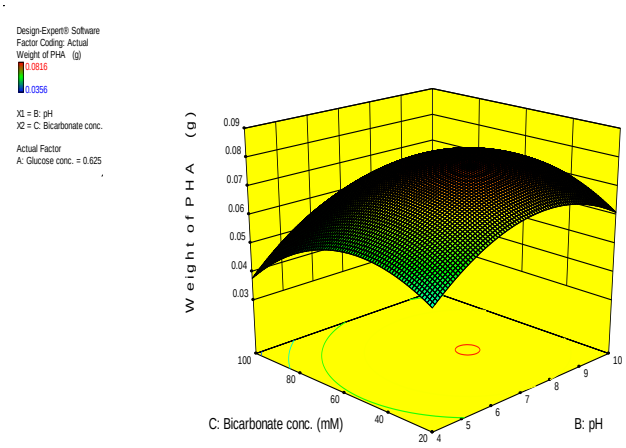

(b)

Biomass

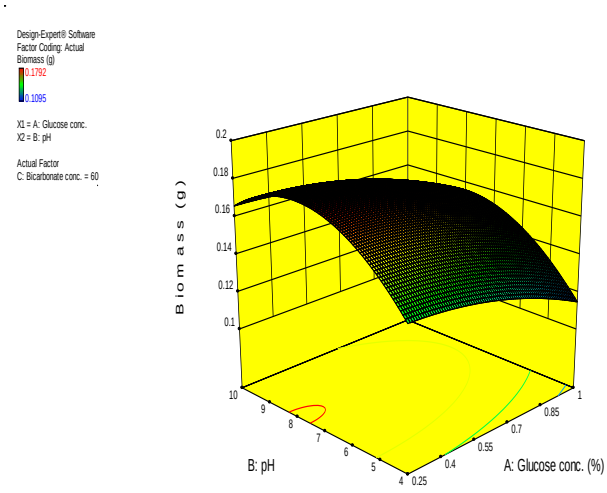

(d)

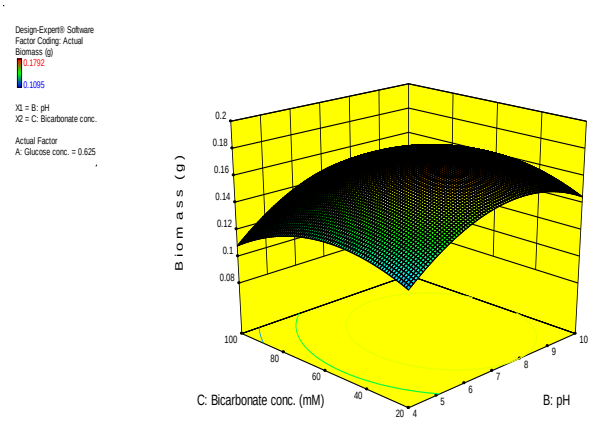

(e)

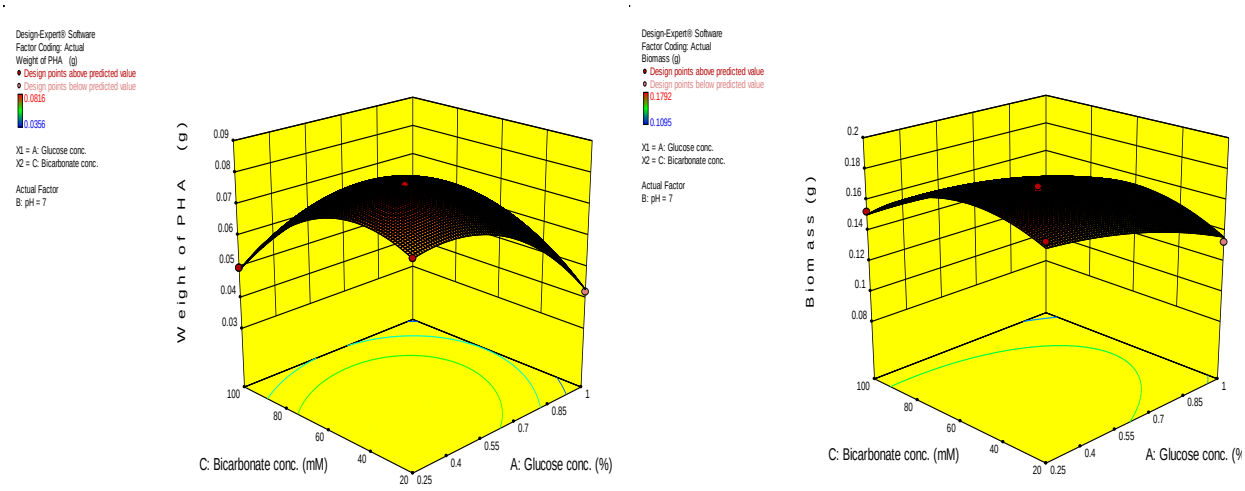

(c) (f)

Fig.5.8 3-D surface plot showing the interaction of A= Glucose concentration (%), B = pH and C = Bicarbonate concentration (mM) on weight of (i) PHA (a,b,c) and (ii) biomass (d,e,f) both measured in g per 100 mL culture by *Serratia* sp. ISTD04.

5.3.8.3 Validation Results

Verification experiments with numerical optimized levels of experimental variables were conducted in order to confirm the suitability of Equations 2 and 3 for maximum response generation **Fig.5.9, Table.5.7**.

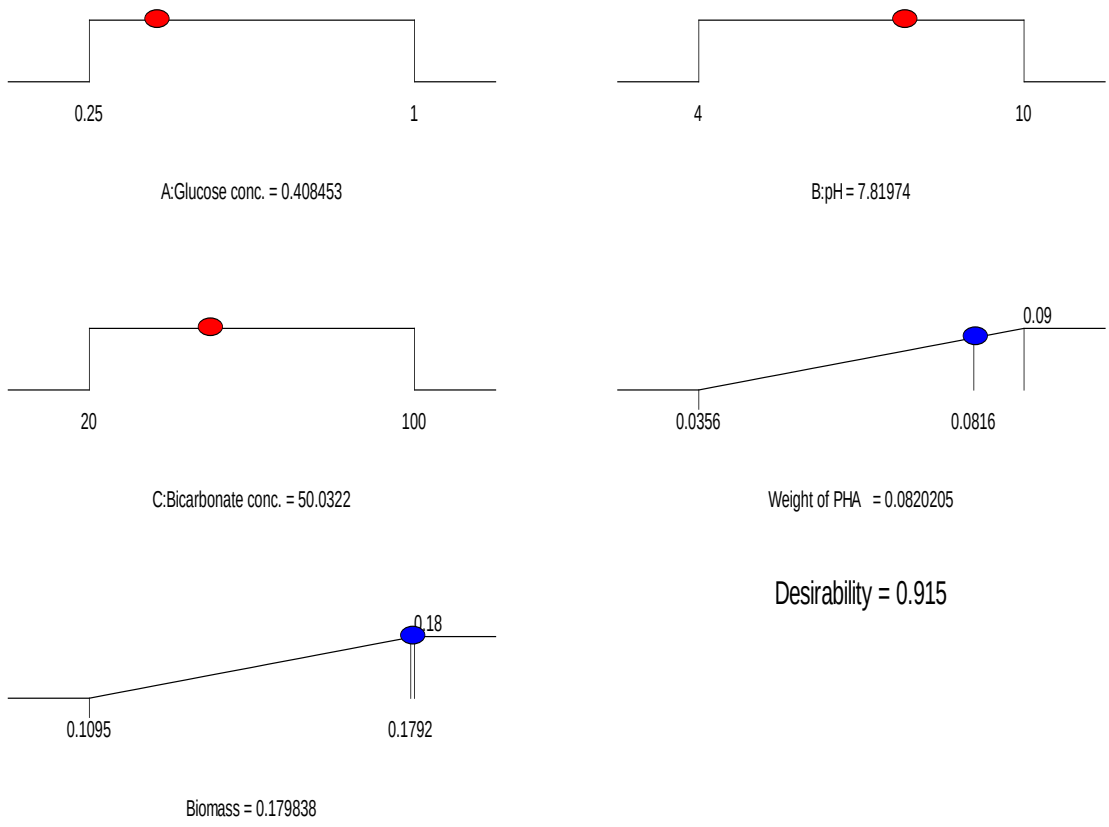

Fig.5.9 Ramps indicate the optimized conditions of factors (glucose concentration%, pH, bicarbonate (mM)) for production of PHA and biomass by *Serratia* sp. ISTD04, predicted by model.

The optimized conditions as predicted by the software for maximum PHA and biomass production were 0.41 % and 50 mM Glucose and bicarbonate concentration respectively at p H 7.8 and the predicted production of PHA and biomass were 0.082 g and 0.180 g per 100 mL culture respectively at desirability 0.915. The weight of PHA and biomass attained after validation experiment at the predicted conditions were found to be 0.0802 g and 0.176 g per 100 mL culture respectively. Thus, the results of the verification experiments established the accuracy of the predicted model **Table. 5.7**.

Table.5.7 Weight of PHA and Biomass obtained from *Serratia* sp. ISDT04 culture (g per 100 mL culture) before and after optimization.

Variable	Optimization condition		PHA yield (mean)			Biomass(mean)		
	Before	After	Optimization			Optimization		
			Before (mean)	After		Before(mean)	After	
				Predicted	Experimental (mean)		Predicted	Experimental (mean)
Glucose%	0.5	0.41						
pH	7	7.81						
Bicarbonate (Mm)	50	50.03	0.0421	0.0820	0.0802	0.1332	0.1800	0.1760

The weight of PHA and biomass (per 100 mL culture) prior to optimization, at the initial experimental conditions of 1 % Glucose and 20 mM bicarbonate concentration at pH 7.6 were found to be 0.0421 and 0.1332 g respectively. Thus, after optimization of concentrations of the two carbon sources and pH, there was an increase of almost 2 and 1.3 folds in the production of PHA and biomass respectively. **Steinbüchel et al (1993)** first reported production of PHV by *Chromobacterium violaceum*. The strain was found to produce 2.48 g per 100 mL PHV from a 300 L scale fed-batch fermentor (**Steinbüchel and Schmack, 1995**). In a previous study by Fukui et al. (1997), PHV production from a recombinant *Ralstonia eutropha* PHB-4 was found to be 0.002 g per 100 mL of cell dry weight. In another study, production of homopolymer poly (3-hydroxyvalerate) (PHV) by a recombinant *Aeromonas hydrophila* strain 4AK4 in shake flasks was reported to be 0.27 g per 100 mL of cell dry weight (**Shen et al., 2009**). Although, the amount of PHV produced by *Serratia* sp. ISTD04 in this study is not at par with some of the previous reports on other bacteria, yet the production of PHV using only mineral media supplemented with bicarbonate as one of the carbon sources makes the finding important. The study opens a new avenue of research involving CO_2 capture and storage as PHA granules in the bacterial cells which can further be harvested to make bioplastics and other composites.

5.4 Conclusion

The present work is the first report of production of homopolymer poly (3-hydroxyvalerate) (PHV), a type of co-polymer along with carbon sequestration by a *Serratia* sp. The GC-MS results confirmed the production of 3-Hydroxyvalerate, which is a monomer of PHV, by *Serratia* sp. ISTD04 cultured in a mineral media supplemented with bicarbonate and glucose as carbon sources. A 2 fold increase in PHA production after optimization demonstrates the successful application of the Box-Behnken design of RSM in process optimization for enhanced PHA production.

Chapter 6: Production, characterization and application of extracellular polymeric substance produced by carbon dioxide sequestering chemolithotrophic bacteria

6. Production, characterization and application of extracellular polymeric substance produced by carbon dioxide sequestering chemolithotrophic bacteria

6.1 Introduction

Comprehensively increasing worldwide temperature is one of the major environmental tribulations that living organisms are facing these days, rising level of CO_2 in the atmosphere speed up this problem in cascading manners. Therefore an necessary requirement to minimize the CO_2 release in the atmosphere or to transformed the atmospheric CO_2 in to different forms (immobilized forms) by applying various methods such as, physical, chemical and biological (**Zevenhoven et al., 2006; Chang and Yang, 2003; Honjo et al., 1996; Murakami and Ikenouchi, 1997; Otsuki, 2001**). The microorganisms utilizes CO_2 as carbon source and form biomass, microbial biomass could be use as raw materials for production of diverse groups of biological materials such as, bioenergy, biodiesel, biohydrogen, polyhydroxyalkanotes (PHAs) and extracellular polymeric substances (EPSs). Based on the chemical composition and bonding linkages, the biopolymers synthesized by microorganisms were divided in to four main categories: polyesters, polyamides, inorganic polyanhydrides, and polysaccharides (**Crescenzi and Dentini, 1996; Rehm, 2009**). Since these microbial polymers synthesized as an protective mechanisms when environmental conditions become unfavorable, it may act as reserve food materials and contribute significantly to cop-up with adverse environmental condition (**Rehm, 2010**). Most of the EPS producer microbes have been illustrated to produce either homo or heteropolysaccharide (**Kumar et al., 2007**). **Kwon et al (1994)** has been reported that bacteria sp. such as *Serratia marcescens*, *Aeromonas salominicida*, and *Pseudomonas* sp. are able to synthesize two different types of polysaccharides. α-D-glucans, β-D-glucans, fructans, and polygalactan comes under the category of homopolysaccharides based on the monomeric composition and nature of the bonds linking. On the other hand heteropolysaccharides are composed of repeating units of D-glucose, D-galactose, l-rhamnose, and *N*-acetylglucosamine (GlcNAc), *N*-acetylgalactosamine (GalNAc), or glucuronic acid (GlcA) and some time non-

carbohydrate components like phosphate, acetyl, and glycerol (**More et al 2014; Ates, 2015**). Homopolysaccharides are synthesized biologically by microbes using specific substrates like sucrose, glucose, while the heteropolysaccharide residues are synthesized intracellularly with the help of precursor molecules which are present crossways the membrane and finally its extracellular polymerization will be facilitated by isoprenoid glycosyl carrier lipids (**Nwodo et al., 2012**). Usually, two form of EPS is well known on the basis of its association with microbial cell wall: EPS attached tightly to the cell wall called tightly bound EPS (TB-EPS) and EPS attached loosely to the cell wall called loosely bound EPS (LB-EPS), EPS of both types can be separated by centrifugation (**Sheng et al., 2010**). The EPS which is not separated easily from the cell wall during the centrifugation is called as capsular EPS and the EPS, which is easily separated from the cell wall and release in to culture supernatant is called as slime EPS.

Numerous bacterial strains have been reported for EPS production, utilizing different carbon source with varies production rates from 0.8 g L^{-1} by *Bacillus* sp. (MBFF19) utilizing glucose as carbon source (**Zheng et al., 2008**) to 27.7 g L^{-1} by *Klebsiella terrigena* (R2) grown on glycerol and ethanol (**Buthelezi et al., 2010**). A significant increase in curiosity about the biological polymers and considering the environmental friendly behaviour creates huge demand of these biomaterials. But the major stumbling block in commercialization of EPS are its less production rate, unavailability of cheap carbon source and cost involve in its processing of the material. Using cost effective substrates (carbon and nutrient source) at some level for production of EPS at larger scale may reduced the production cost of EPS which should make this material marketable. Production media containing waste materials or cheaper carbon and nutrient sources like molasses, sugar beet, flower extracts and sewage sludge have been gaining attention for microbial production of EPS (**More et al., 2014**).

Simultaneously reduction in cost and enhance efficiency of EPS production can be achieved by optimizing the process parameters of EPS production. For optimization of EPS production, some specific sets of parameters should be targeted, which have maximum influence on its production (**Gupta and Thakur, 2016**). Microorganisms are able to carry out their own desirable function with some degree of inhibition, under optimized sets of conditions. A

bioreactor constantly maintains the bacterial growth condition optimum which required running the production experiment for longer duration and its help to achieve maximum production.

To identify the pathways of EPS production in microorganism, proteomics, genomics and metabolomics are the emerging and imperative approach, which quite helpful in finding the mechanism of its biosynthesis and production (**Singh et al., 2014; Kumar et al., 2017b**).

Thus, the comprehensively study of EPS production along with CO_2 sequestration by chemolithotrophic bacteria while convalescing the effectiveness of the procedure through the optimization of effective parameters and large scale product formation at fermentor level may have provides dual benefit of CO_2 sequestration along with cost effective production of EPS. The objectives of the present study were to characterization of EPS produced by chemolithotrophic bacterium *Serratia* sp. ISTD04, optimization of process parameters for production of EPS at fermentor level and its environmental application in removal of dyes and finally characterization of bacterium for production of EPS by genomics and proteomics approach.

6.2 Materials and methods

6.2.1 Chemicals and reagents

All chemicals were procured from Sigma–Aldrich (St. Louis, MO, USA) or Merck (Darmstadt, Germany). All organic solvents and solid chemicals used were of analytical reagent grade.

6.2.2 Microorganism and culture condition

A previously reported carbon concentrating bacterial strain *Serratia* sp. ISTD04 (gene bank accession number- JF276275) isolated from marble rocks of the palaeoproterozoic metasediments of the Aravali Supergroup, Rajasthan, was used for the study of EPS production. The bacterial strain was procured from a chemostat culture maintained at 30 °C, 150 rpm and pH 7.6 in Minimal salt medium (MSM) containing (g L^{-1}): $Na_2HPO_4 \cdot 2H_2O$, 7.8; KH_2PO_4, 6.8; $MgSO_4$, 0.2; $NaNO_3$, 0.085; $ZnSO_4.7H_2O$, 0.05; $ZnCl_2$, 0.02; Ca $(NO_3)_2.4H_2O$, 0.05 and 20 mM $NaHCO_3$ as the sole carbon source (**Bharti et al. 2014a**). Pre-LB cultured of the strain was transfer (1:10 v/v) to mineral medium (MM) with slight modification reported by **Vijayendra et al (2008)**, containing (g L^{-1}): Na_2HPO_4 5.0, KH_2PO_4 6.0, ammonium ferric citrate 2.0, $MgSO_4$

1.0, CaCl2 0.05, yeast extract 0.5, trace elements solution 1 mL, consisting of (g L^{-1}): $FeSO_4.7H_2O$ 5.0, $MnSO_4$ 2.0, $CoCl_2$ 1.0, $ZnCl_2$ 1.0, dissolved in 0.1 N HCl solution pH 7.8 and supplemented with filter sterilized 50 mM $NaHCO_3$ and 5 g L^{-1} glucose as carbon sources and incubated under aerobic conditions at 30 °C and 150 rpm for five days.

6.2.3 Isolation and purification of EPS

LB-EPS have been isolated from bacterial culture by harvesting the 72 h grown bacterial culture by centrifugation for 15 min at 8000 rpm, separated the biomass, added 1:10 volumes of ice cold isopropanol in the culture supernatant, mixed properly and stored at 4 °C for 12 h for precipitation of material. The precipitated material was further separated by using cold centrifugation for 30 min at 4 °C and 15,000 rpm and the pellets were washed with ice cold isopropanol and acetone to purify the material (EPS) (**Vijayabaskar et al., 2011**). The purify EPS was oven dried until a constant weight was achieved and weighed. Weight of the purified and dried EPS was expressed in g L^{-1} of bacterial culture (**Poli et al., 2009**). For isolation of TB-EPS, separated cell biomass after the centrifugation was re-suspended in double distilled water and heated for 30 min at 60 °C in water bath to release TB-EPS in the liquid phase followed by centrifugation at 15,000 rpm, 4 °C for 15 min (**Li and Yang, 2007**). The liquid phase containing TB-EPS was used to measure dry weight using the same procedure as for LB-EPS. The weight of total EPS, which is called broth EPS (B-EPS) was estimated, after adding the weight of LB-EPS and TB-EPS.

6.2.4 Morphological observation of *Serratia* sp. ISTD04 by scanning electron microscopy (SEM)

To observe morphology of *Serratia* sp. ISTD04 cells grown for 0 h, 48 h and 72 h were fixed in glutaraldehyde (1% solution) and paraformaldehyde (2%) buffered with sodium phosphate buffer saline (0.1 M, pH 6.8) for 12–18 h at 4°C after that cells were gently washed with fresh buffer and fixing was performed with the help of osmium tetraoxide (1%) in the beffer for 2 h at 4°C. Smearing of fixed cell was done with poly-L-lysin for 30 min in wet condition. The washing of specimen was done by phosphate buffer and then dehydrated sequence bias with ethanolic water solution (30%, 50%, 70% and 90% ethanol, 5 min each) and dried in CO_2 incubator for 20 min. Specimen mounting was performed on aluminium stubs, and cells coating

were done with 90 Å thick gold-palladium coating in polar on Sc 7640 sputter coater (VG Microtech, East Sussex, TN22, England) for 30 min. finally Coated cells were observed at 25 kV with SEM (Model-Zeiss EVO40) (**Naik et al., 2012**).

6.2.5 Chemical characterization of EPS

6.2.5.1 Estimation of total carbohydrate content of EPS

The total carbohydrate (sugar) content was evaluated by applying standard phenol sulphuric acid method and using glucose as a standard (**Dubois et al., 1956**). In brief, 80 % phenol solution was prepared and 500 µL of this solution was added to 100 µL sample containing 2.5 mg mL^{-1} EPS afterwards vortexing and adding flush of 2 mL H_2SO_4. The mixed solution was cooled at room temperature for 10 min. and then absorbance was recorded at 490nm using distilled water as blank.

6.2.5.2 Estimation of reducing sugar of EPS

Estimation of the reducing sugar content of EPS was performed by using dinitrosalicylic acid (DNS) method and Glucose as a standard (**Shivakumar and Vijayendra, 2006**). In brief 500 µL of DNS was added to 500 µL sample containing 2.5 mg mL^{-1} EPS and heated at 90 °C for 10 min. in water bath afterward 150 µL sodium potassium tartarate (40%) was added to the solution and cooled to room temperature. Finally optical density (O.D) of the sample was taken at 575nm using distilled water as blank.

6.2.5.3 Estimation of protein content of EPS

The protein content of EPS was majored by Bradford method for protein estimation using Bovine Serum Albumin (BSA) as standard (**Bradford, 1976**). In brief 900 µL of Bradford reagent was added to 100 µL EPS sample (EPS concentration 5 mg mL^{-1}) mixed gently and incubated at room temperature for 30 min. in the dark. O.D of the developed colour was recorded at 595 nm using distilled water as blank.

6.2.5.4 Estimation of fatty acid content of EPS

The standard chloroform and methanol extraction procedure followed by **Zhang et al., (2014)** for estimation of lipids and fatty acid component from waste water sludge were opted for

determination of lipids contents in EPS with slight modification in procedure. 200 mg of purified dried EPS power were mixed in to 4 ml solvent mixture of chloroform and methanol (2:1 v/v), incubated to 60 °C for 4 h in water bath. The mixture was centrifuged at 5000 rpm for 15 min. and the supernatant solvent phase was withdrawn and filtered with glass microfiber filter, diameter 47 mm into a pre-weighed glass vial (W1). The extraction procedure was repeated three times. Afterwards, the vial containing the total volume of the supernatant collected from each extraction was put under evaporation at 70 °C and then weighed (W2). The lipid content was calculated by the difference of W_1 and W_2.

The fatty acid content of the ESP = $(W_2-W_1)/200$ mg ×100%.

6.2.6 Structural composition analysis of EPS

Morphology, structural composition, bond angles and bonding patterns of the extracted, purified and dried EPS was further analysed by Scanning electron microscopy (SEM), Energy Dispersive X-ray (EDX) spectroscopy, Fourier Transform Infrared Spectroscopy (FT-IR), Gas Chromatography Mass Spectrometry (GC-MS) and Nuclear Magnetic Resonance (NMR) analysis.

6.2.6.1 SEM-EDX analysis of EPS

SEM analysis was performed for viewing surface texture of the purified and dried EPS produced by *Serratia* sp. ISTD04. The dried EPS powder was mounted on aluminum stubs and sample was coated with 90 Å thick gold-palladium coating in polaron Sc 7640 sputter coater (Carl Zeis, Germany) for 30 min. Coated samples were viewed at 20 KV with scanning electron microscopy (Leo Electron Microscopy Ltd., Cambridge) at various magnification (500 X-10 KX).

Energy Dispersive X-ray (EDX) spectroscopy of dried purified EPS was performed for elemental analysis of qualitative analysis of the elemental composition of EPS. The dried EPS powder was mounted on aluminium stubs and the analysis was performed at 20 kV on Dx4 Prime EDX spectrometer (Bruker, Germany) equipped with X-flash detector.

6.2.6.2 FT-IR analysis

Functional groups analysis of EPS was performed by Fourier Transform Infrared spectroscopy (FT-IR). For FT-IR analysis, dried EPS powder was properly mixed with

potassium bromide (KBr) with the help of motor-pester and compressed to prepare a salt disc of about 3 mm diameter. IR spectroscopy of the disc was recorded Varian 7000 FTIR spectrometer (Perkin-Elmer Inc., Wellesley, MA, USA) at room temperature, in the frequency range of 400 to 4000 cm^{-1}, for 64 scans per sample at a resolution of 4 cm^{-1}.

6.2.6.3 GC-MS analysis

The monomeric composition of EPS was analysed by using GC-MS after hydrolysing and silylation of the dried and powered EPS sample to make non-volatile components in to volatile derivatives (methylsilanes) (**Synytsya and Novak, 2014**). In brief, 5-10 mg of dried powder EPS was hydrolysed with Trifluoroacetic acid (TFA) (1 M) at 100 °C for 8 h followed by reduction for 16 h at room temperature with addition of 100 µL $NaBH_4$ (10 mg in 1 mL of 1M ammonium hydroxide) in the sample after proper mixing. The silylation of the reduced sample was performed using silylating agent, N,O-Bis (trimethylsilyl) trifluoroacetamide (BSTFA) in pyridine at 60 °C for 30 min. The product of this reaction is methylsilanes was used for monomers analysis of EPS by GC-MS analysis. Analysis of linkage present in the monosaccharides and its position were determined by performing permethylation according to **Poli et al. (2009)** followed by hydrolysis and silylation (**Synytsya and Novak, 2014**). Briefly, 5-10 mg of EPS sample was dissolved in 1 mL dimethyl sulphoxide (DMSO) mixed with 50 mg of grounded sodium hydroxide and 0.1 mL of methyl iodide. The prepared samples were kept on an orbital shaker at 30 °C for 5 h followed by solvent extraction of aqueous layer with dichloromethane. The extracted organic phase was washed with water and evaporated to dryness under an air stream. The methylated product was further hydrolysed and silylated as described earlier in this section followed by GC-MS analysis.

Both permethylated and silylated EPS sample were dissolved in pyridine and analyzed by the GC-MS, condition described by **Gupta et al., (2016)** on Shimadzu GC-MS-QP 2010 Plus instrument equipped with a capillary column Rtx-5 (dimensions: 0.25-µm film thickness, 0.25 mm ID, 30 m in length). 1.00 µL of the samples were injected into GC-MS injector port and conditions were set as: initial temperature 50 °C for 2 min; first ramp 5 °C min^{-1} to 250 °C, hold time: 5 min and second ramp 10 °C min^{-1} to 280 °C, hold time: 10 min. The head pressure of the

helium carrier gas was 81.7 kPa and helium flow rate 1.0 mL min^{-1}. All data similarity search were performed with the GC-MS inbuilt standard mass spectra library of NIST-08 and Wiley-8.

6.2.6.4 NMR analysis

The ^{1}H NMR and ^{13}C NMR measurements of pure EPS were performed using Varian Mercury Plus NMR spectrometer that was equipped with ATB and SW Varian probes (5 mm). The purified and dried EPS was dissolved in deuterated water (D_2O), taken as solvent (10 mg mL^{-1}) (**Vijayendra et al. 2008**). ^{1}H spectrum was recorded at 10330.578 Hz, with pulse width of 3.17 s, with pulse duration of 64° and a recycle delay of 1 s. The spectrum was measured with 16 scans. ^{13}C NMR spectra were obtained at 29761.904 Hz, with pulse width of 1.10 s, with pulse duration of 64° and a recycle delay of 0.03 s. The spectrum was measured with 1640 scans (**Gupta et al., 2016)**.

6.2.7 Optimization of EPS production and scale up

6.2.7.1 Culture conditions for optimization of EPS production by *Serratia* sp. ISTD04

The optimization experiments were performed with *Serratia* sp. ISTD04, pre-cultured in LB and inoculated in 250 mL Erlenmeyer flasks under aerobic conditions, with 100 mL of MM at 30 °C and 150 rpm for 72 h and were supplemented with Glucose concentration (0.0-2.5% (w/v)), $NaHCO_3$ concentration (0-200 mM) and pH ranges (5-10) as per experimental design, based on the previous studies carried out on the bacterial strain by **Kumar et al., (2016d).** C:N ratio play crucial role in production of EPS by microorganism (**More et al., 2014**), so in this study C:N ratio (3-40) was also optimized.Finally the weight of EPS (LB-EPS and TB-EPS) was determined by methodology described in section 6.2.4 and weight was expressed in g L^{-1}.

6.2.7.2 Scale-up the production of EPS

The optimized parameters for EPS production along with CO_2 sequestration were used in a 20 L fed batch bioreactor (Adept). LB-precultured cells of *Serratia* sp. ISTD04 were inoculated in (1:100 v/v) an effective volume of 10 L MM, pH 8 supplemented with 10 g L^{-1} glucose and 50 mM $NaHCO_3$. Aeration was provided by the rate of 2 litres per minute (LPM) and stirring

rate 300 rpm. After 48 h, 5 g L^{-1}glucose and 50 mM $NaHCO_3$ were supplemented in the media then 72 h, 2 g yeast extract was added as nitrogen source; finally after 144 h the cultures were harvested and centrifuged at 8000 rpm for 10 min. The bacterial culture was harvested for extraction of EPS as methodology described in **Section 6.2.4.**

6.2.8 Determination of flocculating activity

Samples were taken at desired time for the measurement of flocculating activity by using the method described by **He et al (2002)**. The mixture containing 100 ml kaolin clay suspension (5 g L^{-1}, pH 7.0), 0.2 ml sample (bacterial culture broth as well as supernatant separately) and 1ml $CaCl_2$ solution (1 mg L^{-1}, pH 7.0), was stirred vigorously and left standing for 10 min. The supernatant was measured for absorbance at 550 nm (**Wang et al., 2007**). A control was prepared using the same method but the sample was replaced by distilled water. The flocculating activity was calculated as: Flocculating activity (%) = $(A - B) \div A \times 100$ (1)

Where *A* and *B* are the optical densities of the control and the sample, respectively.

6.2.9 Application of EPS in dyes decolorization

To determine the decolorization activity of EPS a dose of 1.0 ml bacterial culture and 1ml $CaCl_2$ solution (1 mg L^{-1}) was added to the 100 mL of 0.1 % cationic dye (Acridine orange, Crystal violet) and anionic dye (Trypan blue, Methyl orange, Bromothymol blue, Aniline blue) solutions at pH 7.0. After the addition of bacterial culture, the compound in the beaker was mixed using a blender at 200 rpm for 1 min, and then at 40 rpm for another 3 min. The dyes solution was left to settle for 10 min, and then the supernatant was taken for analysis (**Wang et al., 2007**).To determine the dye concentration of each sample, the absorption spectral scan (200‑800 nm) of control and treated reaction mixture was carried on UV-visible (Varian Carry 100 Bio) spectrophotometer (**Mazur et al. 2009; Mishra and Thakur 2011**). The absorbance of each dye was measured using a UV–vis spectrophotometer in scan mode at the maximum wavelength of each dye (607, 470-490, 407, 615, 588, 595-610 nm for trypan blue, acridine orange, methyl orange, bromothymol blue, crystal violet and aniline blue, respectively). The residual concentration of the dye in the samples was then calculated, and the decolorization efficiency was calculated as follows:

Decolorization efficiency (%) = $(A_0 - A) \div A_0 \times 100$ (2)

where A_0 is the initial dye absorbance and A is dye absorbance after the flocculation treatment.

6.2.10 Proteomics and genomics study of chemolithotrophic bacterium *Serratia* sp. ISTD04 for production of EPS

For proteomic analysis, protein content in whole cell lysate (25µg) was resolved by sodium dodecyl sulfate-polyacrylamide gel electrophoresis (SDS-PAGE) on a 6% polyacrylamide stacking gel and a 12% polyacrylamide-resolving gel (**Laemmli, 1970**). Protein bands were visualized by staining with Coomassie brilliant blue R250. Individually each sample lanes were separated into six horizontal sections and each section was further chopped into small pieces (approximately 1 mm^2) and was kept into separate tube. In-gel tryptic digestion and peptide extraction was performed separately according to method described earlier (**Manavalan et al., 2012**). All the fractions of the in-gel digested peptides were analyzed by using liquid chromatography (Tempo nano-LC from Applied Biosystems, Foster City, CA) offline coupled to ABI 5800 Proteomics Analyzer MALDI-TOF/TOF mass spectrometer (Applied Biosystems, Foster City, CA) (**Singh et al., 2017**). Detailed genomic analysis methodology of this strain was described in chapter 3; here we have demonstrated the genes responsible for biosynthesis of EPS and its arrangement on the cluster by antiSMASH ver. 4.1.0 and Rapid Annotations using Subsystems technology (RAST) (**Aziz et al., 2008, Overbeek et al., 2014**).

6.3 Results and discussion

6.3.1 Production of EPS by *Serratia* sp. ISTD04

The *Serratia* sp. strain ISTD04 has been previously reported as a CO_2-sequestering bacterium isolated from marble mining rocks in the Umra area, Rajasthan, India. This strain grows chemolithotrophically on media that contain $NaHCO_3$ as the sole carbon source (**Bharti et al., 2014a; 2014b**). Here this strain was used for production of EPS in presence of $NaHCO_3$ as carbon source and glucose as inducer in MM-media. The EPS production (after acetone washing and drying) in MM-media, pH 7.8, glucose 0.5% (w/v), $NaHCO_3$ 50 mM was found to be 1.44 ±0.10 g L^{-1} culture at 30 °C, harvested after 72 h. The pure EPS appeared as a white amorphous material **(Fig.6.1a and b).** There have been previous reports of EPS production by bacteria isolated from waste water sludge as well as extreme habitats (**Arena et al. 2006; Maugeri et al.**

2002). As far as author knowledge concerned, this is the first report of production of EPS from a chemolithotrophic bacteria *Serratia* sp. isolated from marble mining rocks

(a) (b)

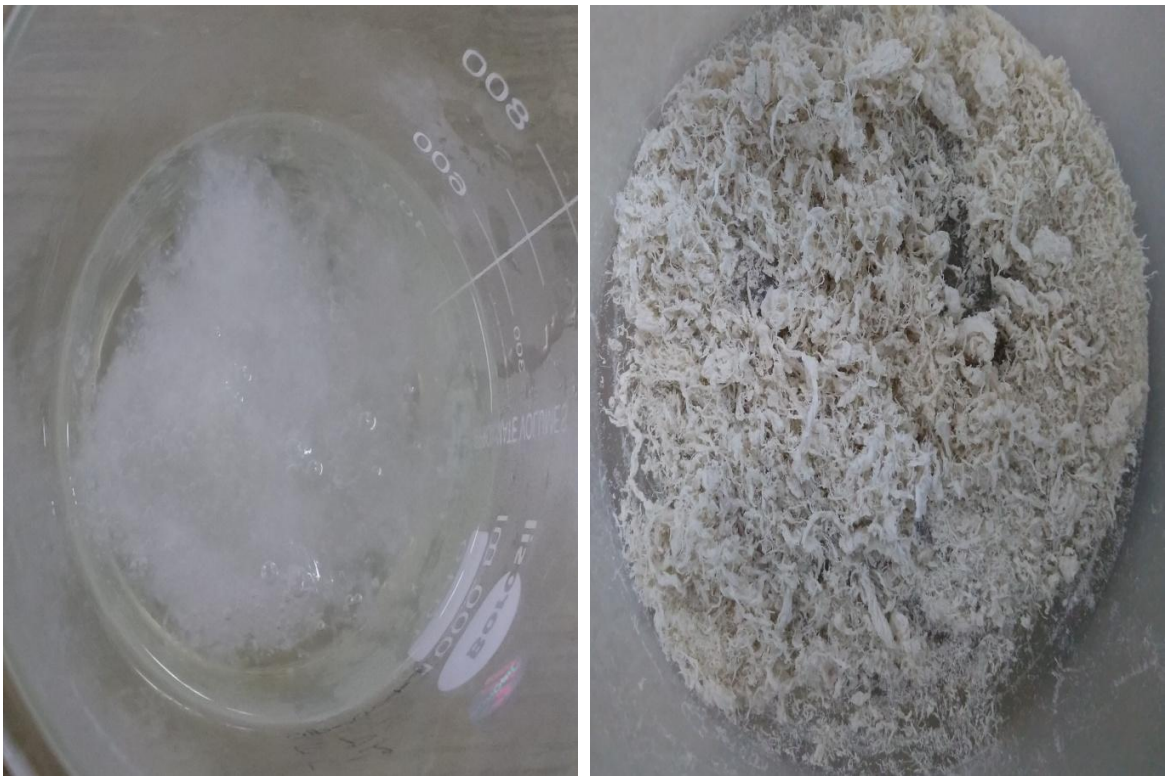

Fig. 6.1 (a) EPS precipitated by ice cold isopropanol (b) EPS purified by isopropanol, acetone and oven dried

6.3.2 Morphological observation of *Serratia* sp. ISTD04 grown in MM- media

SEM observation **Fig.6.2** depicted that, during initial growth of bacteria, production of EPS was less and bacterial cells shows maximum growth, due to availability of carbon, nitrogen and phosphate source in the media. When time passed carbon and nutrients concentration depleted in the media and bacteria came to stress, it shape and morphology also changed, that leads to maximum production of EPS in the media (**Liu et al., 2006)**. That might be the defensive mechanism adopted by the bacteria to cop up with imbalance nutrient condition in the growth media (**Bezawada et al., 2013; Dermlim et al., 1999**).

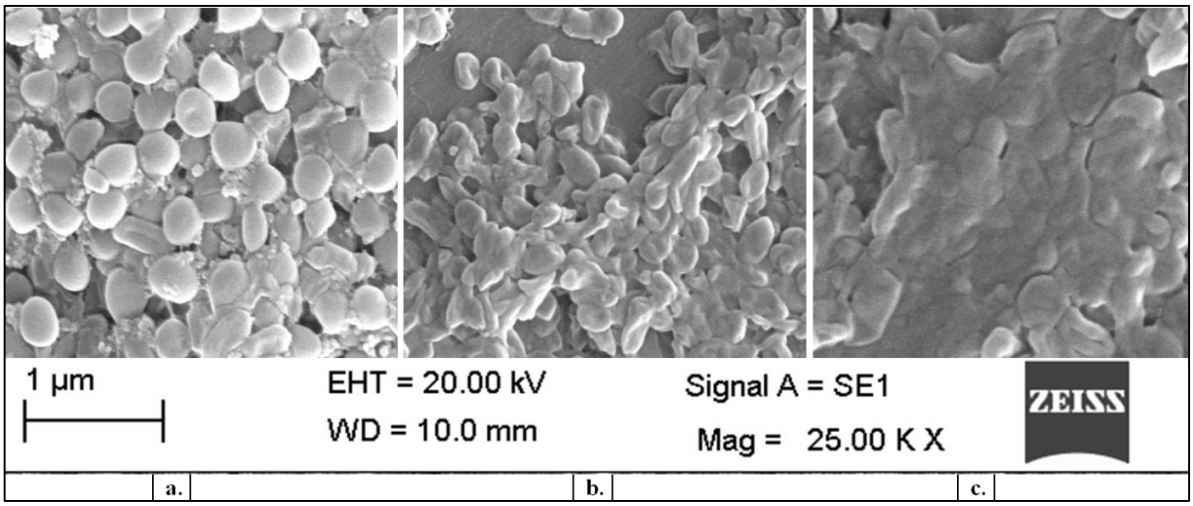

Fig.6.2 SEM images of *Serratia* sp. ISTD04 during EPS production at different time intervals; (**a)** 0h, (**b)** 48 h, and (**c)** 72h in media supplemented with 50 mM $NaHCO_3$ and glucose (0.5%).

6.3.3 Chemical characterization of EPS

6.3.3.1 Estimation of total carbohydrate content of EPS

According to the phenol-sulfuric acid assay, the concentration of total carbohydrates in EPS was found to be 67 % w/w. Standard curve was prepared with Glucose **Fig.6.3**. The results show that carbohydrates are the major component of the EPS. The phenol-sulfuric acid method is a simple and rapid colorimetric technique used for the estimation of total carbohydrates in a sample. The method involves detection of all classes of carbohydrates including mono-, di-, oligo- and polysaccharides. In this method, the concentrated sulfuric acid oxidises any polysaccharides, oligosaccharides, and disaccharides to monosaccharides. Pentoses (5-carbon compounds) and hexoses (6-carbon compounds) are then dehydrated to furfural and hydroxymethyl furfural, respectively. These compounds react with phenol to form a yellow-gold colour, which has absorption maxima at 490 nm. This colour is stable for several hours, and the accuracy of the method falls within ± 2 % under proper experimental conditions.

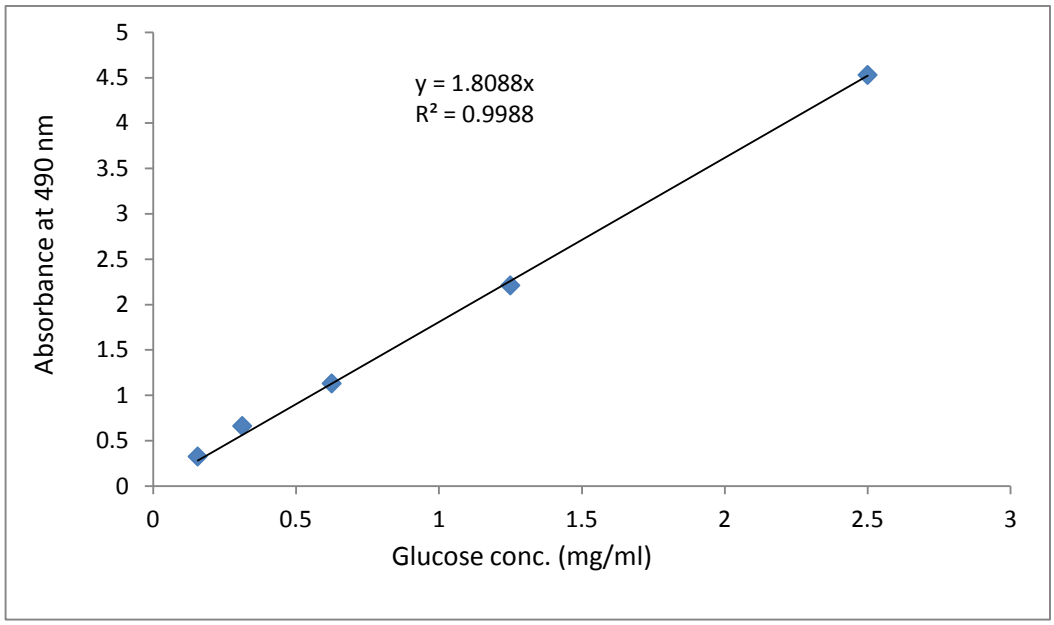

Fig.6.3. Standard curve of Glucose for phenol- sulfuric acid assay.

6.3.3.2 Estimation of reducing sugar content of EPS

3,5-dinitrosalicylic acid (DNS) assay was done for estimation of reducing sugars in EPS. Standard curve was prepared with Glucose **Fig.6.4**. According to this assay, the concentration of reducing sugar in EPS was found to be 34.5 % w/w. The assay reveals that the EPS produced by the bacterial strain is composed almost equally of reducing as well as non-reducing sugars. This method tests the presence of free carbonyl group (C=O), characteristic of reducing sugars. The assay involves the oxidation of the aldehyde (-CHO) functional group, commonly present in glucose and the ketone (C=O) functional group of fructose. Concurrently, DNS is reduced to 3-amino,5-nitrosalicylic acid under alkaline conditions as represented by the following reaction:

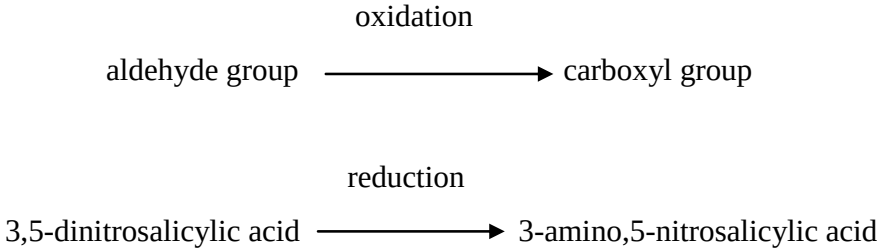

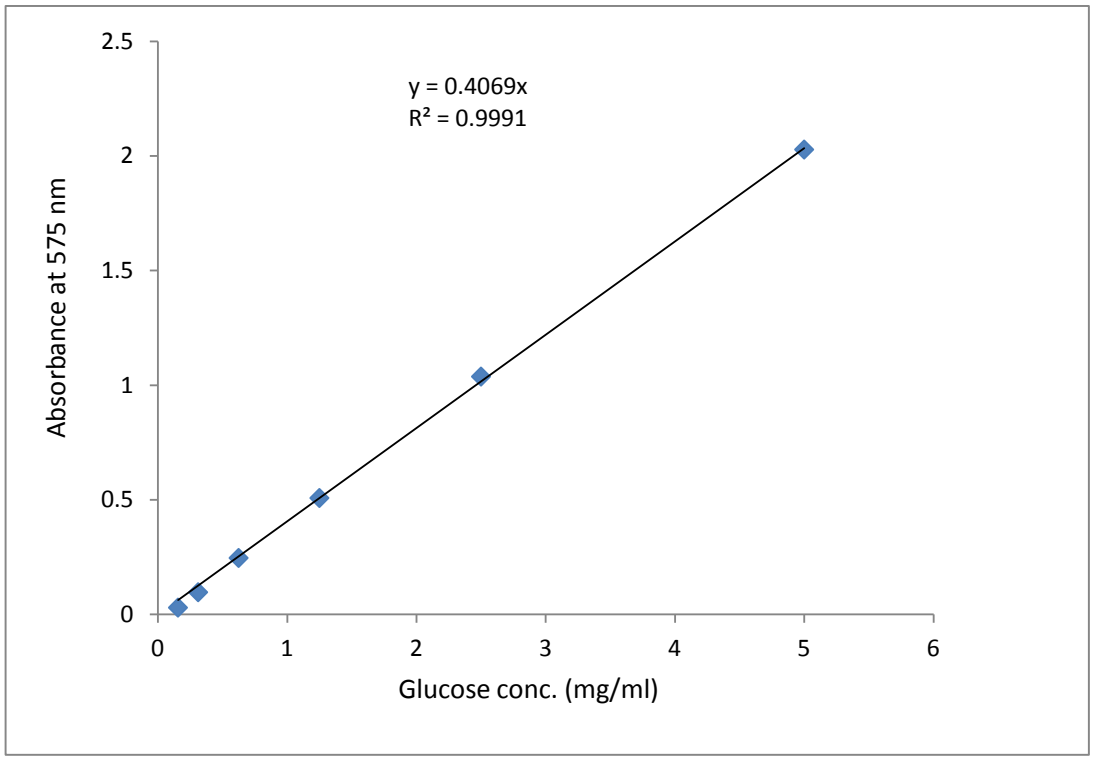

Fig. 6.4 Standard curve of Glucose for 3,5- dinitrosalicyclic acid assay.

6.3.3.3 Estimation of protein concentration of EPS

According to the Bradford assay, the concentration of total protein present in the EPS was found to be 0.54 % w/w (**Fig.6.5**). Thus, the protein content of EPS was found to be very low. The Bradford assay is a colorimetric protein assay, which is based on an absorbance shift of the Coomassie Brilliant Blue G-250 dye. Under acidic conditions, the red colour of the dye is changed to blue as a result of the dye binding to the protein being assayed. The bound form of the dye has absorption maxima at 595 nm. The cationic (unbound) forms are of usually green or red colour. The binding of the dye to the protein results in stabilization of the blue anionic form. The increase in the absorbance at 595 nm is directly proportional to the amount of the bound dye, and thus to the protein concentration in the sample.

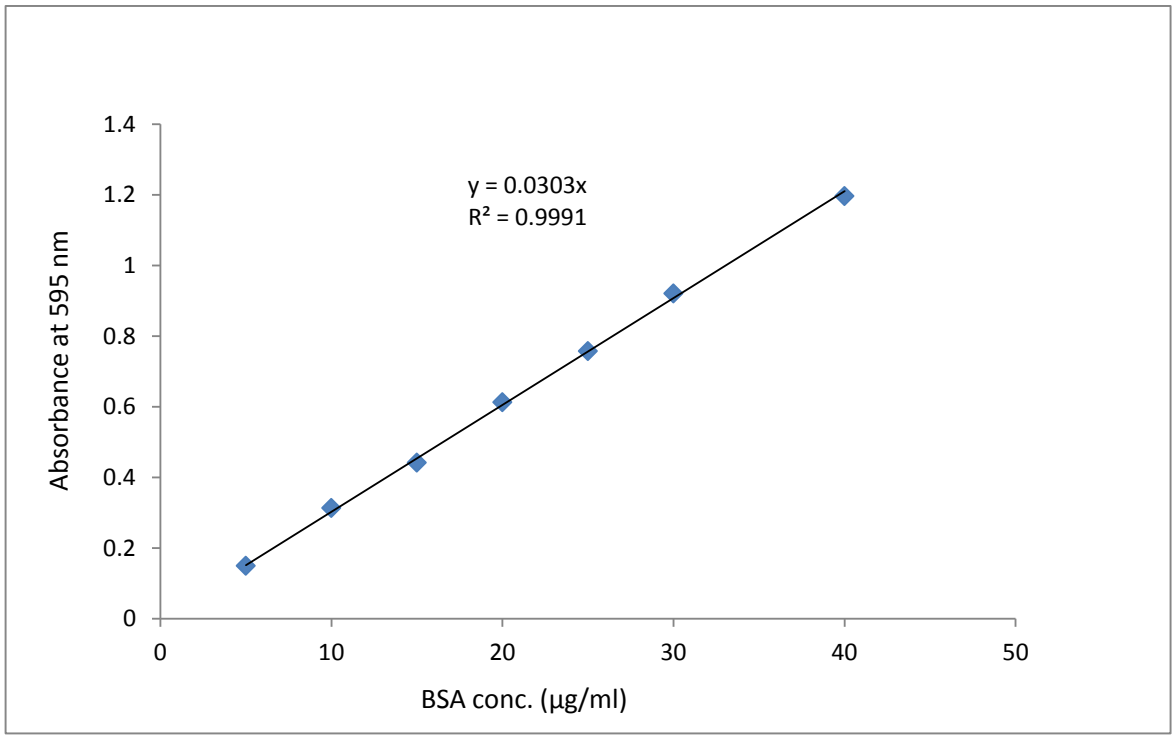

Fig.6.5 Standard curve of BSA for Bradford assay.

6.3.3.4 Estimation of fatty acid content in EPS

Fatty acids content in the EPS was estimated by method described by **Zhang et al., (2014)** using chloroform: methanol (2:1 v/v) and the content were found to be 10.49% w/w of dry EPS. It has been reported that the fatty acids content of the EPS varies from 1-10%, and it play major to minor role in flocculating activities, depends on its fatty acids content of EPS (**Flemming and Wingender, 2010; Tian, 2008; Wingender et al., 1999**). This bacterial strain have been previously reported for production of extracellular fatty acid might be that should be the probable reason of high fatty acid content in the EPS (**Bharti et al., 2014c**).

6.3.4 Structural compositional analysis of EPS

6.3.4.1 SEM-EDX analysis of EPS

The surface view of EPS was analysed using scanning electron microscopy (SEM) at various magnifications ranging from 500 X to 10 KX (**Fig.6.6.a-d**). The polysaccharide appears to be an amorphous white solid under 500 X **Fig. 6.6a**. Higher magnifications reveal a porous, layered texture of EPS, with pore sizes varying in the range from nanometers to micrometers (**Fig.6.6.b-d**). Scanning electron microscope (SEM) is an electron microscope that scans the sample with a focussed beam of electrons to produce the image. The interaction of electrons with atoms in the sample, produce various signals that convey information about the surface topography and composition of the sample. Commonly, in SEM analysis, secondary electrons emitted by sample atoms that are excited by the electron beam, are detected. Scanning of the sample and collection of the emitted secondary electrons, using a special detector, creates an image of the sample displaying the surface topography.

(a) (b)

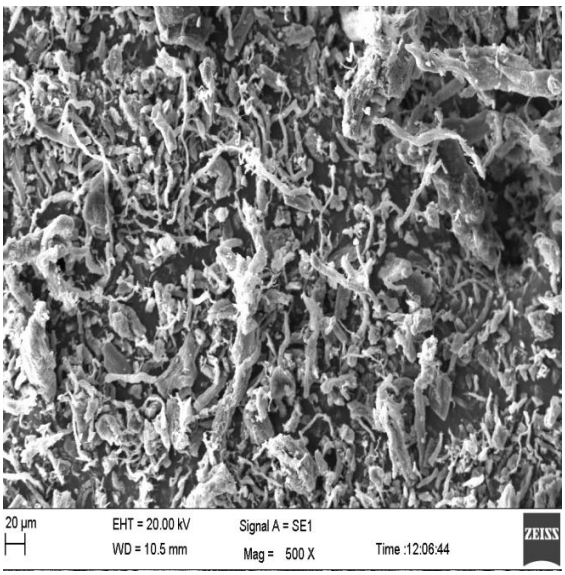

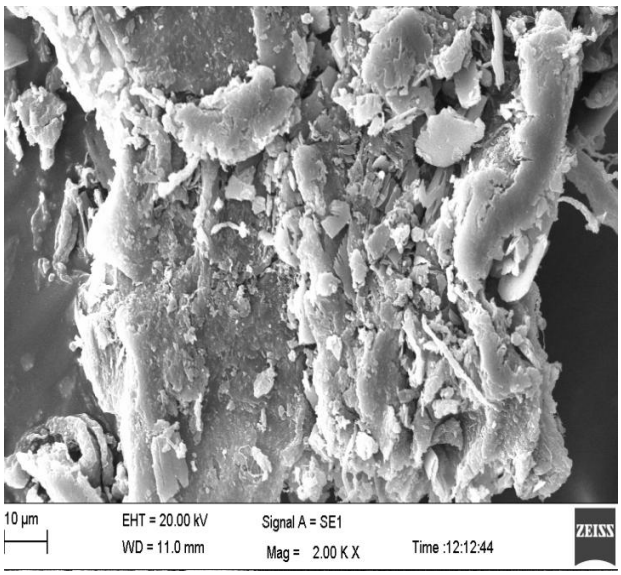

(c) (d)

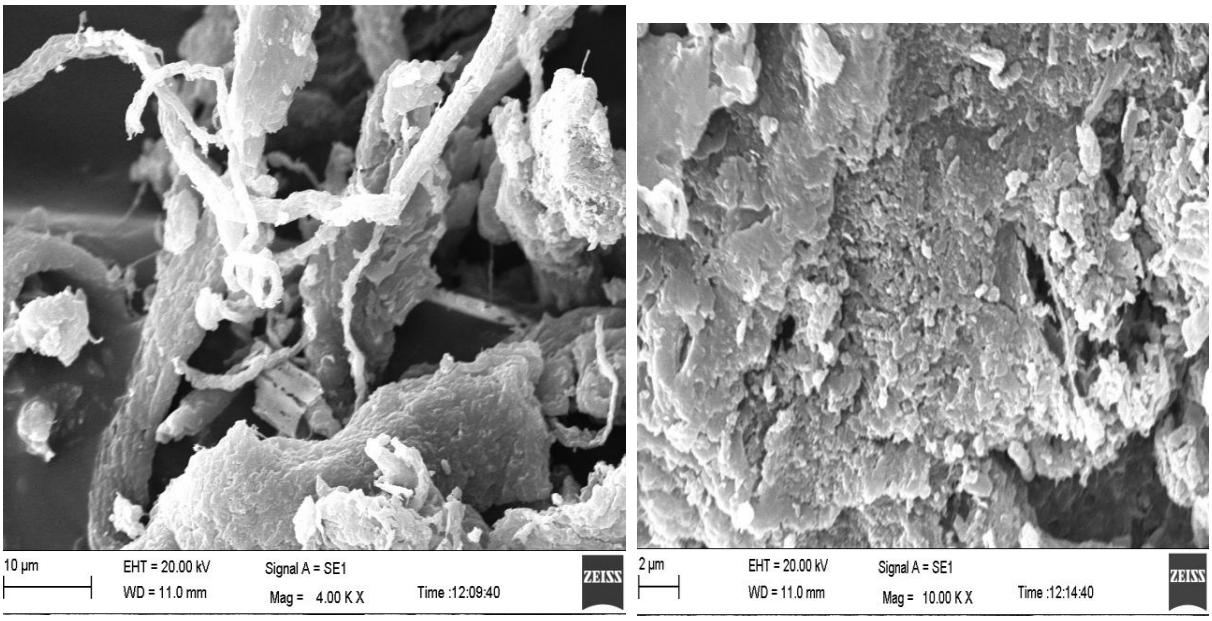

Fig.6.6 SEM viewing of purified EPS extracted from *Serratia* sp. ISTD04 at various magnifications (a-d).

Energy Dispersive X-Ray Spectroscopy (EDX) analysis of the pure and dry basal EPS revealed the dominance of carbon (26.39 at. wt. %) and oxygen (67.87 at. wt. %) along with the presence of other elements like sodium (2.41 at. wt. %), iron (0.58 at. wt. %), phosphorus (1.90 at. wt. %) potassium (0.85 at. wt %) (**Fig.6.7.a,b**). EDX Analysis in terms of abundance, indicating towards the purely organic nature of EPS. EDX is micro-analytical technique used along with SEM to detect the elemental composition of the analysed volume. The analysis involves detection of x-rays emitted following bombardment of electron beam on the sample. The elemental composition of the sampled volume is evaluated from x-ray energy versus counts spectrum.

(a)

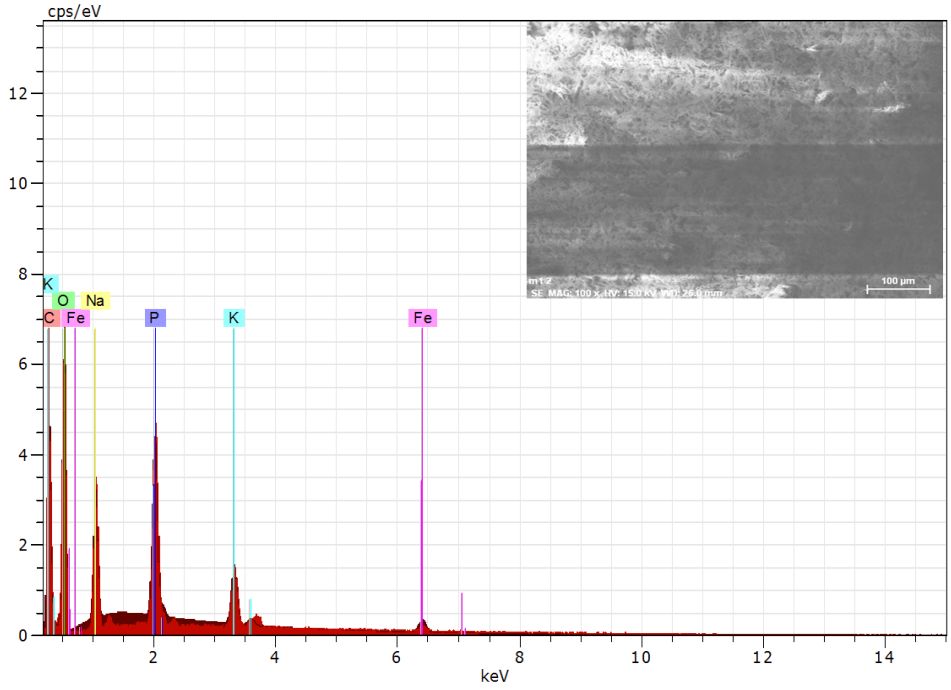

(b)

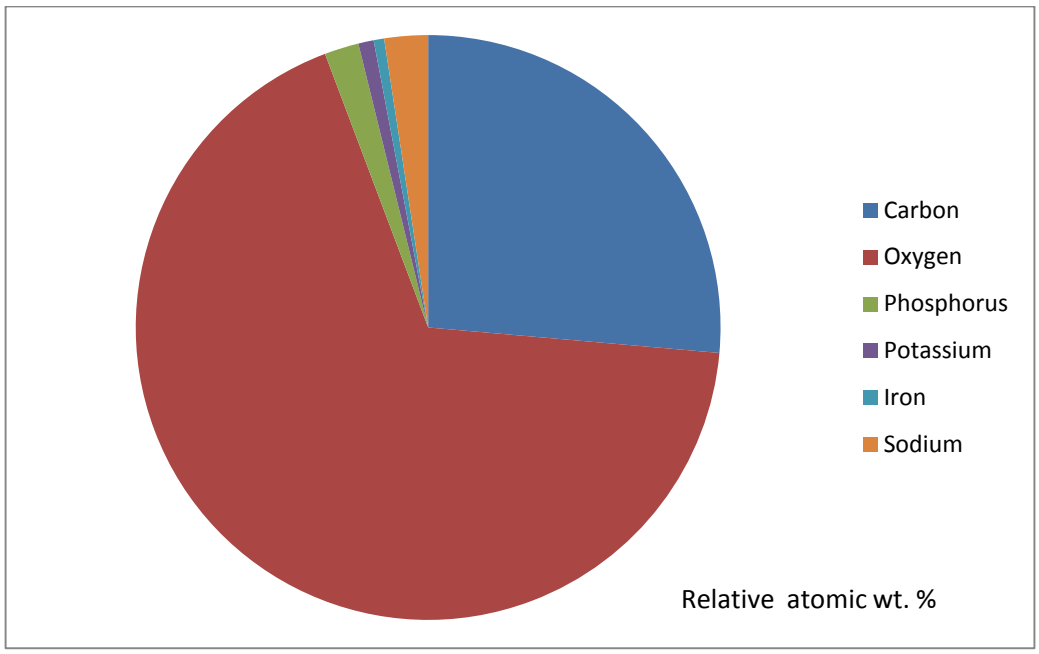

Fig.6.7 Elemental composition of EPS in terms of abundance, as detected by EDX spectrometer (a) peaks of the elements detected (b) relative Atomic wt. percent of the abundant elements.

6.3.4.2 Functional group analysis by FT-IR

The EPS produced by *Serratia* sp. ISTD04 was characterized for functional group composition by FT-IR (**Fig.6.8**). The broad and intense band at 3396.63 cm^{-1} (stretching vibration of hydroxyl groups) and 2929.86 cm^{-1} (C-H stretching of CH2 groups) usually observed in carbohydrates (**Kumar et al., 2015**). The band at 1643.34 cm^{-1} (C=O stretching vibration), 1537.26 cm^{-1} (vibration of C-O), 1414.81 cm^{-1} (CH2 bending and C-O-O stretching vibrations), 1390.67cm^{-1} (bending vibration of C-H), 1153.42 cm^{-1} indicated (C-O-C stretching) and 1078.28 cm^{-1} (C-O stretching) was due to sugar ring vibrations. The band between 1000 and 1100 cm^{-1}, i.e. 1078.28 cm^{-1} was characteristic for the presence of β -glucans due to O-substituted glucose residues (**Kim et al., 2016; Yoshiba et al., 2015**). The band at 854.46 cm^{-1} (C-H variable angle vibration) indicated the presence of β-pyranoside units. The absorption at 707.87 and 543.92 cm^{-1} can be detected in (1→3) - β -D-glucan (**Mathlouthi and Koenig, 1987; Shingel, 2002**). Peak observed and their corresponding bonds annotation was also represented in **Table 6.1**.

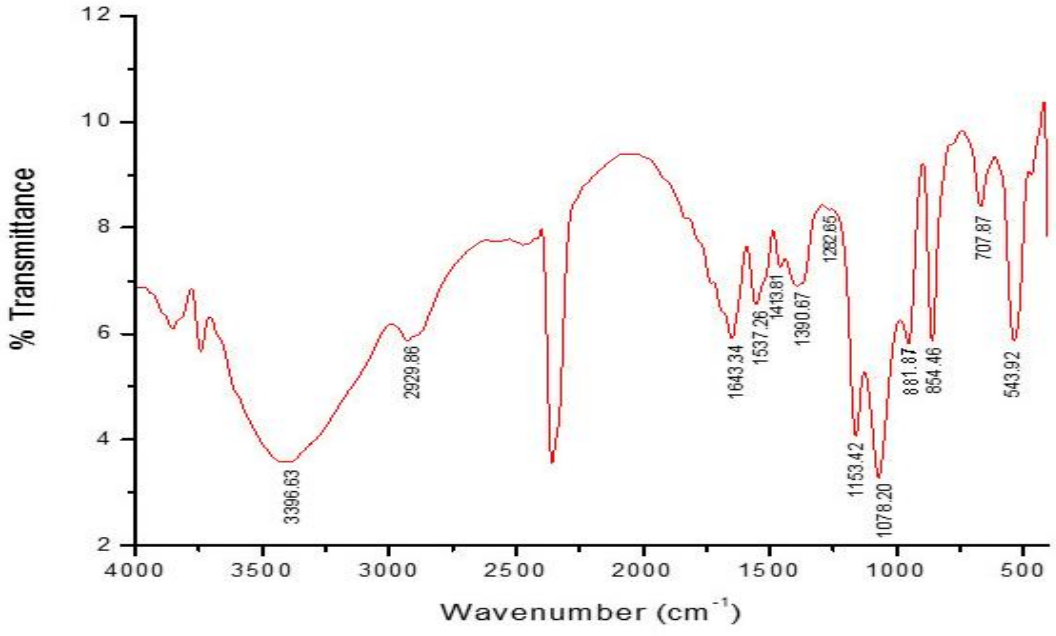

Fig.6.8 FT-IR spectra of EPS produced by *Serratia* sp. ISTD04.

Table.6.1 Peaks observed in FTIR spectrum of EPS produced by *Serratia* sp. ISTD04.

Peak(cm^{-1})	**Bonds and Corresponding annotation**
707.87 and 543.92	(1-3)- *ß*-D-glucan
854.46	C-H variable angle vibration
881.87	Pyranose ring
1078.28	O-substituted glucose residues
1153.42	C-O-C stretching
1390.67	bending vibration of C-H
1414.81	CH2 bending and C-O-O stretching vibrations
1537.26	vibration of C-O
1643.34	C=O stretching vibration
2929.86	C-H stretching of CH2 groups
3396.63	Stretching vibration of hydroxyl groups

6.3.4.3 Monosaccharide composition and Linkage analysis by GC-MS

The monosaccharide components of EPS produced by *Serratia* sp. ISTD04 were analyzed on GC–MS after hydrolysis and silylation (**Synytsya and Novak, 2014)** (**Fig.6.9a**). EPS produced by the bacterium was found to be composed of three types of monosaccharide components, that is, glucose, arabinose and mannose. β-D-glucose was detected at R.T. (Retention Time) 16.600 and 43.101. β-D arabinopyranoside (R.T. 14.890) and β-D-mannofuranose (R.T. 20.703) were also detected in the electron impact fragmentation pattern of the mass spectra. All the detected monosaccharides showed D-configuration. The results were in agreement with the peaks observed in the FT-IR spectrum. Linkage positions of the monosaccharides as determined by methylation analysis revealed the presence of β-D-glucopyranoside, methyl 2,4,6-tri-O-methyl- (R.T. 18.467), which corresponded to 3-linked glucose residue (**Fig.6.9b**) (**Gupta and Thakur, 2016**). Another peak at R.T. 24.917 and 27.367 represent the 2, 3, 4, 5- tetra-O-methyl arising from the terminal branched mannose residues

(**Singh et al., 2017; Leathers et al., 2006)**. The monomer composition and linkage analysis indicated that the EPS is heteropolymer with diverse linkages

(a)

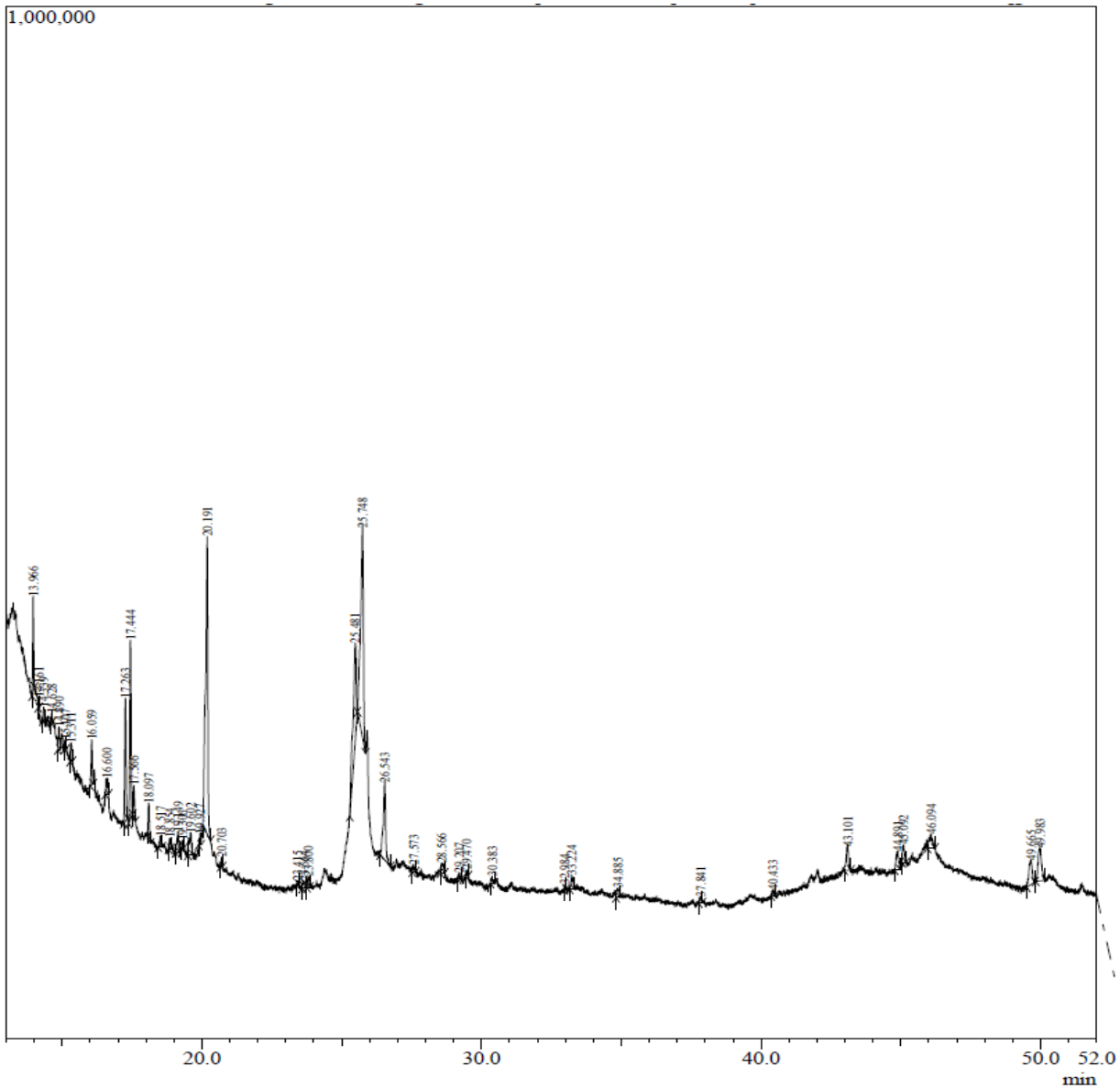

(b)

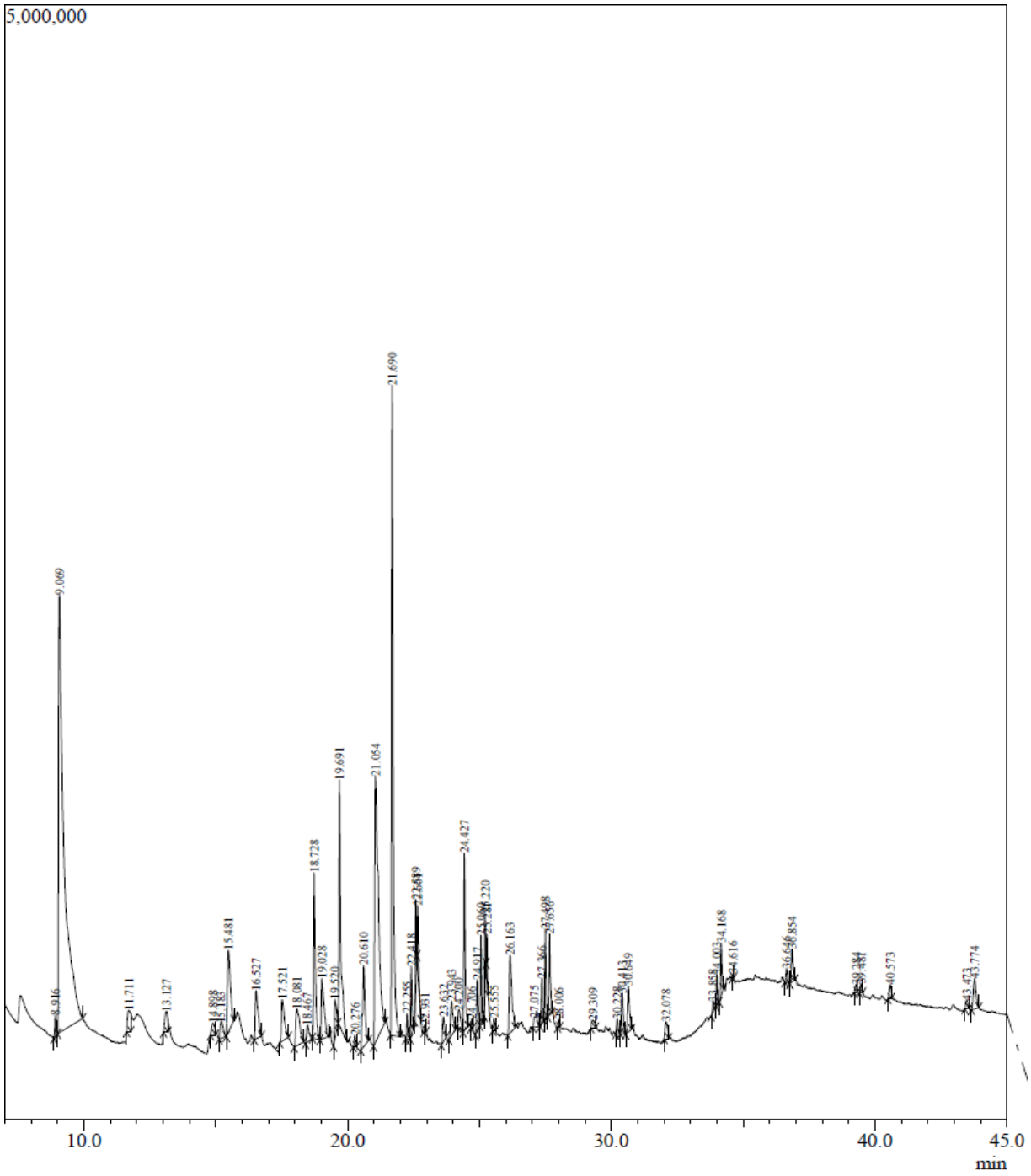

Fig.6.9 (a) GC-MS analysis of monomers composition of EPS produced by Serratia sp. ISTD04 (b) Linkage analysis of EPS.

6.3.4.4 Structural configuration analysis of EPS by ^{13}C and ^{1}H NMR

The ^{13}C NMR spectrum of the pure EPS (**Fig.6.10a**) showed the six well resolved signals at 95.93, 75.96, 74.16, 75.78, 69.67 and 60.61 ppm, that correspond to the six carbons of the pyranose ring at 1st, 4th, 5th, 3rd, 6th and 2nd positions, respectively. The carbon chemical shifts corresponded to β-configured glucopyranose units. The detection of a downfield shifted peak at 69.62 and the presence of a signal at δ 60-61, which is characteristic of glucose moiety indicate β-(2 → 6) backbone structure of EPS (**Bubb, 2003; Poli et al., 2009; Vijayendra et al., 2008**). The ^{1}H NMR (**Fig.6.10b**) revealed the presence of a prominent peak at 4.687 ppm, which is characteristic of β-anomer, while other protons were observed to be present in a series, distributed over a range of 3.773-3.130 ppm (**Vijayendra et al., 2008**).

(a)

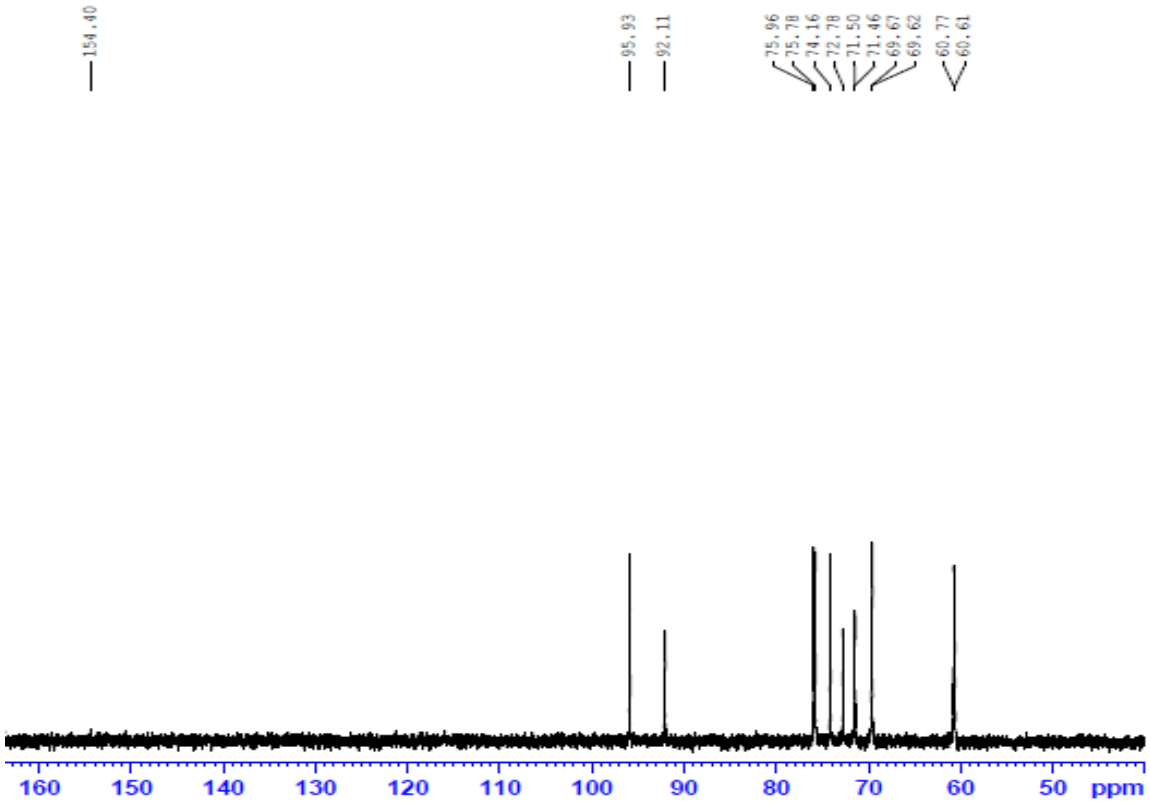

(b)

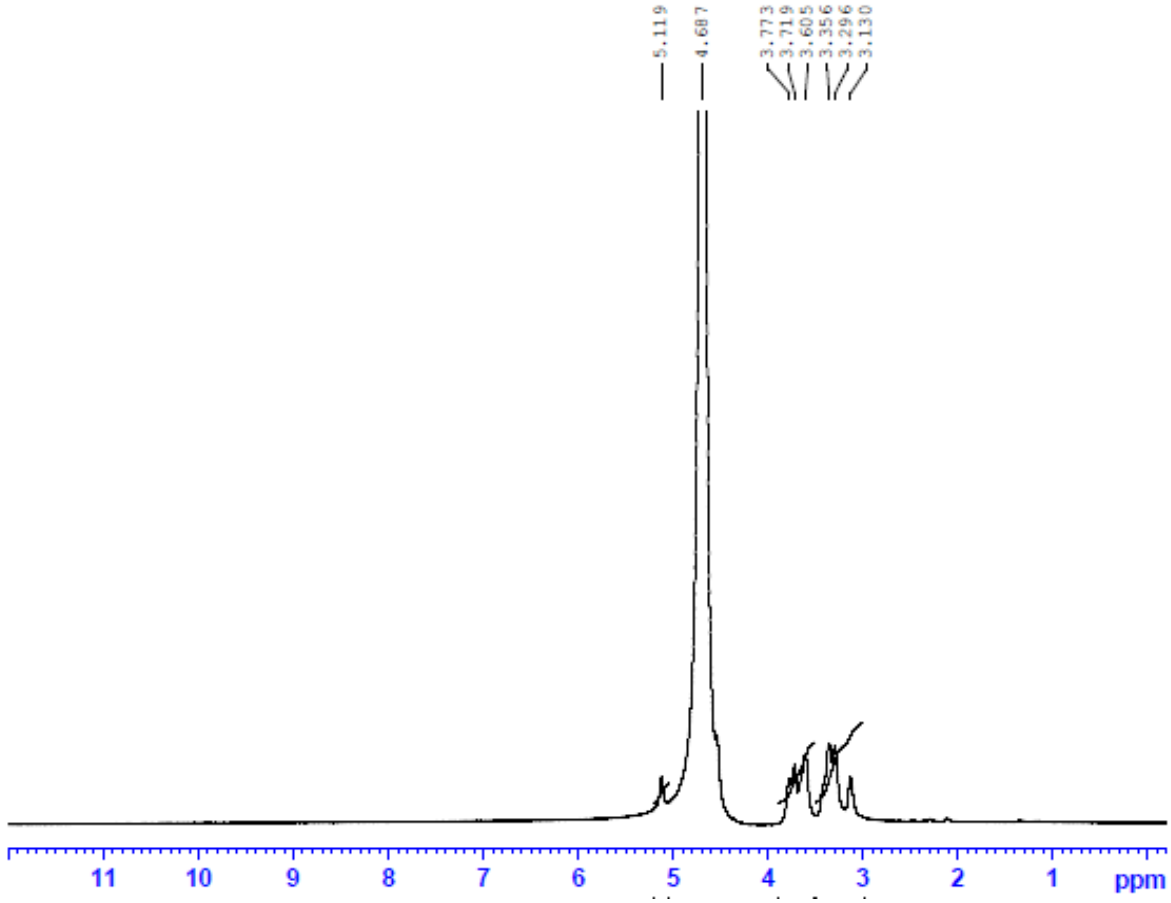

Fig.6.10 (a) ^{13}C and (b) ^{1}H NMR analysis of EPS extracted from *Serratia* sp. ISTD04.

6.3.5 Optimization of production of EPS by *Serratia* sp. ISTD04

To enhance the production yield of EPS, optimization of process parameters, such as glucose concentration, $NaHCO_3$ concentration and pH of the media was performed in triplicates. As before the optimization (Initial condition, glucose 0.5% w/v, $NaHCO_3$ 50 mM, pH 7.8, Duration 72 h) the yield of B-EPS was 1.44 ±0.10 g L^{-1}, which includes 1.33 ±0.08 g L^{-1} and 0.11 ± 0.02 g L^{-1} LB-EPS and TB-EPS respectively. After the optimization the yield of B-EPS was 4.57 ±0.21 g L^{-1} (TB-EPS 4.18 ±0.15 g $L^{-1}$and LB-EPS 0.39 ±0.06 g L^{-1}) at glucose concentration 1% w/v, $NaHCO_3$ 50 mM, pH 8 **Table 6.2, Fig.6.11, a, b, c.**

Table.6.2 Optimization of process parameters for production of EPS by *Serratia* sp. ISTD04

Experiment No	Glucose %(w/v)	NaHCO3 (mM)	C:N	pH	LB EPS (g/L)	TB EPS (g/L)	B-EPS (g/L)
1	-	50	3	7.8	1.13 ±0.11	0.12 ±0.02	1.25 ±0.13
2	0.5	50	10	7.8	1.33 ±0.08	0.11 ± 0.02	1.44 ±0.10
3	1	50	17	7.8	3.41 ±0.13	0.24 ±0.05	3.65 ±0.18
4	1.5	50	25	7.8	2.95 ±0.11	0.18 ±0.03	3.13 ±0.14
5	2	50	32	7.8	2.83 ±0.15	0.19 ±0.02	3.02 ±0.17
6	2.5	50	40	7.8	2.64 ±0.09	0.21 ±0.04	2.85 ±0.13
7	1	-	14	7.8	0.82 ±0.07	0.06 ±0.01	0.88 ±0.08
8	1	20	15	7.8	3.11 ±0.10	0.38 ±0.06	3.39 ±0.16
9	1	50	17	7.8	3.31 ±0.14	0.28 ±0.03	3.59 ±0.17
10	1	100	20	7.8	2.98 ±0.17	0.31 ±0.05	3.29 ±0.22
11	1	150	21	7.8	2.12 ±0.14	0.14 ±0.03	2.26 ±0.17
12	1	200	24	7.8	1.97 ±0.10	0. 17 ±0.02	2.14 ±0.12
13	1	50	17	5.0	1.86 ±0.13	0.15 ±0.04	2.01 ±0.17
14	1	50	17	6.0	2.31 ±0.14	0.28 ±0.03	2.59 ±0.17
15	1	50	17	7.0	3.47 ±0.18	0.37 ±0.04	3.84 ±0.22
16	1	50	17	8.0	4.18 ±0.15	0.39 ±0.06	4.57 ±0.21
17	1	50	17	9.0	3.53 ±0.17	0.33 ±0.04	3.88 ±0.21
18	1	50	17	10	2.52 ±0.16	0.34 ±0.03	2.86 ±0.19

(a) (b)

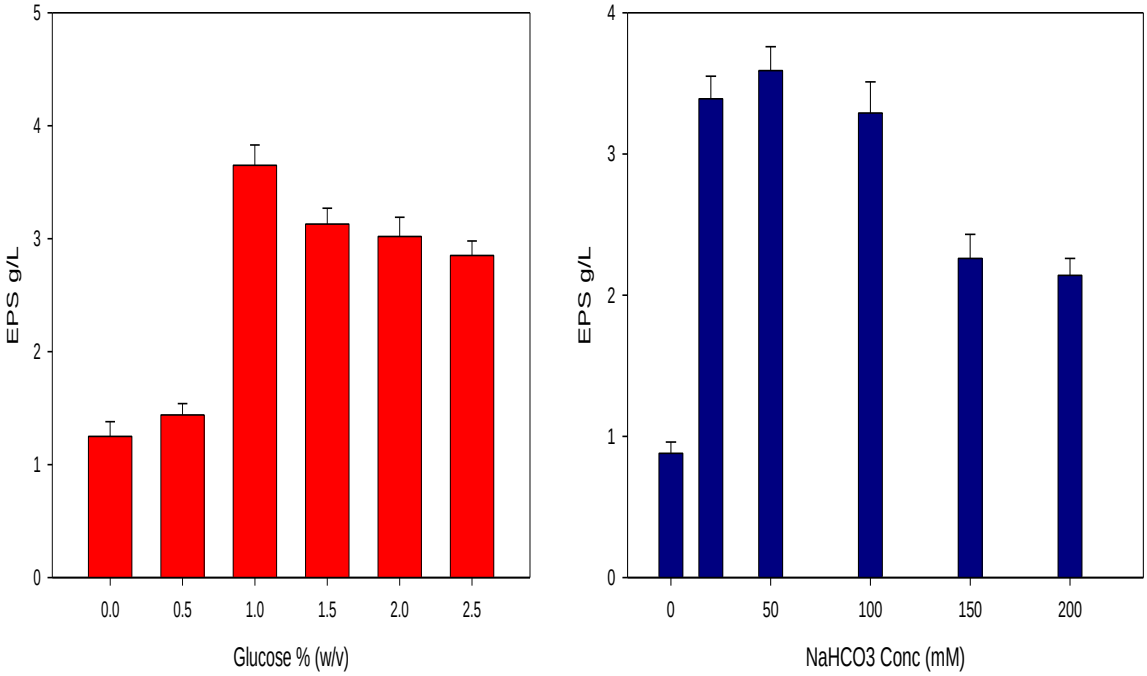

(c)

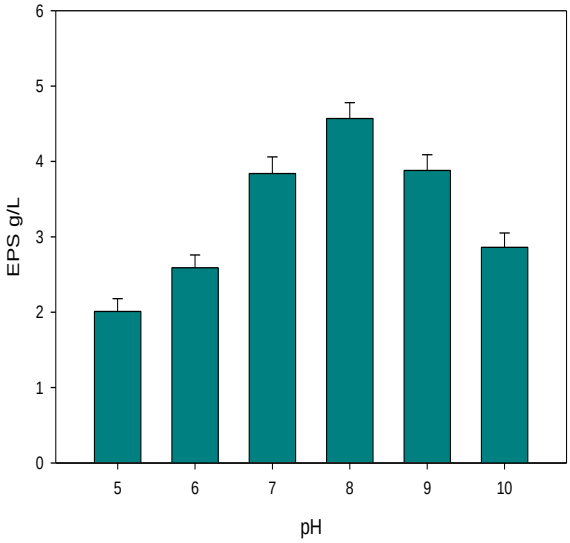

Fig.6.11 Representation of optimization parameters for production of EPS (a) Glucose % (w/v) (b) NaHCO3 Conc (mM) (c) pH.

There are many studies was performed by various researcher for EPS production from pure culture of bacteria using different carbon sources like glucose, sucrose, waste water, waste water sludge and Acetate-Propionate as represented in **Table.6.3**. After the optimization of process parameters 3-fold increase in EPS production by *Serratia* sp. ISTD04 was observed, which confirmed the important of optimization. The production of EPS is influenced by many factors including bacterial growth, carbon and nitrogen sources, pH and temperature (**More et al., 2014; Bezawada et al., 2013**). The EPS production depends upon the type of substrate, i.e., carbon and nitrogen source. There are a number of carbon and nitrogen sources reported to be favored over others by different EPS producing microorganisms (**Sheng et al., 2010; Wingender et al., 1999**).Therefore, EPS production usually takes place during active sugar consumption and is often growth associated. Along with different carbon and nitrogen source, a profound emphasis is given to C/N (carbon/nitrogen) ratio in relation with EPS production. This is due to the fact that the C/N ratio had a great effect on microbial metabolisms and hence on the EPS production. In fact, C/N ratio is critical for EPS production than the type of carbon and nitrogen source. In spite of several reports on C/N ratio relation to EPS, there is no fixed favorable C/N ratio in the literature for production of EPS. The range of C/N ratio is given in literature varies from 0.5 to 100 (specific for the microbes) and increased or decreased in this, affect the chemical nature of EPS and its flocculating properties (**Ye et al. 2011; Bezawada et al., 2013**). Usually, the optimum pH for bacterial production of EPS is also the optimum pH for its growth. The pH of the culture medium significantly influences the EPS production. However, the effect of pH on the production of EPS varies with different microorganisms, operational conditions and medium composition (**Shu and Lung, 2004**). The pH effects are often investigated using the same microorganism in flask experiments with different initial pH values. In general, the optimal medium pH for EPS production varies from 5.0 to 7.0. Several microorganisms have the capability to produce EPS at pH 7 in different media (**Gandhi et al., 1997**). Most of the EPS producing microorganisms require a constant pH for maximum production of EPS. Some of the microorganisms produce more EPS in acidic pH 5.5-6.5 (**Lee et al., 1999**). The extreme pH of the medium (pH 2.0-3.0 or pH higher than 10) affect the biosynthesis of EPS (**Czaczyk and Myszk, 2007**). The maximum production of EPS by *Serratia*

sp. ISTD04 in alkaline condition might be due to its inherent calcite precipitation ability at higher pH, which is facilitated by EPS (**Messner and Sleytr, 1992)**.

Table.6.3 Production of EPS by pure culture of bacteria using different carbon sources.

Microorganism	Carbon source	Yield of EPS (g/L)	Reference
Bacillus licheniformis	sucrose	2.9	Xiong et al., 2010
Proteus mirabilis (TJ-1)	glucose	1.3	Xia et al., 2008
Halomonas sp.	sucrose	1.073	Poli et al., 2009
P. jamilae CP-38	olive mill wastewaters	4.2	Aguilera et al., 2008
Alcaligenes cupidus (KT201)	Sucrose	1.5	Toeda and Kurane, 1991
Klebsiella sp.	Glucose	1.0	Dermlim et al., 1999
P. polymyxa SQR-21	Galactose	3.44	Raza et al., 2011
Citrobacter sp.	Acetate-Propionate	1.5	Fujita et al., 2000
Corynebacterium glutamicum	Sucrose	2.0	He et al., 2002
Bacillus sp. (MBFF19)	Glucose	0.8	Zheng et al., 2008
Serratia sp.1	Waste water sludge	3.44	Bezawada et al., 2013
Bacillus sp. ISTVK1	Waste water and Sucrose	0.31	Gupta and Thakur, 2016

6.3.6 Scale-up the production of EPS at fermentor level

The optimized parameters for EPS production were selected for production of EPS in a 20 L fed batch bioreactor with effective volume 10 L, proper monitoring of bacterial growth and subsequent production of EPS was estimated for 144 h **Fig.6.12**. The EPS was extracted, purified

and weighted **Fig.6.13**. The amount of B-EPS produced by *Serratia* sp. ISTD04 after 144 h was 7.8 ±0.39 g L^{-1} (LB-EPS 6.7 ±0.27 g L^{-1} and TB-EPS 1.1 ±0.12 g L^{-1}). Higher production of EPS in fermentor could possibly be due to stable growth condition, such as pH, aeration, temperature, sterring, carbon source being maintained in the fermentor which could have facilitated better growth of microorganism for production of EPS. Various researcher have been reported the production range of EPS by microorganism at shake flask as well as bioreactor level from 0.8 g L^{-1} - 27.70 g L^{-1} using carbon source like glucose, sucrose, glycerol, acetate and waste water sludge (**More et al., 2014). Bezawada et al. (2013)** have been reported that production of EPS by *Serratia* sp.1 using waste water sludge as carbon source in fermentor was 3.44 g L^{-1}, **Shen et al. (2013)** has reported 6.36 g L^{-1} EPS production from a 5-litre stirred tank fermentor by *Pleurotus pulmonarius*. **Poli et al. (2009)** reported 1.073 g L^{-1} and 1.844 g L^{-1} of EPS, in flasks and bioreactor condition respectively, by a novel *Halomonas* species, in the presence of sucrose in a defined media. In this present study almost 2 fold increments in EPS production was observed in fermentor as compare to shake flask level, which signify the higher production of EPS may leads to reduced its production cost.

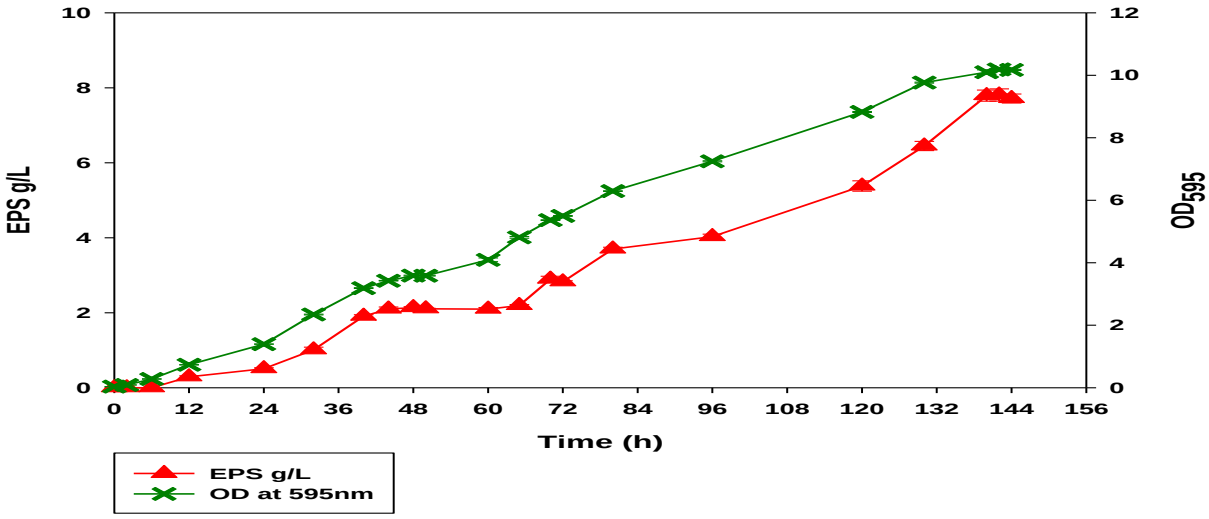

Fig.6.12 Bacterial growth in 20 L fermentor and subsequent production of EPS at various time intervals.

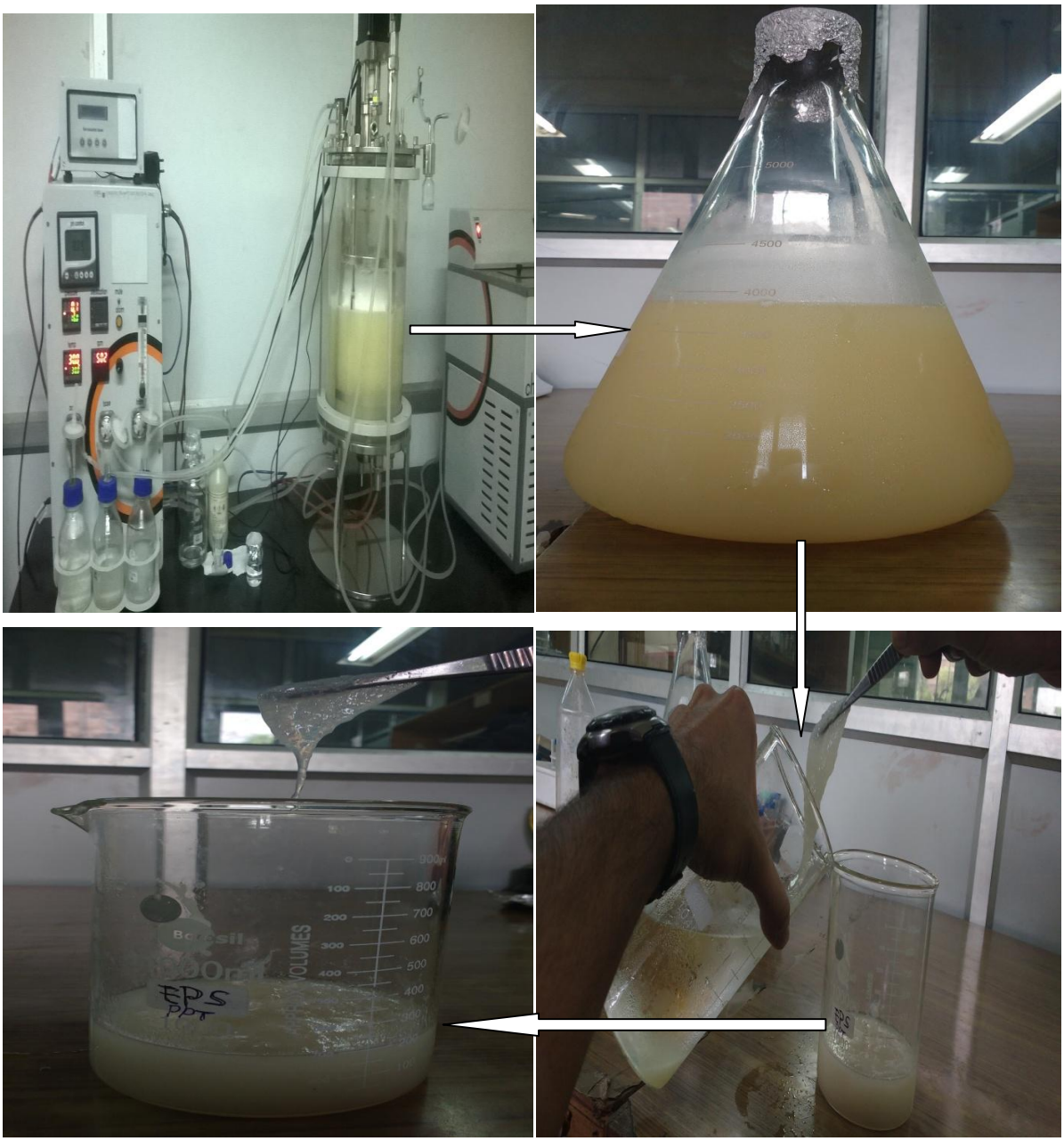

Fig.6.13 Production and precipitation steps of EPS produced by *Serratia* sp. ISTD04 in 20 L fermentor.

6.3.7 Application of EPS produced by *Serratia* sp. ISTD04

6.3.7.1 Determination of flocculating activity of EPS

Bioflocculating characteristic of EPS was evaluated by kaoline test (Jar test) and the results show that, the flocculating activity of bacterial culture broth EPS and supernatant EPS was 68% ±0.9 and 59% ±0.6 respectively **Fig.6.14**. Higher flocculating activity of culture broth EPS (B-EPS) as compare to culture supernatants EPS (LB-EPS) may be due to more protein content in the B-EPS as it is composed of LB-EPS and TB-EPS (**Bezawada et al., 2013**). As compare to previous literature the flocculating activity of EPS are in the range of 61-95% using purified EPS as well as direct bacterial culture broths (**Wang et al., 2007; Bezawada et al., 2013**). Application of purified EPS as flocculating agent may be not a cost effective technique, because major cost involves in centrifugation, precipitation and purification of EPS put some extra cost on its application angle as bioflocculant. Using direct culture broth may be a sustainable approach to reduce the cost involve in application of EPS as bioflocculant.

Fig.6.14 Determination of bioflocculating activity of bacterial culture broth EPS, culture supernatant EPS by Kaoline test (Jar test) using distilled water as blank.

6.3.7.2 Determination of dyes decolorization efficiency of EPS

There are various physical, chemical and biological dyes decolorization technologies previously described by the researcher, such as biodegradation, sorption, ozonolysis, precipitation **(Robinson et al., 2002; Gong et al., 2005**). Although ozonolysis and precipitation are efficient in dye removal, there are some limitations of these processes, such as high-running cost, low-removal efficiency, and labor-intensive operation (**Tarley and Arruda, 2004**). Therefore, developing cost-effective sorbents becomes fairly attractive for the treatment of dye. In recent years, biosorption has been considered as a promising technology for the removal of dyes from industrial effluents and natural waters (**Robinson et al., 2001**). Biosorption can be defined as the uptake of contaminants, via various physicochemical mechanisms including ion exchange, sorption, complexation, chelation, microprecipitation, etc., by biological materials (**Volesky and Schiewer, 1999**). Some biomaterials (Bioflocculants) have been reported to remove dyes, including agricultural byproducts like rice husk, bark and orange peel and microbiological materials such as algae, fungi and bacteria (**Zhang et al., 2009**). Bioflocculants possess functional groups as well as surface charge that could flocculate other compounds such as oil, dyes and algae (**Zhong and Yoshida, 1995**). Considering all these facts EPS produced by *Serratia* sp. ISTD04 were used as bioflocculant for decolorization of six dyes at pH 7 and dye concentration 0.1%. In this study six dyes were selected, such as four anionic dyes (trypan blue, methyl orange, bromothymol blue, aniline blue) and two cationic dyes (acridine orange, crystal violet). The flocculant effectively decolarized the anionic dye, such as trypan blue (40%), methyl orange (25%), bromothymol blue (75%) and aniline blue (60%) **Fig.6.15**. The decolorization activity of of the bioflocculant was much more effective against the cationic dye, such as acridine orange (80%) and crystal violet (95%) **Fig.6.15**. this is might be due to anionic nature of the bioflocculant (EPS). Flocculation in biological systems is generally explained by the bridging mechanism. Particles and cells get aggregated by biopolymer flocculants through bridging and charge neutralization mechanism. During bridging, the biopolymers bring different particles closer by encouraging aggregation. In this case, the biopolymer can absorb to other particles to form flocs. This mechanism explains flocculation by neutral or like charged EPS (**Hantula and Bamford, 1991**). Charge neutralization occurs when the particle surface charge is reduced by

oppositely charged cations and/or bioflocculants. The distance between particles decreases and attractive forces become more effective than the repulsive forces between the particles. The effectiveness of the bridging mechanism depends on the molecular weight of the EPS, the charge on the polymer and the particle, the ionic strength of suspension, and the nature of mixing (**More et al., 2014**). These results show the cost effective production of EPS by chemolithotrophic bacteria *Serratia* sp. ISTD04 and its application as bioflocculant for decolorization of anionic dyes.

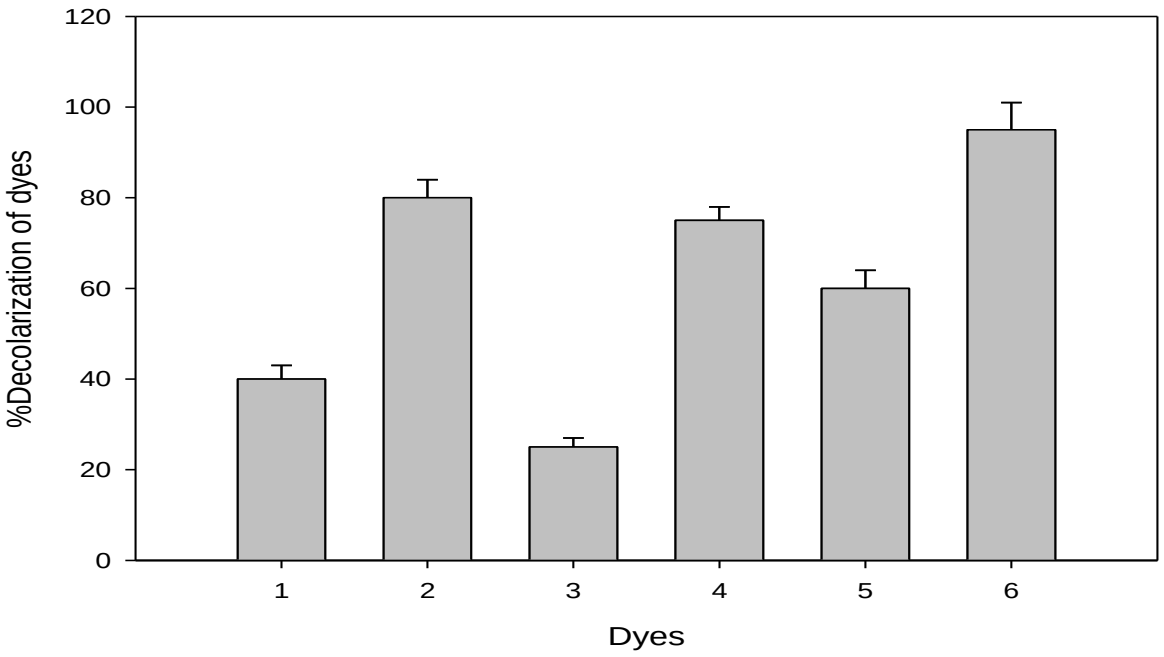

Fig.6.15 Representation of dyes decolorization efficiency of EPS produced by *Serratia* sp. ISTD04 (1) Trypan blue (2) Acridine orange (3) Methyl orange (4) Bromothymol blue (5) Aniline blue (6) Crystal violet.

6.3.8 Proteomics and genomic analysis of chemolithtrophic bacteria *Serratia* sp. ISTD04 for production of EPS

6.3.8.1 Proteomics analysis by Nano LC-MS/MS

In the present study, whole cell soluble protein was separated by SDS-PAGE **Fig.6.16** and divided into six fractions. Each fraction was identified by nano LC-MS/MS for proteomic analysis of *Serratia* sp. ISTD04 grown under 100 mM $NaHCO_3$ as sole carbon source autotrophically. A total of 96 proteins were identified in the protein lysate. The identified proteins fraction was functionally classified according to their biological roles **Table.6.4, Fig.6.17**. The protein profile was dominated by enzyme responsible for CO_2 fixation and carbohydrate metabolism, fatty acid metabolism and alkane biosynthesis. In the present study Ribulose-1,5-bisphosphate carboxylase/oxygenase (RuBisCO) smaller subunit were detected, which is the key enzyme involved in chemolithotrophic fixation of CO_2 by CBB cycle (**Bharti et al., 2014b**), along with RuBisCO five other enzymes were also detected **Table.6.4**. Proteomic analysis of *Serratia* sp. ISTD04 identified the 13 enzymes, which are involved in carbohydrate metabolism pathway as well as EPS production pathway, such as polysaccharide biosynthesis protein, glycosyl transferase family proteins, Lipopolysaccharide biosynthesis protein, capsule polysaccharide biosynthesis protein (**Singh et al., 2017**). Bacterial EPS plays a significant role in overcoming the environmental constraints; often serving as a carbon or energy source in nutrient limiting conditions, which is certainly possible in nutrient stressed environment of marble mines (**Alonso-Sáez et al. 2010**).

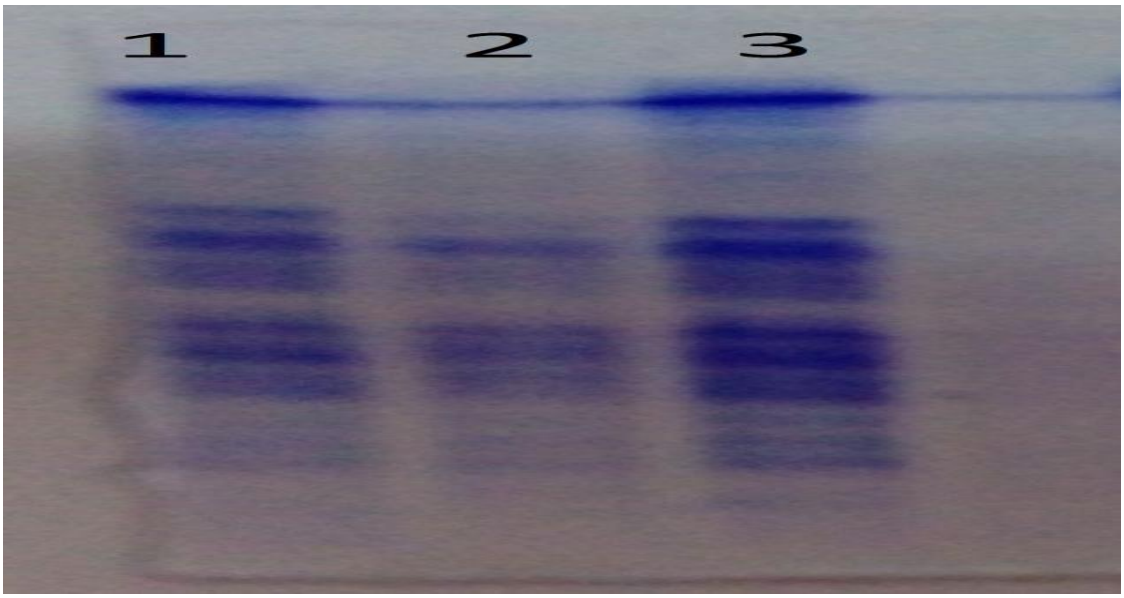

Fig.6.16 Whole cell proteins (triplicate) separated by SDS-PAGE gel from *Serrati*a sp. ISTD04

Table.6.4 Identification and functional classification of proteins involve in different major pathway of *Serratia* sp. ISTD04 grown in MSM containing $NaHCO_3$ as sole carbon source.

Name of protein	**NCBI ID**	**Mol mass**	**pI**	**Score**	**No of peptide match**
CO_2 Sequestration					
RuBisCO smaller subunit	gi|114778451	13585	5.13	19	1
Fructose-1,6-biphosphatase	gi|188532273	36112	5.16	16	3
Phosphoenolpyruvate synthase	gi|238855160	88243	5.59	16	1
Gyceraldehyde-3-phosphate dehydrogenase	gi|222054266	53747	7.88	18	3
Methylmalonyl-CoA mutase	gi|121610330	78579	5.20	15	2
pyruvate flavodoxin oxidoreductase	gi|34558414	20178	7.97	19	1

Fatty acid metabolism					
Acetyltransferase GNAT	gi|78050004	20364	7.56	28	2
2-oxoisovalerate dehydrogenase	gi|238023732	45167	5.94	34	2
Acyltrasferase	gi|323356587	28429	4.96	20	1
Transketolase	gi|292492796	35402	4.85	20	1
Acyl-CoA synthetase	gi|68535669	66479	5.38	19	1
Transaldolases	gi|302670347	68569	6.14	13	1
3-oxoacyl-(acyl carrier protein) synthase III	gi|73541952	34369	5.45	18	3
acyl-CoA dehydrogenase	gi|221632151	48438	5.36	19	1
Acetyl-coA	gi|221195226	173718	5.41	16	1
Carboxylesterase/lipase family	gi|304311021	57227	5.94	18	1
3-oxoacyl-(acyl-carrier-protein) reductase	gi|146337394	26885	7.93	18	1
Alkane biosynthesis					
Short-chain dehydrogenase	gi|254295190	27261	5.82	18	13
Aldehyde dehydrogenase	gi|264679228	54699	5.91	19	1
Alcohol dehydrogenase	gi|169786917	36502	5.72	18	3
Carbohydrate metabolism					
Glycosyl transferase group1family protein	gi|56478615	45189	10.94	39	1
Glycosyl transferase, family 2	gi|209883816	74168	10.17	16	1

Alpha/beta hydrolase family Protein	gi|85708216	31621	5.46	19	2
Glycoside hydrolase family 3protein	gi|182677858	40324	5.51	19	1
Polysaccharide biosynthesis protein	gi|118581801	45969	9.15	18	1
Alpha-glucan phosphorylase	gi|302391852	61083	4.57	18	1
Alpha-glucosidase	gi|148243435	109336	6.04	19	1
Beta-glucosidase	gi|91204997	35337	6.01	19	1
Arabinose efflux permease	gi|300310405	42631	9.04	19	20
Lipopolysaccharide biosynthesis protein	gi|53721460	49418	5.75	27	2
Trehalose synthase	gi|51848581	65000	5.10	19	1
Capsule polysaccharide biosynthesis protein	gi|227820131	36626	8.37	19	3
dTDP-6-deoxy-L-mannose-dehydrogenase	gi|29726016	33553	6.06	19	1

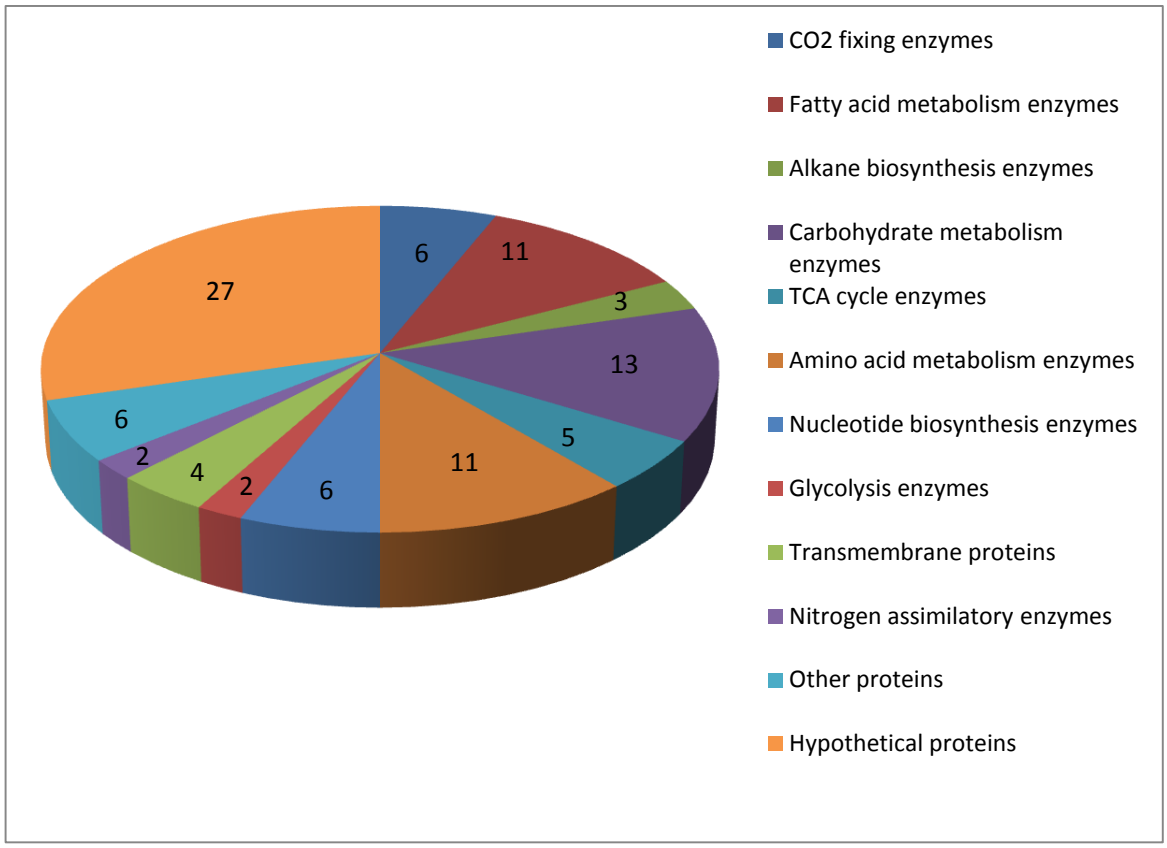

Fig.6.17 Representation of 96 proteins identified by LC-MS/MS in *Serratia* sp. ISTD04 and its functional classification

6.3.8.2 Genomic analysis of *Serratia* sp. ISTD04 for production of EPS

The detailed analysis of genome of *Serratia* sp. ISTD04 has been discussed in chapter 3; here we have discussed the cluster analysis of EPS producing gene and its arrangements. Although EPS related genes are dispersed throughout the whole genome of *Serratia* sp. ISTD04, eight major clusters of genes encoding proteins for the formation of EPS, capsule polysaccharide, lipopolysachharides (LPS), Emulsan have been identified in the genome.

Lipopolysaccharide (LPS) is composed by the O-side chain and core oligosaccharide and lipid which are covalently linked and located at the outer membrane of Gram-negative bacteria. There was 14 genes identified in the cluster 1 having size 15.2 kb and coding various proteins,

such 5 glycosyl transferases (gtfs and gt1), ADP-glyceromanno-heptose 6-epimerase (hldD), ADP-heptose-LPS heptosyltransferase (Rfaf), lipopolysaccharide heptosyltransferase 1 (rfaC), 2 lipopolysaccharide biosynthesis protein (rfbH), ligase (rafL), deacetylase (dac present on negative stand), Putative lipopolysaccharide heptosyltransferase III (rfaQ) and 3-deoxy-D-manno-octulosonic acid transferase (waaA). Genes involves in synthesis of capsular polysachharides in this strain were found in cluster 7 which are present on negative stand (size 30.4 kb) **Table.6.5 Fig.6.18** Genes responsible for polysaccharide biosynthesis, polymerization, and export as well as chain length determinant have been identified. Along with tyrosine kinase transcriptional regulator was also identified in these clusters which regulate the biosynthesis of EPS. Tyrosine kinase was reported to control the initiation of EPS biosynthesis in *Streptococcus thermophilus* (**Minic et al., 2007**), the tyrosine kinase gene identified in cluster 7 may be involved in the regulation of EPS production**.** The discovery of genes encoding Wzx family protein and Wzx specific transporter proteins as well as other characterized EPS proteins in ISTD04 genome imply that Wzy-dependent pathway may be used in Serratia sp. ISTD04 EPS biosynthesis (**Haft et al., 2006**). This pathway was first described in *Salmonella* O-antigen 47 synthesis (**Whitfield, 2006**) and also found for many other polysaccharides, such as that in *Azoarcus* EbN1 and *Rhodospirillum rubrum* (**Haft et al., 2006**), and mauran in *Halomonas Maura* (**Anders et al., 1995**). In this pathway, the lipid-linked repeating units of the polysaccharide are assembled on the cytoplasmic side of the inner membrane and then transported to the periplasmic side of the inner membrane for polymerization and ligation. After some modification in periplasm, the polysaccharide is translocated across the outer membrane (**Whitfield, 2006**). The synthesis pathway involving ABC transporters has been found for group II capsular polysaccharide in *Escherichia coli*, *Haemophilus*, *Neisseria Rhizobium* and *Agrobacterium*. It has different assembly steps and their specific accruing locations (**Whitfield and Roberts, 1999**). In contrast to the Wyz dependent pathway, in ABC transporter pathway, the repeating units are synthesized and polymerized at the inner face of the cytoplasmic membrane, and translocated onto the periplasmic side for ligation with lipid (**Haft et al., 2006**). The final product is then translocated from periplasm to the surface of the outer membrane by interacting with export system of periplasm and outer membrane (**Haft et al., 2006**). Proteins involved in

the ABC transporter dependent pathway, such as the ABC transporter and ligases, are also found in the putative gene clusters of ISTD04, which suggests that this pathway may be also adopted by this strain.

Table.6.5 Genes and protein identified in the clusters analysis of *Serratia* sp. ISTD04 for biosynthesis of EPS.

Cluster No	Size (kb)	Pathway	Nt size range	Genes	Proteins
1. MBDW01000005	**15.2**	**Lipopolysaccharide biosynthesis**	**42623- 57851**		
				hldD	ADP-glyceromanno-heptose 6-epimerase
				Rfaf	ADP-heptose--LPS heptosyltransferase
				rfaC	Lipopolysaccharide heptosyltransferase 1
				rfbH	Lipopolysaccharide biosynthesis protein
				rfaL	Ligase
				gtfs	Glycosyl transferase
				gtfs	Glycosyl transferase
				dac	Deacetylase
				rfaQ	Putative lipopolysaccharide heptosyltransferase III
				gt1	Glycosyl transferase family 1
				gtfs	Glycosyl transferase
				gtfs	Glycosyl transferase
				waaA	3-deoxy-D-manno-octulosonic acid transferase
				rfbH	Lipopolysaccharide biosynthesis protein
2. MBDW01000006	**23.7**	**Stewartan biosynthesis**	**1-23724**		
				gt1	glycosyl transferase family 1
				gtf	glycosyl transferase
				gtf	glycosyl transferase
				WzxE	Polysaccharide biosynthesis protein
				TK	tyrosine-protein kinase
				Wzc	Polysaccharide export protein

				Wxa	undecaprenyl-phosphate alpha-N-acetylglucosaminyl 1-phosphate transferase
				gne	UDP-N-acetylglucosamine 4-epimerase
				cadC	CadC family transcriptional regulator
				narK	nitrate/nitrite transporter
				NarX	two-component system sensor histidine kinase
				NarL	two-component system response regulator
				ipaC	Invasion
				pilD	prepilin peptidase
					hypothetical protein
				ABC	ABC transporter substrate-binding protein
				APC	Peptide ABC transporter ATP-binding protein
				ABC	Peptide ABC transporter ATP-binding protein
				ABCper	Peptide ABC transporter permease
3. MBDW01000035	**22.8**	**Emulsan biosynthesis**	**18435 - 41240**		
				Fist	sigma-54-dependent Fis family transcriptional regulator
				ABC	ABC transporter substrate-binding protein
				MFS	MFS transporter
					Hypothetical protein
				MFS	MFS transporter
					Hypothetical protein
				hem	coproporphyrinogen dehydrogenase
				gt2	glycosyl transferase family 2
				gt2	glycosyl transferase family 2
				dgc	diguanylate cyclise
					Hypothetical protein

				barl	autotransporter outer membrane beta-barrel domain-containing protein
				Qdh	quinate dehydrogenase
				PqqF	coenzyme PQQ biosynthesis protein
4. MBDW01000051	**10.7**	**Polysaccharide B biosynthesis**	**106999 - 117794**		
				wecA	undecaprenyl-phosphate alpha-N-acetylglucosaminyl 1-phosphate transferase
				wxxE	polysaccharide chain length modulation protein
				GNE	UDP-N-acetylglucosamine 2-epimerase
				wecC	UDP-N-acetyl-D-mannosamine dehydrogenase
				RfbB	dTDP-glucose 4,6-dehydratase
				RfbA	glucose-1-phosphate thymidylyltransferase
				wecD	TDP-D-fucosamine acetyltransferase
				wecE	dTDP-4-amino-4,6-dideoxygalactose transaminase
				wzxE	O-antigen translocase
				wecF	4-alpha-L-fucosyltransferase
5. MBDW01000069	**8**	**Emulsan biosynthesis**	**103370 - 111370**		
				UDPGP	UTP--glucose-1-phosphate uridylyltransferase
				UDPglcDH	UDP-glucose 6-dehydrogenase
				CapI	protein CapI (NAD dependent epimerase)
				Trans.Reg	Transcriptional regulator
				TK	thymidine kinase
				adhE	bifunctional acetaldehyde-CoA/alcohol dehydrogenase

6. MBDW01000089	**16.1**	**Emulsan biosynthesis**	**263177 - 279371**		
				Gnd/GntZ	phosphogluconate dehydrogenase (NADP(+)-dependent, decarboxylating)
				ABCsugar	Sugar ABC transporter permease
				TagH	teichoic acid ABC transporter ATP-binding protein
				gt1	glycosyl transferase family 1
				gt1	glycosyl transferase family 1
				GNE	UDP-N-acetylglucosamine 2-epimerase
				gt	glycosyl transferase
				rmlD	dTDP-4-dehydrorhamnose reductase
				rmlC	dTDP-4-dehydrorhamnose 3,5-epimerase
				GalE	UDP-glucose 4-epimerase
				PPM	Phosphomannomutase
7. MBDW01000089	**30.4**	**Capsular polysaccharide biosynthesis**	**282463 - 312886**		
				RND	hemolysin D (RND efflux transporter)
				ABC	Peptidase (ABC transporter)
				DUF4214	DUF4214 domain-containing protein
				AT	acyltransferase
				WbaP	UDP-phosphate galactose phosphotransferase
				gtf2	glycosyl transferase family 1
					hypothetical protein
				GumL	polysaccharide biosynthesis protein
				WzxE	polysaccharide biosynthesis protein
					hypothetical protein
					hypothetical protein

				TK	tyrosine-protein kinase
				GalF	GalU regulator GalF
				UDPGP	UTP--glucose-1-phosphate uridylyltransferase
					hypothetical protein
				DcuC	anaerobic C4-dicarboxylate transporter DcuC
					hypothetical protein
8. MBDW01000092	**20.2**	**fatty acid and saccharide biosynthesis**	**41894 - 62133**		
				FADS2	linoleoyl-CoA desaturase
				FADS2	linoleoyl-CoA desaturase
				FAH	fatty acid hydroxylase
				AP	acid phosphatise
				CoF synt	CoF synthetase
				MBLH	MBL fold metallo-hydrolase
					hypothetical protein
				FabH	3-oxoacyl-ACP synthase
				narI	respiratory nitrate reductase subunit gamma
				narJ	nitrate reductase molybdenum cofactor assembly chaperone
				narH	nitrate reductase subunit beta
				narG	nitrate reductase subunit alpha
				gt	glycosyl transferase
				gt	glycosyl transferase
				CenC	carbohydrate-binding protein
				gt	glycosyl transferase
				gt1	glycosyl transferase family 1

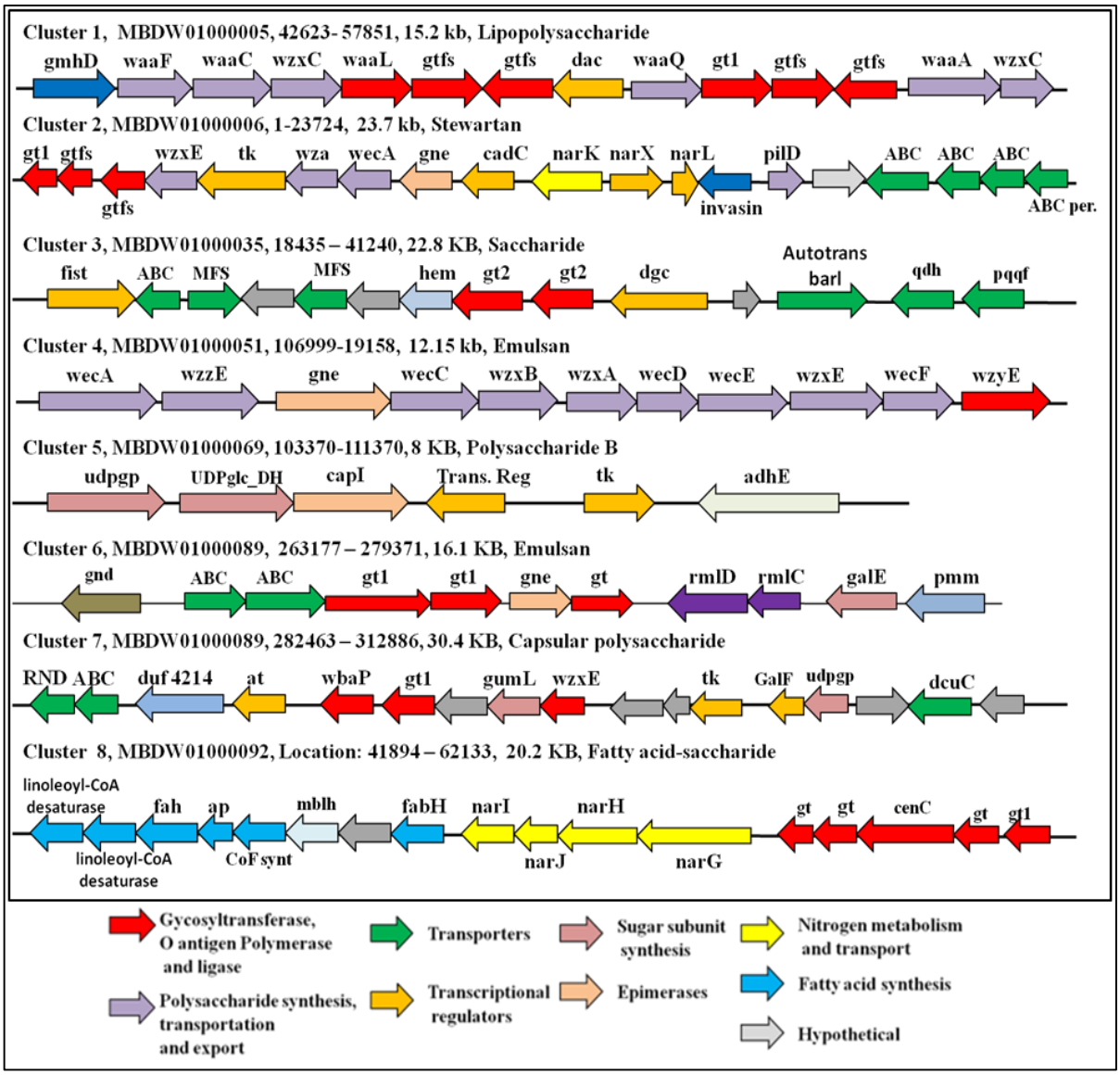

Fig.6.18 Represention of putative gene clusters with contig number, position and size identified in *Serratia* sp. ISTD04 genome responsible for polysaccharide biosynthesis**.**

In the genomic cluster of this strain we have also found the gene responsible for production of Stewartan EPS as well as emulsan **Fig.6.18, Table.6.5** Stewartan EPS is an anionic polymer composed largely of heptasaccharide repeat units that contain galactose, glucose and glucuronic acid in a 3:3:1 ratio (**Nimtz et al., 1996a; Yang et al., 1996**). Its chemical structure is related to that of amylovoran, a polysaccharide and virulence determinant in *Erwinia amylovora*

(**Nimtz et al., 1996b**). Cluster analysis of ISTD04 strain shows 10 % homology with *Pseudomonas cichorii* JBC1 and *Pseudomonas amygdali* pv. Strains, follow the Stewartan EPS production pathway. In this pathway polymer repeat units are assembled on a polyisoprenoid lipid carrier and translocated via the Wzx membrane associated polysaccharide specific transport (PST). Many alkane-degrading bacteria secrete diverse surfactants that facilitate emulsification of hydrocarbons (**Ron and Rosenberg, 2002**). In particular, among surfactant producers, Acinetobacter venetianus RAG-1T (**Vaneechoutte et al., 1999**) has been shown to produce an extracellular anionic lipoheteropolysaccharide, known as emulsan, to aid in the capture and transport of the carbon sources to the cell (**Mercaldi et al., 2008; Marco et al., 2013**). Cluster genes analysis of strain ISTD04 have been shown genes similarity with *Pseudomonas putida* LS46, *Pseudomonas putida* F1**,** *Burkholderia glumae* PG1 19%, 16% and 12% respectively for production of emulsan.

6.4 Conclusion

The present work establishes the potential of the bacterial strain *Serratia* sp. ISTD04 in production of EPS along with CO_2 sequestration. This study highlights the possibility of production of biomaterial such as EPS by chemolithotrophic bacteria utilizing $NaHCO_3$ and glucose as carbon source. The work also demonstrates the optimized production of EPS, scale up at fementor level in feed-batch mode for higher production and its application in removal of dyes. Finally proteomics and genomics analysis of chemolithtrophic *Serratia* sp. ISTD04 highlights the involvement of proteins and genes in production of EPS along with CO_2 sequestration.

Chapter 7:

SUMMARY AND CONCLUSION

7. SUMMARY AND CONCLUSION

Carbon dioxide (CO_2) is one of the major greenhouse gases (GHGs), whose concentration has increased from 270 ppm to approximately 400 ppm after industrial revolution. Increase in CO_2 concentration may be mitigated by autotrophic and heterotrophic carbon fixation by plants and microorganisms. Some microorganisms are able to grow in limiting CO_2 concentrations by employing a CO_2-concentrating mechanism (CCM) by enzymes mainly ribulose-1,5-bisphosphate carboxylase/ oxygenase (RuBisCO) and carboxylating enzymes such as carbonic anhydrase which facilitate the CO_2 fixation. Genomics, Proteomic and metabolomics analysis has become a powerful tool to identified novel genes and protein for fixation of CO_2 and evaluation of enzymes and metabolites for production of value added products. Chemolithotrophic microorganisms can sequester CO_2 and synthesize valuable products such as different types of alkanes/alkenes, fatty acids, PHA, EPS which can be further utilized as raw materials for production of other bio-products.

To understand the microbial sequestration of CO_2 and production of biological materials, a previously reported CO_2 sequestering *Serratia* sp. ISTD04 isolated from marble mining rocks in the Umra area, Rajasthan, India was characterized by genomic analysis. This study leads to infer the carbon dioxide mitigation strategies by bacteria along production of biomaterials such as, bioplastics, EPS and its application. Beside from this, optimization of process parameters for production of biomaterial, its recovery and biorefinery approach may provide a new direction in the research of developing technology for production of biomaterials from CO_2 concentrating bacteria. Utilization of $CaCO_3$ precipitated by bacteria for synthesis of biocomposite material and their further cytotoxicity evaluation on osteosrcoma cell line. Optimized production and characterization of PHA by this strain, also characterization of EPS production, scale-up and its application in removal of dyes. The conclusive summary of all the objectives of the present work has been discussed bellow.

Chapter 3 described, bacteria *Serratia* sp. ISTD04 isolated from marble mines is a novel organism which performs chemolithoautotrophic CO_2 assimilation. Genomic analysis of *Serratia* sp. ISTD04 revealed the presence of PRK and other CBB pathway genes. However, the RuBisCo gene could not be identified in the genome assembly. The carbonic anhydrase, AN important

enzyme which facilitate the sequestrating mechanism of CO_2 is also present in the genome. Enzymes like phosphoenolpyruvate (PEP) carboxylase, malic enzymes, and PEP carboxykinase, which help in anaplerotic assimilation of CO_2, are also present in the genome of *Serratia* sp. ISTD04. Important transcriptional regulator, such as LTTR, HTH type and CysB- like protein transcription regulator which are known for CO_2 fixation are also identified in the genome. EPS biosynthesis ability of this strain is also investigated at genomic level, presence of various EPS synthesis enzymes such as UDP-glucose 6-dehydrogenase, phosphoglucomutase, Galactose-1-phosphate uridylyltransferase, UDP-galactose-4-epimerase, Mannose-6-phosphate isomerase, phosphomannomutase, glucans biosynthesis glucosyltransferase H, polysaccharide biosynthesis protein, capsular polysaccharide translocation, glycogen/starch/alpha-glucan phosphorylases family protein and many more in the genome, confirm this strain as an potential candidate for EPS production. This strain is well known fatty acid production; Enzymes for fatty acid metabolism such as acetyl-CoA carboxlases, malonyl Co-ACP transacylase, 3-ketoacyl ACP-synthase, and 3-ketoacyl ACP-reductase are identified in the genome. Cluster analysis of PHA biosynthesis revealed the presence of enzymes like β-ketoacyl-CoA thiolase and acetoacetyl-CoA dehydrogenase, which as well known for PHA biosynthesis. Genomic analysis of this strain confirmed that; this strain could be used as potential candidate for simultaneous sequestration of CO2 as well as production of biological materials.

Chapter 4 described, $CaCO_3$ precipitated by CO_2 sequestering *Serratia* sp. ISTD04 were used as raw material along with $NaNO_3$ and Si for the synthesis of biocomposite material by sol-gel process under ambient environmental condition has been performed successfully. The material synthesized by sol-gel process have essential features similar to Na_2O-containing bioactive materials, mainly the formation of crystalline phase $Na_2Ca_2Si_3O_9$ after sintering the material at 1200 °C for 2 h and formed hydroxyl apatites like amorphous phase when its incubated in SBF, 1.5SBF and DMEM for 25 days without losing its crystallinity, this study showed that this material exhibits good bioactivity, biodegradability as well as mechanical properties. Ions exchange ability of this material in aqueous environment was analyzed by ICP-MS analysis and result confirmed the exchange of ions takes place between the material and aqueous environment, which favour the formation of hydroxyl apatites. MTT-assay confirmed that this material and their supernatant did not have any cellular cytotoxicity so this material

could be use in biomedical application, although various analysis still required before its application in biomedical field.

Chapter 5 described, screening of CO_2 sequestering chemolithotrophic bacteria *Serratia* sp. ISTD04 for production of biomass and PHA, further optimization of process parameters were performed by using statistical approach Response Surface Methodology (RSM) for improved production of PHA and biomass. The bacterial strain was screened for PHA production based on Nile red staining followed by visualization under fluorescence microscope. Spectrofluorometric measurement of Nile red fluorescence of the bacterial culture was also done. Confirmatory analysis of PHA accumulation by GC–MS revealed the presence of 3-hydroxyvalerate (PHV), which is a co-polymer of polyhydroxybutrate (PHB). Detection of characteristic peaks in the FT-IR spectrum further confirmed the production of PHA by the bacterium. RSM was used for optimization of pH and carbon sources concentrations for higher PHA production. The result of optimization experiment revealed, almost a 2 fold increament in the production of PHA as compare to un-optimized condition. Thus this study establishes the production of PHV by *Serratia* sp. ISTD04.

Chapter 6 established the potential of the chemolithotrophic bacterial *Serratia* sp. ISTD04 in production of EPS along with CO_2 sequestration. This study highlights the possibility of production of biomaterial such as EPS by chemolithotrophic bacteria utilizing $NaHCO_3$ and glucose as carbon source. Further characterization of EPS was performed by SEM, EDX, GC-MS, FT-IR, NMR and its constituent like total sugar, reducing sugar, protein content and fatty acid content was estimated. The work also demonstrates the optimized production of EPS at shake flask level and the optimized condition was adopted for production of EPS at fementor level in feed-batch mode for scale-up the production and its environmental application such as removal of various dyes. Finally proteomics analysis of *Serratia* sp. ISTD04 and cluster analysis of genes of chemolithtrophic *Serratia* sp. ISTD04 highlight the involvement of various proteins and genes in the production of EPS along with CO_2 sequestration.

REFERENCES

1. Abbasi, Z., Bahrololoom, M.E., Shariat, M.H., Bagheri, R., 2015 Bioactive Glasses in Dentistry: A Review. JDB. 2015, 2.
2. Abraham, A., Mathew, A.K., Sindhu, R., Pandey, A., Binod, P., 2015. Potential of rice straw for bio-refining: an overview. Bioresour. Technol. 215, 29–36.
3. Aguilera, M., Quesada, M.T., del Águila, V.G., Morillo, J.A., Rivadeneyra, M.A., Ramos-Cormenzana, A., Monteoliva-Sánchez, M., 2008. Characterisation of *Paenibacillus jamilae* strains that produce exopolysaccharide during growth on and detoxification of olive mill wastewaters. Bioresour. Technol. 99, 5640–5644.
4. Alonso-Sáez, L., Galand, P.E., Casamayor, E.O., Pedrós-Alió, C., Bertilsson, S., 2010. High bicarbonate assimilation in the dark by Arctic bacteria. ISME Journal 4, 1581–1590.
5. Amachi, T., Bowien, B., 1979. Characterization of two fructose bisphosphatase isoenzymes from the hydrogen bacterium *Nocardia opaca* 1b. J. Gen. Microbiol. 113, 347–56.
6. Anders, H. J., A. Kaetzke, P. Kampfer, W. Ludwig, and G. Fuchs**.** 1995. Taxonomic position of aromatic-degrading denitrifying pseudomonad strains K 172 and KB 740 and their description as new members of the genera Thauera, as Thauera aromatica sp. nov., and Azoarcus, as Azoarcus evansii sp. nov., respectively, members of the beta subclass of the Proteobacteria. Int J Syst Evol Microbiol, 45, 327.
7. Aresta, M., Dibenedetto, A., Dumeignil, F., 2013. Biorefinery: from biomass to chemicals and fuels. Green Process. Synth. 2, 87–88.
8. Arp, G., Reimer, A., Reitner, J., 1999. Calcification in cyanobacterial biofilms of alkaline salt lakes. Eur. J. Phycol. 34, 393–403.
9. Ates, O., 2015. Systems Biology of Microbial exopolysaccharides Production. Front Bioeng Biotechnol. 3, 200.
10. Atomi, H., 2002. Microbial enzymes involved in carbon dioxide fixation. J. Biosci. Bioeng. 94, 497–505.
11. Aylward, F.O., Tremmel, D.M., Starret,t G.J., Bruce, D.C., Chain, P., Chen, A., 2013. Complete Genome of Serratia sp. Strain FGI 94, a Strain Associated with Leaf-Cutter Ant Fungus Gardens. Genome Announc. 1, e23912.

12. Aziz, R. K., Bartels, D., Best, A. A., DeJongh, M., Disz, T., Edwards, R. A., Meyer, F., 2008. The RAST Server: rapid annotations using subsystems technology. BMC genomics, 9, 75.
13. Badger, M.R., Price, G.D., 1992. The CO2 concentrating mechanism in cyanobacteria and microalgae. Physiol. Plant. 84, 606–615.
14. Badger, M.R., Price, G.D., 2003. CO2 concentrating mechanisms in cyanobacteria: molecular components, their diversity and evolution. J. Exp. Bot. 54, 609–622.
15. Badger, M.R., Price, G.D., Long, B.M., Woodger, F.J., 2006. The environmental plasticity and ecological genomics of the cyanobacterial CO2 concentrating mechanism. J. Exp. Bot. 57, 249–265.
16. Bai, L. *Qi*, X., Zhang, Y., Yao, C., Guo, L., Jiang, R., Zhang, R., Li, Y., 2013. A new GntR family regulator Ste1 in *Streptomyces* sp. 139. Appl. Microbiol. Biotechnol. 97, 8673−8682.
17. Bainbridge, G., Anralojc, P. J., Madgwick, P. J., Pitts, J. E., Parry, M. A., 1998. Effect of mutation of lysine-128 of the large subunit of ribulose bisphosphate carboxylase/oxygenase from *Anacystis nidulans.* Biochem. J., 336, 387-393.
18. Balamurugan, A., Ballossier, G., Michel, J., Kannan, S., Benhayoune, H., Rebelo, A.H.S., Ferreira, J.M., 2007. Sol gel derived SiO2–CaO–MgO–P2O5 bioglass system-preparation and in vitro characterization. J Biomed Mater Res Part B Appl Biomater. 83B-546.
19. Ballering, K.S., Kristich, C.J., Grindle, S.M. Oromendia, A., Beattie, D.T., Dunny, G.M., 2009. Functional genomics of Enterococcus faecalis: multiple novel genetic determinants for biofilm formation in the core genome. J. Bacteriol. 191, 2806−2814.
20. Bandaru, V.V.R., Somalanka, S.R., Mendu, D.R., Madicherla, N.R., Chityala, A., 2006. Optimization of fermentation conditions for the production of ethanol from sago starch by co-immobilized amyloglucosidase and cells of Zymomonas mobilis using response surface methodology. Enzyme Microb. Technol. 38, 209–214.
21. Bao, HD., Guo, Z.X., Yu, J., 2008. Effect of electrically inert particulate filler on electrical resistivity of polymer/multi-walled carbon nanotube composites. Polymer. 49, 3826.

22. Barabesi, C., Galizzi, A., Mastromei, G., Rossi, M., Tamburini, E., Perito, B., 2007. Bacillus subtilis gene cluster involved in calcium carbonate biomineralization. J. Bacteriol. 189, 228–235.
23. Bar-Even, A., Noor, E., Lewis, N.E., Milo, R., 2010. Design and analysis of synthetic carbon fixation pathways. Proc. Natl. Acad. Sci. U.S.A. 107, 8889–8894.
24. Belova, L.L., Sokolov, A.P., Sidorov, I.A., Trotsenko, Y.A., 1997. Purification and characterization of NADPH-dependent acetoacetyl – CoA reductase from Methylobacterium extorquens. FEMS Microbiol. Lett. 156, 275–279.
25. Berg, I.A., 2011. Ecological aspects of the distribution of different autotrophic CO2 fixation pathways. Appl. Environ. Microbiol. 77, 1925–1936.
26. Berg, I.A., Kockelkorn, D., Ramos-Vera, W.H., Say, R.F., Zarycki, J., 2010. Autotrophic carbon fixation in Archaea. Nat. Rev. Microbiol. 8, 447–460.
27. Berlanga, M., Montero, M.T., Fernández-Borrell, J., Guerrero, R., 2006. Rapid spectrofluorometric screening of poly-hydroxyalkanoate-producing bacteria from microbial mats. Int. Microbiol. 9, 95-102.
28. Beudeker, R.F., Gottschal, J.C., Kuenen, J.G., 1982. Reactivity versus flexibility in *thiobacilli*.
29. Bezawada, J., Hoang, N.V., More, T.T., Yan, S., Tyagi, N., Tyagi, R.D., Surampalli, R.Y., 2013.Production of extracellular polymeric substances (EPS) by Serratia sp.1 using wastewater sludge as raw material and flocculation activity of the EPS produced. J Environ Manage.128 83-91.
30. Bharti, R.K., Srivastava, S., Thakur, I. S., 2014a. Production and characterization of biodiesel from carbon dioxide concentrating chemolithotrophic bacteria, *Serratia* sp. ISTD04. Bioresour. Technol. 153, 189-197.
31. Bharti, R.K., Srivastava, S., Thakur, I.S., 2014b. Isolation, purification, characterization and mass spectroscopic analysis of carbonic anhydrase from *Serratia* sp. for sequestration of carbon dioxide and formation of calcite. J. Environ. Chem. Eng. 2, 31–39.
32. Bharti, R.K., Srivastava, S., Thakur, I.S., 2014c. Proteomic analysis of carbon concentrating chemolithotrophic bacteria Serratia sp. for sequestration of carbon dioxide. PLoS One 9, 1–10.

33. Bharti, R.K., Srivastava, S., Thakur, I.S., 2014d. Extraction of extracellular lipids from chemoautotrophic bacteria *Serratia* sp. ISTD04 for production of biodiesel. Bioresour. Technol. 165, 201–204.
34. Bi, C., Su, P., Muller, J., Yeh, Y.C., Chhabra, S.R., Beller, H.R., Singer, S.W., Hillson, N.J., 2013. Development of a broad-host synthetic biology toolbox for Ralstonia eutropha and its application to engineering hydrocarbon biofuel production. Microb. Cell Fact. 12, 107.
35. Boetzer, M., Henkel, C.V., Jansen, H.J., Butler, D., Pirovano, W., 2011. Scaffolding pre-assembled contigs using SSPACE. Bioinformatics 27, 578–579.
36. Bose, H., Satyanarayana, T., 2017. Microbial carbonic anhydrases in biomimetic carbon sequestration for mitigating global warming: prospects and perspectives. Front. Microbiol. 8, 1615.
37. Bradford, M.M., 1976. A rapid and sensitive method for the quantitation of microgram quantities of protein utilizing the principle of protein-dye binding. Anal Biochem. 72, 7, 248–254.
38. Brandt, J.U., Jakob, F., Behr. J., Geissler. A.J., Vogel, R.F., 2016. Dissection of exopolysaccharide biosynthesis in *Kozakia* baliensis. Microb Cell Fact. 15, 1, 170.
39. Brigham, C.J., Budde, C.F., Holder, J.W., Zeng, Q., Mahan, A.E., Rha, C., Sinskey, A.J., 2010. Elucidation of beta-oxidation pathways in Ralstonia eutropha H16 by examination of global gene expression. J. Bacteriol. 192, 5454–5464.
40. Brigham, C.J., Zhila, N., Shishatskaya, E., Volova, T.G., Sinskey, A.J., 2012. Manipulation of Ralstonia eutropha carbon storage pathways to produce useful bio-based products. Subcell Biochem. 64, 343–366.
41. Brinker, J., Scherer, G.W., 1990. Sol–gel science: the physics and chemistry of sol–gel processing. Boston, MA, Academic Press.
42. Bubb,W.A., 2003. NMR spectroscopy in the study of carbohydrates: Characterizing the structural complexity. Concepts Magn Reson. 19, 1-19. DOI: 10.1002/cmr.a.10080.
43. Buchanan, B.B., Arnon, D.I., 1990. A reverse Krebs cycle in photosynthesis: consensus at last. Photosynth. Res. 24, 47–53.

44. Budde, C.F., Riedel, S.L., Willis, L.B., Rha, C., Sinskey, A.J., 2011. Production of poly (3- hydroxybutyrate-co-3-hydroxyhexanoate) from plant oil by engineered Ralstonia eutropha strains. Appl. Environ. Microbiol. 77, 2847–2854.
45. Buick, R., 1992. The antiquity of oxygenic photosynthesis: evidence from stromatolites in sulphate-deficient archaean lakes. Science 255, 74–77.
46. Campbell, B.J., Engel, A.S., Porter, M.L., Takai, K., 2006. The e-proteobacteria: key players in sulphidic habitats. Nat. Rev. Microbiol. 4, 458–468.
47. Cannon, G.C., Heinhorst, S., Kerfeld, C.A., 2010. Carboxysomal carbonic anhydrases: structure and role in microbial CO2 fixation. Biochimica et Biophysica Acta. 1804, 382–392.
48. Chaitanya, K., Mahmood, S.K., Kausar, R., Sunilkumar, N., 2014. Biotechnological production of Polyhydroxyalkonates by various isolates: A Review. Int. J. Pharm. Sci. Invent. 3, 01-11.
49. Chang, E.H., Yang, S.S., 2003. Some characteristics of microalgae isolated in Taiwan for biofixation of carbon dioxide. Bot Bull Acad Sin. 44, 43–52.
50. Cheah, W.Y., Ling, T.C., Juan, J.C., Lee, D.J., Chang, J.S., Show, P.L., 2016. Biorefineries of carbon dioxide: from carbon capture and storage (CCS) to bioenergies production. Bioresour. Technol. 215, 346–356.
51. Cheah, W.Y., Show, P.L., Chang, J.S., Ling, T.C., Juan, J.C., 2015. Biosequestration of atmospheric CO2 and flue gas-containing CO2 by microalgae. Bioresour. Technol. 184, 190–201.
52. Chen, Q.Z., Ahmed, I., Knowles, J.C., Nazhat, S.N., Boccaccini, A.R., Rezwan, K., 2008. Collagen release kinetics of surface functionalized 4555 bioglass (R)-based porous scaffolds. J Biomed Mater Res Part A. 86A, 87.
53. Chen, Q.Z., Rezwan, K., Francon, V., Armitage, D., Nazhat, S.N., Jones, F.H., Boccaccini, A.R., 2007. Surface functionalization of bioglass((R))-derived porous scaffolds. Acta Biomater. 3, 551.
54. Chen, Q.Z., Thompson, I.D., Boccaccini, A.R., 2006. 45S5 Bioglass (R)-derived glass–ceramic scaffolds for bone tissue engineering. Biomaterials. 27, 2414.

55. Chen, Q-Z ., Li, Y., Jin, L-Y., Julian, M.W., Quinn., Komesaroff, P.A., 2010. A new sol–gel process for producing Na2O-containing bioactive glass ceramics. Acta Biomater, 6, 4143–4153.
56. Chen, W., Sommerfeld, M., Hu, Q., 2011. Microwave-assisted Nile red method for in vivo quantification of neutral lipids in microalgae. Bioresour. Technol. 102, 135-141.
57. Choi, S., Drese, J.H., 2009. Adsorbent materials for carbon dioxide capture from large anthropogenic point sources. ChemSusChem 2, 796–854.
58. Choudhary, R., Koppala, S., Swamiappan, S., 2015. Bioactivity studies of calcium magnesium silicate prepared fromeggshell waste by sol–gel combustion synthesis. J. Asi. Ceram. Soc. 3, 173–177.
59. Chung, W.C., Chen, L.L., Lo, W.S., Kuo, P.A., Tu, J., Kuo, C.H., 2013. Complete Genome Sequence of Serratia marcescens WW4. Genome Announc. 1, e12613.
60. Clark, J.H., Buldarni, V., Deswarte, F.I.E., 2006. Green chemistry and the biorefinery: a partnership for a sustainable future. Green Chem. 8, 853–860.
61. Clupper, D.C., Hench, L.L., 2003. Crystallization kinetics of tape cast bioactive glass 45S5. J Non-Cryst Solids, 318, 43.
62. Clupper, D.C., Mecholsky, J.J., LaTorre, G.P., Greenspan, D.C., 2002. Bioactivity of tape cast and sintered bioactive glass–ceramic in simulated body fluid. Biomaterials. 23, 2599.
63. Cokoja, M., Bruckmeier, C., Rieger, B., Herrmann, W.A., Kühn, F.E., 2011. Transformation of carbon dioxide with homogeneous transition-metal catalysts: a molecular solution to a global challenge? Angew. Chem. Int. Ed. Engl. 50, 8510–8537.
64. Conesa, A., Götz, S., García-Gómez, J. M., Terol, J., Talón, M., & Robles, M., 2005. Blast2GO: a universal tool for annotation, visualization and analysis in functional genomics research. Bioinformatics, *21*, 18, 3674-3676.
65. Connor, M.R., Atsumi, S., 2010. Synthetic biology guides biofuel production. J. Biomed. Biotechnol. http://dx.doi.org/10.1155/2010/541698.
66. Cooksey, K.E., Guckert, J.B., Williams, S.A., Callis, P.R., 1987. Fluorometric determination of the neutral lipid content of microalgal cells using Nile red. J. Microbiol. Methods. 6, 333–45.

67. Cotton, C.A.R., Edlich-Muth, C., Bar-Even, A., 2018. Reinforcing carbon fixation: CO2 reduction replacing and supporting carboxylation. Curr. Opin. Biotechnol. 49, 49–56.
68. Crescenzi, V., Dentini, M., 1996. "Microbes in polymer chemistry," in Hydrogels and Biodegradable Polymers for Bioapplications, ACS Symposium Series. 627, 221–232.
69. Dangel, A.W., Tabita F.R., 2015. CbbR, the Master Regulator for Microbial Carbon Dioxide Fixation. J. Bacteriol. 197, 3488–3498.
70. De Silva, G., Ranjith, P., Perera, M., 2015. Geochemical aspects of CO2 sequestration in deep saline aquifers: a review. Fuel. 155, 128–143.
71. De, M.W., Verbeken, K., De, B.N., Verstraete, W., 2010. Influence of the calcium dosage on the effectiveness of bacterially induced carbonate precipitation on limestone. Ecol Eng 36, 99-111.
72. Dean-Mo, L., 1997. Fabrication of hydroxyapatite ceramic with controlled porosity. J Mater Sci: Mater Med. 8, 227–32.
73. Défarge, C., 2011. Organomineralization. In *Encyclopedia of Geobiology*, Springer: Dordrecht, The Netherlands, 697–701.
74. Dermlim, W., Prasertsan, P., Doelle, H., 1999. Screening and characterization of bioflocculant produced by isolated Klebsiella sp. Appl. Microbiol. Biotechnol 52, 698-703.
75. Dubois, M., Gilles, K.A., Hamilton, J.K., Rebers, P.A., Smith, F., 1956. Colorimetric method for determination of sugars and related substances. Analytical Chemistry 28, 350-356.
76. Dupraz, C., Visscher, P.T., Baumgartner, L.K., Reid, R.P., 2004. Microbe-mineral interactions: Early carbonate precipitation in a hypersaline lake (Eleuthera Island, Bahamas). Sedimentology,
77. Ee, R., Lim, Y.L., Tee, K.K., Yin, W.F., 2014. Chan KG. Quorum sensing activity of *Serratia fonticola* strain RB-25 isolated from an ex-landfill site. 14, 5136–5146.
78. Elbakidze, L., McCarl, B., 2007. Sequestration offsets versus direct emission reductions: consideration of environmental co-effects. Ecol Econ. 60, 564–571.
79. ElMekawy, A., Hegab, H.M., Mohanakrishna, G., Elbaz, A.F., Bulut, M., Pant, D., 2016. Technological advances in CO2 conversion electro-biorefinery: a step toward commercialization. Bioresour. Technol. 215, 357–370.

80. Engin, B., Demirtas, H., Eken, M., 2006. Temperature effects on egg shells investigated by XRD, IR and ESR techniques Radiat. Phys. Chem., 75, 268–277.
81. Ercole, C., Cacchio, P., Botta, A.L., Centi, V., Lepidi, A., 2007. Bacterially induced mineralization of calcium carbonate: the role of exopolysaccharides and capsular polysaccharides. Microsc. Microanal. 13, 42–50.
82. Esparza, M., Cárdenas, J.P., Bowien, B., Jedlicki, E., Holmes, D.S., 2010. Genes and pathways for CO2 fixation in the obligate, chemolithoautotrophic acidophile, Acidithiobacillus ferrooxidans, carbon fixation in A. ferrooxidans. BMC Microbiol 10, 229.
83. Ferreira, S.L.C., Bruns, R.E., Ferreira, H.S., Matos, G.D., David, J.M., Brandao, G.C., da Silva, E.G.P., Portugal, L.A., dos Reis, P.S., Souza, A.S., dos Santos, W.N.L., 2007. Box-Behnken design: an alternative for the optimization of analytical methods. Anal. Chim. Acta 597, 179–186.
84. Ferrer, M.R., Quevedo-Sarmiento, J., Rivadeneyra, M.A., Bejar, V., Delgado, G., Ramos-Cormenzana, A., 1988. Calcium carbonate precipitation by two groups of moderately halophilic microorganisms at different temperatures and salt concentrations. Curr. Microbiol. 17, 221–227.
85. Field, C.B., Behrenfeld, M.J., Randerson, J.T., Falkowski, P., 1998. Primary production of the biosphere: integrating terrestrial and oceanic components. Science 28, 237–240.
86. Figueroa, D.J., Fout, T., Plasynski, S., McIlvried, H., Srivastava, R.D., 2008. Advances in CO2 capture technology—The U.S. department of energy's carbon sequestration program. Int. J. Greenhouse Gas Control. 2, 9–20.
87. Finn, R.D., Bateman, A., Clements, J., Coggill, P., Eberhardt, R.Y., Eddy, S.R., Heger, A., Hetherington, K., Holm, L., Mistry, J., Sonnhammer, E.L., Tate, J., Punta, M., 2014. Pfam: the protein families database. Nucleic Acids Res 42, D222–D230.
88. Flemming, H.C., Wingender, J., 2010. The biofilm matrix. Nat. Rev. Microbiol. 8, 623-633.
89. Fondi, M., Rizzi, E., Emiliani, G., Orlandini, V., Berna, L., Papaleo M.C., Perrin, E., Maida, I., Corti, G, Bellis, G.D., Baldi, F., Dijkshoorn, Lenie., Vaneechoutte, M., Fani, R., 2013. The genome sequence of the hydrocarbon-degrading *Acinetobacter venetianus* VE-C3 . Res Microbiol. 164, 439-449.

90. Fowles, M., 2007. Black carbon sequestration as an alternative to bioenergy. Biomass Bioenergy 31, 426–432.
91. Fujita, M., Ike, M., Tachibana, S., Kitada, G., Kim, S.M., Inoue, Z., 2000. Characterization of a bioflocculant produced by *Citrobacter* sp.-TKF04 from Acetic and Propionic acids. J. Biosci. Bioeng. 89, 40-46.
92. Fukui, T., A. Yoshimoto., M. Matsumoto., S. Hosokawa., T. Saito, H. Nishikawa., T. Kenkichi., 1976. Enzymatic synthesis of poly-3-hydroxybutyrate in Zoogloea ramigera. Arch. Microbiol. 110, 149-156.
93. Fukui, T., Abe, H., Doi, Y., 2002. Engineering of Ralstonia eutropha for production of poly (3-hydroxybutyrate-co-3-hydroxyhexanoate) from fructose and solid state properties of the copolymer. Biomacromolecules 3, 618–624.
94. Fukui, T., Kichise, T., Yoshida, Y., Doi, Y., 1997. Biosynthesis of poly (3-hydroxybutyrate-co-3-hydroxyvalerate-co-3-hydroxy-heptanoate) terpolymers by recombinant *Alcaligenes eutrophus*. Biotechnol. Lett. 19, 1093–1097.
95. Gallois, A., Grimont, P. A. D. 1985. Pyrazines responsible for the potatolike odor produced by some *Serratia* and *Cedecea* strains. Applied and Environmental Microbiology 50, 1048–1051.
96. Ghosh, P., Swati, Thakur, I.S., 2014. Enhanced removal of COD and color from landfill leachate in a sequential bioreactor. Bioresour. Technol. 170, 10–19.
97. Gibson, J.L., Tabita, F.R., 1987. Organization of phosphoribulokinase and ribulose bisphosphate carboxylase/oxygenase genes in *Rhodopseudomonas* (*Rhodobacter) sphaeroides*. J. Bacteriol. 169, 3685–90.
98. Gnansounou, E., Pandey, A., 2017. Classification of Biorefineries Taking into Account Sustainability Potentials and Flexibility. Life-Cycle Assessment of Biorefineries. EPFLChapter- 226362. doi:10.1016/B978-0-444-63585-3.00001-2.
99. Gong, R, Ding, Y., Li, M., Yang, C., Liu, H., Sun, Y., 2005.Utilization of powdered peanut hull as biosorbent for removal of anionic dyes from aqueous solution, Dyes Pigments 64, 187–192.
100. Greenspan, D.C., Zhong, JP., Latorre, G.P., 1994. Effect of surface area to volume ratio on in vitro surface reactions of bioactive glass particulates. Bioceramics. 7, 28-35.

101. Grostern, A., Alvarez-Cohen, L.,2013. RubisCO-based CO2 fixation and C1 metabolism in the actinobacterium *Pseudonocardia dioxanivorans* CB1190. Environ Microbiol. 15, 11, 3040–53.
102. Gumel, A.M., Annuar, M.S.M., 2012. Biosynthesis and characterization of Polyhydroxyalkanoates copolymers produced by *Pseudomonas putida* Bet001 isolated from palm oil mill effluent. PLoS ONE. 7 (9). e45214. doi:10.1371/journal.pone.0045214.
103. Gupta, A., Kumar, M., Thakur, I.S., 2017. Analysis and optimization of process parameters for production of Polyhydroxyalkanoates along with wastewater treatment by Serratia sp. ISTVKR1. Bioresour. Technol. 242, 55–59.
104. Gupta, A., Thakur, I.S., 2016. Study of optimization of wastewater contaminant removal along with extracellular polymeric substances (EPS) production by a thermotolerant Bacillus sp. ISTVK1 isolated from heat shocked sewage sludge. Bioresour. Technol. 213, 21–30.
105. Haft, D. H., Paulsen, I.T., Ward, N., Selengut, J. D., 2006. Exopolysaccharide-associated protein sorting in environmental organisms: the PEPCTERM/ EpsH system. Application of a novel phylogenetic profiling heuristic. BMC Biology 4, 29.
106. Hammes, F., Verstraete, W., 2002. Key roles of pH and calcium metabolism in microbial carbonate precipitation. Environ. Sci. Biotechnol. 1, 3–7.
107. Hanai, T., Atsumi, S., Liao, J.C., 2007. Engineered synthetic pathway for isopropanol production in Escherichia coli. Appl. Environ. Microbiol. 73, 7814–7818.
108. Hansen, S., Vollan, V. B., Hough, E., Andersen, K., 1999. The crystal structure of Rubisco from *Alcaligenes eutrophus* reveals a novel central eight-stranded P-barrel formed by pstrands from four subunits. J. Mol. Biol., 288, 609-621.
109. Hantula, J., Bamford, D.H., 1991. Bacteriophage resistance and flocculation deficiency of Flavobacterium sp. are phenotypically interrelated. Appl. Microb. Biotech. 36, 105-108.
110. Harpel, M.R., Larimer, F.W., Hartman, F.C., 2002. Multifaceted roles of Lysl66 of ribulose-bisphosphate carboxylase/ oxygenase as discerned by product analysis and chemical rescue of site-directed mutants. Biochemistry, 41, 1390.

111. Hayashi, N. R., Arai, H., Kodama, T., Igarashi, Y., 1999. The *cbbQ* genes, located downstream of the Form I and Form II RubisCO genes, affect the activity of both RubisCOs. Biothem. Biophys. Res. Commun., 265,177-l 83.
112. He, N., Li, Y., Chen, J., Lun, S.Y., 2002. Identification of a novel bioflocculant from a newly isolated Corynebacterium glutamicum. Biochem. Eng. J. 11, 137-148.
113. Hench, L.L., 1997. Sol–gel materials for bioceramic applications. Curr Opin Solid State Mater Sci. 2, 604.
114. Hench, L.L., 1998. Bioceramics. J Am Ceram Soc. 81, 1705.
115. Hench, L.L., 2006. The story of Bioglass. J Mater Sci – Mater Med. 17, 967–78.
116. Hench, L.L., Splinter, R.J., Allen, W.C., Greenlee, T.K., 1971. Bonding mechanisms at the interface of ceramic prosthetic materials. J Biomed Mater Res Symp. 334, 117–41.
117. Hench, L.L., Splinter, R.J., Allen, W.C., Greenlee, T.K., 1971. Bonding mechanisms at the interface of ceramic prosthetic materials. J Biomed Mater. 5, 117-141.
118. Henstra, A.M., Sipma, J., Rinzema, A., Stams, A.J., 2007. Microbiology of synthesis gas fermentation for biofuel production. Curr. Opin. Biotechnol. 18, 200–206.
119. Hernandez, J. M., Baker, S. H., Lorbach, S. C., Shively, J.M., Tabita, F. R., 1996. Deduced amino acid sequence, functional expression, and unique enzymatic properties of the Form I and Form II ribulose bisphosphate carboxylase/oxygenase from the chemoautotrophic bacterium *Thiobacillus denitrzjicans.* J. Bacterial., 178,347-356.
120. Hicks, N., Vik, U., Taylor, P., Ladoukakis, E., Park, J., Kolisis, F., Jakobsen, K.S., 2017. Using prokaryotes for carbon capture storage. Trends Biotechnol. 35, 22–32.
121. Hicks, N., Vik, U., Taylor, P., Ladoukakis, E., Park, J., Kolisis, F., Jakobsen, K.S., 2017. Using prokaryotes for carbon capture storage. Trends Biotechnol. 35, 22–32.
122. Hidalgo-Cantabrana, C., Sánchez, B., Milani, C., Marco, Margolles, V.A., Ruas-Madiedo, Patricia., 2014. Genomic Overview and Biological Functions of Exopolysaccharide Biosynthesis in *Bifidobacterium* spp. Appl. Environ. Microbiol. 80, 9-18.
123. Hillebrand, M., Pflugmacher, S., Hahn, A., 2016. Toxicological risk assessment in CO2 capture and storage technology. Int. J. Greenhouse Gas Control 55, 118–143.
124. Hong, C., Hao, H., & Haiyun, W., 2009. Process optimization for PHA production by activated sludge using response surface methodology. Biomass Bioenergy. 33, 721-727.

125. Honjo, K., 1996. R&D for technology to solve global warming. J Mater Process Technol 59,
126. Horken, K.M., Tabita, F. R., 1999. The "green" Form I ribulose 1,5_bisphosphate carboxylase/oxygenase from the nonsulfur purple bacterium *Rhodobacter capsulatus.* J. Bacteriol., 181, 3935-3941.
127. Hoseinabadi, A., Rasooli, I., Taran, M., 2015. Isolation and Identification of Poly β-Hydroxybutyrate over-Producing Bacteria and optimization of production medium. Jundishapur. J. Microbiol. 8, 7. e16965. doi: 10.5812/jjm.16965v2.
128. Hoshino, Y., Utsunomiya, T., Abe, O., 1981. The thermal-decomposition of sodiumnitrate and the effects of several oxides on the decomposition. Bull Chem Soc Jpn. 54, 1385.
129. Hoskisson, P.A., Rigali, S., 2009. Chapter 1: Variation in form and function the helix-turn-helix regulators of the GntR superfamily. Adv. Appl. Microbiol. 69, 1−22.
130. https://www.co2.earth/ for recent CO2 concentration in atmosphere.
131. Hu, S.I., Drake, H.L., Wood, H.G., 1982. Synthesis of acetyl coenzyme A from carbon monoxide, methyltetrahydrofolate, and coenzyme A by enzymes from Clostridium thermoaceticum. J. Bacteriol. 149, 440–448.
132. Hu, Y., Holden, J.F., 2006. Citric acid cycle in the hyperthermophilic archaeon Pyrobaculum islandicum grown autotrophically, heterotrophically, and mixotrophically with acetate. J. Bacteriol. 188, 4350–4355.
133. Huber, H., Gallenberger, M., Jahn, U., Eylert, E., Berg, I.A., Kockelkorn, D., Eisenreich, W., Fuchs, G., 2008. A dicarboxylate/4-hydroxybutyrate autotrophic carbon assimilation cycle in the hyperthermophilic Archaeum Ignicoccus hospitalis. Proc. Natl. Acad. Sci. U.S.A. 105, 7851–7856.
134. Hügler, M., Huber, H., Molyneaux, S.J., Vetriani, C., Sievert, S.M., 2007. Autotrophic CO2 fixation via the reductive tricarboxylic acid cycle in different lineages within the phylum Aquificae: evidence for two ways of citrate cleavage. Environ. Microbiol. 9, 81–92.
135. Hügler, M., Huber, H., Stetter, K.O., Fuchs, G., 2003. Autotrophic CO2 fixation pathways in archaea (Crenarchaeota). Arch. Microbiol. 179, 160–173.

136. Hugler, M., Wirsen, C.O., Fuchs, G., Taylor, C.D., Sievert, S.M., 2005. Evidence for autotrophic CO2 fixation via the reductive tricarboxylic acidcycle by members of the ε subdivision of Proteobacteria. J. Bacteriol. 187, 3020–3027.
137. Hutmacher, D.W., 2000. Scaffolds in tissue engineering bone and cartilage. Biomaterials. 21, 2529–43.
138. Iwata, T., Furuhashi, Y., Su, F., Doi, Y., 2001. Single crystal morphologies of biodegradable aliphatic polyesters RIKEN. 42. Focused on Ecomolecular Science Research. J. Basic Microbiol. 47, 103–117.
139. J. Dunbar, S.A., Eichorst, L. V., Gallegos-Graves, L.V., Silva, Xie, G., S., Hengartner., N.W., Evans, R.D, Hungate, B.A., Jackson, R.B., Megonigal, J.P., Schadt, C.W., Vilgalys, R., Zak, D.R., Kuske, C.R., 2012. Common bacterial responses in six ecosystems exposed to 10 years of elevated atmospheric carbon dioxide. Environ Microbiol. 14, 1145–58.
140. Jajesniak, P., Ali, H.E.M.O., Wong, T.S., 2014. Carbon dioxide capture and utilization using biological systems: opportunities and challenges. J. Bioprocess. Biotech. 4, 155.
141. Janssen,P.J., Houdt, R.V., Moors, H., Monsieurs, Pieter., Morin, N., Michaux, A., Benotmane, M.A., Leys, N., Vallaeys, T., Lapidus, A., Monchy, S.B., Me´ digue, C., Taghavi, S., McCorkle, Sean., Dunn, John., Lelie, D., Mergeay, M., 2010. The Complete Genome Sequence of Cupriavidus metallidurans Strain CH34, a Master Survivalist in Harsh and Anthropogenic Environments. PLoS ONE 5, e10433.
142. Jessop, P.G., 2006. Homogeneous catalysis using supercritical fluid: recent trends and system studied. Supercrit. J. Fluids 38, 211–223.
143. Jiang, K., 2011. Genomic and Molecular Analysis of the Exopolysaccharide Production in the Bacterium Thauera aminoaromatica MZ1T (Doctral Dissertation) (http://trace. tennessee.edu/utk_graddiss/984) (Last accessed: 11.11.2017).
144. Johnson, E.J., MacElroy, R.D., 1973. Regulation in the chemolithotroph *Thiobacillus* neapolitanus*:* fructose-1,6-diphosphate. Arch. Microbiol. 93, 23–28.
145. Jones, J.R., 2009. New trends in bioactive scaffolds: the importance of nanostructure. J Eur Ceram Soc. 29, 1275.

146. Joshi, S., Kozlowski, M., Richens, S., Comberbach, D. M. 1989. Chitinase and chitobiase production during fermentation of genetically improved *Serratia liquefaciens*. Enzyme Microb. Technol. 11, 289–296.
147. Kaplan, A., Reinhold, L., 1999. CO_2 concentrating mechanisms in photosynthetic microorganisms. Ann Rev Plant Physio Plant Mol Biol. 50, 539-559.
148. Karlsson, J., Clarke, A.K., Chen, Z.Y., Hugghins, S.Y., Park, Y.I., 1998. A novel alpha-type carbonic anhydrase associated with the thylakoid membrane in Chlamydomonas reinhardtii is required for growth at ambient CO2. EMBO J. 17, 1208–1216.
149. Kawaguchi, T., Decho, A.W., 2002. A laboratory investigation of cyanobacterial extracellular
150. Keller, M.W., Schut, G.J., Lipscomb, G.L., Menon, A.L., Iwuchukwu, I.J., Leuko, T.T., Thorgersen, M.P., Nixon, W.J., Hawkins, A.S., Kelly, R.M., Adams, M.W.W., 2013. Exploiting microbial hyperthermophilicity to produce an industrial chemical, using hydrogen and carbon dioxide. Proc. Natl. Acad. Sci. U.S.A. 110, 5840–5845.
151. Kerfeld, C.a., Heinhorst, S., Cannon, G.C., 2010. Bacterial microcompartments. Annu. Rev. Microbiol. 64, 391–408.
152. Khandpur, P., Jabeen, E.T., Rohini, K.V.L., Laxminarayana, V.Y., 2012. Study on production, extraction and analysis of Polyhydroxyalkanoate (PHA) from bacterial isolates. IOSR. J. Pharm. Biol. Sci. 1, 31-38.
153. Khanna, S., Srivastava, A.K., 2005. Recent advances in microbial polyhydroxyalkanoates. Process Biochem. 40, 607–619.
154. Khosla, K., Rathour, R., Maurya, R., Maheshwari, N., Gnansounou, E., Larroche, C., Thakur, I.S., 2017. Biodiesel production from lipid of carbon dioxide sequestrating bacterium and lipase of psychrotolerant Pseudomonas sp. ISTPL3 immobilized on biochar. Bioresour. Technol. 245, 743–750.
155. Kim, B.S., 2000. Production of poly (3-hydroxybutyrate) from inexpensive substrates. Enzym. Microbial. Tec. 27, 774–7.
156. Kim, G., Jo, B.H., Kang, D.G., Kim, C.S., Choi, Y.S., 2012. Biomineralizationbased conversion of carbon dioxide to calcium carbonate using recombinant carbonic anhydrase. Chemosphere 87, 1091–1096.

157. Kim, P.I., Bai, H., Bai, D., Chae, H., Chung, S., Kim, Y., Park, R., Chi, Y.T., 2004. Purification and characterization of a lipopeptide produced by Bacillus thuringiensis CMB26. J. Appl. Microbiol. 97, 942–949.
158. Kim, Y.R., Hwang, J., Koh, H.J., Jang, K., Lee, J.D., Choi, J., Yang, C.S., 2016. The targeted delivery of the c-Src peptide complexed with schizophyllan to macrophages inhibits polymicrobial sepsis and ulcerative colitis in mice. Biomaterials 89, 1–13.
159. Kimura, K., Yamaoka, M., Kamisaka, Y., 2004. Rapid estimation of lipids in oleaginous fungi and yeasts using Nile red fluorescence. J. Microbiol. Methods, 56, 331–338.
160. Knorre, H., Krumbein, K.E., 2000. Bacterial calcification. Microbial Sediments. Springer–Verlag, Berlin. 25–31.
161. Knothe, G., 2008. "Designer" biodiesel: optimizing fatty ester composition to improve fuel properties. Energy Fuels 22, 1358–1364.
162. Kokubo, T., . Takadama, H., 2006. How useful is SBF in predicting in vivo bone bioactivity? Biomaterials, 27, 2907–2915.
163. Kokubo, T., 1998. Apatite formation on surfaces of ceramics, metals and polymers in body environment Acta. Mater., 46, 2519–2527.
164. Kolodziej, R., Scheib, J., 2014. Bio-based Isobutanol – A Versatile, Viable Next Generation Biofuel. Digital Refining (www.digitalrefining.com/article/1000899).
165. Kornmann, H., Duboc, P., Marison, I., von Stockar, U., 2003. Influence of nutritional factors on the nature, yield, and composition of Exopolysaccharides produced by *Gluconacetobacter xylinus* I-2281. Appl Environ Microbiol. 69, 6091–8.
166. Kroll, R.G., 1990. Microbiology of extreme environments. McGraw-Hill, New York.
167. Kuenen, G., Bos, P., 1989. Habitats and ecological niches of chemolitho(auto)trophic bacteria.
168. Kumar, A.S., Mody, K., Jha, B., 2007. Bacterial exopolysaccharides-a perception.
169. Kumar, M., Gazara, R.K., Verma, S., Kumar, M., Verma, P.K., Thakur, I.S., 2016a. Genome sequence of carbon dioxide-sequestering Serratia sp. strain ISTD04 isolated from marble mining rocks. Genome Announc. 4, 5, e01141–16
170. Kumar, M., Gazara, R.K., Verma, S., Kumar, M., Verma, P.K., Thakur, I.S., 2016b. Genome sequence of Pandoraea sp. ISTKB, a lignin degrading β-proteobacterium, isolated from the rhizospheric soil. Genome Announc. 4, 6 e01240-16.

171. Kumar, M., Ghosh, P., Khosla, K., Thakur, I.S., 2016c. Biodiesel production from municipal secondary sludge. Bioresour. Technol. 216, 165–171.
172. Kumar, M., Ghosh, P., Khosla, K., Thakur, I.S., 2018. Recovery of polyhydroxyalkanoates from municipal secondary wastewater sludge. Bioresour. Technol. 255, 111–115.
173. Kumar, M., Gupta, A., Thakur, I.S., 2016d. Carbon dioxide sequestration by chemolithotrophic oleaginous bacteria for production and optimization of polyhydroxyalkanoate. Bioresour. Technol. 213, 249–256.
174. Kumar, M., Gupta, J., Thakur, I.S., 2016e. Production and optimization of polyhydroxyalkanoate from oleaginous bacteria Bacillus sp. ISTC RRJMB 5, 80–89.
175. Kumar, M., Khosla, K., Thakur, I.S., 2017a. Optimization of process parameters for the production of biodiesel from carbon dioxide sequestering bacterium. JEES 3, 43–50.
176. Kumar, M., Morya, R., Gnansounou, E., Larroche, C., Thakur, I.S., 2017b. Characterization of carbon dioxide concentrating chemolithotrophic bacteriumSerratia sp. ISTD04 for production of biodiesel. Bioresour. Technol. 243, 893–897.
177. Kumar, M., Singh, J., Singh, M.K., Singhal, A., Thakur, I.S., 2015. Investigating the degradation process of kraft lignin by b-proteobacterium, Pandoraea sp. ISTKB. Environ. Sci. Pollut. Res. 22, 15690–15702.
178. Kumar, M., Sundaram, S., Gnansounou, E., Christian Larroche, C., Thakur, I.S., 2017c. Carbon dioxide capture, storage and production of biofuel and biomaterials by bacteria: a review. Bioresour. Technol. http://dx.doi.org/10.1016/j.biortech.2017.09. 050.
179. Laemmli, U.K., 1970. Cleavage of structural proteins during the assembly of the head of bacteriophage T4. Nature. 227, 680–685.
180. Lakshmi, R., Velmurugan, V., Sasikumar, S., 2013. Combust. Sci. Technol., 185, 1777–1785.
181. Laudisio, G., Branda, F., 2001. Sol-gel synthesis and crystallization of 3CaO.2SiO2 glassy powders. Thermochim Acta. 370, 119-124.
182. Lawrencin, C.T., El Amin, S.F., Ibim, S.E., Willoughby, D.A., Attavia, M., Allcock, H.R., Ambrosio, A.A., 1996. A highly porous 3-dimensional polyphosphazene polymer matrix for skeletal tissue regeneration. J Biomed Mater Res 30, 2, 133–8.

183. Leathers, T.D., Nunnally, M.S., Price, N.P., 2006. Co-production of schizophyllan and arabinoxylan from corn fiber. Biotechnol. Lett. 28, 623–626.
184. Lee, J.H., Park, D.O., Park, S.W., Hwang, E.H., Oh, J.I., Kim, Y.M., 2009. Expression and regulation of ribulose 1,5-bisphosphate carboxylase/ oxygenase genes in *Mycobacterium* sp. strain JC1 DSM 3803. J Microbiol 47, 297–307.
185. Lee, J.W., Na, D., Park, J.M., Lee, J., Choi, S., Lee, S.Y., 2012. Systems metabolic engineering of microorganisms for natural and non-natural chemicals. Nat. Chem. Biol. 8, 536–546.
186. Lee, S. J., Yoon, B.-D., Oh, H.-M., 1998. Rapid method for the determination of lipidfrom the green alga *Botryococcusbraunii*, Biotechnol Tech. 12, 553–6.
187. Lee, S.Y., 1996. Plastic bacteria? Progress and prospects for polyhydroxyalkanoate production in bacteria. Trends. Biotechnol. 14, 431–438.
188. Lee, S.Y., 1996. Plastic bacteria? Progress and prospects for polyhydroxyalkanoate production in bacteria. Trends. Biotechnol. 14, 431–438.
189. LeGeros, R.Z., 2002. Properties of osteoconductive biomaterials: calcium phosphates. Clin Orthop Relat Res. 395, 81- 98.
190. Leung, D.Y.C., Caramanna, G., Mercedes, M.M.-V., 2014. An overview of current status of carbon dioxide capture and storage technologies. Renewable Sustainable Energy Rev. 39, 426–443.
191. Li, B.Z., Balan, V., Yuan, Y.J., Dale, B.E., 2010. Process optimization to convert forage and sweet sorghum bagasse to ethanol based on ammonia fiber expansion (AFEX) pretreatment. Bioresour. Technol. 101, 1285–1292.
192. Li, R., Clark, A.E., Hench, L.L., 1991. An Investigation of Bioactive Glass Powders by Sol-Gel Processing. J Appl Biomater. 2, 231-239.
193. Li, X.Y., Yang, S.F., 2007. Influence of loosely bound extracellular polymeric substances (EPS) on the flocculation, sedimentation and dewaterability of activated sludge. Water Research 41, 1022-1030.
194. Li, Y., Zhao, R., Liu, T., Zhao, J., 2015. Does urbanization lead to more direct and indirect household carbon dioxide emissions? Evidence from China during 1996–2012. J. Clean. Prod. 102, 103–114.

195. Lindberg, P., Park, S., Melis, A., 2010. Engineering a platform for photosynthetic isoprene production in cyanobacteria, using Synechocystis as the model organism. Metab. Eng. 12, 70–79.
196. Liu, J.R., Liu, C.T., Edwards, E.A., Liss, S.N., 2006. Effect of phosphorus limitation on microbial floc structure and gene expression in activated sludge. Water Sci. Technol 54, 247-255.
197. Liu, X., Ding, C., . Chu, P.K., 2004. Mechanism of apatite formation on wollastonite coatings in simulated body fluids. Biomaterials, 25, 1755–1761.
198. López-Cuellar, M., Alba-Flores, J., Rodríguez, J., Pérez-Guevara, F., 2011. Production of polyhydroxyalkanoates (PHAs) with canola oil as carbon source. Int. J. BiolMacromol. 48, 74–80.
199. Lu, J., Tappel, R.C., Nomura, C.T., 2009. Mini-review: Biosynthesis of poly(hydroxyalkanoates). Polym. Rev. 49, 226–248.
200. Lugg, H., Sammons, r., Marquis, L.P.M., Hewitt, c. J., Yong, P., Paterson-Beedle, M., Redwood, M. D., Stamboulis, A., Kashani, M., Jenkins, M., Macaskie, L. E., 2008. Polyhydroxybutyrate accumulation by a *Serratia* sp. Biotechnol. Lett. 30, 481-491.
201. Luoma, P., Vanhanen, J., Tommila, P., 2011. Distributed Bio-Based Economy—Driving Sustainable Growth, Sitra..
202. Ma, F., Hannab, M.A., 1999. Biodiesel production: a review. Bioresour. Technol. 70, 1–15.
203. MacElroy, R.D., Mack, H.M., Johnson, E.J., 1972. Properties of phosphoribulokinase from *Thiobacillus neapolitanu*s. J. Bacteriol. 112, 532–38
204. Madhavan, A., Sindhu, R., Binod, P., Sukumaran, R.K., Pandey, A., 2017. Strategies for design of improved biocatalysts for industrial applications. Bioresour. Technol. http://dx.doi.org/10.1016/j.biortech.2017.05.031.
205. Madhuvilakku, R., Shakkthivel, P., 2013. Biodiesel synthesis by TiO2-ZnO mixed oxide nanocatalyst catalyzed palm oil transesterification process. Bioresour. Technol. 150, 55–59.
206. Madison, L.L., Huisman, G.W., 1999. Metabolic engineering of poly(3-hydroxyalkanoates): From DNA to plastic. Microbiol. Mol. Biol. Rev. 63, 21–53.

207. Magdouli, S., Brar, S.K., Blais, J.F., Tyagi, R.D., 2015. How to direct the fatty acid biosynthesis towards polyhydroxyalkanoates production? Biomass Bioenerg. 74, 2 6 8 - 2 7 9.

208. Maheshwari, N., Kumar, M., Thakur, I.S., Srivastava, S., 2017. Recycling of carbon dioxide by free air CO2 enriched (FACE) Bacillus sp. SS105 for enhanced production and optimization of biosurfactant. Bioresour. Technol. 242, 2–6.

209. Manavalan, T., Manavalan, A., Thangavelu, K.P., Heese, K., 2012. Secretome analysis of *Ganoderma lucidum* cultivated in sugarcane bagasse. J. Proteomics 77, 298–309.

210. March, J.J., Lebherz, H.G., 1992. Fructose bisphosphate aldolases: an evolutionary history. Trends Biochem. Sci. 17, 110–13.

211. Maria, V.O., Sergey, V.T., Galina A.D., Elena, V.B., Maria N.T., Margarita, Y.G., 2016. Genomic insights into metabolic versatility of a lithotrophic sulfur-oxidizing diazotrophic Alphaproteobacterium *Azospirillum thiophilum.* FEMS Microbiology Ecology, 92, 199.

212. Mathlouthi, M., Koenig, J.L., 1987. Vibrational spectra of carbohydrates. Adv. Carbohydr. Chem. Biochem. 44, 7–89.

213. Matsuyama, T., Murakami, T., Fujita, M., Fujita, S., Yano, I., 1986. Extracellular vesicle formation and biosurfactant production by *Serratia marcescens*. J. Gen. Microbiol 132, 865–875.

214. Matter, J.M., Stute, M., Snæbjörnsdottir, S.Ó., Oelkers, E.H., Gislason, S.R., Aradottir,E.S., Sigfusson, B., Gunnarsson, I., Sigurdardottir, H., Gunnlaugsson, E., Axelsson, G., Alfredsson, H.A., Wolff-Boenisch, D., Mesfin, K., de la Fernandez, R.T.D., Hall, J., Dideriksen, K., Broecker, W.S., 2016. Rapid carbon mineralization for permanent disposal of anthropogenic carbon dioxide emissions. Science 352, 1312–1314.

215. Mazur, M., Krywko-Cendrowska, A., Krysińsk, P., Rogalski, J., 2009. Encapsulation of laccase in a conducting polymer matrix: a simple route towards polypyrrole microcontainers. Synth Met 159, 1731–1738.

216. Meijer, W.G., Enequist, H.G., Terpstra, P., Dijkhuizen. L., 1990. Nucleotide sequences of the genes encoding fructosebisphosphatase and phosphoribulokinase from *Xanthobacter flavus* H4-14. J. Gen. Microbiol. 136, 2225–30.

217. Mercaldi, M.P., Dams-Kozlowska, H., Panilaitis, B., Joyce, A.P., Kaplan, D.L., 2008. Discovery of the dual polysaccharide composition of emulsan and the isolation of the emulsion stabilizing component. Biomacromolecules 9, 1988-1996.
218. Merrick, J.M., M. Doudoroff., 1960. Enzymatic synthesis of poly-3-hydroxybutyric acid in bacteria. Nature (London) 189, 890-892.
219. Messner, P., Sleytr, U.B., 1992. Crystalline bacterial cell-surface layers. Adv. Microb. Physiol. 33, 213–275.
220. Millennium development goals indicators, 2014. Carbon dioxide emissions (CO2), thousand metric tons of CO2 (CDIAC).
221. Minic, Z., C, Marie., C, Delorme., Faurie, J.M., Mercier, G., Ehrlich, D., Renault, P., 2007. Control of EpsE, the Phosphoglycosyltransferase Initiating Exopolysaccharide Synthesis in Streptococcus thermophilus, by EpsD Tyrosine Kinase? J.Bictriol. 189, 1351-1357.
222. Minoda, A., Weber, A.P.M., Tanaka, K., Miyagishima, S.Y., 2010. Nucleusindependent control of the rubisco operon by the plastid-encoded transcription factor Ycf30 in the red alga *Cyanidioschyzon merolae*. Plant Physiol 154, 1532–1540.
223. Mishra, M., Thakur, I.S., 2011. Purification, characterization and mass spectroscopic analysis of thermo-alkalotolerant β- 1, 4-endoxylanase from Bacillus sp. and its potential for dye decolorization. Int Biodeterior Biodegrad 65, 301-308.
224. Moazami, N., Ranjbar, R., Ashori, A., Tangestani, M., Nejad, A.S., 2011. Biomass and lipid productivities of marine microalgae isolated from the Persian Gulf and the Qeshm Island. Biomass Bioenerg. 35, 1935–1939.
225. Mohapatra, S., Samantaray, D. P., Samantaray, S. M., 2014. Phylogenetic heterogeneity of the rhizospheric soil bacterial isolates producing PHAs revealed by comparative analysis of 16s-rRNA. Int. J. Curr. Microbiol. App. Sci. 3.5, 680-690.
226. Montenero, A., Gnappi, G., Ferrari, F., Cesari, M., Salvioli, E., Mattogno, L., Kaciulisand, S., Fini M., 2000. Sol-gel derived hydroxyapatite coatings on titanium substrate. J. Mater. Sci. 35, 2791–2797 .
227. More, T.T., Yadav, J.S.S., Yan, S., Tyagi, R.D., Surampalli, R.Y., 2014. Review extracellular polymeric substances of bacteria and their potential environmental applications. J. Environ. Manage. 144, 1–25.

228. Moreira, D., Pires, J.C.M., 2016. Atmospheric CO2 capture by algae: negative carbon dioxide emission path. Bioresour. Technol. 215, 371–379.
229. Moriya, Y., Itoh, M., Okuda, S., Yoshizawa, A.C., Kanehisa, M., 2007. KAAS: an automatic genome annotation and pathway reconstruction server. Nucleic Acids Res, 35, 182-185.
230. Mosmann, T., 1983. Rapid colorimetric assay for cellular growth and survival: application to proliferation and cytotoxicity assays. J Immunol Methods. 65, 55-63.
231. Możejko-Ciesielska, J., Kiewisz, R., 2016. Bacterial polyhydroxyalkanoates: Still fabulous?. Microbiological research. 192, 271-282.
232. Muller, H., Furnkranz, M., Grube, M., Berg, G., 2013. Genome Sequence of *Serratia plymuthica* Strain S13, an Endophyte with Germination- and Plant-Growth-Promoting Activity from the Flower of Styrian Oil Pumpkin. Genome Announc. 1, e00594–13.
233. Müller, J., MacEachran, D., Burd, H., Sathitsuksanoh, N., Bi, C., Yeh, Y.C., Lee, T.S., Hillson, N.J., Chhabra, S.R., Singer, S.W., Beller, H.R., 2013. Engineering of Ralstonia eutropha H16 for autotrophic and heterotrophic production of methyl ketones. Appl. Environ. Microbiol. 79, 4433–4439.
234. Murakami, M., Ikenouchi, M., 1997. The biological CO2 fixation and utilization project by RITE Screening and breeding of microalgae with high capability in fixing CO2. Energy Convers Manage. 38, S493-S497.
235. Muynck, W.D., Cox, K., DeBelie, N., Verstraete, W., 2008. Bacterial carbonate precipitation as and alternative surface treatment for concrete. Const Build Mater. 22, 875–885.
236. N. He, Y. Li, J. Chen, S.Y. Lun, Identification of a novel bioflocculant from a newly isolated Corynebacterium glutamicum, Biochem. Eng. J. 11 (2002) 137–148.
237. Naik, U. C., Srivastava, S., Thakur, I.S., 2012. Isolation and characterization of Bacillus cereus IST105 from electroplating effluent for detoxification of hexavalent chromium. Environ Sci Pollut Res. 19, 3005–3014.
238. Nanda, S., Reddy, S. N., Mitra, S. K., Kozinski, J. A., 2016. The progressive routes for carbon capture and sequestration. Energy Science and Engineering. 4, 99–122.

239. Navarro, M., del Valle, S., Martinez, S., Zeppetelli, S., Ambrosio, L., Josep., Planell, A., Ginebra, M.P., 2004. New macroporous calcium phosphate glass ceramic for guided bone regeneration. Biomaterials 25, 4233–4241.
240. Neupane, S., Finlay, R.D., Kyrpides, N.C., Goodwin, L., Alstrom, S., Lucas, S., Land, M., Han, J., Lapidus, A., Cheng, J.F., Bruce, D., Pitluck, S., Peters, L., Ovchinnikova, G., Held B, Han, C., Detter J.C., Tapia, R., Hauser, L., Ivanova, N., Pagani, I., Woyke, T., Klenk, H.P., Högberg, N., 2012. Complete genome sequence of the plant-associated Serratia plymuthica strain AS13. Stand Genomic Sci. 7, 22–30.
241. Newman, J., Gutteridge, S., 1994. Structure of an effectorinduced inactivated state of ribulose 1,5_bisphosphate carboxylase/ oxygenase: the binary complex between enzyme and xylulose 1,5_bisphosphate. Structure, 2,495-502.
242. Nimtz, M., Mort, A., Domke, T., Wray, V., Zhang, Y., Qiu, F., Coplin, D., Geider, D., 1996a. Structure of amylovoran, the capsular exopolysaccharide from the fire blight pathogen *Erwinia amylovora*. Carbohydr Res. 287, 59–76.
243. Nimtz, M., Mort, A., Wray, V., Domke, T., Zhang, Y., Coplin, D.L., and Geider, K. 1996b. Structure of stewartan, the capsular exopolysaccharide from the corn pathogen *Erwinia stewartii*. Carbohydr Res. 288, 189–201.
244. Noble, R.R.P., Stalker, L., Wakelin, S.A., Pejcic, B., Leybourne, M.I., Hortle, A.L., Michael, K., 2012. Biological monitoring for carbon capture and storage – a review and potential future developments. Int. J. Greenhouse Gas Control 10, 520–535.
245. Noda, I., Green, P.R., Satkowski, M.M., Schechtman, L.A., 2005. Preparation and properties of a novel class of polyhydroxyalkanoate copolymers. Biomacromolecules. 6, 580–586.
246. Numata, K., Morisaki, K., TomizawaS., Ohtani, M., Demura, T., Miyazaki, M., Nogi, Y., Deguchi, S., Doi, Y., 2013. Synthesis of poly- and oligo (hydroxyalkanoate)s by deep-sea bacteria, *Colwellia* spp., *Moritella* spp., and *Shewanella* spp., Polym. J. 45, 1094–1100.
247. Nwodo, U.U., Green, E., Okoh, A.I., 2012. Bacterial exopolysaccharides: functionality and prospects. Int. J. Mol. Sci. 13, 14002–14015.

248. Ogunjobi, A. A., Ogundele, A.O., Fagade, O.E., 2011. "Production of Polyhydroxyalkanoates by *Pseudomonas putrefaciens* from cheap and renewable carbon substrates", EJEAFChe. 10, 2806-2815.
249. Olson, D.G., McBride, J.E., Shaw, A.J., Lynd, L.R., 2012. Recent progress in consolidated bioprocessing. Curr. Opin. Biotechnol. 23, 396–405.
250. Otsuki, T., 2001. A study for the biological CO2 fixation and utilization system. Sci Total Environ. 277, 21–5.
251. Overbeek, R., Olson, R., Pusch, G. D., Olsen, G. J., Davis, J. J., Disz, T., Vonstein, V., 2013. The SEED and the Rapid Annotation of microbial genomes using Subsystems Technology (RAST). Nucleic Acids Res, 42, D206-D214.
252. Paital, S.R., Dahotre, N.B., 2009. Calcium phosphate coatings for bio-implant applications: Materials, performance factors, and methodologies. Mater. Sci. Eng. R, 66, 1–70.
253. Paoli, G.C., Tabita, F.R., 1998. Aerobic chemolithoautotrophic growth and RubisCO function in Rhodobacter capsulatus and a spontaneous gain of function mutant of Rhodobacter sphaeroides. Arch. Microbiol. 170, 8–17.
254. Peitl, O., Zanotto, E.D., Hench, L.L., 2001. Highly bioactive P2O5–Na2O–CaO–SiO2 glass–
255. Pengpeng, Li., Amy, H.Y., Kwok, J.J., Tingting, R., Dongqing, X., Weiwu, W., Frederick, C.L., 2015. Comparative Genome Analyses of Serratia marcescens FS14 Reveals Its High Antagonistic Potential. PLoS ONE 10. doi.org/10.1371/journal.pone.0123061.
256. Peplinski, K., Ehrenreich, A., Döring, C., Bömeke, M., Reinecke, F., Hutmacher, C., Steinbüchel, A., 2010. Genome-wide transcriptome analyses of the "Knallgas" bacterium *Ralstonia eutropha* H16 with regard to polyhydroxyalkanoate metabolism. Microbiology. 156, 2136–2152.
257. Peters, M., Köhler, B., Kuckshinrichs, W., Leitner, W., Markewitz, P., Müller, T.E., 2011. Chemical technologies for exploiting and recycling carbon dioxide into the value chain. ChemSusChem 4, 1216–1240.

258. Plewinski, M., Schickle, K., Lindner, M., Weber, M., Fischer, H., 2013. The effect of crystallization of bioactive bioglass 45S5 on apatite formation and degradation. Dent Mater. 29, 1256-1264.
259. Poblete-Castro, I., Binger, D., Oehlert, R., Poblete-Castro, M.R., 2014. Comparison of mcl-Poly (3-hydroxyalkanoates) synthesis by different Pseudomonas putida strains from crude glycerol: citrate accumulates at high titer under PHA-producing conditions. BMC Biotechnol. 14, 962.
260. Poli, A., Kazak, H., Gurleyendag˘, B., Tommonaro, G., Pieretti, G., Oner, E.T., Nicolaus, B., 2009. High level synthesis of levan by a novel Halomonas species growing on defined media. Carbohydr. Polym. 78, 651–657.
261. Pötter, R., Steinbüchel, A., 2005. Poly(3-hydroxybutyrate) granule-associated proteins: Impacts on poly(3-hydroxybutyrate) synthesis and degradation. Biomacromolecules. 6, 552–560.
262. Price, G.D., Sueltemeyer, D., Klughammer, B., Ludwig, M., Badger, M.R., 1998. The functioning of the CO_2 concentrating mechanism in several cyanobacterial strains: a review of general physiological characteristics, genes, proteins and recent advances. Can J Bot 76, 973-1002.
263. Pühler, A., Vorhölte,r F.J., Schneiker, S., Goesmann, A., Krause, L., Bekel, T., Kaiser, O., Linke, B., Patschkowski, T., Rückert, C Schmid, J., Sidhu, V.K., Sieber .V., Tauch. A., Watt, S.A., Weisshaar, B., Becker, A., Niehaus, K., Pühler, A., 2008. The genome of *Xanthomonas campestris* pv. campestris B100 and its use for the reconstruction of metabolic pathways involved in xanthan biosynthesis. J Biotechnol. 134, 33–45.
264. Purushotham, P., Arun, P.V., Prakash, J.S., Podile, A.R., 2012. Chitin binding proteins act synergistically with chitinases in Serratia proteamaculans. PLoS One. 7, e36714.
265. Ragsdale, S.W., Wood, H.G., 1985. Acetate biosynthesis by acetogenic bacteria: evience that carbon monoxide dehydrogenase is the condensing enzyme that catalyzes the final steps of the synthesis. J. Biol. Chem. 260, 3970–3977.
266. Rahaman, M.S.A., Cheng, L.-H., Xu, X.-H., Zhang, L., Chen, H.-L., 2011. A review of carbon dioxide capture and utilization by membrane integrated microalgal cultivation processes. Renewable Sustainable Energy Rev. 15, 4002–4012.

267. Ramila, A., Balas, F., Vallet-Regi, M., 2002. Synthesis routes for bioactive sol–gel glasses: alkoxides versus nitrates. Chem Mater. 14, 542.
268. Raza, W., Makeen, K., Wang, Y., Xu, Y., Qirong, S., 2011. Optimization, purification, characterization and antioxidant activity of an extracellular polysaccharide produced by *Paenibacillus polymyxa* SQR-21. Bioresour. Technol. 102, 6095–6103.
269. Reddy, M.V., Mohan, S.V., 2015. Polyhydroxy alkanoates Production by Newly Isolated Bacteria Serratia ureilytica Using Volatile Fatty Acids as Substrate: Bio-Electro Kinetic Analysis. J. Microb. Biochem. Technol. 7, 1.
270. Rehm, B., 2009. Microbial Production of Biopolymers and Polymer Precursors: Applications and Perspectives. Norfolk: Caister Academic.
271. Rehm, B.H., 2010. Bacterial polymers: biosynthesis, modifications and applications. Nature reviews. Microbiology, 8, 8, 578.
272. Ren, Q., Sierro, N., Witholt, B., Kessler, B., Fab,G., 2000. An NADPHdependent 3-ketoacyl reductase of Pseudomonas aeruginosa, provides precursors for medium-chain-length poly-3 hydroxyalkanoate biosynthesis in *Escherichia coli*. J. Bacteriol. 182, 2978-81.
273. Riding, R., 2006. Cyanobacterial calcification, carbon dioxide concentrating mechanisms, and
274. Rippel, S., Bowien, B., 1984. Phosphoribulokinase from *Rhodopseudomonas acidophil*a. Arch. Microbiol. 139, 207–12.
275. Rittmann, S., Seifert, A., Herwig, C., 2015. Essential prerequisites for successful bioprocess development of biological CH4 production from CO2 and H2. Crit. Rev. Biotechnol. 35, 141–151.
276. Rivadeneyra, M.A., Delgado, G., Ramos, C.A., Delgado, R., 1998. Biomineralization of carbonates by Halomonas eurihalina in solid and liquid media with different salinities: crystal formation sequence. Res. Microbial., 149, 227-287.
277. Rivadeneyra, M.A., Parraga, J., Delgado, R., Ramos-Cormenzana, A., Delgado, G., 2004. Biomineralization of carbonates by Halobacillus trueperi in solid and in liquid media with different salinities. FEMS Microbiol Ecol 48, 39–46.

278. Robinson, T., Chandran, B. Nigam, P., 2002. Removal of dyes from a synthetic textile dye effluent by biosorption on apple pomace and wheat straw, Water Res. 36, 2824–2830.
279. Robinson,T., McMullan, G., Marchant, R., Nigam, P., 2001. Remediation of dyes in textile effluent: a critical review on current treatment technologies with a proposed alternative, Bioresour. Technol. 77, 247–255.
280. Rodriguez-Navarro, C., Rodriguez-Gallego, M., Ben, C.K., González-Mu˜noz, M.T., 2003. Conservation of ornamental stone by *Myxococcus xanthus* induced carbonate biomineralization. Appl Environ Microbiol. 69, 2182–2193.
281. Rodriguez-Navarro, C., Ruiz-Agudo, E., Luque, A., Rodriguez-Navarro, A.B., Ortega-Huertas, M., 2009. Thermal decomposition of calcite: Mechanisms of formation and textural evolution of CaO nanocrystals. Am. Mineral. 94, 578–593.
282. Role of a GntR-family response regulator LbrA in Listeria monocytogenes biofilm formation. PLoS ONE. 8, e70448.
283. Romagnoli, S., Tabita, F.R., 2006. A novel three-protein two-component system provides a regulatory twist on an established circuit to modulate expression of the *cbbI* region of *Rhodopseudomonas palustris* CGA010. J Bacteriol 188, 2780–2791.
284. Ron, E.Z., Rosenberg, E., 2002. Biosurfactants and oil bioremediation. Curr. Opin. Biotechnol. 13, 249-252.
285. Rothermich, M.M., Guerrero, R., Lenz, R.W., Goodwin, S., 2000 Characterization, seasonal occurrence, and diel fluctuation of poly(hydroxyalkanoate) in photosynthetic microbial mats. Appl. Environ. Microbiol. 66, 4279–4291.
286. Saini, R., Kapoor, R., Kumar, R., Siddiqi, T.O., Kumar, A., 2011. CO2 utilizing microbes – a comprehensive review. Biotechnol. Adv. 29, 949–960.
287. Saiz, E., Goldman, M., Gomez-Veg, J.M., Tomsia, A.P., Marshall, G.W., Mar-shall, S.J., 2002. In vitro behavior of silicate glass coatings on Ti6Al4V. Biomaterials, 23, 3749–3756.
288. Sakakura, T., Choi, J.C., Yasuda, H., 2007. Transformation of carbon dioxide. Chem. Rev. 107, 2365–2387.
289. Saravanapavan, P., Hench, L.L., 2003. Dissolution of bioactive gel–glass powders in the SiO2–CaO system. Key Eng Mat. 213, 240–242.

290. Saravanapavan, P., Jones, J.R., Pryce, RS., Hench, L.L., 2003. Bioactivity of gel–glass powders in the CaO–SiO2 system: a comparison with ternary (CaO–P2O5–SiO2) and quaternary glasses (SiO2–CaO–P2O5–Na2O). J Biomed Mater Res Part A. 66A, 110.
291. Sawaya, M.R., Cannon, G.C., Heinhorst, S., Tanaka, S., Williams, E.B., Yeates, T.O., Kerfeld, C.A., 2006. The structure of beta-carbonic anhydrase from the carboxysomal shell reveals a distinct subclass with one active site for the price of two. J. Biol. Chem. 281, 7546–7555.
292. Schafer, S., Barkowski, C., Fuchs, G., 1986. Carbon assimilation by the autotrophic thermophilic archaebacterium Thermoproteus neutrophilus. Arch. Microbiol. 146, 301–308.
293. Schirmer, A., Rude, M.A., Li, X., Popova, E., del Cardayre, S.B., 2010. Microbial biosynthesis of alkanes. Science 329, 559–562.
294. Schnitzer, M., 1991. Soil organic matter—the next 75 years. Soil Sci. 151, 41–58.
295. Schubert, P., Steinbuchel, A., Schlegel, H.G., 1988. Cloning of the Alcaligenes eutrophus Genes for Synthesis of Poly-3-Hydroxybutyric Acid (PHB) and Synthesis of PHB in Escherichia coli. ASM. 170, 5837-5847.
296. Schwander, T., Borzyskowski, L.S., Burgener, S., Cortina, N.S., Erb, T.J., 2016. A synthetic pathway for the fixation of carbon dioxide in vitro. Science. 354, 900–904.
297. Sheikh, A.Q., Skinder, B.H., Pandit, A.K., Ganai, B.A., 2014. Terrestrial carbon sequestration as a climate change mitigation activity. J. Pollut. Eff. 2, 110. http://dx.doi. org/10.4172/2375-4397.1000110.
298. Shen, J.W., Shi, C.W., Xu, C.P., 2013. Exopolysaccharides from Pleurotus pulmonarius: fermentation optimization, characterization and antioxidant activity. Food Technol. Biotechnol. 51, 520–527.
299. Shen, X. W., Yang, Y., Jian, J., Wu, Q., Chen, G. Q., 2009. Production and characterization of homopolymer poly (3-hydroxyvalerate) (PHV) accumulated by wild type and recombinant *Aeromonas hydrophila* strain 4AK4. Bioresour. Technol. 100, 4296-4299.
300. Sheng, G.P., Yu, H.Q., Li, X.Y., 2010. Extracellular polymeric substances (EPS) of microbial aggregates in biological wastewater treatment systems: a review. Biotechnol Adv. 28, 882-894.

301. Shimizu, R., Chou, K., Orita, I., Suzuki, Y., Nakamura, S., Fukui, T., 2013. Detection of phase-dependent transcriptomic changes and Rubisco-mediated CO2 fixation into poly (3-hydroxybutyrate) under heterotrophic condition in *Ralstonia eutropha* H16 based on RNA-seq and gene deletion analyses. BMC Microbiol. 13, 169.
302. Shin, J., Song, Y., Jeong, Y., Cho, B-K., 2016. Analysis of the Core Genome and Pan-Genome of Autotrophic Acetogenic Bacteria. Front. Microbiol. 7, 1531.
303. Shingel, K.I., 2002. Determination of structural peculiarities of dextran, pullulan and γ - irradiated pullulan by Fourier-transform IR spectroscopy. Carbohydr. Res. 337, 1445–1451.
304. Shivakumar, S., Vijayendra, S.V.N., 2006. Production of exopolysaccharides by Agrobacterium sp. CFR-24 using coconut water – a byproduct of food industry. Lett Appl Microbiol 42, 477–482.
305. Shively, J.M., Ball, F., Brown, D.H., Saunders, R.E., 1973. Functional organelles in prokaryotes: polyhedral inclusions (carboxysomes) of Thiobacillus neapolitanus. Science 182, 584–586.
306. Shively, J.M., English, R.S., Baker, S.H., Cannon, G.C., 2001. Carbon cycling: the prokaryote contribution. Curr. Opin. Microbiol. 4, 301–306.
307. Shively, J.M., Keulen, G., Meijer, W.G., 1998. SOMETHING FROM ALMOST NOTHING: Carbon Dioxide Fixation in Chemoautotrophs. Annu Rev Microbiol. 52, 191-230
308. Siebert, K., Bowien, B., 1984. Evidence for an octameric structure of phosphoribulokinase from *Alcaligenes* eutrophus. Biochim. Biophys. Acta 787, 208–14.
309. Sillers, R., Chow, A., Tracy, B., Papoutsakis, E.T., 2008. Metabolic engineering of the nonsporulating, non-solventogenic Clostridium acetobutylicum strain M5 to produce butanol without acetone demonstrate the robustness of the acid-formation pathways and the importance of the electron balance. Metab. Eng. 10, 321–332.
310. Singh, J., Thakur, I.S., 2015. Evaluation of cyanobacterial endolithic Leptolyngbya sp. ISTCY101, for integrated wastewater treatment and biodiesel production: a toxicological perspective. Algal Res. 11, 294–303.

311. Singh, J., Tripathi, R., Thakur, I.S., 2015. Immobilized lipase from Schizophyllum commune ISTL04 for the production of fatty acids methyl esters from cyanobacterial oil. Bioresour. Technol. 188, 214–218.
312. Singh, M.K., Kumar, M., Thakur, I.S., 2017. Proteomic characterization and schizophyllan production by *Schizophyllum commune* ISTL04 cultured on *Leucaena leucocephala* wood under submerged fermentation. Bioresour. Technol. 236, 29–36.
313. Singh, M.K., Singh, J., Kumar, M., Thakur, I.S., 2014. Novel lipase from basidiomycetes Schizophyllum commune ISTL04, produced by solid state fermentation of Leucaena leucocephala seeds. J. Mol. Catal. B: Enzyme 110, 92–99.
314. Siriphannon, P., Kameshima Y, Yasumori, A., Okada, K., Hayashi, S., 2002. Formation of hydroxyapatite on CaSiO3 powders in simulated body fluid. J Eur Ceram Soc. 22, 511-520.
315. Smith, K.S., Ferry, J.G., 2000. Prokaryotic carbonic anhydrases. FEMS Microbiol. Rev. 24, 335–366.
316. Srivastava, S., Bharti, R., Thakur, I.S., 2015a. Characterization of bacteria isolated from palaeoproterozoic metasediments for sequestration of carbon dioxide and formation of calcium carbonate. Environ. Sci. Pollut. Res. 22, 1499–1511.
317. Srivastava, S., Bharti, R., Verma, P., Thakur, I.S., 2015b. Cloning and expression of gamma carbonic anhydrase from Serratia sp. ISTD04 for sequestration of carbon dioxide and formation of calcite. Bioresour. Technol. 188, 209–213.
318. Steinbüchel, A., Debzi, E.M., Marchessault, R.H., Timm, A., 1993. Synthesis and production of poly (3-hydroxyvaleric acid) homopolyester by Chromabacterium violaceum. Appl. Microbiol. Biotechnol. 39, 443–449.
319. Steinbüchel, A., Schmack, G., 1995. Large-Scale production of poly (3-hydroxyvaleric Acid) by fermentation of Chromobacterium violaceum, processing, and characterization of the homopolyester. J. Environ. Polym. Degr. 3, 243–258.
320. Stoor, P., Soderling, E., Salonen, J.I., 1998. Antibacterial effects of a bioactive glass paste on oral microorganisms. Acta Odontol Scand. 56, 161-165.
321. Subramanian, S.B., Yan, S., Tyagi, R.D., Surampalli, R.Y., 2010. Extracellular polymeric substances (EPS) producing bacterial strains of municipal wastewater sludge:

isolation, molecular identification, EPS characterization and performance for sludge settling and dewatering. Water Res. 44, 2253–2266.

322. Sundaram, S., Thakur, I.S., 2015. Biosurfactant production by a CO2 sequestering Bacillus sp. strain ISTS2. Bioresour. Technol. 188, 247–250.
323. Synytsya, A., Novak, M., 2014. Structural analysis of glucans. Ann. Transl. Med. 2, 17.
324. Tabita, F.R., 1980. Pyridine nucleotide control and subunit structure of phosphoribulokinase from photosynthetic bacteria. J. Bacteriol. 143, 1275–80.
325. Tabita, F.R., 2009. The hydroxypropionate pathway of CO2 fixation: Fait accompli. Proc. Natl. Acad. Sci. USA 106, 21015–21016.
326. Tan, G-Y. A., Chen, C.L. , Li, L., Ge, L., Wang, L., Razaad, I.M.N., Li, Y., Zhao, Lei., Mo, Y., Wang, J-Y., 2014. Start a Research on Biopolymer Polyhydroxyalkanoate (PHA): A Review. Polymers. 6, 706-754.
327. Tanahashi, M., Yao, T., Kokubo, T., Minoda, M., Miyamato, T., Nakamura, T., Yamamuro, T., 1994. "Apatite coating on organic polymers by a biomimetic process" J. Am. Ceram. Soc. 77, 2805-2808.
328. Tanaka, K., Miyawaki, K., Yamaguchi, A., Khosravi-Darani, K., Matsusaki, H., 2011. Cell growth and P(3HB) accumulation from CO2 of a carbon monoxide-tolerant hydrogenoxidizing bacterium, Ideonella sp. O-1. Appl. Microbiol. Biotechnol. 92, 1161–1169.
329. .
330. Tarley,C.R.T., Arruda, M.A.Z., 2004. Biosorption of heavy metals using rice milling byproducts: characterisation and application for removal of metals from aqueous effluents, Chemosphere. 54, 987–995.
331. Tavangarian, F., Emadi, R., 2011. Nanostructure effects on the bioactivity of forsterite bioceramicMater. Lett., 65, 740–743.
332. Temenoff, J.S., Mikos, A.G., 2000. Injectable biodegradable materials for orthopaedic tissue engineering. Biomaterials. 21, 2405–12.
333. Terazono, K., Hayashi, N.R., Igarashi, Y., 2001. CbbR, a LysR-type transcriptional regulator from *Hydrogenophilus thermoluteolus*, binds two *cbb* promoter regions. FEMS Microbiol Lett 198, 151–157.
334. Thauer, R.K., 2007. A fifth pathway of carbon fixation. Science 318, 1732–1734.

335. Tian, Y., 2008. Behaviour of bacterial extracellular polymeric substances from activated sludge: a review. Int. J. Environ. Pollut. 32, 78-89.
336. Toeda, K., Kurane, R., 1991. Microbial flocculant from *Alcaligenes cupidus* KT201(Microbiology & fermentation Industry). J. Agric. Biolog. Chem. 55, 2793-2799.
337. Tomita, K., T. Saito., T. Fukui., 1983. Bacterial metabolism of poly-p-hydroxybutyrate. Biochemistry of metabolic processes. Elsevier Science Publishing, Inc., New York. 353-366.
338. Toyoda, K., Yoshizawa, Y., Arai, H., Ishii, M., Igarashi, Y., 2005. The role of two CbbRs in the transcriptional regulation of three ribulose-1,5- bisphosphate carboxylase/oxygenase genes in *Hydrogenovibrio marinus* strain MH-110. Microbiology 151, 3615–3625.
339. Tracy, B.P., Jones, S.W., Fast, A.G., Indurthi, D.C., Papoutsakis, E.T., 2012. Clostridia: the importance of their exceptional substrate and metabolite diversity for biofuel and biorefinery applications. Curr. Opin. Biotechnol. 23, 364–381.
340. Trichet, J., Défarge, C., 1995. Non-biologically supported organomineralization. Inst. Oceanogr. Bull, 14, 203–236.
341. Tripathi, R., Singh, J., Thakur, I.S., 2015. Characterization of microalga Scenedesmus sp. ISTGA1 for potential CO2 sequestration and biodiesel production. Renewable Energy 74, 774–781.
342. Trusler, J.P.M., 2017. Thermophysical properties and phase behavior of fluids for application in carbon capture and storage processes. Annu. Rev. Chem. Biomol. Eng. 8, 381–402.
343. Tsai, Y., Sawaya, M.R., Cannon, G.C., Cai, F., Williams, E.B., Heinhorst, S., Kerfeld, C.A., Yeates, T.O., 2007. Structural analysis of CsoS1A and the protein shell of the Halothiobacillus neapolitanus carboxysome. PLoS Biol. 5, 1345–1354.
344. Van den Bergh, E.R.E., Baker, S.C., Raggers, R.J., Terpstra, P., Woudstra EC, Dijkhuizen, L., Meijer, W.G., 1996. Primary structure and phylogeny of the Calvin cycle enzymes transketolase and fructosebisphosphate aldolase of *Xanthobacter flavu*s. J. Bacteriol. 178, 888–93.

345. Van den Bergh, E.R.E., van der Kooij, T.A.W., Dijkhuizen, L., Meijer, W.G., 1995. Fructosebisphosphatase isoenzymes of the chemoautotroph *Xanthobacter flavu*s. J. Bacteriol. 177, 5860–64

346. Vaneechoutte, M., Tjernberg, I., Baldi, F., Pepi, M., Fani, R., Sullivan, E.R., van der Toorn, J., Dijkshoorn, L., 1999. Oil-degrading Acinetobacter strain RAG-1 and strains described as 'Acinetobacter venetianus sp. nov.' belong to the same genomic species. Res. Microbiol. 150, 69-73.

347. Venkata Mohan, S., Nikhil, G.N., Chiranjeevi, P. Chiranjeevi, Reddy, C.N., Rohit, M.V., Kumar, A.N., Sarkar, O., 2016. Waste biorefinery models towards sustainable circular bioeconomy: critical review and future perspectives. Bioresour. Technol. 215, 2–12.

348. Venkata Mohan, S., Velvizhi, G., Krishna, K.V., Babu, M.L., 2014. Microbial catalyzed electrochemical systems: a bio-factory with multi-facet applications. Bioresour. Technol. 165, 355–364.

349. Videmšek, U., Hagn, A., Suhadolc, M., Radl, V., Knicker, H., Schloter, M., Vodnik, D., 2009. Abundance and diversity of CO2-fixing bacteria in grassland soils close to natural carbon dioxide springs. Microb. Ecol. 58, 1–9.

350. Vijayabaskar, P., Babinastarlin, S., Shankar, T., Sivakumar, T., Anandapandian, K.T.K., 2011. Quantification and Characterization of exopolysaccharides from Bacillus subtilis (MTCC 121). Adv. Biol. Res. 5, 71–76.

351. Vijayendra, S.V.N., Palanivel, G., Mahadevamma, S., Tharanathan, R.N., 2008. Physico-chemical characterization of an exopolysaccharide produced by a non-ropy strain of Leuconostoc sp. CFR 2181 isolated from dahi, an Indian traditional lactic fermented milk product. Carbohydr. Polym. 72, 300–307.

352. Volesky, B., Schiewer, S., 1999. Biosorption of metals. Encyclopedia of Bioprocess Technology,Wiley, New York. 433–453.

353. Vuyisich, M., Arefin, A., Davenport, K., Feng, S., Gleasner, C., McMurry, K., Parson-Quintana, B., Price, J., Scholz, M., Chain, P., 2014. Facile, High Quality Sequencing of Bacterial Genomes from Small Amounts of DNA. Int J Genomics. 434575, 8.

354. Wang, D., Zhang, Y., Pohlmann, E.L., Li, J., Roberts, G.P., 2011. The poor growth of *Rhodospirillum rubrum* mutants lacking RubisCO is due to the accumulation of ribulose-1,5-bisphophate. J Bacteriol 193, 3293–3303.
355. Wang, S.G., Gong, W.X., Liu, X.W., Tian, L., Yue, Q.Y., Gao, B.Y., 2007. Production of a novel bioflocculant by culture of *Klebsiellamobilis* using dairy wastewater. Biochem. Eng. J. 36, 81e86
356. Wang, W., Lu, X., 2013. Microbial synthesis of alka(e)nes. Front. Bioeng. Biotechnol. 1, 10.
357. Wang, X., Falcone, D. L., Tabita, F.R., 1993. Reductive pentose phosphate-independent CO, fixation in *Rhodobacter sphaeroides* and evidence that ribulose bisphosphate carboxylase/ oxygenase activity serves to maintain the redox balance of the cell. J. Bacterial., 175, 3372-3379.
358. Wassinger, A., Zhang, L., Tracy, E., Munson Jr, R.S., Kathariou, S., Wang, H.H., 2013.
359. Wei, X., Sayavedra-Soto, L.A., Arp, D.J., 2004. The transcription of the *cbb* operon in *Nitrosomonas europaea*. Microbiology 150, 1869–1879.
360. Whitfield, C., 2006. Biosynthesis and assembly of capsular polysaccharides in Escherichia coli. Annu. Rev. Biochem. 75:39-68.
361. Whitfield, C., and I. S. Roberts**.** 1999. Structure, assembly and regulation of expression of capsules in Escherichia coli. Molecular microbiology 31, 1307-1319.
362. Wingender, J., Neu, T.R., Flemming, H.C., 1999. Microbial Extracellular Polymeric Substances: Characterization, Structure and Function. Springer-Verlag, Berlin Heidelberg, New York.
363. Wood, A.P., Kelly, D.P., Thurston, C.F., 1977. Simultaneous operation of three catabolic pathways in the metabolism of glucose by *Thiobacillus* A2. Arch. Microbiol. 113, 265–74.
364. Wood, H.G., 1991. Life with CO or CO2 and H2 as a source of carbon and energy. FASEB J. 5, 156–163.
365. Xia, S., Zhang, Z., Wang, X., Yang, A., Chen, L., Zhao, J., Leonard, D., Jaffrezic-Renault, N., 2008. Production and characterization of a bioflocculant by *Proteus mirabilis* TJ-1. Bioresour. Technol. 99, 6520-6527.

366. Xie, Y., Wu, G., Tang, J., Luo, R., Patterson, J., Liu, S., Huang, W., He, G., Gu, S., Li, S., Zhou, X., Lam, T-W., Li, Y., Xu, X., Wong, G.K., Wang, J., 2014. SOAPdenovo-Trans: de novo transcriptome assembly with short RNASeq reads. Bioinformatics 30, 1660 –1666.

367. Xiong, Y., Wang, Y., Yu, Y., Li, Q., Wang, H., Chen, R., He, N., 2010. Production and characterization of a novel bioflocculant from Bacillus licheniformis. Appl. Environ. Microbiol. 76, 2778-2782.

368. Yan, S., Tyagi, R.D., Surampalli, R.Y., 2006. Polyhydroxyalkanoates (PHA) production using wastewater as carbon source and activated sludge as microorganisms. Water Sci. Technol. 53, 6, 175–180.

369. Yan, S., Tyagi, R.D., Surampalli, R.Y., 2006. Polyhydroxyalkanoates (PHA) production using wastewater as carbon source and activated sludge as microorganisms. Water. Sci. Technol. 53, 175–180.

370. Yang, B.Y., Gray, J.S., and Montgomery, R., 1996. The structure of stewartan, a capsular polysaccharide produced by *Erwinia stewartii* strain DC283. Carbohydr Res 296, 183– 201.

371. Ye, F., Ye, Y., Li, Y., 2011. Effect of C/N ratio on extracellular polymeric substances (EPS) and physicochemical properties of activated sludge flocs. J. Hazard. Mater. 188, 37-43.

372. Ye, Z., Li, X., Cheng, Y., Liu, Z., Tan, G., Zhu, F., Fu, S., Deng, Z., Liu, T., 2016. Evaluation of 3-hydroxypropionate biosynthesis in vitro by partial introduction of the 3-hydroxypropionate/ 4-hydroxybutyrate cycle from Metallosphaera sedula. J. Ind. Microbiol. Biotechnol. 43, 1313–1321.

373. Yeates, T.O., Kerfeld, C.A., Heinhorst, S., Cannon, G.C., Shively, J.M., 2008. Protein-based organelles in bacteria: carboxysomes and related microcompartments. Nat. Rev. Microbiol. 6, 681–691.

374. Yoshiba, K., Sato, T., Osumi, T., Ulset, A.S.T., Christensen, B.E., 2015. Conformation of carboxylated schizophyllan in aqueous solution. Carbohydr. Polym. 134, 1–5.

375. Yu, J., 2014. Bio-based products from solar energy and carbon dioxide. Trends Biotechnol. 32, 5–10.

376. Yu, M., Du, Y., Jiang, W., Chang, W.L., Yang, S.T., Tang, I.C., 2012. Effects of different replicons in conjugative plasmids on transformation efficiency, plasmid stability, gene expression and n-butanol biosynthesis in Clostridium tyrobutyricum. Appl. Microbiol. Biotechnol. 93, 881–889.
377. Zamarreno, D.V., Inkpen, R., May, E., 2009. Influence of temperature on biocalcification by non-sporing freshwater bacteria. Geomicrobiol J. 26, 1–12.
378. Zerbino, D.R., Birney, E., 2008. Velvet: algorithms for de novo short read assembly using de Bruijn graphs. Genome Res 18, 821– 829.
379. Zevenhoven, R., Eloneva, S., Sebastian, T., 2006. Chemical fixation of CO2 in carbonates: routes to valuable products and long-term storage. Catal Today. 115, 73–79.
380. Zhang, X., Yan, S., Tyagi, R.D., Surampalli, R.Y., Valero, J.R., 2014. Wastewater sludge as raw material for microbial oils production. Appl Energy 135, 192–201.
381. Zhang, X.S., García-Contreras, R., Wood, T.K., 2008. Escherichia coli transcription factor YncC (McbR) regulates colonic acid and biofilm formation by repressing expression of periplasmic protein YbiM (McbA). ISME J. 2, 615−631.
382. Zhang, Z., Lian, B., Hou, W., Chen, M., Li, X., Li, Y., 2011. Bacillus mucilaginosus can capture atmospheric CO2 by carbonic anhydrase. Afr. J. Microbiol. Res. 5, 106–112.
383. Zhang, Z., Xia, S., Wang, X., Yang, A., Xu, B., Chen, L., Zhu, Z., Zhao, J., Jaffrezic-Renault, N., Leonard, D., 2009. A novel biosorbent for dye removal: Extracellular polymeric substance(EPS) of *Proteus mirabilis* TJ-1. Journal of Hazardous Materials. 163, 279–284.
384. Zheng, Y., Ye, Z.-L., Fang, X.-L., Li, Y.-H., Cai, W.-M., 2008. Production and characteristics of a bioflocculant produced by Bacillus sp. F19. Bioresour. Technol. 99, 7686-7691.
385. Zhu, C., Nomura, C.T., Perrotta, J.A., Stipanovic, A.J., Nakas, J.P., 2010. Production and characterization of poly-3-hydroxybutyrate from biodiesel-glycerol by *Burkholderia cepacia* ATCC 17759. Biotechnol. Progr. 26, 424-430.
386. Zuriani, R., Vigneswari, S., Azizan, M. N. M., Majid, M. I. A., Amirul, A. A., 2013. A high throughput nile red fluorescence method for rapid quantification of intracellular bacterial polyhydroxyalkanoates. Biotechnol. and Bioprocess Eng. 18, 472-478.

Manish kumar

LOHIT HOSTEL, ROOM NO-123 JAWAHARLAL NEHRU UNIVERSITY, NEW DELHI-110067, INDIA, +91-9818122475

Email id **manishkumar.bt@gmail.com**
manish73_ses@jnu.ac.in

OBJECTIVES

Bioprocess and Biorefinery
Approach for production of Biofuel and Biomaterials

EDUCATIONAL QUALIFICATION

CLASS	YEAR	SCHOOL \ COLLEGE	BOARD \ UNIVERSITY	PERCENTAGE \ CGPA
Ph.D	2014-present	Jawaharlal Nehru University	Jawaharlal Nehru University	-
M.Sc. Environmental Sciences	2012-2014	Jawaharlal Nehru University	Jawaharlal Nehru University	88.60%
B.Tech in Biotechnology	2012	ICFAI University	ICFAI University	8.34
Intermediate (12^{th})	2002	Gaya College Gaya	Bihar intermediate education council	69%
High School (10^{th})	2000	Agrawal High School	Bihar Board	69%

Publications

1. **Manish Kumar**, Pooja Ghosh, Khushboo Khosla, Indu Shekhar Thakur. Biodiesel production from municipal secondary sludge. Bioresource Technology 216 (2016) 165–171.

2. **Manish Kumar**, Asmita Gupta, Indu Shekhar Thakur. Carbon dioxide sequestration by chemolithotrophic oleaginous bacteria for production and optimization of polyhydroxyalkanoate. Bioresource Technology 213 (2016) 249–256.

3.**Manish Kumar**, Rajesh Kumar Gazara , Sandhya Verma , Madan Kumar, Praveen Kumar Verma, Indu Shekhar Thakur. Genome sequence of carbon dioxide sequestering Serratia sp. ISTD04 isolated from marble mining rocks. Genome announcements 2016. Genome Announc 4(5):e01141-16. doi:10.1128/genomeA.01141-16.

4. **Manish Kumar**, Juhi Gupta, Indu Shekhar Thakur. Production and optimization of polyhydroxyalkanoate from oleaginous bacteria Bacillus sp. ISTC1. RR: Journal of Microbiology and Biotechnology 2016, 5: 3.

5. Madan Kumar, Rajesh Kumar Gazara, Sandhya Verma, **Manish Kumar**, Praveen Kumar Verma and Indu Shekhar Thakur. Genome Sequence of Pandoraea sp. ISTKB, a lignin degrading β-proteobacterium, isolated from the rhizospheric soil. Genome announcement 2016. Genome Announc 4(6):e01240-16. doi:10.1128/genomeA.01240-16.

6. **Manish Kumar**, Khushboo Khosla and Indu Shekhar Thakur. Optimization of Process Parameters for the Production of Biodiesel from Carbon dioxide Sequestering Bacterium. Journal of Energy and Environmental Sustainability, 3 (2017) 43-50.

7. **Manish Kumar**, Raj Morya, Edgard Gnansounou, Christian Larroche and Indu Shekhar Thakur. Characterization of carbon dioxide concentrating chemolithotrophic bacterium *Serratia* sp. ISTD04 for production of biodiesel. Bioresource Technology 243 (2017) 893–897.

8. **Manish Kumar**, Smita Sundaram, Edgard Gnansounou ,Christian Larroche and Indu Shekhar Thakura. Carbon dioxide capture, storage and production of biofuel and biomaterials by bacteria: A Review. Bioresource Technology 247 (2018) 1059–1068.

9. **Manish Kumar**, Pooja Ghosh, Khushboo Khosla, Indu Shekhar Thakur. Recovery of polyhydroxyalkanoates from municipal secondary wastewater sludge. Bioresource Technology 255 (2018) 111–115.

10. Indu Shekhar Thakur, **Manish Kumar**, Sunita J. Varjani, Yonghong Wu, Edgard Gnansounou, Sindhu Ravindran. Sequestration and utilization of carbon dioxide by chemical and biological methods for biofuels and biomaterials by chemoautotrophs: Opportunities and challenges. Bioresource Technology. 256 (2018) 478–490.

11. Raj Morya[1], **Manish Kumar[1]**, Indu Shekhar Thakur. Utilization of glycerol by *Bacillus* sp. ISTVK1 for production and characterization of Polyhydroxyvalerate. Bioresource Technology Reports 2 (2018) 1-6. doi.org/10.1016/j.biteb.2018.03.002.
1. Raj Morya and Manish Kumar have equal contribution in this work.

12. Madan Kumar, Sandhya Verma, Rajesh Kumar Gazara, **Manish Kumar**, Ashok Pandey, Praveen Kumar Verma, Indu Shekhar Thakur. Genomic and proteomic analysis of lignin degrading and Polyhydroxyalkanoate accumulating β-proteobacterium Pandoraea sp. ISTKB. Biotechnology for Biofuels. *(2018) 11:154*
https://doi.org/10.1186/s13068-018-1148-2.

TRAINING/ SEMINAR/ TRIPS ATTENDED

- Oral presentation on Carbon dioxide sequestration and production of Biomaterials by *bacillus* sp. ISTC1 in Bacillus ACT 2015 organized by Jawaharlal Nehru University New Delhi, India from October 27-31, 2015.
- Poster presentation in UGC-SAP-DSA-2 AND MoEFCC sponsored National Conference on Environmental Pollutants: Impact Assessment and Remediation (NCEPIAR-2016) organized by School of Environmental Sciences, Jawaharlal Nehru University, New Delhi from 18-19 march 2016.
- Poster presentation on Carbon dioxide sequestration and production of Biomaterials in National Science Day sponsored by Department of Science and Technology, Government of India organized by Jawaharlal Nehru University, New Delhi India, held on 28th February, 2015 and 28th February 2016.
- Oral presentation on Carbon dioxide sequestration and production of biomaterial by chemolithotrophic bacteria.International conference on strategies for Environmental Protection and Management (ICSEPM-2016), held during December 11-13, 2016 at Jawaharlal Nehru University, New Delhi.
- Oral presentation on Optimization of process parameters:Biodiesel production from carbon dioxide sequestering bacterium.ISEES International conference on Sustainable Energy aand Environment Challenges (SEEC-2017), held during 26-28 february 2017, Centre of Innovative and Applied Bioprocessing, Mohali, India.

AREAS OF INTEREST

- Bio-energy , Bio-fuel
- Biomaterials
- Biovalorization
- Clean energy technology
- Spreading Environmental awareness

PERSONAL DETAILS

1. Father's Name: Ramashish Sharma
2. Mother's Name: Indramani Devi
3. Date of Birth: 10/12/1984
4. Sex: Male
5. Marital Status: Unmarried

DECLARATIONS

I hereby declare that all the information given above is true.

Bioresource Technology 213 (2016) 249–256

Contents lists available at ScienceDirect

Bioresource Technology

journal homepage: www.elsevier.com/locate/biortech

Carbon dioxide sequestration by chemolithotrophic oleaginous bacteria for production and optimization of polyhydroxyalkanoate

Manish Kumar, Asmita Gupta, Indu Shekhar Thakur *

School of Environmental Sciences, Jawaharlal Nehru University, New Delhi 110067, India

HIGHLIGHTS

- Carbon concentrating *Serratia* sp. ISTD04 was screened for PHA production.
- Screening for PHA production was done on the basis of Nile red fluorescence.
- GC–MS analysis revealed the presence of 3-hydroxyvalerate, monomer of PHV.
- There was a 2 fold increase in PHA production following optimization by RSM.

ARTICLE INFO

Article history:
Received 30 December 2015
Received in revised form 6 February 2016
Accepted 9 February 2016
Available online 18 February 2016

Keywords:
CO_2 sequestration
Polyhydroxyalkanoate
3-Hydroxyvalerate
Serratia sp.
Response Surface Methodology

ABSTRACT

The present work involved screening of a previously reported carbon concentrating oleaginous bacterial strain *Serratia* sp. ISTD04 for production of PHA and optimization of process parameters for enhanced PHA and biomass generation. The selected bacterial strain was screened for PHA production based on Nile red staining followed by visualization under fluorescence microscope. Spectrofluorometric measurement of Nile red fluorescence of the bacterial culture was also done. Confirmatory analysis of PHA accumulation by GC–MS revealed the presence of 3-hydroxyvalerate. Detection of characteristic peaks in the FT-IR spectrum further confirmed the production of PHA by the bacterium. Response Surface Methodology was used for optimization of pH and carbon sources' concentrations for higher PHA production. There was almost a 2 fold increase in the production of PHA following optimization as compared to un-optimized condition. The study thus establishes the production of PHA by *Serratia* sp. ISTD04.

1. Introduction

The world today is facing twin crises of rising carbon dioxide (CO_2) emission leading to climate change as well as environmental deterioration by accumulation of non-biodegradable compounds such as plastics. On one hand, the concentration of CO_2, the primary green house gas, has increased approximately 43% since industrial revolution and is projected to further increase by 60% in 2100 if the current trend continues. CO_2 capture and storage by autotrophic biota and some chemoautotrophic and chemolithoautotrophic bacteria possessing CO_2 fixing enzymes like Ribulose-1,5-bisphosphate carboxyl-ase/oxygenase (Rubisco), is one of the mitigation options (Bharti et al., 2014a).

On the other hand, global plastic production, mostly derived from fossil fuels, has been continuously rising with almost 299 million tons of plastics produced in 2013 which was 3.9% higher than 2012's output and is projected to further increase at a moderate rate in the coming years. Some bacteria have the capability to naturally accumulate, within their cells, such biopolymers that exhibit similar physical and mechanical properties to oil-based plastics. Therefore, one of the most cost effective and sustainable methods to alleviate this dual challenge of high CO_2 and plastic accumulation is through culturing of such microorganism that are capable of fixing atmospheric CO_2 along with production of easily degradable biopolymers.

Poly (hydroxyalkanoate)s (PHAs) are biodegradable, biocompatible and thermostable biopolymers that are synthesized by several bacteria as intracellular materials for the storage of carbon/energy usually in the presence of high carbon concentration and growth limiting nutrient environments. Structurally, PHAs are polyesters, which contain (*R*)-hydroxyacyl monomeric units. Depending on the bacterial strain employed and the growth substrates supplied, PHA can be synthesized as homopolymers or copolymers or even their mixture. Among the nearly 150 different PHA monomers

* Corresponding author. Tel.: +91 011 26704321 (O); fax: +91 011 26717586.
E-mail addresses: asmitagupta5@gmail.com (A. Gupta), isthakur@hotmail.com (I.S. Thakur).

http://dx.doi.org/10.1016/j.biortech.2016.02.038
0960-8524/

AMERICAN SOCIETY FOR MICROBIOLOGY | genomeAnnouncements

Genome Sequence of Carbon Dioxide-Sequestering *Serratia* sp. Strain ISTD04 Isolated from Marble Mining Rocks

Manish Kumar,[a] Rajesh Kumar Gazara,[b] Sandhya Verma,[b] Madan Kumar,[a] Praveen Kumar Verma,[b] Indu Shekhar Thakur[a]

School of Environmental Sciences, Jawaharlal Nehru University, New Delhi, India[a]; National Institute of Plant Genome Research, New Delhi, India[b]

R.K.G. and S.V. contributed equally to this work.

The *Serratia* sp. strain ISTD04 has been identified as a carbon dioxide (CO_2)-sequestering bacterium isolated from marble mining rocks in the Umra area, Rajasthan, India. This strain grows chemolithotrophically on media that contain sodium bicarbonate ($NaHCO_3$) as the sole carbon source. Here, we report the genome sequence of 5.07 Mb *Serratia* sp. ISTD04.

Received 23 August 2016 **Accepted** 31 August 2016 **Published** 20 October 2016

Citation Kumar M, Gazara RK, Verma S, Kumar M, Verma PK, Thakur IS. 2016. Genome sequence of carbon dioxide-sequestering *Serratia* sp. strain ISTD04 isolated from marble mining rocks. Genome Announc 4(5):e01141-16. doi:10.1128/genomeA.01141-16.

Address correspondence to Indu Shekhar Thakur, isthakur@hotmail.com, or Praveen Kumar Verma, pkv@nipgr.ac.in.

Increase in CO_2 concentration can be mitigated by autotrophic and heterotrophic carbon fixation by plants and microorganisms (1). Some microorganisms, in addition to carbon dioxide fixation, also produce value-added products (2). *Serratia* sp. strain ISTD04 was isolated from marble mining rocks of the palaeoproterozoic metasediments of the Aravali Supergroup, Rajasthan, India, by enrichment in minimal salt media with increasing concentration of $NaHCO_3$ as the carbon source (3). The bacterium is characterized by chemolithotrophic fixation of carbon dioxide which is supported by the presence of ribulose-1,5-bisphosphate carboxylase/oxygenase (RuBisCo), carbonic anhydrase, and carboxylases (4). The strain was studied in detail for CO_2 sequestration along with biodiesel and polyhydroxyalkanoate (PHA) production (5, 6).

Whole-genome shotgun sequencing of *Serratia* sp. strain ISTD04 was performed on the Illumina Miseq platform and resulted in 2,073,386 paired-end reads of 151-bp length. After filtering the raw reads using NGS tool kit (v2.3.1), high-quality 1,485,793 paired-end reads were obtained. The genome assembly was performed using Velvet (v1.2.10) (7), SOAPdenovo (8), and gsassembler using a k-mer value of 79 for primary assembly. SSPACE (9) was used to perform scaffolding of the primary assembled contigs that generated 120 scaffolds, with an N_{50} scaffold size of 1,03,262 bp. The maximum scaffold length was 3,28,633 bp and minimum scaffold length was 210 bp. The NCBI prokaryotic genome annotation pipeline (PGAP) was used for the identification of candidate gene models. Furthermore, Pfam (10) annotation was carried out to assign functional domains to the predicted gene models. The pathways and the genes involved were predicted with the help of the KEGG Automatic Annotation Server (KAAS) (11).

The total genome size of *Serratia* sp. strain ISTD04 is 5.07 Mb with a G+C content of 59.98%. The assembly resulted in a coverage of 81×. A total of 4,563 protein coding gene models were predicted by PGAP. Moreover, 75 tRNAs, 8 rRNAS (2 5S rRNAs, 4 16S rRNAs, and 2 of 23S rRNAs), and 12 noncoding RNAs (ncRNAs) were also identified. In addition, 88 pseudo genes were predicted, among which were 6 frame-shifted pseudogenes. PGAP annotated 3,765 (82.51%) of the total predicted genes. In addition, Pfam annotation was assigned to 4,234 genes (92.78%) and 1,498 genes (32.82%) were predicted by the KAAS tool to be involved in various pathways.

Serratia sp. ISTD04 is a novel organism which performs chemolithoautotrophic carbon dioxide assimilation. Genome analysis of *Serratia* sp. ISTD04 revealed the presence of phosphoribulokinase (PRK) and other CBB pathway genes. However, the RuBisCo gene could not be identified in the genome assembly (12). The carbonic anhydrase, an important facilitator enzyme, is also present in the genome (13). Anaplerotic CO_2 assimilating enzymes *viz.* phosphoenolpyruvate (PEP) carboxylase, malic enzymes, and PEP carboxykinase, are present in the genomic analysis (14). Enzymes for fatty acid metabolism such as acetyl-CoA carboxlases, malonyl Co-ACP transacylase, 3-ketoacyl ACP-synthase, and 3-ketoacyl ACP-reductase are present (4). Enzymes involved in PHA synthesis like β-ketoacyl-CoA thiolase and acetoacetyl-CoA dehydrogenase were also identified in the genome sequence (6). Therefore, this strain can be applied to sequester CO_2 and value-added products.

Accession number(s). This whole-genome shotgun project has been deposited at DDBJ/ENA/GenBank under the accession no. MBDW00000000. The version described in this paper is version MBDW01000000.

ACKNOWLEDGMENTS

We thank the University with Potential for Excellence-UGC (UPOE), JNU, New Delhi, India, for providing funds for publication charges.

FUNDING INFORMATION

The funders had no role in study design, result interpretation, data collection, or the decision to submit the research work.

REFERENCES

1. **Saini R, Kapoor R, Kumar R, Siddiqi TO, Kumar A.** 2011. CO_2 utilizing microbes—A comprehensive review. Biotechnol Adv **29**:949–960. http://dx.doi.org/10.1016/j.biotechadv.2011.08.009.

Bioresource Technology 216 (2016) 165–171

Contents lists available at ScienceDirect

Bioresource Technology

journal homepage: www.elsevier.com/locate/biortech

Biodiesel production from municipal secondary sludge

Manish Kumar, Pooja Ghosh, Khushboo Khosla, Indu Shekhar Thakur *

School of Environmental Sciences, Jawaharlal Nehru University, New Delhi 110067, India

HIGHLIGHTS

- Municipal secondary sludge was found to be an ideal feedstock for biodiesel.
- Optimization by Response surface methodology enhanced the biodiesel yield.
- Biodiesel yield under optimum conditions was 20.76 ± 0.04% of sludge solids.
- Analysis of FAME profile revealed a good quality biodiesel.

ARTICLE INFO

Article history:
Received 29 March 2016
Received in revised form 18 May 2016
Accepted 19 May 2016
Available online 21 May 2016

Keywords:
Secondary sludge
Fatty acid methyl esters (FAMEs)
In situ transesterification
Biodiesel
Response surface methodology

ABSTRACT

In the present study, feasibility of biodiesel production from freeze dried sewage sludge was studied and its yield was enhanced by optimization of the *in situ* transesterification conditions (temperature, catalyst and concentration of sludge solids). Optimized conditions (45 °C, 5% catalyst and 0.16 g/mL sludge solids) resulted in a 20.76 ± 0.04% biodiesel yield. The purity of biodiesel was ascertained by GC–MS, FT-IR and NMR (^{1}H and ^{13}C) spectroscopy. The biodiesel profile obtained revealed the predominance of methyl esters of fatty acids such as oleic, palmitic, myristic, stearic, lauric, palmitoleic and linoleic acids indicating potential use of sludge as a biodiesel feedstock.

1. Introduction

High energy prices, coupled with uncertainties about future petroleum supplies and an increasing recognition of the environmental impacts of fossil fuels, have led to global interests in developing biodiesel. However, at present, biodiesels cannot compete economically in the market. Considering the fact that up to 85% of the overall biodiesel production cost is associated with the feedstock or raw material (Sheik et al., 2014), wastewater sludge rich in lipids is a cost-effective alternative of biodiesel production (Chisti, 2007; Mondala et al., 2009). With increasing urbanization and industrialization, wastewater treatment plants will be producing higher quantities of sludge each year making it a readily available feedstock for biodiesel production (Olkiewicz et al., 2012). Also, it has been demonstrated that dry sludge is largely comprised of fatty acids and steroids. With the fatty acids from sludge predominantly in the range of C10 to C18, these are excellent for the production of biodiesel (Kargbo, 2010).

Bacterial species present in sludge either assimilate lipids from the wastewater or synthesize them de novo from other carbon sources, and store them intracellularly as neutral lipids, for example, triacylglycerides (TAGs), wax esters (WEs) or polyhydroxyalkanoates (PHAs). Availability of municipal sludge at minimal cost makes them a cost-effective feedstock for biodiesel production. Additionally, it solves the environmental issues associated with sludge treatment and disposal. (Mondala et al., 2009). Further, *in situ* transesterification eliminates some conventional processing steps by combining the lipid extraction and fuel conversion steps into a single step which can greatly reduce the cost of biodiesel production.

Determining the optimum conditions is important for improving the performance of a system, a process, or a product in order to obtain the maximum benefit from it. Traditional approach of optimizing one-variable-at-a-time (OVAT) for a multivariable system is not only time and labor intensive but often results in missing out the interactive effects between the components (Bandaru et al., 2006). Response surface methodology (RSM) is a suitable multivariate statistical technique which not only assists in understanding the interactions of different variables and predicts maximized response, but also is rapid and economical with fewer experiments and minimal resource utilization. Amongst

* Corresponding author.
E-mail addresses: manishkumar.bt@gmail.com (M. Kumar), pooja.ghosh9@gmail.com (P. Ghosh), khushboo912@gmail.com (K. Khosla), isthakur@hotmail.com (I.S. Thakur).

http://dx.doi.org/10.1016/j.biortech.2016.05.078
0960-8524/

Research & Reviews: Journal of Microbiology and Biotechnology

e-ISSN:2320-3528
p-ISSN:2347-2286

Production and Optimization of Polyhydroxyalkanoate from Oleaginous Bacteria *Bacillus Sp.* ISTC1

Manish Kumara, Juhi Guptaa, and Indu Shekhar Thakura*

School of Environmental Sciences, Jawaharlal Nehru University, New Delhi-110067, India

Research Article

Received date: 26/07/2016
Accepted date: 23/09/2016
Published date: 26/09/2016

***For Correspondence**

Indu Shekhar Thakur, School of Environmental Sciences, Jawaharlal Nehru University, New Delhi-110067, India, Tel: +0091-011-26704321.

E-mail: isthakur@hotmail.com

Keywords: Optimization; Polyhydroxyalkanoate; 3-hydroxyvalerate; *Bacillus sp*; Response surface methodology

ABSTRACT

The present effort involved isolation and screening of bacterial strain *Bacillus* sp. ISTC1 for production of PHA and optimization of selected process parameters for enhanced production of PHA and biomass. Screening of selected bacterial strain for PHA production was based on Nile red staining, fluorescence microscopic visualization, spectrofluorometric measurement of Nile red fluorescence of the bacterial culture having 0.5% (w/v) glucose as carbon source. The presence of 3-hydroxyvalerate revealed by GC–MS served as a confirmatory analysis of PHA accumulation. Detection of characteristic functional group by FT-IR further confirmed the production of PHA by the bacterium. Response Surface Methodology (RSM) was used for optimization of pH, time duration and carbon source concentrations for an increased PHA production. On equating the optimized condition with the pre-optimized one, there was almost a 60% increase in the production of PHA. Therefore the finding thus established the production of PHA by *Bacillus* sp. ISTC1.

INTRODUCTION

As we all know because of human intervention, world is welcoming us with so many bizarre complications but apart from these our human race is creating a bigger mess in terms of the plastic industry. With continuous growth for more than 50 years, global plastic production in 2012 rose to 288 million tonnes-a 2.8% increase compared to 2011 and situation wasn't better at all for the year 2013. It has been continuously rising with almost 299 million tons of plastics produced in 2013 which was 3.9% higher than 2012's output and is expected to further increase at an alarming rate in the near future. A fortunate advantage with, such biopolymers that exhibit alike physical and mechanical properties to oil-based plastics. There are certain bacterial species having natural accumulation capacity within their cells. Therefore, one of the long-term and cost effective strategy to culturing such type of microbes which can accumulate and produced easily degradable biopolymers which ultimately will help us in controlling this flooding situation of plastic industry. Polyhydroxyalkanoates (PHAs) are biodegradable, biocompatible and thermostable biopolymers that are synthesized by several bacteria as reserve food materials as source of energy [1] usually in the presence of growth limiting nutrient condition. Structurally, they are polyesters, which contain (R)-hydroxyacyl monomeric units. PHA can be synthesized as homopolymers or copolymers or even their mixture based on the selected bacterial strain and supply of growth substrates. Among the nearly 150 different PHA monomers identified till now, Poly (3-hydroxybutyrate) (PHB), a short chain length PHA (scl-PHA) having 3 to 5 carbon atom, is the first and perfectly-characterized form. Other forms, commonly synthesized by microbes are medium chain length PHAs (mcl-PHA) having 6 to 14 carbon atom like poly-b-hydroxyvalerate (PHV), poly (3-hydroxyhexanoate) (PHH), poly (3-hydro-xyoctanoate) (PHO) [2] and copolymers like Poly (3-hydroxybutyrate-co-3-hydroxyvalerate) (PHBV) and poly (β 3-hydroxybutyrate-co-3hydroxyhexanoate) (PHBHHx) [3], long-chain length PHA (lcl-PHA) containing 15 or more carbon atoms or copolymer of scl-mcl PHA copolymer consisting of monomeric subunits with 4 to12 carbons [4]. Both Gram positive and Gram negative bacteria have been known to produce PHA but the synthesis pathway may be different such as an enoyl-CoA hydratase, Methyl malonyl-CoA pathway for PHBV synthesis from sugars represented by *Ralstonia*

AMERICAN SOCIETY FOR MICROBIOLOGY | genomeAnnouncements

Genome Sequence of *Pandoraea* sp. ISTKB, a Lignin-Degrading Betaproteobacterium, Isolated from Rhizospheric Soil

Madan Kumar,[a] Rajesh Kumar Gazara,[b] Sandhya Verma,[b] Manish Kumar,[a] Praveen Kumar Verma,[b] Indu Shekhar Thakur[a]

School of Environmental Sciences, Jawaharlal Nehru University, New Delhi, India[a]; National Institute of Plant Genome Research, New Delhi, India[b]

R.K.G. and S.V. contributed equally to this article.

We report here the genome sequence of *Pandoraea* sp. ISTKB, a betaproteobacterium isolated from rhizospheric soil in the backwaters of Alappuzha, Kerala, India. The strain is alkalotolerant and grows on medium containing lignin as a sole carbon source. Genes and pathways related to lignin degradation were complemented by genomic analysis.

Received 9 September 2016 **Accepted** 12 September 2016 **Published** 3 November 2016

Citation Kumar M, Gazara RK, Verma S, Kumar M, Verma PK, Thakur IS. 2016. Genome sequence of *Pandoraea* sp. ISTKB, a lignin-degrading betaproteobacterium, isolated from rhizospheric soil. Genome Announc 4(6):e01240-16. doi:10.1128/genomeA.01240-16.

Address correspondence to Praveen Kumar Verma, pkv@nipgr.ac.in, or Indu Shekhar Thakur, isthakur@hotmail.com.

Lignin is recalcitrant to degradation due to its complex and heterogeneous structure (1). Although industry based on plant polysaccharides will add to the already large amount of lignin generation (2), sustainable biorefinery can be possible if polysaccharides and lignin are utilized in improved ways. Fungi are well-known lignin degraders, but in recent years the focus has been on bacterial degradation, since bacteria are more adapted to extreme environments and are easy to manipulate at the genetic level (3, 4). *Pandoraea* sp. ISTKB is an alkalotolerant strain, and the degradation and decolorization potential of kraft lignin and various dyes have been investigated with this strain (5). Pretreatment of sugarcane bagasse by *Pandoraea* sp. ISTKB under submerged and solid state conditions was also studied in detail (6). Insight into genomic analysis might help us to understand the novel enzymes and pathways responsible for lignin degradation and biovalorization.

The draft genome of *Pandoraea* sp. ISTKB was sequenced using the Illumina MiSeq platform, which generated 2,139,250 paired-end reads of 151-bp length. Raw reads were filtered using the NGS toolkit version 2.3.1 to obtain 1,597,718 high-quality paired-end reads. The genome assembly was performed using Velvet version 1/2/10 (7), SOAPdenovo (8), and gsAssembler using a *k*-mer value of 57 for primary assembly. Scaffolding for the primary assembled contigs was performed using SSPACE (9) to generate 115 scaffolds, with an N_{50} scaffold size of 132,761 bp (maximum scaffold length: 545,170 bp; minimum scaffold length: 258 bp). Genes were identified using the NCBI Prokaryotic Genome Annotation Pipeline (PGAP). The functional annotation of the genome sequence was also performed using Pfam (10). Pathway analysis was carried out using the KEGG Automatic Annotation Server (KAAS) (11).

The total genome size of *Pandoraea* sp. ISTKB is 6.37 Mb, and a coverage of 65× was achieved. The strain had a G+C content of 62.05% and a total of 5,356 protein-coding genes were predicted. The bacterium contained 54 tRNAs, six rRNAs (two copies each for 5S, 16S, and 23S), and four ncRNAs. Additionally, 154 pseudogenes were also identified, out of which 12 were frame-shifted pseudogenes. With PGAP, 68.59% of the predicted proteins were annotated. In addition, Pfam annotation was assigned to 4,603 genes (85.94%), and the KAAS tool predicted 1,351 genes (25.22%) to be involved in different pathways.

The draft genome revealed the presence of putative genes responsible for the degradation of lignin and lignin-derived aromatic compounds. The lignin-degrading enzymes identified were DyP-type peroxidases, peroxidases, multicopper oxidases, esterases, coniferyl-alcohol dehydrogenase, coniferyl-aldehyde dehydrogenase, etherases, methyltransferases, and vanillate O-demethylase oxidoreductase. Genes responsible for the catabolism of aromatic compounds identified in the genome assembly were 4-hydroxybenzoate 3-monooxygenase, vanillate monooxygenase ferredoxin subunit, salicylate hydroxylase, protocatechuate 3,4-dioxygenase, gentisate 1,2-dioxygenase, catechol 2,3-dioxygenase, extradiol ring-cleavage dioxygenase, catechol 1,2-dioxygenase, phthalate 4,5-dioxygenase, protocatechuate 4,5-dioxygenase, hydroxyquinol 1,2-dioxygenase, 3-phenylpropionate dioxygenase, and various other oxidoreductases. Additionally, genes for oxidative stress and redox signaling, such as glutathione peroxidase, glutathione synthase, glutathione reductase, thioredoxin, thioredoxin reductase, catalases, and superoxide dismutases, were also present. These findings indicate that *Pandoraea* sp. ISTKB could potentially have an application in lignocellulosic biomass valorization.

Accession number(s). This whole-genome shotgun project has been deposited at DDBJ/ENA/GenBank under the accession number MAOS00000000. The version described in this paper is the first version, MAOS01000000.

ACKNOWLEDGMENTS

Madan Kumar is grateful to the Council of Scientific and Industrial Research (CSIR), New Delhi, for Senior Research Fellowship. P.K.V. thanks the National Institute of Plant Genome Research, New Delhi, for financial support.

Bioresource Technology 243 (2017) 893–897

Contents lists available at ScienceDirect

Bioresource Technology

journal homepage: www.elsevier.com/locate/biortech

Characterization of carbon dioxide concentrating chemolithotrophic bacterium *Serratia* sp. ISTD04 for production of biodiesel

Manish Kumar [a], Raj Morya [a], Edgard Gnansounou [c], Christian Larroche [b], Indu Shekhar Thakur [a,*]

[a] School of Environmental Sciences, Jawaharlal Nehru University, New Delhi 110067, India
[b] Polytech Clermont-Ferrand, Université Blaise Pascal, Aubière, France
[c] Swiss Federal Institute of Technology Lausanne (EPFL), Lausanne, Switzerland

HIGHLIGHTS

- Characterization of Carbon dioxide concentrating *Serratia* sp. was performed by LC–MS/MS.
- Carboxylase and enzyme for fatty acid metabolism was confirmed by LC–MS/MS.
- Proteomic analysis revealed the carbon dioxide sequestration and production of Biofuel.
- Characterization of Bio-hydrocarbon and biofuel was performed by GC–MS.

ARTICLE INFO

Article history:
Received 12 June 2017
Received in revised form 11 July 2017
Accepted 12 July 2017
Available online 14 July 2017

Keywords:
Serratia sp. ISTD04
LC–MS/MS
Hydrocarbon
Biofuel
Carbon dioxide concentrating mechanism (CCM)

ABSTRACT

Proteomics and metabolomics analysis has become a powerful tool for characterization of microbial ability for fixation of Carbon dioxide. Bacterial community of palaeoproterozoic metasediments was enriched in the shake flask culture in the presence of $NaHCO_3$. One of the isolate showed resistance to $NaHCO_3$ (100 mM) and was identified as *Serratia* sp. ISTD04 by 16S rRNA sequence analysis. Carbon dioxide fixing ability of the bacterium was established by carbonic anhydrase enzyme assay along with proteomic analysis by LC–MS/MS. In proteomic analysis 96 proteins were identified out of these 6 protein involved in carbon dioxide fixation, 11 in fatty acid metabolism, indicating the carbon dioxide fixing potency of bacterium along with production of biofuel. GC–MS analysis revealed that hydrocarbons and FAMEs produced by bacteria within the range of C_{13}–C_{24} and C_{11}–C_{19} respectively. Presence of 59% saturated and 41% unsaturated organic compounds, make it a better fuel composition.

1. Introduction

Carbon dioxide (CO_2) is one of the major greenhouse gases (GHGs), whose concentration has increased from 270 ppm to approximately 380 ppm after industrial revolution (Shrestha and Lal, 2006). Increase in CO_2 concentration may be mitigated by autotrophic and heterotrophic carbon fixation by plants and microorganisms. Some microorganisms are able to grow in limiting CO_2 concentrations by employing a CO_2-concentrating mechanism (CCM) by enzymes mainly ribulose-1,5-bisphosphate carboxylase/oxygenase (RuBisCO) and carboxylating enzymes such as carbonic anhydrase which facilitate the CO_2 fixation (Badger et al., 2006). Proteomic and metabolomics analysis has become a powerful tool for investigating changes in prokaryotic protein expression for fixation of carbon dioxide and evaluation of enzymes and metabolites for production of biofuel and value added products (Bharti et al., 2014a). Some microbes can sequester CO_2 and synthesize valuable products such as different types of alkanes/alkenes, which can be further utilized for production of biofuel or biofuel additives. Alkanes/Alkenes are the metabolic product of some chemolithotrophic bacteria which are directly synthesized from fatty acid intermediates by decarbonylation of fatty acid precursor such as fatty aldehyde (Schirmer et al., 2010). The synthesis of hydrocarbons by microorganisms depends significantly on the culture conditions and its growth that present a way for its physiological directive. Intracellular as well as extracellular hydrocarbons (C_{15}–C_{24}) produced by *Vibrio furnissii* a halotolerant bacterium has been reported and range of hydrocarbons meeting to kerosene and light oil (Bharti et al., 2014a; Ladygina et al., 2006). Yeasts can produce a broad range of hydrocarbons from C_{10} to C_{34}, which include n-alkanes as well as some unsaturated and branched components (Ladygina et al., 2006). Bacteria are able to synthesize fatty acids inherently which act as precursor molecule for their cell wall/cell

* Corresponding author.
E-mail address: isthakur@hotmail.com (I.S. Thakur).

http://dx.doi.org/10.1016/j.biortech.2017.07.067
0960-8524/

Journal of Energy and Environmental Sustainability, 3 (2017) 43-50

An official publication of the International Society for Energy, Environment and Sustainability (ISEES)

Journal of Energy and Environmental Sustainability

Journal homepage : www.jees.in

Optimization of Process Parameters for the Production of Biodiesel from Carbon dioxide Sequestering Bacterium

Manish Kumar, Khushboo Khosla and Indu Shekhar Thakur*

School of Environmental Sciences, Jawaharlal Nehru University, New Delhi-110067, India

ARTICLE INFO

Received : 01 May 2017
Accepted : 17 May 2017

Keywords:
Serratia sp. ISTD 04; Fatty Acid Methyl Esters (FAMEs); *In situ* transesterification; Biodiesel; Response surface methodology

ABSTRACT

In the study, the process of *in-situ* transesterification for biodiesel production from a carbon dioxide sequestering chemolithotrophic bacterial strain *Serratia*sp. ISTD04 was optimized. The optimization of process parameters was carried out in order to enhance the yield and reduce the cost of biodiesel production. *Serratia*sp. ISTD04 was grown in MSM in the presence of sodium bicarbonate as the sole carbon source. The bacterial biomass harvested after 48 hours was utilized for biodiesel production. Box–Behnken design and Response surface methodology were used to optimize the *in-situ* transesterification, by carrying out the optimization study on three process parameters- Temperature, Duration and Catalyst concentration. Under optimized conditions of- 40.52°C, 22.93hrs and 2.04% v/v of methanol, a biodiesel yield of 41.47% was obtained. The characterization of biodiesel was further done by GC–MS, FT-IR and NMR (H^1 and C^{13}).

1. Introduction

Green-house gases (GHGs) are one of the most serious environmental issues which raise a question mark on existence of the earth. Carbon dioxide (CO_2), one of the major GHGs, concentration was stable at about 270 ppm which has increased approximately 38% which is 380 ppm after industrial revolution. It is predicted that by the middle of this century the concentration of CO_2 will be reached to 600 ppm and by the end of the century it is likely to reach 700 ppm [Shrestha and Lal, 2006]. Increase in CO_2 concentration may be mitigated by autotrophic and heterotrophic carbon fixationby plants and microorganisms. CO_2 mitigation strategy includes- improving energy efficiency, capturing and sequestering CO_2 and use of alternative fuels (biohydrocarbon, biodiesel, etc.) [Bharti et al., 2014a]. One of the most effective and alternative methods to check the increasing levels of CO_2 is by using microorganisms as some of them are capable of fixing atmospheric carbon dioxide in to valuable products with the help of their enzymatic machinery [Kumar et al., 2016a]. Some microbes synthesize valuable products such as biodiesel and polyhydroxyalaka notes along with sequestration of CO_2 [Kumar et al., 2016a].Hydrocarbons (Alkanes/alkenes) have been widely distributed among organisms, that are including bacteria, fungi, algae, higher plants, and animals [Han et al., 1969] and they are the metabolic product of some chemolithotrophic bacteria which are produced from fatty acidsand triacylglycerol (TAG). Triacylglycerols (TAG) are fatty acid trimesters of glyceroland its properties vary depending on their fatty acid composition. The occurrence of TAG as energystock is widespread among eukaryotic organisms such as yeast, fungi, plants and animals, whereas, occurrence of TAG in bacteria has only rarely been described [Alvarez et al., 2000]. Biosynthesisand accumulation of TAG has been reported in bacteria belonging to the actinomycetes group, such as Streptomyces, Nocardia, Rhodococcus, Mycobacterium, etc. [Alvarez et al., 2002].These microorganisms utilize diverse types of carbon sources such as sugars, organic acids, alcohols, n-alkanes, branched alkanes, phenylalkanes, oils and coal for biosynthesis of TAG[Alvarez et al., 2000]. The excess availability ofcarbon and limiting nitrogen in the growth medium enhances the synthesis of TAG inside bacterium, because in such a situation, cellular growth is impaired and the cells utilize the carbon sourcemainly for the biosynthesis of neutral lipids [Alvarez et al., 2002].The extraction of lipids from bacterial biomass and further its transesterification is one of the challenging and cost intensive process. Lipids extracted by Sonication [Belarbi et al., 2000] helps to disrupt the cells and encourage better lipid extraction, but this method also adds significant mechanical and chemical costs. Bligh and Dyer method of lipids extraction [Bligh and Dyer, 1959]

* Corresponding Author: *isthakur@hotmail.com*

Bioresource Technology 247 (2018) 1059–1068

Contents lists available at ScienceDirect

Bioresource Technology

journal homepage: www.elsevier.com/locate/biortech

Review

Carbon dioxide capture, storage and production of biofuel and biomaterials by bacteria: A review

Manish Kumar[a], Smita Sundaram[b], Edgard Gnansounou[c], Christian Larroche[d], Indu Shekhar Thakur[a,*]

[a] School of Environmental Sciences, Jawaharlal Nehru University, New Delhi 110 067, India
[b] Advanced Instrument Research Facility, Jawaharlal Nehru University, New Delhi 110 067, India
[c] Swiss Federal Institute of Technology Lausanne (EPFL), Lausanne, Switzerland
[d] Polytech Clermont-Ferrand, Université Blaise Pascal, Aubière, France

ARTICLE INFO

Keywords:
Bacteria
Biodiesel
Biomaterial
Carbon dioxide sequestration
Microorganisms

ABSTRACT

Due to industrialization and urbanization, as humans continue to rely on fossil fuels, carbon dioxide (CO_2) will inevitably be generated and result in an increase of Global Warming Gases (GWGs). However, their prospect is misted up because of the environmental and economic intimidation posed by probable climate shift, generally called it as the "green house effect". Among all GWGs, the major contributor in greenhouse effect is CO_2. Mitigation strategies that include capture and storage of CO_2 by biological means may reduce the impact of CO_2 emissions on environment. The biological CO_2 sequestration has significant advantage, since increasing atmospheric CO_2 level supports productivity and overall storage capacity of the natural system. This paper reviews CO_2 sequestration mechanism in bacteria and their pathways for production of value added products such as, biodiesel, bioplastics, extracellular polymeric substance (EPS), biosurfactants and other related biomaterials.

1. Introduction

The increase in concentration of carbon dioxide (CO_2) by anthropogenic activities such as change in land use pattern, deforestation, industrialization, transportation and modern life style leads to global climate shift, which is one of the critical environmental challenges that the world is facing today. The atmospheric concentration of CO_2 is presently 408 ppm (CO2 earth, 2017). As one of the potent Global Warming Gas (GWG), CO_2 has increased by approximately 43% since industrial revolution and is expected to further increase to 60% in 2100 if the current trend continues (Kumar et al., 2016c). Mitigation strategy of CO_2 can be attained mainly by three possible ways: primarily by improving energy efficiency of existing engine technology and proper fossil fuel utilization, secondly by CO_2 sequestration and the lastly by facilitating the uses of unconventional fuels such as biohydrocarbon, biodiesel, etc. (Bharti et al., 2014a). Storage and utilization of captured CO_2 by autotrophic biota and some microorganism such as algae, cyanobacteria, chemoautotrophic and chemolithoautotrophic bacteria having CO_2 fixing mechanism supported by key enzyme like Ribulose-1,5-bisphosphate carboxylase/oxygenase (RuBisCO) and facilitated by enzyme like carbonic anhydrase (CA) is one of the mitigation options (Bharti et al., 2014b; Kumar et al., 2016a). Increasing demand of petroleum oil and its derivatives as well as rising retail prices necessitate the search for alternative biomaterials. Biodiesel is mono-alkyl esters of long-chain fatty acids derived from fats, oils or lipids. Lipids feed stokes such as bacteria, cyanobacteria, algae, jatropha, palm trees and soybeans have been used as source of lipids for production of biodiesel. Bacteria possess significant advantages over photosynthetic organism e.g. higher plants and microalgae, which have been the main focus of attention, for production of environmental friendly fuel oil. Fatty acids, alcohols and alkanes are fundamental organic components for production of biofuel. Bacteria are capable of synthesizing intracellular as well as extracellular fatty acid (Bharti et al., 2014a). Intracellular fatty acid is used by bacteria as precursor molecules for biosynthesis of their own cell envelopes (Moazami et al., 2011). Bacteria synthesize fatty acids similar to plants, using acetyl-CoA with ATP as the source of energy and NADPH as the source of reducing equivalents (Bharti et al., 2014b). Hydrocarbons such as alkanes and alkenes are produced directly from fatty acid metabolites by decarboxylation of fatty aldehydes (Schirmer et al., 2010).

Microorganisms obtain their food and energy via assorted adaptation in environment for survival. Accumulation of polyhydoxyalkanoate (PHA) is survival strategy adopted by microorganisms against the stress responses exerted by environment (Kumar et al., 2016c). Among

* Corresponding author.
E-mail address: isthakur@hotmail.com (I.S. Thakur).

http://dx.doi.org/10.1016/j.biortech.2017.09.050
Received 30 July 2017; Received in revised form 5 September 2017; Accepted 6 September 2017
Available online 08 September 2017

Bioresource Technology 255 (2018) 111–115

Contents lists available at ScienceDirect

Bioresource Technology

journal homepage: www.elsevier.com/locate/biortech

Recovery of polyhydroxyalkanoates from municipal secondary wastewater sludge

Manish Kumar[a], Pooja Ghosh[b,1], Khushboo Khosla[a,1], Indu Shekhar Thakur[a,*]

[a] School of Environmental Sciences, Jawaharlal Nehru University, New Delhi 110067, India
[b] Centre for Rural Development and Technology, Indian Institute of Technology, New Delhi 110016, India

ARTICLE INFO

Keywords:
Sewage sludge
Mixed microbial culture
Polyhydroxyalkanoates
Bioplastic
Response Surface Methodology

ABSTRACT

In the current study, the feasibility of utilizing municipal secondary wastewater sludge for Polyhydroxyalkanoate (PHA) extraction was improved by optimization of various parameters (temperature, duration and concentration of sludge solids). Optimized process parameters resulted in PHA recovery of 0.605 g, significantly higher than un-optimized conditions. The characterization of PHA was carried out by GC–MS, FT-IR and NMR (^{1}H and ^{13}C) spectroscopy. The PHA profile was found to be dominated by mcl PHA (58%) along with other diverse PHA. The results of the present study show rich diversity of PHA extracted from a raw material which is readily available at minimal cost. In conclusion, exploring the potential of wastes for production of bioplastics not only reduces the cost of bioplastic production, but also provides a sustainable means for waste management.

1. Introduction

Rapid depletion of petroleum reserves and persistence of conventional synthetic plastics in the environment are considered important ecological problems. Thus, there is a need for alternatives to petroleum-based plastics. One such alternative is Polyhydroxyalkanoate (PHA), commonly known as bioplastic, which is a polymer produced by bacteria and has the advantage of being biodegradable and biocompatible. (Kumar et al., 2016b). It has been estimated that globally, production capacities of bioplastics till 2018 is going to increase by 300% (European Bioplastics, 2013). However, the main obstacle to the growth of bioplastic market is its high production cost, poor recycling facilities and inefficient waste handling technology (Brockhaus et al., 2016). There are innumerous reports of PHA production from pure bacterial cultures, but the major portion of the production cost is spent on media sterilization and maintenance of reactor (Reddy and Mohan, 2012). Hence, it has become imperative to search for worthwhile and cost effective feedstock alternatives for PHA production.

Wastewater treatment sludge containing mixed microbial consortia (MMC) is a potential feedstock for PHA production. Utilizing wastewater treatment sludge for producing PHA will also reduce the environmental burden of sludge disposal (Reddy and Mohan, 2012). Rapidly increasing population, urbanization and industrialization leads to production of excess amount of sludge every year, making it a readily available and more economical feedstock for bioplastic production (Bengtsson et al., 2008). Microbial species such as bacteria, yeasts, fungi present in sludge, synthesize the biopolymers triacylglycerol (TAG), wax esters (WEs) or PHA de novo with the availability of excess carbon source, particularly when nitrogen or phosphorus is limiting in the growth media (Kumar et al., 2017b).

Substantial efforts have gone towards PHA production using mixed culture of molasses (Albuquerque et al., 2010), sludge and municipal wastewater (Morgan-Sagastume et al., 2014), effluent of olive oil, designed synthetic wastewater (Reddy and Mohan, 2012). However, along with screening of low cost sustainable alternatives for PHA production, finding the optimum conditions for maximal PHA extraction is also essential. The solvent extraction method is not very environment friendly; apart from this it is economically more feasible when compared to green solvent extraction methods such as enzymatic digestion, mechanical cell disruption and the use of supercritical carbon dioxide, therefore making it an attractive method for PHA recovery (Anis et al., 2013). The action of the solvent at temperature above 50 °C will speed up the cell disruption, solubilize the intracellular PHA granules and ultimately increase the purity of polymer (Lee, 1996; Anis et al., 2013).

Response Surface Methodology (RSM) is one of the well known statistical techniques, commonly used for optimization. This optimization tool not only facilitates understanding of the interactions among different variables and estimate the maximum response generation, but

* Corresponding author.
E-mail address: indushekhart@gmail.com (I.S. Thakur).
[1] Pooja Ghosh and Khushboo Khosla have contributed equally to this work.

https://doi.org/10.1016/j.biortech.2018.01.031
Received 11 December 2017; Received in revised form 4 January 2018; Accepted 5 January 2018
Available online 08 January 2018
0960-8524/

Bioresource Technology 256 (2018) 478–490

Contents lists available at ScienceDirect

Bioresource Technology

journal homepage: www.elsevier.com/locate/biortech

Review

Sequestration and utilization of carbon dioxide by chemical and biological methods for biofuels and biomaterials by chemoautotrophs: Opportunities and challenges

Indu Shekhar Thakur[a,d,*], Manish Kumar[a], Sunita J. Varjani[b,d], Yonghong Wu[c], Edgard Gnansounou[d], Sindhu Ravindran[e]

[a] School of Environmental Sciences, JawaharNehru University, New Delhi 110067, India
[b] Gujarat Pollution Control Board, Sector-10A, Gandhinagar 382010, Gujarat, India
[c] State Key Laboratory of Soil and Sustainable Agriculture, Institute of Soil Science, Chinese Academy of Sciences, 71 East Beijing Road, Nanjing 210008, China
[d] Bioenergy and Energy Planning Research Group (BPE), IIC, ENAC, Station 18, Ecole Polytechnique Fédérale de Lausanne (EPFL), CH-1015 Lausanne, Switzerland
[e] Microbial Processes and Technology Division, CSIR-NIIST, Trivandrum, India

ARTICLE INFO

Keywords:
Biofuel and biorefineries
Biomaterials
Catabolic pathways
Carbon dioxide capture and utilization
Organic synthesis

ABSTRACT

To meet the CO_2 emission reduction targets, carbon dioxide capture and utilization (CCU) comes as an evolve technology. CCU concept is turning into a feedstock and technologies have been developed for transformation of CO_2 into useful organic products. At industrial scale, utilization of CO_2 as raw material is not much significant as compare to its abundance. Mechanisms in nature have evolved for carbon concentration, fixation and utilization. Assimilation and subsequent conversion of CO_2 into complex molecules are performed by the photosynthetic and chemolithotrophic organisms. In the last three decades, substantial research is carry out to discover chemical and biological conversion of CO_2 in various synthetic and biological materials, such as carboxylic acids, esters, lactones, polymer biodiesel, bio-plastics, bio-alcohols, exopolysaccharides. This review presents an over view of catalytic transformation of CO_2 into biofuels and biomaterials by chemical and biological methods.

1. Introduction

Emission of Global Warming Gases (GWGs) is the mainly responsible causes, which trigger the global warming and subsequently climate shift. Carbon dioxide (CO_2), being the most rampant of GWGs, concentration has increases by somehow 32% since the Industrial Revolution, from approximately 280 part per million (ppm) to 400 ppm until now (De Silva et al., 2015; Cheah et al., 2016). The power sector is the foremost CO_2 emitter requires strict CO_2 management technology and thus various strategies have been made so far to move forward to achieve "low carbon society" (Cheah et al., 2015; Li et al., 2015). In current years, endeavours have been made to extend technologies and processes for CO_2 capture, storage and utilization (CCU), which includes liquids, solids, membranes as adsorbents and biological methods (Choi and Drese, 2009; Rahaman et al., 2011; Olson et al., 2012). However, CO_2 is incredibly striking as reaction media in biphasic catalysis as it is copious, harmless, non-flammable easily available and renewable carbon source for production of value added products such as fuels and chemicals (Peters et al., 2011). Therefore, catalytic mechanism and reaction media are developed based on economic feasibility and activation of CO_2 for uses it as eco-friendly carbon source. Considerable development is made so far in catalytic utilization of CO_2, as a substitute of reaction medium, reactant, reagent and promoter due to its exclusive physical properties (Cokoja et al., 2011; Trusler, 2017).

Several chemical processes, photochemical, electrochemical, biochemical and microwave-assisted conversion of CO_2 are reported since last five decades (Choi and Drese, 2009; Leung et al., 2014). To understand the molecular mechanism adopted by biological system for utilization of CO_2 and developing the advance technology, it is important to know the basic chemistry of CO_2. Although CO_2 is a non-polar molecule, but it contains two polar C=O bonds and exhibits two varying reaction sites, such as electrophilic carbon atom and nucleophilic oxygen atoms. The chemical bonding of a third atom of oxygen and some other atom with carbon atom is exergonic reaction and as a result CO_2 can be transformed into carboxylates, lactones, carbamates, urea, isocyanates and carbonates (Choi and Drese, 2009). Apart from oxidised form of CO_2 its reduced form such as formates, oxalates, formaldehyde, carbon monoxide, methanol and methane are produced by endergonic reaction mechanism (Jessop, 2006). Therefore, major

* Corresponding author at: School of Environmental Sciences, Jawaharlal Nehru University, New Delhi 110067, India.
E-mail addresses: indushekhart@gmail.com (I.S. Thakur), yhwu@issas.ac.cn (Y. Wu), edgard.gnansounou@epfl.ch (E. Gnansounou).

https://doi.org/10.1016/j.biortech.2018.02.039
Received 9 January 2018; Received in revised form 6 February 2018; Accepted 7 February 2018
Available online 10 February 2018
0960-8524/

Bioresource Technology Reports 2 (2018) 1–6

Contents lists available at ScienceDirect

Bioresource Technology Reports

journal homepage: https://www.journals.elsevier.com/bioresource-technology-reports

Utilization of glycerol by *Bacillus* sp. ISTVK1 for production and characterization of Polyhydroxyvalerate

Raj Morya [1], Manish Kumar [1], Indu Shekhar Thakur *

School of Environmental Sciences, Jawaharlal Nehru University, New Delhi 110067, India

ARTICLE INFO

Article history:
Received 20 February 2018
Received in revised form 7 March 2018
Accepted 8 March 2018
Available online 14 March 2018

Keywords:
Bioplastic
Polyhydroxyvalerate
Glycerol
TEM
Bacillus sp.
Cell dry weight

ABSTRACT

Plastic due to its light weight and low cost is a first choice for daily use product, which now can be replaced by Bioplastics. The current study demonstrates the screening of a previously reported thermotolerant bacterium strain *Bacillus* sp. ISTVK1 isolated from wastewater treatment plant for production of PHA by utilizing pure glycerol as carbon source. Primary screening of the selected bacterium strain was performed by Nile red staining and afterward visualization under a fluorescence microscope. Nile red fluorescence measurement of bacterial culture was also investigated based on absorbance of spectrofluorometer. GC–MS, ^{1}H NMR, TEM, and FT-IR analysis revealed that the produced material is PHV, which is *co*-polymer of PHB. Optimization of process parameters was performed to enhance the production of PHA. A substantial increase in PHA production from 1.29 g/L to 4.44 g/L (85.19% of CDW) was observed after optimization of process parameters, shows the importance of optimization.

1. Introduction

Industrialization and modernization lead to increase in the lifestyle of the people, and we are bound to use the synthetic products such as plastics. Now, these days plastics are appealing and most of the things around us is made up of plastic. Production of the plastics reached from 2 million metric tonnes (Mt) in 1950 to 8300 Mt in 2015. Out of total plastic produced till date, only 600 Mt recycled, 2500 Mt is in use, 800 Mt incinerated, and a considerable section 4900 Mt dumped into the environment may be in the landfill or in the ocean (Geyer et al., 2017). Non-biodegradable petroleum based plastic waste dumped into the environment affects the water dwellers, groundwater quality, soil productivity and finally chemicals release from the plastic degradation enters into the foodchain (Porras et al., 2017).

One of the best alternatives to synthetic plastic is the bio-degradable polyhydroxyalkanoates (PHAs) which has enormous potential to replace the Petro based non-degradable plastic. These polymers have diverse applications, it can be employed either for packaging and coating materials (Porras et al., 2017); its biodegradable nature makes PHA a strong contender in control drug delivery carrier (Essel and Carus, 2012). PHA show a considerable temperature tolerance, mechanical properties, and biodegradability these properties makes them economically viable and Environment-friendly, it will help in reducing the carbon footprint. According to literature, 1 kg PHA production can save up to 2 kg carbon dioxide and 30 MJ of energy from fossil resources (Essel and Carus, 2012). However, significant area of concern of the growing PHA industry is the raw material since food crops and vegetable oils primarily being utilized as carbon source for production of PHA (Thakur et al., 2018).

But these carbon sources compete with the food supply which forced scientists to search for cost effective substrate which doesn't compete to the food supply. For instance, when corn was used as carbon source as a substitute for glucose, 0.67 kg of glucose can be extracted from 1 kg of corn (Borglum, 1980), and this much amount of glucose can be used as a carbon source to yield 0.27 kg PHA (Kim et al., 1994). Subsequently, 1,26,000 tonnes of corn would increase the production of 34,000 tonnes of PHA (Jiang et al., 2016). Hence, it is necessary to exploit substrates which are non-food-based or waste generated from household and industries as a carbon source for the sustainable synthesis of PHA. PHA can be generated by utilizing various types of wastes as a substrate like lignin derivatives (Kumar et al., 2017b), municipal wastewater (Gupta et al., 2017), pulp, paper and cardboard industry wastewater (Bhuwal et al., 2013), starch industry wastewater (Grazia et al., 2017), wastewater sludge (Kumar et al., 2018a), glycerol (Mohandas et al., 2017) and carbon dioxide (Kumar et al., 2016b).

Glycerol is the major by-product of biodiesel industry (Kalia et al., 2016); further produced glycerol is processed and utilized in production of various chemicals and products such as, healthcare products, cosmetics, and sweetener. An inversely proportional relationship exists between the biodiesel production and cost of glycerol in the market (Rodríguez-Contreras et al., 2015). Utilizing glycerol as carbon source by microorganism is appealing area of research for production of PHAs

* Corresponding author.
E-mail address: isthakur@hotmail.com (I.S. Thakur).
[1] Raj Morya and Manish Kumar have equal contribution in this work.

https://doi.org/10.1016/j.biteb.2018.03.002
2589-014X/

Kumar *et al. Biotechnol Biofuels (2018) 11:154*
https://doi.org/10.1186/s13068-018-1148-2

Biotechnology for Biofuels

RESEARCH Open Access

Genomic and proteomic analysis of lignin degrading and polyhydroxyalkanoate accumulating β-proteobacterium *Pandoraea* sp. ISTKB

Madan Kumar[1], Sandhya Verma[2], Rajesh Kumar Gazara[2], Manish Kumar[1], Ashok Pandey[3], Praveen Kumar Verma[2*] and Indu Shekhar Thakur[1*]

Abstract

Background: Lignin is a major component of plant biomass and is recalcitrant to degradation due to its complex and heterogeneous aromatic structure. The biomass-based research mainly focuses on polysaccharides component of biomass and lignin is discarded as waste with very limited usage. The sustainability and success of plant polysaccharide-based biorefinery can be possible if lignin is utilized in improved ways and with minimal waste generation. Discovering new microbial strains and understanding their enzyme system for lignin degradation are necessary for its conversion into fuel and chemicals. The *Pandoraea* sp. ISTKB was previously characterized for lignin degradation and successfully applied for pretreatment of sugarcane bagasse and polyhydroxyalkanoate (PHA) production. In this study, genomic analysis and proteomics on aromatic polymer kraft lignin and vanillic acid are performed to find the important enzymes for polymer utilization.

Results: Genomic analysis of *Pandoraea* sp. ISTKB revealed the presence of strong lignin degradation machinery and identified various candidate genes responsible for lignin degradation and PHA production. We also applied label-free quantitative proteomic approach to identify the expression profile on monoaromatic compound vanillic acid (VA) and polyaromatic kraft lignin (KL). Genomic and proteomic analysis simultaneously discovered Dyp-type peroxidase, peroxidases, glycolate oxidase, aldehyde oxidase, GMC oxidoreductase, laccases, quinone oxidoreductase, dioxygenases, monooxygenases, glutathione-dependent etherases, dehydrogenases, reductases, and methyltransferases and various other recently reported enzyme systems such as superoxide dismutases or catalase–peroxidase for lignin degradation. A strong stress response and detoxification mechanism was discovered. The two important gene clusters for lignin degradation and three PHA polymerase spanning gene clusters were identified and all the clusters were functionally active on KL–VA.

Conclusions: The unusual aerobic '-CoA'-mediated degradation pathway of phenylacetate and benzoate (reported only in 16 and 4–5% of total sequenced bacterial genomes), peroxidase-accessory enzyme system, and fenton chemistry based are the major pathways observed for lignin degradation. Both *ortho* and *meta* ring cleavage pathways for aromatic compound degradation were observed in expression profile. Genomic and proteomic approaches provided

*Correspondence: pkv@nipgr.ac.in; isthakur@hotmail.com; isthakur@mail.jnu.ac.in
[1] School of Environmental Sciences, Jawaharlal Nehru University, New Delhi, 110067, India
[2] National Institute of Plant Genome Research, Aruna Asaf Ali Marg, New Delhi 110067, India
Full list of author information is available at the end of the article